



Quashie, Neils Benjamin (2008) *Purine transport in plasmodium falciparum*. PhD thesis.

<http://theses.gla.ac.uk/165/>

Copyright and moral rights for this thesis are retained by the author

A copy can be downloaded for personal non-commercial research or study, without prior permission or charge

This thesis cannot be reproduced or quoted extensively from without first obtaining permission in writing from the Author

The content must not be changed in any way or sold commercially in any format or medium without the formal permission of the Author

When referring to this work, full bibliographic details including the author, title, awarding institution and date of the thesis must be given

# **Purine Transport in *Plasmodium falciparum***

**Neils Benjamin Quashie**

**Division of Infection Immunity  
Institute of Biomedical and Life Sciences**



This thesis is submitted for the degree of Doctor of Philosophy

Faculty of Biomedical and Life Sciences

University of Glasgow

© Neils B. Quashie, January 2008

## Abstract

Purine transport in malaria parasites has become an important potential drug target because the malaria parasite is unable to synthesis purine *de novo* and has to salvage it from the host milieu through transporter(s). Knowledge of the number, selectivity and kinetic parameters of the transporters expressed by the parasite would therefore facilitate a rational purine-based chemotherapy of malaria

The rates of transport of radiolabeled purines into *Plasmodium falciparum*-infected erythrocytes were measured using classical uptake techniques. We found that the uptake of purine into intact parasite-infected erythrocytes was mediated by the endogenous human erythrocyte nucleoside and nucleobase transporters (hENT1 and hFNT1) rather than the parasite-induced New Permeation Pathways (NPP). The overall rate of purine uptake was observed to be approximately doubled in parasite-infected cells compared to uninfected cells and the rate of adenosine uptake was seen to be faster than hypoxanthine in parasite-infected cells. It was observed that transport of hypoxanthine and adenine through the hFNT1 was unexpectedly inhibited by furosemide. This inhibition by furosemide of [<sup>3</sup>H]-hypoxanthine and [<sup>3</sup>H]-adenine uptake was not through inhibition of the NPP, as it was observed equally in infected and uninfected hRBC.

To gain further understanding of purine transport in the malaria parasite, uptake was measured in saponin-freed *P. falciparum* trophozoites. Treatment of parasite infected erythrocytes with saponin render both the erythrocyte membrane and the parasitophorous vacuole membrane permeable to solutes, allowing transport to be measured across the parasite membrane. The data obtained from the uptake assays were analysed using Michaelis Menten plots to obtain the kinetic properties ( $K_m$  and  $V_{max}$ ) of the parasite's purine transporters. Three separate and novel transport activities were identified in saponin-freed *P. falciparum* trophozoites: (i) a high affinity hypoxanthine transporter with a secondary capacity for purine nucleosides, named PfNT1, (ii) a separate high affinity transporter for uptake of adenine (named PfADET1) and (iii) a low affinity/high capacity adenine carrier (denoted PfADET2). Additionally, the presence in the parasite of a low affinity adenosine transporter designated PfLAAT, with kinetic properties similar to that previously reported by other research groups was also confirmed. At room temperature,

uptake of hypoxanthine through PfNT1 was observed to be 12-fold more efficient than adenosine.

The gene encoding the high affinity hypoxanthine/nucleoside transporter *PfNT1* was disrupted by a single crossover event and the parasite clones obtained were designated 3D7 $\Delta$ *PfNT1*. The characteristics of purine uptake into parasites lacking a functional *PfNT1* gene were then compared to uptake in wild-type parasites. The high affinity uptake of hypoxanthine or adenosine was completely abolished in 3D7 $\Delta$ *PfNT1*, whereas uptake of 25 $\mu$ M [ $^3$ H]-adenosine (through the low affinity transporter, PfLAAT) was similar in both 3D7 $\Delta$ *PfNT1* and wild-type *P. falciparum* parasites. Adenine transport was observed to increase in 3D7 $\Delta$ *PfNT1*, presumably to partly compensate for the loss of the high affinity hypoxanthine transporter.

An improved microfluorometric technique for determining parasite's sensitivity to antimalarial drugs was developed and the method was used to evaluate antiplasmodial potential of a small number of purine analogues. A 'hypoxanthine-like' purine analogue, JA-32, was found to inhibit the uptake of hypoxanthine by PfNT1, supporting the potential of purine transporters as targets for antimalarial drug development.

The findings from this study provide evidence that purine salvage in *P. falciparum* is predominantly based on the highly efficient uptake of hypoxanthine by PfNT1 and secondarily on the high capacity uptake of nucleosides by a lower affinity carrier. The exact contribution to the overall purine salvage in parasite by the two transporters of adenine is not clear. Indeed, the issue of whether Plasmodium can utilise adenine as a purine source is controversial. These findings re-emphasise the importance of purine transporters as targets for novel antimalarial drugs and open the gateway for a systematic purine-based chemotherapy of malaria.

# Table of Contents

<b>Abstract.....</b>	<b>i</b>
<b>Table of Contents .....</b>	<b>iii</b>
<b>List of Tables .....</b>	<b>viii</b>
<b>List of Figures.....</b>	<b>ix</b>
<b>List of Recent Publications.....</b>	<b>xiii</b>
<b>Acknowledgements.....</b>	<b>xiv</b>
<b>Dedication .....</b>	<b>xv</b>
<b>Declaration.....</b>	<b>xvi</b>
<b>Abbreviations.....</b>	<b>xvii</b>
<b>1 General Introduction .....</b>	<b>1</b>
1.1 Background to the study .....	2
1.2 Malaria- The disease burden .....	4
1.3 Economic burden of malaria .....	5
1.4 Life cycle of the malaria parasite .....	6
1.5 Manifestation of malaria .....	7
1.6 Laboratory diagnosis of malaria .....	8
1.7 Chemotherapy of Malaria .....	9
1.7.1 Chloroquine.....	9
1.7.2 Sulphadoxine/pyrimethamine (SP) .....	10
1.7.3 Quinine.....	10
1.7.4 Primaquine .....	11
1.7.5 Artemisinin or Qinghaosu .....	11
1.8 Resistance to Antimalarial Drugs .....	13
1.9 Vaccines to combat malaria? .....	15
1.10 Search for novel antimalarial drugs: purine transporters as a potential chemotherapeutic target .....	17
1.11 An Overview of the Biochemistry of Plasmodium .....	17
1.12 Mode of Transport in cells .....	19
1.13 Purine transport in human cells.....	22
1.14 Purine metabolism in mature uninfected human erythrocytes.....	25
1.15 Transportation systems in infected erythrocytes.....	27
1.15.1 The New Permeation Pathway .....	28
1.15.2 The Parasitophorous Vacuole Membrane .....	30
1.16 Chemical structures of purines.....	31
1.17 Salvage and metabolism of purine in parasitic protozoa .....	32
1.18 Purine metabolism in <i>P. falciparum</i> .....	32
1.19 The Equilibrative Nucleoside Transporters .....	34
1.20 Identification of ENT transporter genes in <i>Plasmodium falciparum</i> .....	36
1.21 Cellular location of <i>P. falciparum</i> purine transporters .....	38
1.22 Purine antimetabolites as antimalarial drugs .....	39
1.23 Nucleoside and Nucleobase transport in other apicomplexa .....	41
1.24 Studies on <i>P. falciparum</i> purine transport published after conclusion of our own characterisation of purine salvage in isolated trophozoites.....	43

1.25	Aims and objectives of study .....	44
<b>2</b>	<b>Materials and methods .....</b>	<b>45</b>
2.1	<i>In vitro</i> cultivation of <i>P. falciparum</i> .....	46
2.1.1	Parasite lines/clones .....	46
2.1.2	Preparation of culture media .....	46
2.1.3	Processing of red blood cells for parasite culture .....	46
2.1.4	Culturing of malaria parasites .....	46
2.1.5	Synchronization of culture .....	47
2.1.6	Staining of malaria parasites .....	47
2.1.7	Cryopreservation of malaria parasites.....	48
2.1.8	Thawing of cyopreserved malaria parasites.....	48
2.1.9	Red blood cell counts using Improved Neubauer haemocytometer.....	49
2.2	Purine transport assays.....	49
2.2.1	Chemicals used in the transport assays.....	49
2.2.2	Preparation of saponin-freed <i>P. falciparum</i> trophozoites for transport assays 49	
2.2.3	Percoll enrichment of infected erythrocytes .....	50
2.2.4	Measurement of purine uptake in saponin-freed <i>P. falciparum</i> trophozoites.. .....	51
2.2.5	Time-dependent uptake of permeant.....	51
2.2.6	Dose-dependent uptake of permeant.....	52
2.2.7	Processing of sample after uptake assay .....	53
2.3	Molecular Techniques.....	53
2.3.1	Extraction of parasite DNA using Instagene.....	53
2.3.2	DNA extraction using the phenol-chloroform method .....	54
2.3.3	Purification of DNA using a mini-, midi- and max-prep kit.....	54
2.3.4	Polymerase chain reaction (PCR) .....	55
2.3.5	Determination of DNA concentrations by spectrophotometry .....	55
2.3.6	Agarose electrophoresis of DNA .....	55
2.3.7	Amplification of ENT DNA fragments .....	56
2.3.8	Purification of the ENT DNA fragments .....	62
2.3.9	Plasmid used in preparing DNA construct.....	62
2.3.10	Restriction digestion of ENT DNA or pCAM-BSD plasmid .....	65
2.3.11	Ligation of ENT fragment into pCAM-BSD.....	65
2.3.12	Transforming DH5 $\alpha$ cells with (pCAM-BSD/ENT).....	66
2.3.13	Retrieval and purification of pCAM-BSD/ENT.....	67
2.3.14	Sequencing of pCAM-BSD/ENT.....	68
2.4	Transfection of <i>P. falciparum</i> by electroporation.....	68
2.4.1	Selection of transfected <i>P. falciparum</i> parasites .....	68
2.4.2	Verification of integration by PCR .....	69
2.4.3	Cloning of 3D7 $\Delta$ PfNT1 parasites.....	71
2.4.4	Confirmation of Integration by Southern blot analysis.....	72
2.5	Isotopic method for testing sensitivity to antimalarial drugs.....	74
2.6	PicoGreen <sup>®</sup> Method for drug sensitivity assays.....	75
2.7	Data analysis .....	76
<b>3</b>	<b>Purine transport into uninfected and <i>P. falciparum</i> infected human erythrocytes .....</b>	<b>78</b>
3.1	Summary .....	79
3.2	Introduction .....	80
3.3	Adenosine uptake into Percoll <sup>™</sup> -enriched <i>P. falciparum</i> infected erythrocytes is not consistent with salvage through the NPP .....	83

3.4	Hypoxanthine uptake into uninfected erythrocytes and Percoll-enriched <i>P. falciparum</i> -infected erythrocytes occurs mainly through hFNT1 and is inhibited by furosemide.....	86
3.5	Adenine transport into uninfected human erythrocytes is inhibited by furosemide .....	88
3.6	Discussion .....	90
3.7	Conclusions .....	92
<b>4</b>	<b>Purine transport in saponin-freed <i>P. falciparum</i> trophozoites .....</b>	<b>93</b>
4.1	Summary .....	94
4.2	Background .....	95
4.2.1	Mechanism of permeabilisation of <i>P. falciparum</i> infected erythrocytes .....	96
4.2.2	Hypoxanthine, the preferred purine source for <i>P. falciparum</i> .....	97
4.3	Preparation of saponin-freed <i>P. falciparum</i> (clone 3D7) trophozoites for uptake studies .....	98
4.4	Data analysis .....	99
4.5	High affinity hypoxanthine transport in saponin-freed <i>P. falciparum</i> trophozoites .....	100
4.5.1	Time dependent uptake of hypoxanthine into saponin-freed <i>P. falciparum</i> trophozoites .....	100
4.5.2	Determination of $K_m$ and $V_{max}$ values for the high affinity hypoxanthine transporter .....	101
4.5.3	Inhibitory effect of other purines on the high affinity hypoxanthine transporter .....	102
4.6	Inhibitory effect of purine analogues on the high affinity hypoxanthine transporter .....	103
4.7	Inhibition of high affinity hypoxanthine transport by Pyrimidines .....	104
4.8	High affinity adenosine transport into saponin-freed <i>P. falciparum</i> trophozoites.....	105
4.8.1	Time dependent uptake of adenosine .....	105
4.8.2	Determination of the $K_m$ and inhibition profile for the high affinity adenosine transport .....	106
4.9	Transport of adenine into saponin-freed <i>P. falciparum</i> trophozoites .....	107
4.9.1	Uptake of adenine is mediated by a separate high affinity transporter .....	107
4.9.2	Determination of $K_m$ and $V_{max}$ for PfADET1 .....	108
4.9.3	Inhibition profile of PfADET 1 .....	111
4.10	A very low affinity/high capacity transporter of adenine exists in saponin-freed <i>P. falciparum</i> trophozoites .....	112
4.11	Low affinity transport of adenosine in saponin-freed <i>P. falciparum</i> trophozoites .....	113
4.11.1	Existence of a low affinity adenosine transporter in <i>P. falciparum</i> trophozoites confirmed .....	113
4.11.2	Determination of $K_m$ and $V_{max}$ of PfLAAT.....	115
4.12	Effect of dipyrindamol on the low affinity adenosine transporter .....	116
4.13	Summary of results: Profile of purine transport in <i>P. falciparum</i> trophozoites.....	118
4.14	Proposed model for purine transport in saponin-freed <i>P. falciparum</i> trophozoites .....	119
4.15	Discussion .....	120
4.16	Conclusions .....	123

<b>5</b>	<b>Generation of <i>P. falciparum</i> clones with disrupted Equilibrative Nucleoside Transporter- encoding genes .....</b>	<b>124</b>
5.1	Summary .....	125
5.2	Introduction .....	126
5.2.1	Four genes encode Equilibrative Nucleoside Transporters in <i>P. falciparum</i> .....	127
5.2.2	Alignment of amino acids of the four ENT proteins .....	128
5.3	Alignment of the nucleotides of the four genes encoding for ENT in <i>P. falciparum</i> .....	130
5.4	Phylogenic tree of the four genes encoding for ENT in <i>P. falciparum</i> .....	133
5.5	Sequencing of <i>PfNT1</i> (PF13_0252) in <i>P. falciparum</i> clone 3D7 .....	134
5.6	Preparation of plasmid constructs for disruption of the equilibrative nucleoside transporter genes .....	135
5.7	Preparation of pCAM/BSD-ENT construct .....	138
5.8	Transformation of DH5 $\alpha$ competent cells with pCAM/BSD-ENT construct ...	138
5.9	Transfection of <i>P. falciparum</i> by electroporation .....	140
5.10	Confirmation of integration of 3D7 $\Delta$ <i>PfNT1</i> , 3D7 $\Delta$ <i>PfNT2</i> and 3D7 $\Delta$ <i>PfNT3</i> in uncloned parasite cultures .....	141
5.11	Cloning of parasites with disrupted <i>PfNT1</i> .....	143
5.12	Molecular characterisation of 3D7 $\Delta$ <i>PfNT1</i> clones .....	145
5.12.1	PCR characterisation of 3D7 $\Delta$ <i>PfNT1</i> clones .....	145
5.12.2	Southern blot analysis of 3D7 $\Delta$ <i>PfNT1</i> clones .....	145
5.13	Discussion .....	148
5.14	Conclusions .....	150
<b>6</b>	<b>Characterisation of purine transport parameters in <i>P. falciparum</i> parasites lacking the gene encoding the Equilibrative Nucleoside Transporter 1 protein (PfNT1). .....</b>	<b>151</b>
6.1	Summary .....	152
6.2	Introduction .....	153
6.3	Kinetic characterisation of parasites- summary of procedure .....	154
6.4	High affinity Adenosine transport is abolished in clone 3D7 $\Delta$ <i>PfNT1</i> -D6 .....	155
6.5	High affinity Hypoxanthine transport in clone 3D7 $\Delta$ <i>PfNT1</i> -D6 is abolished... ..	156
6.6	High affinity adenine transport is not abolished in clone 3D7 $\Delta$ <i>PfNT1</i> -D6 .....	157
6.7	Low affinity adenosine transporter is not abolished in clone 3D7 $\Delta$ <i>PfNT1</i> -D6 ..	158
6.8	Sensitivity of parasites lacking PfNT1 to JA- and NA- compounds .....	159
6.9	Discussion .....	161
6.10	Conclusion .....	163
<b>7</b>	<b>Development of an improved microfluorimetric method for <i>in vitro</i> assessment of the susceptibility of <i>P. falciparum</i> to purine antimetabolites .....</b>	<b>164</b>
7.1	Summary .....	165
7.2	Introduction .....	166
7.3	PicoGreen <sup>®</sup> fluorescence is directly proportional to DNA concentration .....	168
7.4	Blood quenches fluorescence of PicoGreen <sup>®</sup> .....	170
7.5	Reversing the quenching effect of blood on PicoGreen <sup>®</sup> fluorescence by saponin treatment .....	172
7.6	Comparison of the improved PicoGreen <sup>®</sup> method with [ <sup>3</sup> H]-hypoxanthine uptake method .....	174



7.7	Test of purine analogues for antiplasmodial activities using the improved PicoGreen <sup>®</sup> method .....	177
7.8	Discussion .....	180
7.9	Conclusion .....	182
<b>8</b>	<b>General Discussion .....</b>	<b>183</b>
8.1	Purine transport activity in <i>P. falciparum</i> parasites with intact erythrocyte membranes .....	185
8.2	Purine transport activity in <i>P. falciparum</i> parasites with permeabilised erythrocyte membranes .....	186
8.3	Purine transport in <i>P. falciparum</i> parasites lacking <i>PfNT1</i> .....	189
8.4	Purine-based antimalarial drugs .....	192
<b>9</b>	<b>Appendix .....</b>	<b>195</b>
9.1	Composition of solutions .....	196
9.1.1	Cryopreservation solution .....	196
9.1.2	Cytomix .....	196
9.1.3	Denaturation solution for Southern blot .....	196
9.1.4	6 X DNA loading dye .....	196
9.1.5	LB agar .....	196
9.1.6	LB medium .....	196
9.1.7	Neutralisation solution for Southern blot .....	196
9.1.8	SOC .....	196
9.1.9	20 X SSC .....	197
9.1.10	50 X TAE .....	197
9.1.11	5 X TBE .....	197
9.1.12	1 X TE .....	197
<b>10</b>	<b>Reference List .....</b>	<b>198</b>

## List of Tables

<b>Table 1.1:</b> Physiological average concentrations of salvageable purines in mammalian cells or tissues .....	<b>24</b>
<b>Table 2.1:</b> A table showing the size of each of the four <i>P. falciparum</i> equilibrative nucleoside transporter genes, the size of each fragment cloned into pCAM/BSD and the primer pairs used to amplify each of the DNA fragments. ....	<b>61</b>
<b>Table 2.2:</b> Cycling condition for the amplification of the four <i>P. falciparum</i> equilibrative nucleoside transporter genes. ....	<b>61</b>
<b>Table 2.3:</b> Primers used to check integration of the episomes: <i>PfNT1</i> , <i>PfNT2</i> , <i>PfNT3</i> and <i>PfNT4</i> . ....	<b>69</b>
<b>Table 2.4:</b> Primer combinations used to check integration of the episome. ....	<b>70</b>
<b>Table 4.1:</b> Summary of the kinetic studies of saponin-freed <i>P. falciparum</i> trophozoites. ....	<b>118</b>
<b>Table 6.1 :</b> Sensitivity of <i>P. falciparum</i> clones 3D7 $\Delta$ <i>PfNT1</i> -D6 and wild type (3D7 clones of <i>P. falciparum</i> ) to JA- and NA-compounds .....	<b>160</b>
<b>Table 7.1</b> Fluorescence intensity reading for blood of haematocrit 1 – 5%, spiked with 1000 ng/ml salmon sperm DNA .....	<b>170</b>
<b>Table 7.2</b> Mean IC <sub>50</sub> values for chloroquine and pyrimethamine determined by the PicoGreen® or [ <sup>3</sup> H]-hypoxanthine accumulation assay .....	<b>175</b>
<b>Table 7.3:</b> <i>In vitro</i> antiplasmodial activity of purine analogues against <i>P. falciparum</i> clone 3D7 using the improved PicoGreen® method .....	<b>179</b>
<b>Table 8.1:</b> Comparison of K <sub>m</sub> Values obtained from various studies. ....	<b>190</b>

## List of Figures

<b>Figure 1.1:</b> Distribution of Malaria in the world as at April 2004.....	4
<b>Figure 1.2:</b> The life Cycle of <i>P. falciparum</i> Malaria Parasite.....	6
<b>Figure 1.3:</b> Site of action of most of the available antimalarial drugs.....	12
<b>Figure 1.4:</b> Chemical structures of some of the commonly used antimalarial drugs.....	12
<b>Figure 1.5:</b> Representation of an intra-erythrocytic <i>P. falciparum</i> trophozoite, highlighting key parasite intracellular compartments and the site of action of some of the major classes of antimalarial drugs .....	13
<b>Figure 1.6:</b> The global distribution of malaria .....	14
<b>Figure 1.7:</b> Antigens listed according to the stage in which they would be expected to provoke a protective immune response.....	16
<b>Figure 1.8:</b> The relative permeability of the lipid bilayer of cell to different classes of molecules .....	20
<b>Figure 1.9:</b> Mechanism of transport in cells showing simple diffusion, facilitated diffusion, active uptake and active extrusion of compounds. ....	21
<b>Figure 1.10:</b> Nucleoside transport mediated by the concentrative nucleoside transporter (CNT) and equilibrative nucleoside transporter (ENT) .....	23
<b>Figure 1.11:</b> Schematic representation of adenosine metabolism in human erythrocytes...	26
<b>Figure 1.12:</b> Transport systems before and after parasite invasion of the erythrocyte .....	28
<b>Figure 1.13:</b> Models for the formation and induction of the new permeability pathway (NPP) in <i>P. falciparum</i> -infected human RBCs.....	29
<b>Figure 1.14:</b> Chemical structures of purines .....	31
<b>Figure 1.15:</b> The purine pathway in <i>P. falciparum</i> .....	34
<b>Figure 1.16:</b> Topology of mammalian members of the ENT family .....	35
<b>Figure 1.17:</b> Structures of some of the inhibitors of the exogenous purine transporters ....	36
<b>Figure 1.18:</b> Stage-dependent gene expression of the four <i>P. falciparum</i> members of the equilibrative nucleoside transporter family, throughout the intraerythrocytic cycle of the parasite. ....	38
<b>Figure 1.19:</b> Chemical structures of adenosine analogues.....	40
<b>Figure 1.20:</b> Structural formula of HPMPA, an acyclic purine nucleoside phosphonate.....	40
<b>Figure 2.1:</b> Classical uptake technique .....	51
<b>Figure 2.2:</b> DNA sequence of gene encoding for ENT in <i>P. falciparum</i> . This is the gene with plasmDB accession number PF13_0252 (designated <i>PfNT1</i> ). ....	57
<b>Figure 2.3:</b> DNA sequence of genes encoding for ENT in <i>P. falciparum</i> . This is the gene with plasmDB accession number, PF14_0662 (designated: <i>PfNT2</i> ). ....	58
<b>Figure 2.4:</b> DNA sequence of genes encoding for ENT in <i>P. falciparum</i> . This is the gene with plasmDB accession number MAL8P1.32 (designated <i>PfNT3</i> ).....	59
<b>Figure 2.5:</b> Unspliced DNA sequence of genes encoding for ENT in <i>P. falciparum</i> . This is the gene with plasmDB accession number PFA0160C (designated <i>PfNT4</i> ). ....	60
<b>Figure 2.6:</b> Schematic presentation of the vector pCAM-BSD. ....	63

<b>Figure 2.7:</b> DNA sequence of the 4519bp pCAM-BSD. ....	64
<b>Figure 2.8:</b> PCAM-BSD/ENT construct showing the restriction sites for Sac II and Bam H1 .....	67
<b>Figure 2.9:</b> Confirmation of integration in <i>P. falciparum</i> transfectant lacking the <i>ENT</i> gene. .....	70
<b>Figure 2.10:</b> A typical Michaelis-Menten plot.....	77
<b>Figure 3.1:</b> The sources of hypoxanthine in infected erythrocyte, proposed by Berman and colleagues (Berman <i>et al.</i> , 1991). ....	81
<b>Figure 3.2:</b> Schematic presentation of an infected human erythrocyte showing location of purine transporters and the new permeation pathway.....	82
<b>Figure 3.3:</b> Adenosine transport in <i>P. falciparum</i> -infected and uninfected human erythrocytes with inhibition by NBMPR. ....	85
<b>Figure 3.4:</b> Adenosine transport in <i>P. falciparum</i> -infected and uninfected human erythrocytes with inhibition by furosemide. ....	86
<b>Figure 3.5:</b> Transport of 1 $\mu$ M [ $^3$ H]-Hypoxanthine in <i>P. falciparum</i> -infected and uninfected human erythrocytes with inhibition by furosemide. ....	87
<b>Figure 3.6:</b> Adenine transport in uninfected human erythrocytes with inhibition by furosemide.....	89
<b>Figure 4.1:</b> A <i>P. falciparum</i> -infected erythrocyte showing the presence of the different membranes before and after saponin permeabilisation of the RBC.....	97
<b>Figure 4.2:</b> Hypoxanthine transport in saponin-freed <i>P. falciparum</i> trophozoites. ....	100
<b>Figure 4.3:</b> Characterization of a high affinity <i>P. falciparum</i> hypoxanthine transporter..	101
<b>Figure 4.4:</b> Characterization of a high affinity <i>P. falciparum</i> hypoxanthine transporter..	102
<b>Figure 4.5:</b> Uptake of 30 nM [ $^3$ H]-hypoxanthine in the presence or absence of purine analogues JA-23, JA-24 and JA 32. ....	103
<b>Figure 4.6:</b> Effect of pyrimidines on the transport of 30 nM [ $^3$ H]-hypoxanthine by saponin-freed <i>P. falciparum</i> trophozoites. ....	104
<b>Figure 4.7:</b> Uptake of low concentrations of [ $^3$ H]-adenosine in isolated <i>P. falciparum</i> trophozoites.....	105
<b>Figure 4.8:</b> Uptake of low concentrations of [ $^3$ H]-adenosine in saponin-freed <i>P.</i> <i>falciparum</i> trophozoites. ....	106
<b>Figure 4.9:</b> Characterization of a high affinity adenine transporter in <i>P. falciparum</i> trophozoites (Transport of 1 $\mu$ M [ $^3$ H]-adenine). ....	108
<b>Figure 4.10:</b> Characterization of a high affinity adenine transporter in saponin-freed <i>P.</i> <i>falciparum</i> trophozoites (Transport of 0.05 $\mu$ M [ $^3$ H]-adenine). ....	109
<b>Figure 4.11:</b> Characterization of a high affinity adenine transporter in <i>P. falciparum</i> trophozoites (Michaelis-Menten plot).....	110
<b>Figure 4.12:</b> Uptake of 0.05 $\mu$ M [ $^3$ H]-adenine into saponin-freed <i>P. falciparum</i> trophozoites in the presence of varying concentrations of other purines.....	111
<b>Figure 4.13:</b> Uptake of 10 $\mu$ M [ $^3$ H]-adenine by <i>P. falciparum</i> trophozoites.....	112
<b>Figure 4.14:</b> Low affinity transport of adenosine in saponin-freed <i>P. falciparum</i> trophozoites (at room temperature).....	114

<b>Figure 4.15:</b> Low affinity transport of adenosine in saponin-freed <i>P. falciparum</i> trophozoites (at 6 °C).	114
<b>Figure 4.16:</b> Transport of 25 µM [ <sup>3</sup> H]-adenosine into saponin-freed <i>P. falciparum</i> trophozoites (Michaelis-Menten plot).	115
<b>Figure 4.17:</b> Structure of Dipyridamol.	116
<b>Figure 4.18:</b> Effect of dipyridamole (1-25 µM) on the uptake of 25 µM [ <sup>3</sup> H]-adenosine at 6 °C by saponin-freed <i>P. falciparum</i> trophozoites.	117
<b>Figure 4.19:</b> Proposed model of purine transport systems in <i>P. falciparum</i> trophozoites.	119
<b>Figure 5.1:</b> Strategy for disruption of the ENT locus.	127
<b>Figure 5.2:</b> Alignment of the predicted amino acid sequences from the four ENT encoding genes in <i>P. falciparum</i> .	129
<b>Figure 5.3:</b> Alignment of the four genes encoding for equilibrative nucleoside transporter in <i>P. falciparum</i> .	132
<b>Figure 5.4:</b> Phylogenetic tree, with bootstrap values, of the four genes encoding for ENT in <i>P. falciparum</i> and TbAT1 of <i>T. brucei</i> . The scale bar represents the distances as numbers of substitutions per site.	133
<b>Figure 5.5:</b> Sequencing of <i>PfNT1</i> .	135
<b>Figure 5.6:</b> Amplification of <i>PfNT1</i> (PF13_0252).	136
<b>Figure 5.7:</b> Amplification of <i>PfNT2</i> and <i>PfNT3</i> DNA fragments.	137
<b>Figure 5.8:</b> Amplification of <i>PfNT4</i> DNA fragment.	137
<b>Figure 5.9:</b> Verification of presence of <i>PfNT1</i> insert in plasmid pCAM/BSD-PfNT1 by PCR.	139
<b>Figure 5.10:</b> Verification of the presence of <i>PfNT1</i> inserts in the plasmid pCAM/BSD- <i>PfNT1</i> by restriction digestion with <i>Bam</i> HI and <i>Sac</i> II.	140
<b>Figure 5.11:</b> PCR analysis of uncloned <i>PfNT1</i> transfectants, pCAM/BSD- <i>PfNT1</i> and wild type 3D7 parasites.	141
<b>Figure 5.12:</b> PCR analysis of uncloned PfNT2 to verify integration of pCAM/BSD-PfNT2 into parasite's genome.	142
<b>Figure 5.13:</b> PCR analysis of uncloned PfNT3 to verify integration of pCAM/BSD-PfNT2 into parasite's genome.	142
<b>Figure 5.14:</b> PCR analysis of the three clones of <i>PfNT1</i> transfectants, pCAM/BSD- <i>PfNT1</i> and wild type 3D7 parasites.	144
<b>Figure 5.15:</b> PCR analysis of genomic DNA from the wild-type 3D7, uncloned pCAM/BSD- <i>PfNT1</i> transfected parasite population and two of the 3D7Δ <i>PfNT1</i> clones (B11 and D6).	145
<b>Figure 5.16:</b> Separation of 12 µl of restriction digested DNA with <i>Xmn</i> I of wild type (3D7 of <i>P. falciparum</i> ) and DNA from four 3D7Δ <i>PfNT1</i> clones on 0.8% agarose gel prior to Southern blotting.	146
<b>Figure 5.17:</b> Gene disruption strategy.	147
<b>Figure 5.18:</b> Southern blot showing the wild type locus and the digested products of the clones by <i>Xmn</i> I.	147

<b>Figure 6.1:</b> Flow diagram for the production of 3D7 $\square$ <i>PfNT1</i> clones and wild-type control parasites used to assess purine transport in <i>P. falciparum</i> .....	<b>154</b>
<b>Figure 6.2:</b> Purine transport in <i>P. falciparum</i> trophozoites of clone 3D7 $\Delta$ <i>PfNT1</i> -D6 lacking <i>PfNT1</i> (Transport of 0.25 [ $^3$ H]-adenosine at 22 °C).....	<b>155</b>
<b>Figure 6.3:</b> Purine transport in <i>P. falciparum</i> trophozoites lacking PfNT1 (transport of 0.4 $\mu$ M [ $^3$ H]-hypoxanthine at 22 °C) .....	<b>156</b>
<b>Figure 6.4:</b> Purine transport in <i>P. falciparum</i> trophozoites lacking PfNT1 (Transport of 1 $\mu$ M [ $^3$ H]-adenine at 22 °C).....	<b>157</b>
<b>Figure 6.5:</b> Purine transport in <i>P. falciparum</i> trophozoites lacking PfNT1 (Transport of 25 $\mu$ M [ $^3$ H]-adenosine at 6 °C) .....	<b>158</b>
<b>Figure 7.1:</b> Relationship between PicoGreen <sup>®</sup> fluorescence and salmon sperm DNA.....	<b>169</b>
<b>Figure 7.2:</b> The absorption spectra of oxygenated haemoglobin and deoxy haemoglobin .....	<b>171</b>
<b>Figure 7.3:</b> Effect of saponin treatment on PicoGreen <sup>®</sup> fluorescence .....	<b>173</b>
<b>Figure 7.4:</b> Representative graph showing chloroquine responses of <i>P. falciparum</i> lines obtained with the improved PicoGreen <sup>®</sup> method.....	<b>176</b>
<b>Figure 7.5:</b> Representative graph showing chloroquine responses of <i>P. falciparum</i> lines obtained with the traditional [ $^3$ H]-hypoxanthine incorporation method.....	<b>176</b>
<b>Figure 7.6:</b> Structures of the purine analogues designated JA-32 and JA-23 .....	<b>177</b>
<b>Figure 7.7:</b> Representative graph showing the response of <i>P. falciparum</i> 3D7 clone to purine analogues .....	<b>178</b>
<b>Figure 8.1:</b> Model of purine uptake into intraerythrocytic <i>P. falciparum</i> trophozoites....	<b>187</b>

## List of Recent Publications

**Quashie N.B.**, Dorin-Semlat D., Bray P., Biagini G., Doerig C., Lisa C. Ranford-Cartwright L., de Koning H.P. (2008) A comprehensive model of purine uptake by the malaria parasite *Plasmodium falciparum*: identification of four purine transport activities in intraerythrocytic parasites. *Biochem J.* **411** (287–295)

Dorin-Semlat, D., **Quashie, N.**, Halbert, J., Sicard, A., Doerig, C., Peat, E., Ranford-Cartwright, L., & Doerig, C. (2007) Functional characterization of both MAP kinases of the human malaria parasite *Plasmodium falciparum* by reverse genetics. *Mol. Microbiol.* **65**, 1170-1180.

Gudin, S., **Quashie, N.B.**, Candlish, D., Al Salabi, M.I., Jarvis, S.M., Ranford-Cartwright, L.C., & de Koning, H.P. (2006) *Trypanosoma brucei*: a survey of pyrimidine transport activities. *Exp. Parasitol* **114**, 118-125.

**Quashie, N.B.**, de Koning, H.P., & Ranford-Cartwright, L.C. (2006) An improved and highly sensitive microfluorimetric method for assessing susceptibility of *Plasmodium falciparum* to antimalarial drugs in vitro. *Malar. J.* **5**, 95.

## Acknowledgements

I wish to sincerely thank my supervisors, Drs Lisa Ranford-Cartwright and Harry de Koning for their genuine support in diverse ways throughout my PhD program. There would not have been any better supervision than that offered by this pair!

My sincere thanks goes to Dr Dominique Dorin-Semblat of INSERM U609, Wellcome Trust centre for Molecular Parasitology for her advice on molecular techniques including her personal interest in my project, not forgetting the gentle smile and encourage I constantly received from her boss, Prof Christian Doering. I am also grateful to Dr Pat Bray of the Liverpool School of Tropical medicine for his technical advice on transport assays. The advice and suggestions received from my assessor, Prof Jeremy Mottram, are very much appreciated.

The Government of Ghana provided financial support for my PhD training through the GETFUND. I thank the University of Ghana Medical School for encouraging me to undertake the PhD program.

My profound gratitude goes to Liz Peat for her excellent technical support for the entire period of my laboratory work. Fiona McMonagle and Dorothy Armstrong are also acknowledged for their technical support. I wish to thank Boris Rodenko and Denise Candlish for being the first to introduce me to the transport assays. I appreciate the help and support of all my colleagues in GBRC especially Anne, Matt, Pius, Mohammed, Hassan, Nasser, Charles, Georgina, David and the many others.

Finally, I would like to thank my daughter, Ama Palm Quashie who suffered long neglect as a result of the PhD programme. I sincerely thank my friend, Nancy who became my wife in the course of the programme, for all that she has been to me. I take this opportunity to express my profound gratitude to my mother for her constant support even at this stage of my life. I also thank my sister, Mrs Elizabeth Quaynor for the encouragement through the frequent phone calls she made to Glasgow, not forgetting the support I received from the other members of my family.



## Dedication

This thesis is dedicated to my daughter, **Ama Palm Quashie** and the **One Unborn**

## **Declaration**

This thesis and the results presented in it are entirely my own work.

**Neils Benjamin Quashie**

## Abbreviations

μCi	Micro Curie
μg	Microgram
μl	Microlitre
μM	Micromolar
Ade	Adenine
Ado	Adenosine
AP	Alkaline Phosphatase
BLAST	Basic Local Alignment Search Tool
bp	Base Pair
BSA	Bovine Serum Albumin
BCP	Benzothiocarboxypurine
CO <sub>2</sub>	Carbon dioxide
CQ	Chloroquine
dATP	Deoxyadenosine Triphosphate
dTTP	Deoxythymidine Triphosphate
dGTP	Deoxyguanosine Triphosphate
dCTP	Deoxycytidine Triphosphate
DEPC	Diethylpyrocarbonate
dNTP	Deoxynucleotide Triphosphate
DMSO	Dimethyl Sulphoxide
DNA	Deoxyribonucleic Acid
DNase	Deoxyribonuclease
dsDNA	Double stranded DNA
DTT	1,4-dithio-DL-threitol
<i>E. coli</i>	<i>Escherichia coli</i>
EDTA	Ethylenediamine tetraacetic acid
ENT	Equilibrative nucleoside transporter
g	Gram
HCl	Hydrochloric acid
Hypx	Hypoxanthine
IC <sub>50</sub>	50% Inhibitory Concentration
Kb	Kilo base

KCl	Potassium Chloride
kD	Kilo Dalton
K <sub>M</sub>	Michaelis Menten constant
KO	Knock Out
L	Litre
LB	Luria-Bertani
M	Molar
mg	Milligram
MgCl <sub>2</sub>	Magnesium Chloride
mRNA	Messenger RNA
N <sub>2</sub>	Nitrogen
NaCl	Sodium chloride
NAD	Nicotine Adenine Dinucleotide
NADP	Nicotine Adenine Dinucleotide Phosphate
NaHCO <sub>3</sub>	Sodium bicarbonate
nM	Nanomolar
NTP	Nucleotide 5' Triphosphate
O <sub>2</sub>	Oxygen
OD	Optical Density
PBS	Phosphate Buffered Saline
PCR	Polymerase Chain Reaction
RBC	Red Blood Cell
PCV	Packed cell volume
PPP	Pentose Phosphate Pathway
QBC	Quantitative Buffy Coat
RNA	Ribonucleic Acid
SDS	Sodium Dodecyl Sulfate
SOC	Super Optimal broth-Catabolite repression
SSC	Sodium Chloride- Sodium Citrate
ssDNA	Single stranded DNA
T	Thymine
TAE	Tris-acetate EDTA
TBE	Tris-borate EDTA
TCA	Trichloroacetic acid
TE	Tris-EDTA

---

$T_m$	Melting point temperature
TRIS	2-amino-2-hydroxymethyl-1, 3-propanediol
UV	Ultra Violet
V	Volts
$V_{max}$	maximum velocity
WHO	World Health Organisation
$\alpha$	Alpha
$\beta$	Beta
$\gamma$	Gamma
$\lambda$	Lambda

## **CHAPTER ONE**

### **1 General Introduction**

## 1.1 Background to the study

Malaria, caused by protozoan parasites of the genus *Plasmodium*, is responsible for a significant proportion of the recorded morbidity and mortality, especially among children living in the tropics and subtropical areas of the world (Gubler, 1998;WHO, 2005). Of the four species of *Plasmodium* that infect humans, *Plasmodium falciparum*, *Plasmodium malariae*, *Plasmodium vivax* and *Plasmodium ovale*, the first is the most virulent ((WHO, 2005). It must, however, be added that reports from recent studies indicate that non-human primate plasmodia are the source of malaria outbreaks among humans in some parts of the world. In this regard, the groups of Kanbara and Conway have described cases of naturally acquired infection with *Plasmodium knowlesi* in Thailand and Malaysia respectively (Jongwutiwes *et al*, 2004;Singh *et al*, 2004).

Chemotherapy remains the mainstay of malaria control; however the malaria parasites, especially *P. falciparum*, have developed resistance to most of the antimalarial drugs currently available.(White, 2004). Resistance of *P. vivax* to chloroquine has also been reported (Rieckmann *et al*, 1989;Baird *et al*, 1991). The emergence and spread of *P. falciparum* parasites resistant to antimalarial drugs limits the treatment of the disease and makes its management difficult. This situation calls for the prompt identification and development of new antimalarial drugs. Unlike pyrimidine (which could be synthesised from glutamine and bicarbonate), the malaria parasites are incapable of *de novo* synthesis of the purine ring and have to depend on uptake of preformed purines from the host milieu through transporters. The salvage mechanism of purine has therefore become a target for novel antiplasmodial compounds (Gero *et al*, 2003;Joet *et al*, 2003). The identification and selection of appropriate inhibitors and cytotoxic compounds as antiplasmodial agents will depend on the detailed knowledge of the kinetic characteristics of the purine transporters. It is, therefore, an objective of this study to identify and characterise transporters of purine in *P. falciparum* in order to facilitate a purine-based chemotherapy of malaria.

Prior to this study, two groups of researchers – Carter and co and Parker and co – investigated the characteristics of *P. falciparum* purine transporter expressed in the oocytes of *Xenopus laevis* (Parker *et al*, 2000;Carter *et al*, 2000). Although this first cloning and characterisation in *Plasmodium* of the Equilibrative Nucleoside Transporter (ENT) family was undoubtedly a breakthrough, the discrepancies between their findings caused some controversy. With regard to substrate affinities, the *K<sub>m</sub>* for adenosine was determined as

13 and 320  $\mu\text{M}$  by the groups of Ullman (Carter *et al*, 2000) and Baldwin (Parker *et al*, 2000) respectively. In terms of substrate specificity, Parker and colleagues demonstrated the uptake of nucleobases such as hypoxanthine, whereas the group of Ullman could not measure any uptake of these compounds. Whilst Carter and colleagues reported that the transporter was inhibited by 10  $\mu\text{M}$  dipyridamole, a report from the group of Baldwin showed otherwise. Reasons for these significant differences have been hard to find. However, one possible cause of these discrepancies could be the system in which the transporter was expressed, i.e. *Xenopus* oocytes. Though the *Xenopus* oocyte system has been widely used and has yielded highly valuable data on human transporters (Griffith & Jarvis, 1991; Wright *et al*, 2002; Beene *et al*, 2003), yet it is also true, as with any heterologous expression system, that the functional properties of the expressed proteins may be affected by the activities of indigenous proteins (Buyse *et al*, 1997). It is, therefore, possible that the kinetic values reported by the two research groups may not accurately reflect that of the transporters when they exist in their natural location (i.e. the plasma membrane of parasite). Furthermore, the fact that the Plasmodium genome is extremely A+T-rich (Gardner *et al*, 2002) (*PfNT1* is 72% A+T) explains the reported difficulties of expressing other *P. falciparum* ENT genes in this system (Downie *et al*, 2006). Furthermore, in the study by Carter and co, a parasite clone different from that of Parker and Downie studies (W2 and 3D7, respectively), which had a single amino acid difference in their *PfNT1* gene (Leu replacing Phe, at position 385) was used.

Since concern is heightened in the light of the marked differences in the reports of the two groups it became necessary that purine transport be re-assessed using isolated *P. falciparum* parasites and that genes are subsequently matched to known transport activities by reverse genetics. Purine transport into saponin-freed *P. falciparum* trophozoites was therefore investigated in this study, followed by disruption of each of the known *P. falciparum* ENT genes.



## 1.2 Malaria- The disease burden

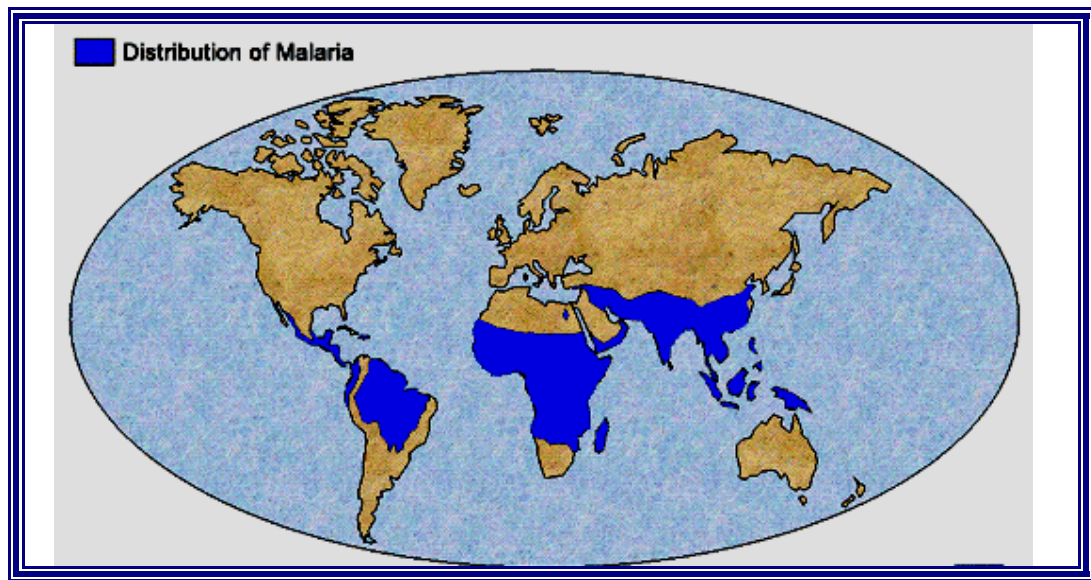


Figure 1.1: Distribution of Malaria in the world as at April 2004.

The deep blue colour indicates *P. falciparum* malaria endemic countries of the world. Reproduced with permission from the Centre for Disease Control (<http://www.cdc.gov/malaria/impact>).

According to a World Health Organization report, an estimated 350 to 500 million clinical cases of malaria occur each year, resulting in more than 1 million deaths (WHO, 2005). Over 80% of these deaths occur among children living in sub-Saharan Africa. Globally, an estimated 40% of the world's population are at risk of the disease in about 90 countries (see Figure 1.1). *Plasmodium falciparum* is responsible for about 95% of malaria deaths worldwide and has a mortality rate of 1-3% (WHO, 2005).

The wide variation in the burden of the disease between different regions of the world has been attributed to several factors, such as the 'variation in parasite species, differences in levels of socio-economic development and differences among the vulnerable groups in different parts of the world' (WHO, 2005). *Plasmodium falciparum*, the most virulent of the different species of the parasite affecting human, is usually a common species in Africa south of the Sahara, hence the reported high incidence of malaria from this area. The climatic conditions in this part of the world favour the growth and multiplication of Anopheles mosquitoes, the vector responsible for transmission of the parasites (CDC, 2004). At temperatures below 18°C (66°F), development of *P. falciparum* in the mosquito is retarded such that the intrinsic period in the vector exceeds the longevity of the insect

(Patz & Olson, 2006). *P. vivax* can, however, grow and multiply even at lower ambient temperatures, giving it a wider geographical range extending into the temperate regions. Socio-economic determinants such as ‘poverty, quality of housing and access to health care and health education, as well as the existence of active malaria control programmes’ among others could influence malaria transmission (WHO, 2005). It is obvious that poorer countries are likely to suffer the brunt of the disease, mostly because of the limited resources to combat the disease. The proportion of the vulnerable groups in different regions of the world where malaria transmission is stable may also contribute to the observed variation in the disease burden.

### 1.3 Economic burden of malaria

In addition to the high burden of mortality and morbidity, malaria severely limits productivity in most disease-endemic countries of the world. A report by Gallup and Sachs indicated that the disease imposes substantial costs to governments as well as families within the communities of the world (Gallup & Sachs, 2001). The economic burden on society, according to the report, takes the form of drugs purchased for home management of malaria, expenses incurred in travelling for treatment at clinics and hospitals, lost days of work, and children’s absence from school. Other effects of the disease mentioned in the report include expenses for preventive measures and expenses for burial in case of deaths.

A survey conducted in six sub-Saharan African countries indicated that the cost of vector control through the use of mosquito coils, aerosol sprays, treated bed nets and mosquito repellents ranged between US\$ 0.05 and US\$ 2.08 per person per month (Shepard *et al*, 1991). The report also revealed that ‘on average, a family of five spends US\$ 55 annually on disease prevention alone and between US\$ 0.39 and US\$ 3.84 per person on its treatment’ (Shepard *et al*, 1991; Russell, 2004). Globally, about US\$1800 million is spent annually on both the direct costs (prevention and control) and on indirect cost such as loss to productivity and time costs (Foster S & Phillips M, 1998; Malaney *et al*, 2004).

## 1.4 Life cycle of the malaria parasite

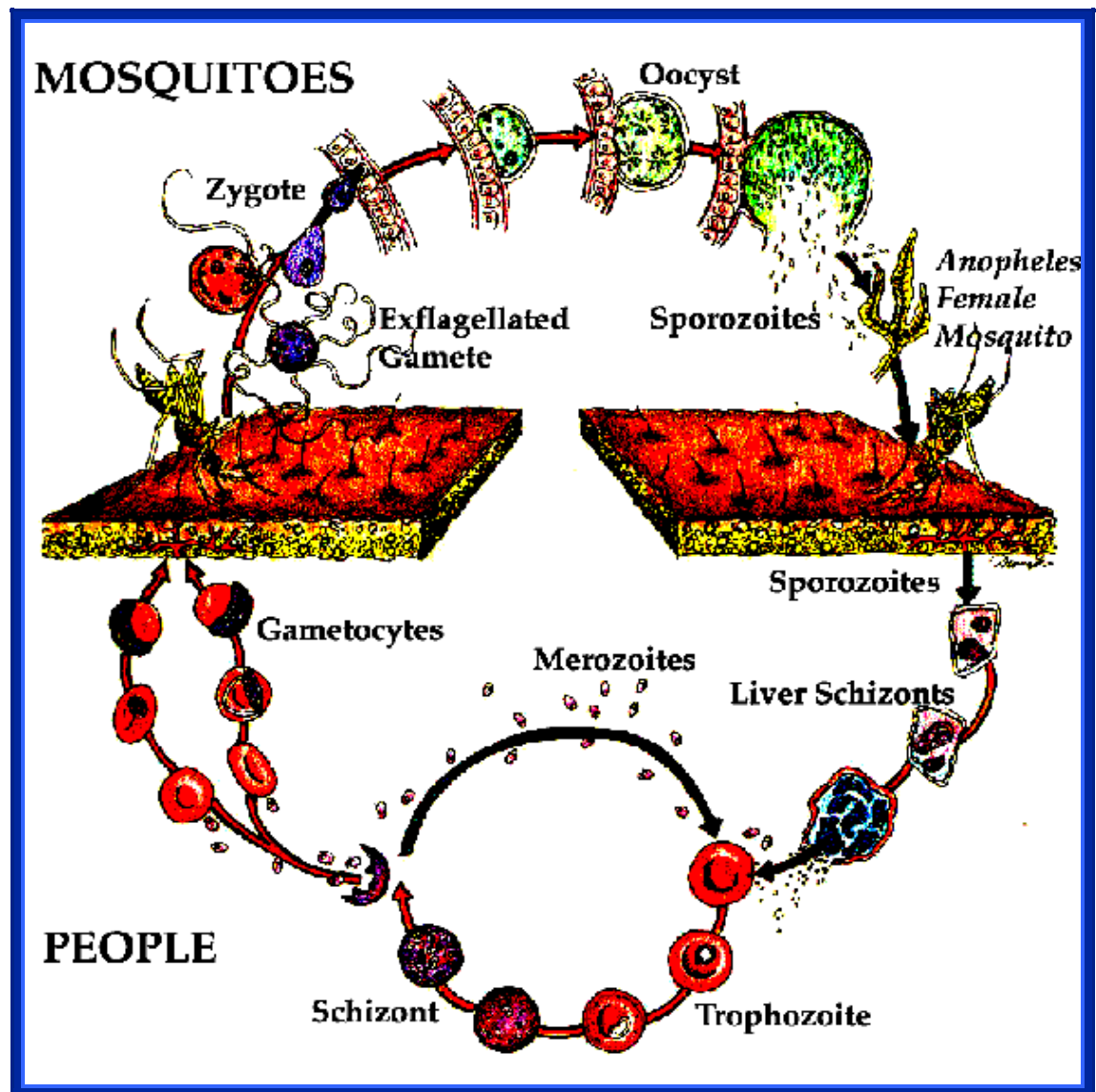


Figure 1.2: The life Cycle of *P. falciparum* Malaria Parasite.

(Reproduced with permission from: <http://www.malariatest.com/cycle>).

The life cycle of *Plasmodium* is complex and specific to the parasite species. The life cycle of *P. falciparum* infection is shown in Figure 1.2 and described below. Malaria parasites are transmitted to human when, in the course of taking a blood meal, an infected female *Anopheles* mosquito injects infectious sporozoites contained in its salivary glands into the peripheral circulation (Carucci *et al*, 1998). The sporozoites immediately invade the liver hepatocytes and undergo rounds of asexual multiplication over the next 5-7 days, producing thousands of merozoite forms of the parasite. When the infected hepatocyte ruptures, the merozoites are released into the peripheral circulation and they quickly invade

the red blood cells (RBC). It has been reported that after the invasion of the RBCs, the parasites (ring forms) seemly lie dormant for up to 15 hours(Kirk, 2001). After this period, there is a rapid increase in metabolic and biosynthetic activities within the infected cell whilst the parasites develop from the trophozoite to reach the schizont stage, which occurs at 36 hours post-invasion. The schizont matures fully within the next 12 hours (approximately 48 hours post invasion). At this stage the parasite (schizont) has divided to produce 16–20 daughter cells (merozoites). It is worth noting that this part of the lifecycle is 72 hours for *P. malariae*. Upon the rupture of the erythrocyte, the released merozoites re-invade other RBC to carry on with the asexual erythrocytic cycle. It is the synchronous release of merozoites and toxic metabolic waste into the blood stream that causes the periodic fever associated with malaria. Some merozoites do not begin the divisions of schizogony, but rather differentiate into male (microgametocyte) and female (macrogametocyte) sexual forms (Figure 1.2). These sexual forms are then taken from the bloodstream by a feeding female *Anopheles* mosquito and fertilise in the mosquito midgut to form zygotes. The zygotes differentiate into motile forms, called ookinetes, which then migrate through the mosquito gut wall to form oocysts on the external gut wall. Replication occurs within the oocyst on the gut wall to form thousands of sporozoites. The infective sporozoites are released into the mosquito haemocoel and move to the salivary glands, where they await injection into another human host and thereby complete the life cycle. It must also be noted that with an infection with *P. vivax*, there are occasions where some of the invaded sporozoites do not immediately grow and divide after entering the hepatocyte, but rather remain in a dormant, hypnozoite stage for weeks or months. This may lead to relapse malaria, which is mostly found associated with *P. vivax* infections.

## 1.5 Manifestation of malaria

Clinical symptoms of malaria caused by an infection of *P. falciparum* manifest in many forms, some of which mimic other diseases such as typhoid, meningitis and gastroenteritis. The age, immune status, intensity of transmission and the *Plasmodium* species most often determine the symptoms. According to a WHO report, the disease shows flu-like symptoms with a rapid increase in temperature for those living in non-endemic areas (WHO, 1990). In disease-endemic areas, the symptoms are modified by immunity and the associated fever is often intermittent, occurring with periodicity (WHO, 2005). It has been observed that, particularly in children, the fever is variable with no periodicity. Other

manifestations of the disease observed in children are pallor, nausea, vomiting and refusal of feeds, lethargy, restlessness, headache, diarrhoea and cough (WHO, 2005). Severe forms of malaria, which are mostly associated with an infection with *P. falciparum*, include vomiting, diarrhoea, cerebral malaria, severe anaemia, algid malaria, hepatic-renal syndrome and black water fever among others (WHO, 2005).

## 1.6 Laboratory diagnosis of malaria

Direct microscopic examination of intracellular parasites on Giemsa's-stained blood films is currently the gold standard for definitive diagnosis of malaria (WHO, 2005). Laboratory diagnosis of malaria by microscopy has many advantages over the other available methods, as it allows for quantification of parasite density and also for differentiation of the species (Bloland, 2001). Distinction between the sexual forms of the parasite (gametocytes) and the asexual forms is also possible with this method. However a major limitation of microscopy is that it can give false negative results if the blood smear is made when *P. falciparum* parasites are at trophozoites or schizont form, since these parasites are sequestered in the vessels of the internal organs and are not present in peripheral blood

Fluorescent microscopy can also be used for laboratory diagnosis of malaria. Methods employed under this include the quantitative buffy coat (QBC) method (Baird *et al*, 1992; Benito *et al*, 1994), the Kawamoto acridine orange method (Kawamoto, 1991), and the Benzothiocarboxypurine (BCP) method (Makler *et al*, 1991; Cook, 1992). Fluorescence microscopy has the advantage of providing rapid results but the equipment and reagents required are considerably more expensive than for light microscopy.

Molecular diagnostic techniques such as Polymerase Chain Reaction (PCR) have also been developed for the identification of the presence of the malaria parasite in biological samples such as the blood (Vu *et al*, 1995). In this method, two primers, flanking the target sequence, and Taq polymerase, are used in successive cycles of DNA denaturation and extension to generate many copies of the target sequence. The genes mostly targeted in *P. falciparum* are the merozoite surface protein-1 (MSP1), merozoite surface protein-2 (MSP2) and glutamine rich protein (GLURP). The amplified gene can be detected using internal probes (for which there are many types) or by gel electrophoresis. Although this technique is expensive and requires an expert to perform, it is very sensitive and highly

specific. This method is not used routinely in the diagnosis of malaria in disease endemic areas of the world.

The recently developed Rapid Diagnostic Tests (RDTs) uses rapid immuno-chromatographic techniques to detect specific antigens produced by malaria parasites that are present in the blood of infected or recently infected individuals. Whilst some RDTs can detect the presence of only *P. falciparum*, others can detect the presence of the other species of Plasmodium. The most commonly used tests detect the *P. falciparum* histidine-rich protein-2 (pHRP-2) and the parasite lactate dehydrogenase (pLDH) (Howard *et al*, 1986). These two antigens are present in the blood of infected people during the asexual stages of the parasite. The tests are rapid, simple to perform and have good detection limits. However a disadvantage of the method is that parasite antigen continues to circulate after the infection has been cleared, for example by chemotherapy, which can lead to false positives.

## 1.7 Chemotherapy of Malaria

Antimalarial drugs can be classified into two broad groups of compounds, namely blood schizonticides and tissue schizonticides. Blood schizonticides kill the erythrocytic stages of the parasite within the red blood cells whilst tissue schizonticides destroy the liver stages of the parasite (Black *et al*, 1986). Some of the common antimalarial drugs belonging to these classes are discussed in the next sub-sections of this thesis.

### 1.7.1 Chloroquine

Chloroquine, a potent blood schizonticidal drug, is effective against all asexual forms of the malaria parasites (Black *et al*, 1986). The drug is also effective against gametocytes of *P. vivax*, *P. malariae*, and *P. ovale*. The mechanism of action of chloroquine remains unclear. Being a weak base, the drug may concentrate in the acidic lysosome of the parasites. It has been reported that chloroquine interferes with the parasite's metabolism of haemoglobin (Ward, 1988). Haeme (ferriprotoporphorin IX), a by-product of haemoglobin digestion, is very toxic to the parasite and is converted by polymerisation in the food vacuole to harmless haemozoin. Chloroquine is thought to exert its antimalarial effect by preventing the polymerization of the toxic haeme released during the proteolysis of

haemoglobin leading to the accumulation of the toxic free haeme, which eventually kills the parasite. The mechanism of this blockade has not been established.

Chloroquine was the drug of choice in many disease endemic countries for the treatment of uncomplicated malaria and for chemoprophylaxis until the late 1950s when *P. falciparum* parasites that are resistant to the drug emerged and spread throughout the world. The drug is now not recommended for treatment of *P. falciparum*, but is still effective against the other 3 species of malaria, although there have been reports of resistance in *P. vivax* (Rieckmann *et al*, 1989; Baird, 2004).

### 1.7.2 Sulphadoxine/pyrimethamine (SP)

Sulphadoxine/pyrimethamine (SP), marketed under the trade name Fansidar<sup>®</sup>, is a blood schizonticide with fixed-dose combination of 500 mg sulphadoxine and 25 mg pyrimethamine. Both drugs are antifolates and interfere with the synthesis of thymidylate in the parasite. Sulphadoxine competes with para-aminobenzoic acid (PABA) for binding to the enzyme dihydropteroate synthase in the synthesis of dihydropteroate, an essential compound needed for folic acid synthesis (Hyde, 2002). Pyrimethamine inhibits the actions of dihydrofolate reductase, which is necessary for folic acid synthesis in the parasite (Black *et al*, 1986). When both drugs are combined, synergy occurs making the combination drug more efficacious than the monotherapy drugs (Chulay *et al*, 1984).

### 1.7.3 Quinine

Quinine, which is found in the bark of the American cinchona tree, is also a blood schizonticide. Quinine is used for the treatment of severe forms of malaria in most disease endemic areas. The drug, which is reported to destroy the trophozoite stage in the erythrocytes, has no effect on the exo-erythrocytic stages that develop in the liver or the gametocytic stage. Though the mode of action of quinine is not well understood, it is thought to be similar to that of chloroquine, causing cytotoxicity by inhibiting the polymerisation of haeme into haemozoin, with the consequent built up of free haeme, which is toxic to the parasite (Yakuob *et al*, 1995). Another proposed mode of action is that the drug forms a complex with double-stranded DNA to prevent strand separation or that it blocks DNA replication and transcription.

### 1.7.4 Primaquine

Primaquine, a tissue schizonticide, is a member of the 8 aminoquinoline group of compounds used for treatment of malaria infection especially those caused by *P. vivax* or *P. ovale*. It is used in 'radical cure' to destroy the hypnozoites which are lodged in the liver cells. For effective treatment of such an infection primaquine is usually combined with chloroquine or quinine. Although the mechanism of action of primaquine is not well understood, it is thought to interfere with the electron transport chain in the parasite. Studies in a cell-free assay of protein transport through the Golgi apparatus performed by Hiebsch and his colleagues also showed that primaquine works by inhibiting the formation of functional transport vesicles (Hiebsch *et al*, 1991).

### 1.7.5 Artemisinin or Qinghaosu

Artemisinin, a sesquiterpene lactone, is an ancient Chinese medicine, derived from the plant *Artemisia annua*, which grows in the wild in China and elsewhere. Artemisinin acts on blood schizonts and young gametocytes. Derivatives of artemisinin are artemether, artesunate, arteether and artelinate. These compounds are quickly converted to their active plasma metabolite, dihydroartemisinin, which is the active compound that exhibits the anti-malarial activity (Wilairatana *et al*, 1998). Though the specific mechanism of action of artemisinin is not known, it is thought that the iron in the iron-porphyrin complex (from the breakdown of haemoglobin) 'reduces the peroxide bond in artemisinin generating high-valent iron-oxo species resulting in a cascade of reactions that produce reactive oxygen radicals which damage the parasite leading to its death' (Cumming *et al*, 1997). A 2005 study investigating the mode of action of artemisinin using a yeast model also demonstrated that the 'drug acts on the electron transport chain, generates local reactive oxygen species, and causes the depolarization of the mitochondrial membrane' (Li *et al*, 2005). Due to the short half-life of the derivatives they are recommended for combination with drugs of longer half-life (White, 2004).

Artemisinin combination therapy (ACT) has been shown to be effective in the treatment of chloroquine-resistant malaria (Price *et al*, 1996). ACTs have become the first line antimalarial drug in many malaria-endemic countries, and to date there is no confirmed case of drug resistance.



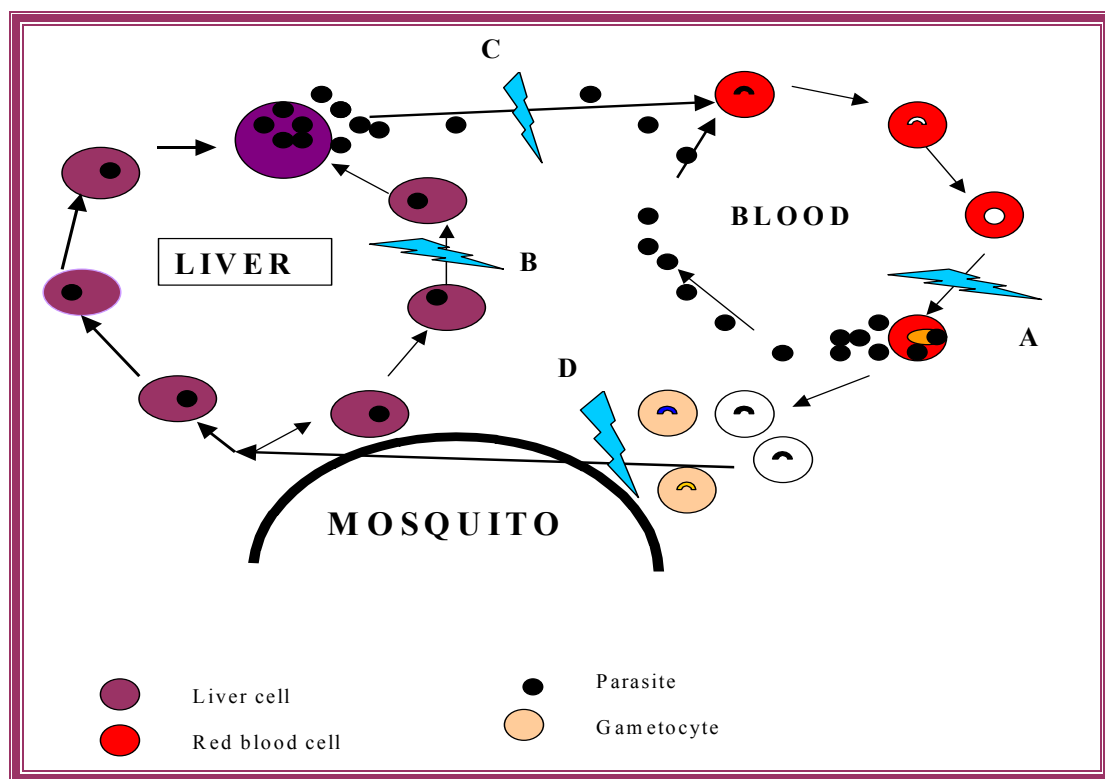


Figure 1.3: Site of action of most of the available antimalarial drugs.

A=site of action of blood schizonticides (eg chloroquine, mefloquine, quinine, sulphadoxine, pyrimethamine) used in the treatment of acute disease; B=site of action of tissue schizonticides (eg primaquine) used for radical cure i.e. to destroy the hypnozoites (*P. vivax* or *P. ovale* infection); C=site of action of most of the common drugs used for chemoprophylaxis (eg chloroquine, mefloquine, pyrimethamine); D=site of action of gametocidal drugs (eg artemisinin).

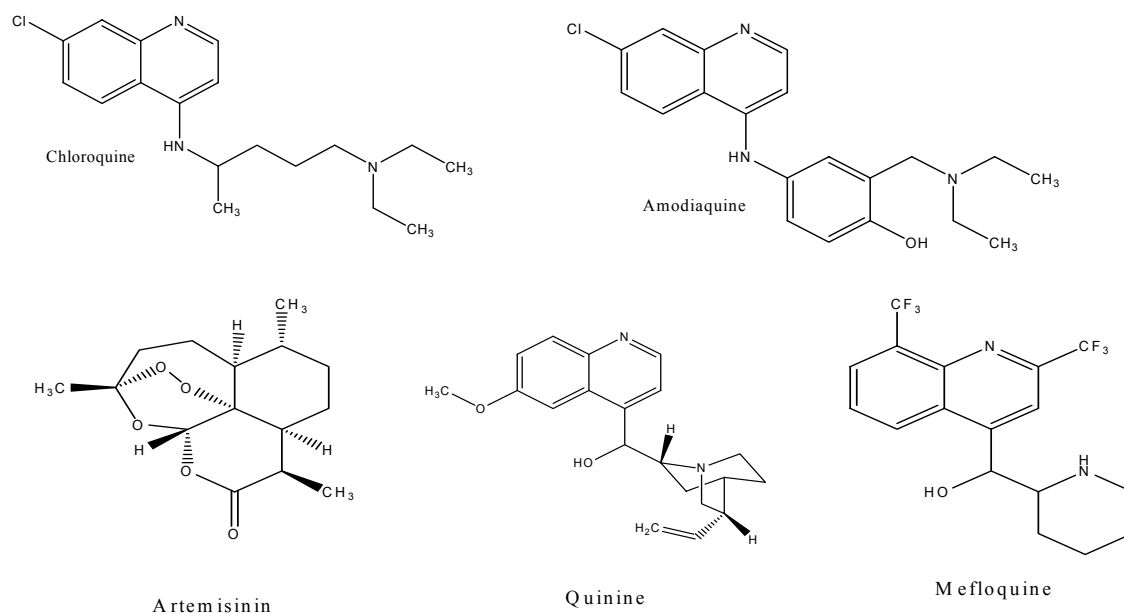
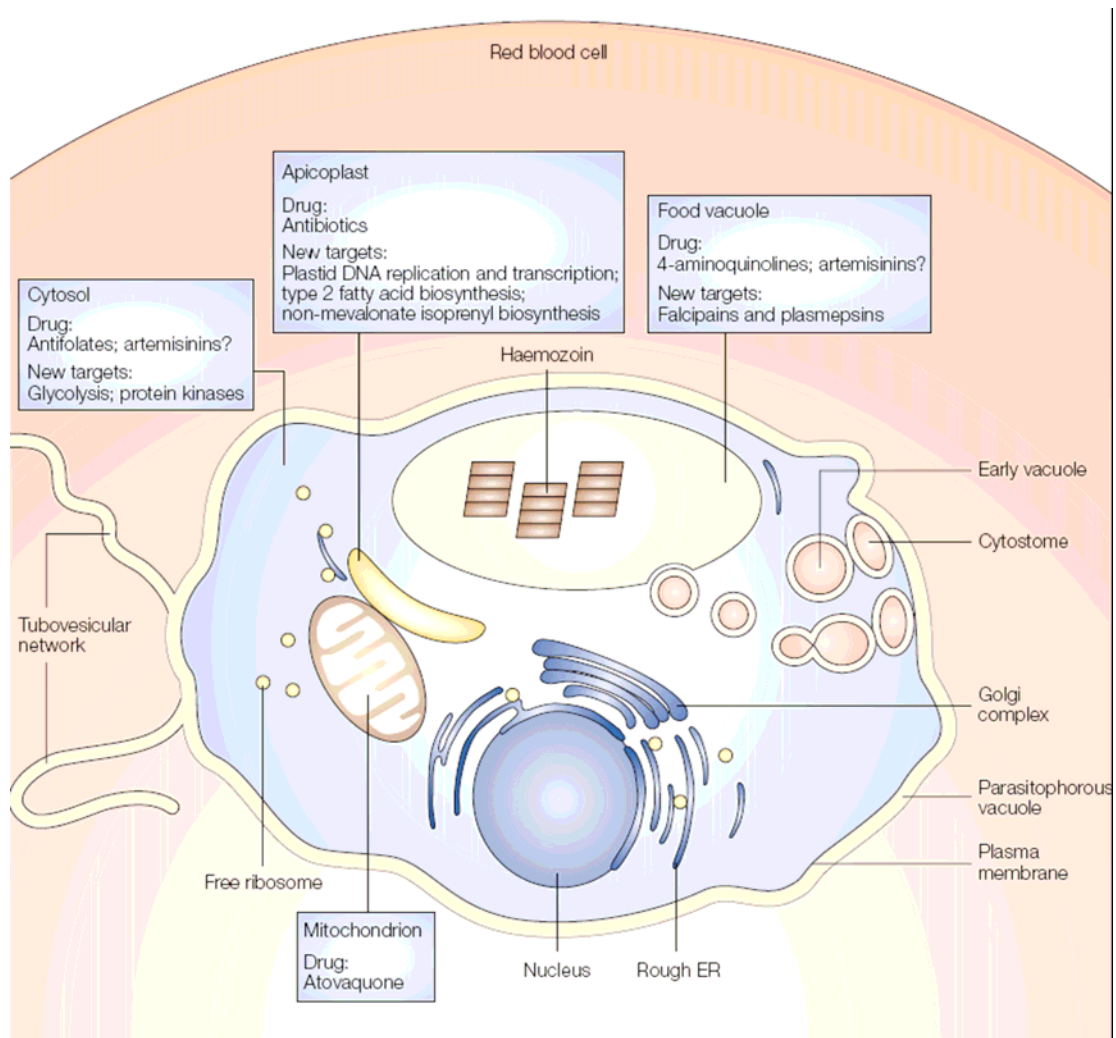


Figure 1.4: Chemical structures of some of the commonly used antimalarial drugs.

A summary of antimalarial drug targets in *Plasmodium* is shown in Figure 1.5



**Figure 1.5: Representation of an intra-erythrocytic *P. falciparum* trophozoite, highlighting key parasite intracellular compartments and the site of action of some of the major classes of antimalarial drugs.**

(Reproduced with permission from Fidock *et al.*, 2004).

## 1.8 Resistance to Antimalarial Drugs

*P. falciparum* has developed resistance to most of the available antimalarial drugs (White, 2004). This situation is a major public health problem, hindering the control and treatment of the disease. Antimalarial drug resistance is defined as the ‘ability of a parasite strain to survive and multiply despite the administration and absorption of drug given in doses equal to or higher than those usually recommended but within the tolerance level of the subject’ (Bruce-Chwatt, 1986). Resistance to the major antimalarial drug, chloroquine, was

believed to have emerged in 1957 both in Colombia and along the then Cambodia-Thailand border area (Moore & Lanier, 1961). However it was not until 1960 that resistance in these areas was confirmed (Moore & Lanier, 1961; Payne, 1987). Thereafter, resistance to the drug spread throughout Southeast Asia in the 1970s (Chongsuphajaisiddhi *et al*, 1979). The first observation of the parasite's resistance to the drug in Africa was made in East Africa (Tanzania) in 1977 (Payne, 1987; Payne, 1988). From East Africa, resistance to the drug spread throughout the continent. The worldwide distribution of parasites resistant to chloroquine is shown in Figure 1.6. Several factors have contributed to the rapid development and spread of parasite resistance, including human behaviour, vector and parasite biology, pharmacokinetics and economics (Bloland, 2001).

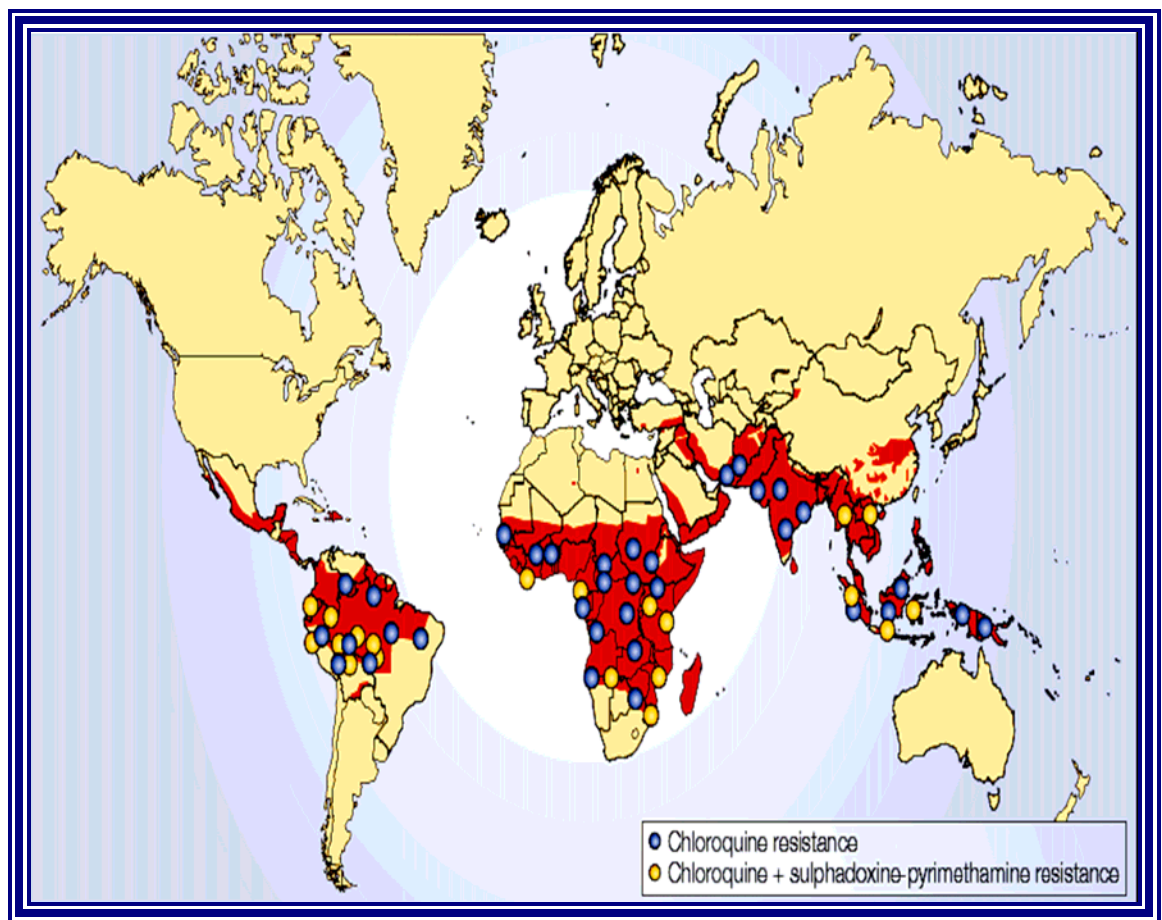


Figure 1.6: The global distribution of malaria.

The global distribution of malaria (in red) showing areas where *Plasmodium falciparum* resistance to the most commonly used antimalarial drugs, chloroquine and sulphadoxine-pyrimethamine, has been documented (Reproduced with permission from Fidock *et al.*, 2004).

## 1.9 Vaccines to combat malaria?

A vaccine against malaria is an important option for the control or elimination of malaria in disease endemic countries of the world, and progress has been made in the development of an effective vaccine, although there is currently no vaccine clinically available.

According to Gardiner and colleagues, there are three separate but overlapping approaches in malaria vaccine development (Gardiner *et al*, 2005). The first is a pre-erythrocytic vaccine that would act in a way to prevent the invasion of hepatocytes by the sporozoites injected from the mosquito during a blood meal. The second is a blood-stage vaccine that would prevent development of the disease, especially in vulnerable groups such as children and pregnant women. The third is a transmission blocking vaccine that would prevent the parasites from developing in the mosquito and thereby stop transmission of the disease.

A report by the Malaria Vaccine Initiative (MVI) indicates that ‘each malaria infection presents thousands of antigens to the human host immune system and understanding which of these antigens is important and thus a useful target for vaccine development has been a difficult task’ (MVI, 2006 [<http://www.malariavaccine.org>]). It is on record that the parasite goes through different stages in its lifecycle and at each point it presents a different subset of molecules for the immune system to combat, making the selection of a single antigen for vaccine development difficult (MVI, 2006).

The presence of ‘multiple infections comprising different species and strains of parasites in a single episode of the disease also pose a challenge to the development of an effective vaccine’ (MVI, 2006). Notwithstanding these difficulties, some antigens have been identified and are currently receiving attention in vaccine development (Figure 1.7)

Results from the field trial of a malaria vaccine named RTS, S/AS02A in Mozambique showed a promising outcome. The outcome indicates a reduction in the risk of malaria infection among children by 30% (Alonso *et al*, 2004). Additionally, the vaccine, which carries two proteins, RTS and S, recognised by the immune system reduced the risk of young children developing severe malaria by 77%. Bojang and his colleagues also carried out a randomised trial of the efficacy of RTS, S/AS02A against natural *P. falciparum* infection in semi-immune Gambian men (Bojang *et al*, 2001). The estimated efficacy of

the vaccine during the first nine months of follow up was reported as 71% (Bojang *et al*, 2001).

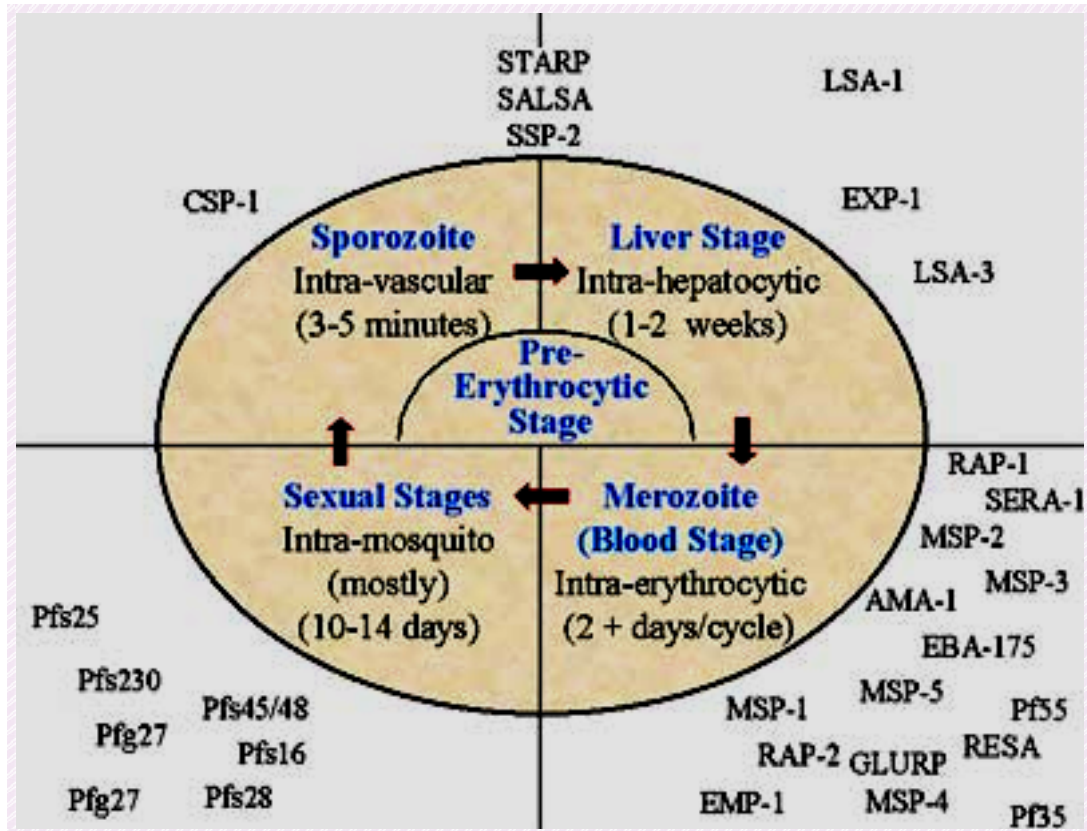


Figure 1.7: Antigens listed according to the stage in which they would be expected to provoke a protective immune response.

Reproduced with permission from Malaria Vaccine Initiative (MVI)  
<http://www.malariavaccine.org/mal-vac2-challenge.htm#Top>.

## **1.10 Search for novel antimalarial drugs: purine transporters as a potential chemotherapeutic target**

The emergence and spread of *P. falciparum* parasites resistant to currently available antimalarial drugs calls for an immediate identification and development of novel antiplasmodial compounds. Compounds that take advantage of the unique metabolic pathways of the parasite are likely to make selective antimalarial drugs. In this respect, purine transporters of the malaria parasite can be considered good targets for novel antiplasmodial drugs. This is because the parasite is unable to synthesise purine *de novo* and has to salvage it from the host through nucleoside/nucleobase transporters (Kirk, 2001). Compounds that would inhibit these transporters could be considered as potential antimalarial drugs, since in the absence or reduction of purine salvage the parasite would be unable to synthesise nucleic acids and many common metabolites and therefore unable to replicate. In this regard, a well-characterised purine transporter will provide information that would facilitate the identification of lead compounds for future drug development. Alternatively, subversive substrates or cytotoxic compounds could be developed for selective delivery into the parasite via these transporters to cause parasite death whilst sparing the host cells.

## **1.11 An Overview of the Biochemistry of Plasmodium**

The intra-erythrocytic stages of the malaria parasite obtain their basic energy needs through the glycolytic pathway (Sherman, 1979). It had been observed that there is more than 75 times utilization of glucose in infected erythrocytes than in non-infected cells (Ginsburg, 1994). The measurement of a high-level activity of lactate dehydrogenase (LDH) in parasitized erythrocytes confirms that the parasite metabolises glucose through glycolysis (Ginsburg, 1994). NAD is also regenerated from NADH in the parasite (Makler *et al*, 1993; Becker & Kirk, 2004). The detection in parasitized erythrocytes of some of the enzymes involved in the pentose phosphate pathway (PPP) indicates that PPP may be operational in the parasites (Sherman, 1979; Ginsburg, 1994). The PPP is likely to be the source of ribose sugar required by the parasite for the synthesis of nucleotides (Sherman, 1979; Ginsburg, 1994). Although the presence of the electron transport chain and oxidative phosphorylation within infected erythrocytes has been reported, there is no evidence to

suggest the existence of the tricarboxylic acid cycle (citric acid cycle) cycle in the parasite (Uyemura *et al*, 2000).

Malaria parasites obtain most of their supply of protein from the ordered degradation of haemoglobin. It has been reported that about 70% of the host cell haemoglobin is digested through a mechanism initiated by the parasite (Rudzinska *et al*, 1965; Krugliak *et al*, 2002). Of this quantity of protein, only 16% is utilized by the parasite to make its own protein (Rudzinska *et al*, 1965; Krugliak *et al*, 2002). Additionally the parasites are capable of *de novo* synthesis of some amino acids and can also salvage some of the host's amino acid (Kirk, 2001; Krugliak *et al*, 2002). Some amino acids such as alanine, aspartate and glutamate can be synthesised by the parasite through the process of carbon fixation (Sherman, 1979). In contrast to a previous report that the parasite excretes most of the amino acids from haemoglobin degradation (Krugliak *et al*, 2002), Liu and co provided evidence showing that the parasites rely on haemoglobin degradation, for all its amino acid supply and parasite growth was enhanced when cultures were supplemented with isoleucine, the only amino acid absent from the haemoglobin (Liu *et al*, 2006).

The malaria parasites require purines for the synthesis of important biomolecules such as DNA and RNA. Since the parasites are incapable of *de novo* synthesis of this important compound, they salvage it from the host (Ginsburg, 1994; Kirk, 2001). The primary purine required by the parasite is reported to be hypoxanthine (Reyes *et al*, 1982). Additionally parasites are able to convert adenosine taken up from the host to hypoxanthine through the process of deamination and dephosphorylation (Reyes *et al*, 1982). This is because *P. falciparum* possessed the purine salvage enzymes: adenosine deaminase, purine nucleoside phosphorylase, hypoxanthine-guanine phosphoribosyltransferase (PRTase), xanthine PRTase and at a lower activity level adenine PRTase and adenosine kinase (Reyes *et al*, 1982). The parasite is able to synthesise its own pyrimidines from bicarbonate and glutamine (Kirk, 2001).

The intraerythrocytic malaria parasite has most of the enzymes involved in the metabolism of glycerides and fatty acids (Matesanz *et al*, 1999; Mitamura & Palacpac, 2003). The parasite can thus synthesise most of its lipid requirement.

The blood-stage malaria parasite possesses a functional vitamin B6 *de novo* biosynthesis pathway (Gengenbacher *et al*, 2006). One of the most important vitamins required by the

parasite is folate, which is used in the replication of parasite DNA. Since the parasite is unable to utilize preformed folate, it synthesises dihydrofolate from GTP, para-aminobenzoic acid and glutamate (Kirk, 2001). Pantothenate, the precursor of coenzyme A, is an essential nutrient for the intraerythrocytic stage of the malaria parasite. Yet it appears that the vitamin is the only one not available in the erythrocytes (Saliba & Kirk, 2001). The parasites, therefore, have to salvage it from the outside milieu through an  $H^+$ -coupled transporter (Saliba & Kirk, 2001). Available evidence suggests that the only vitamin that the parasite does not seem to require is biotin. In support of this, growth of *P. falciparum* in the presence of several biotin antagonists, including avidin has been demonstrated (Geary *et al*, 1985).

## 1.12 Mode of Transport in cells

The lipid bilayer of cell membrane serves as a barrier, controlling the movement of polar molecules across the plasma membrane (Figure 1.8). This allows the cells to maintain concentrations of solutes in their cytosol (Alberts *et al*, 1994).

Transport of inorganic ions and small hydrophilic organic molecules across this barrier is therefore facilitated by specific transmembrane proteins (Alberts *et al*, 1994). The membrane transport proteins have been reported to be 'multipass transmembrane proteins with their polypeptide chains traversing the lipid bilayer multiple times' (Alberts *et al*, 1994). This enables specific hydrophilic solutes to cross the membrane without coming into contact with the hydrophobic interior of the lipid bilayer. The two major membrane transport proteins are carrier protein (permeases or transporters) and channel protein (Alberts *et al*, 1994). Whilst carrier protein binds the solute to be transported and undergoes conformational changes in order to translocate the solute across the membrane, the Channel protein translocates solutes by forming 'hydrophilic pores that extend across the lipid bilayer, which when open allows specific solutes such as inorganic ions to pass through' (Alberts *et al*, 1994). All channel proteins and some carrier proteins are involved in a transport process referred to as passive transport or facilitated diffusion (Figure 1.9) allowing solutes to pass through down their concentration gradient. If the solute is charged a combination of the influence of the electrical gradient and the concentration gradient, referred to as the electrochemical gradient, is the net driving force behind the translocation. In contrast to the above processes is simple diffusion, where solute translocation occurs



freely, down their concentration gradient without the involvement of channel or carrier proteins (see (Figure 1.9) [(Alberts *et al*, 1994)]).

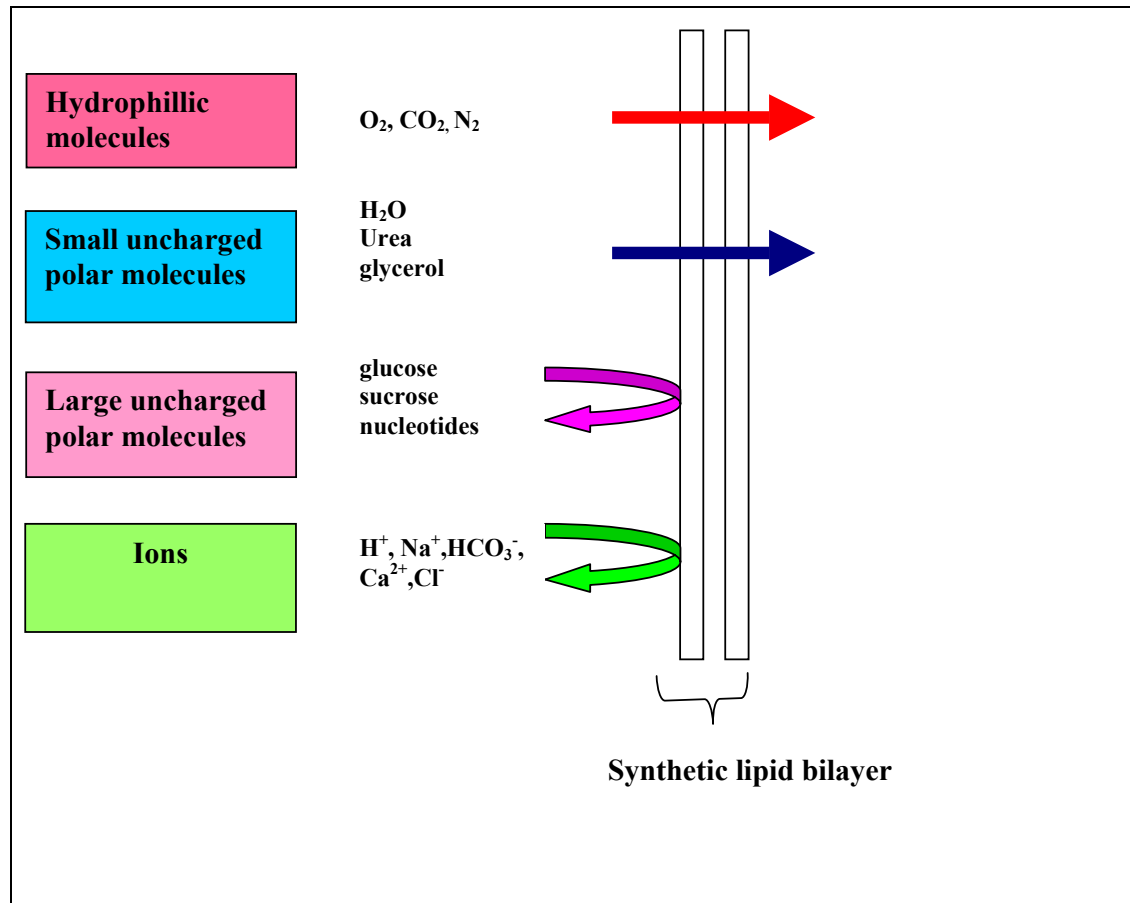


**Figure 1.8:**The relative permeability of the lipid bilayer of cell to different classes of molecules.

The smaller the molecule and the fewer hydrogen bonds it forms with water the more rapidly the molecule diffuses across the lipid bilayer. Redrawn from (Alberts *et al*, 1994).

Active transport, which is mostly mediated by carrier proteins, is a process where solutes are pumped across the membrane against their electrochemical gradient (uphill). This process is coupled to energy (ATP hydrolysis or an ion gradient) [(Alberts *et al*, 1994)].

ABC transporter proteins belong to a super family of transporters each of which contains a highly conserved ATP-Binding Cassette (ABC) [(Alberts *et al*, 1994)]. They mostly function as efflux transporters (Pastor-Anglada *et al*, 2005). One of such class of transporters is the multidrug resistance (MDR) protein, which is implicated in *P. falciparum* antimalarial drug resistance.

Passive and active membrane transport systems exist in protozoan organisms (Tanabe, 1990a; Tanabe, 1990b; Bakker-Grunwald, 1992). Protozoan active transporters are likely to use the proton-motive force whereas mammalian transport uses the sodium gradient across the membrane. Examples of primary active transport are ion pumps and ABC transporters/P-glycoproteins. The latter category is directly implicated in chloroquine resistance.

Uptake of purines in *P. falciparum* is reported to be mediated by facilitated diffusion involving transporters located on the plasma membrane of the parasite (Parker *et al*, 2000; Rager *et al*, 2001).

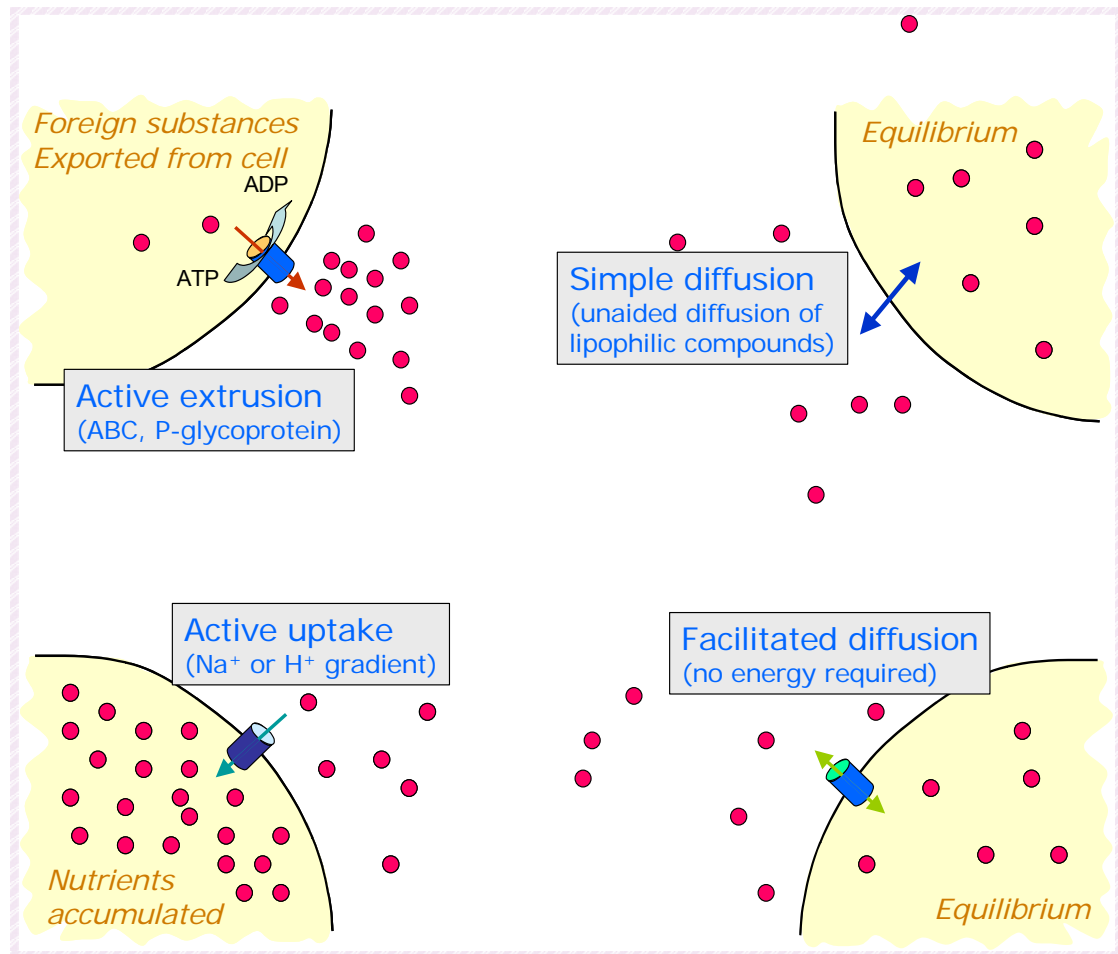


Figure 1.9: Mechanism of transport in cells showing simple diffusion, facilitated diffusion, active uptake and active extrusion of compounds.

Each of these processes is marked appropriately in the figure. The red dots represent the chemical compound being transported and the arrows shows the direction of movement of the compound. The blue cylinders represent the transporter in the plasma membrane of the cell.

## 1.13 Purine transport in human cells

Nucleoside transporters play key roles in the salvage of nucleosides used in biosynthesis of nucleic acids (Baldwin *et al*, 1999) and in regulating endogenous adenosine concentrations in the human central nervous system (Mubagwa & Flameng, 2001). Additionally adenosine is involved in the ‘regulation of blood flow, myocardial slow action potentials, lymphocyte function, glucose metabolism, and neurotransmission’ (Mubagwa & Flameng, 2001; Rosales *et al*, 2004). Even though the effects of adenosine involve a variety of different cells, ‘its action is basically inhibitory in nature and involves the interaction of adenosine with several adenosine-specific receptors on the cell surface, which are coupled to membrane-associated adenylate cyclase’ (Yeung & Green, 1983). Purine transport systems in human cells also mediate the uptake of many synthetic nucleoside analogues used in cancer (and viral) chemotherapy (Sundaram *et al*, 2001).

Mammalian cells possess two major nucleoside transporter families: (i) equilibrative nucleoside transporter (ENT) and (ii) concentrative nucleoside transporter (CNT), which is  $\text{Na}^+$ -dependent (Baldwin *et al*, 2004; Gray *et al*, 2004; Kong *et al*, 2004). In human plasma membrane, transport of nucleosides is brought about by members of ‘the concentrative,  $\text{Na}^+$ -dependent (CNT) and equilibrative,  $\text{Na}^+$ -independent (ENT) nucleoside transporter families’ (Gray *et al*, 2004; Kong *et al*, 2004). ‘CNTs are expressed in a tissue-specific fashion whilst ENTs are present in most, possibly all, cell types’ (Baldwin *et al*, 2004).

As shown schematically in Figure 1.10, ‘the equilibrative transport system mediates nucleoside transport in both directions depending on the nucleoside concentration gradient across the plasma membrane whilst the concentrative transport system is  $\text{Na}^+$ -dependent and the movement of nucleoside, regardless of its concentration gradient, is coupled to that of the sodium ion’ (Podgorska *et al*, 2005).

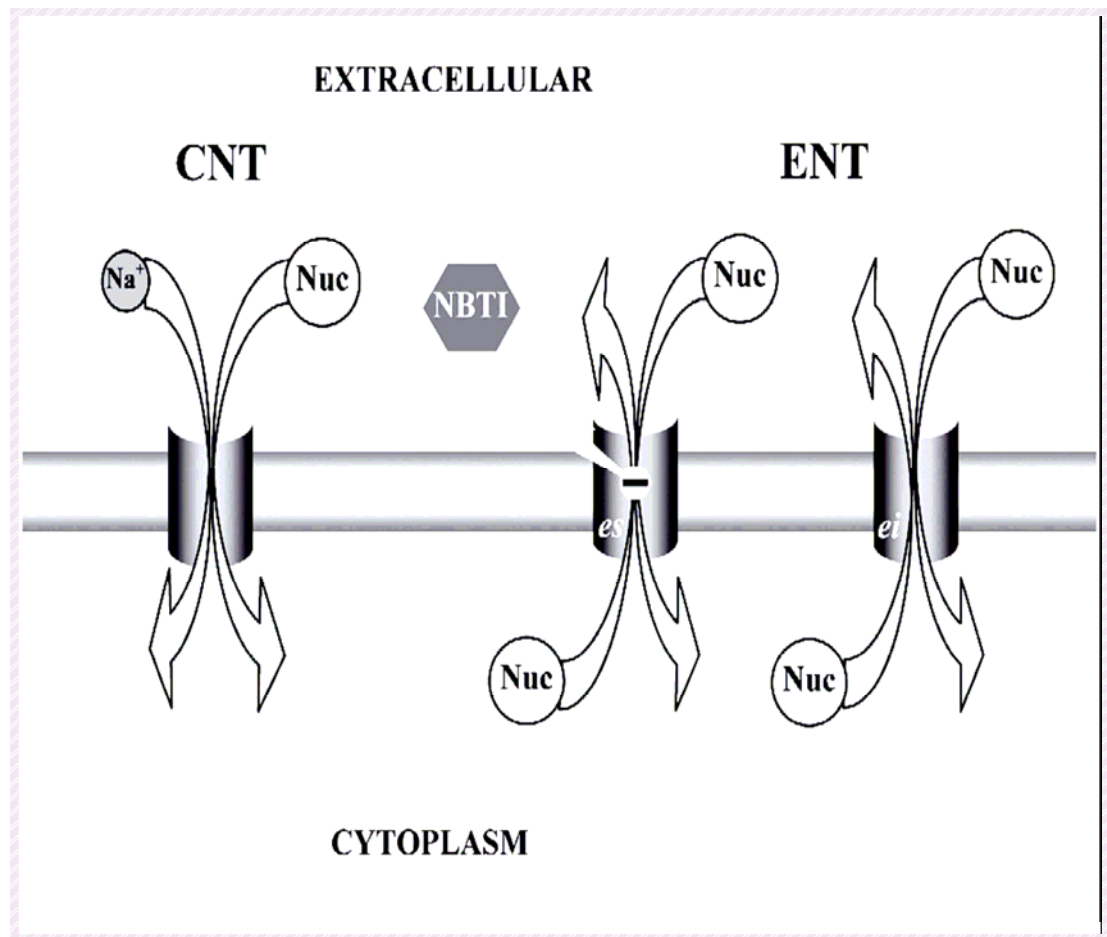


**Figure 1.10: Nucleoside transport mediated by the concentrative nucleoside transporter (CNT) and equilibrative nucleoside transporter (ENT).** There are two types of ENT, NBMPR equilibrative sensitive (es) and equilibrative insensitive (ei). Nuc=nucleoside; NBT1=nitrobenzylthioinosine.

Four nucleoside transporters exhibiting characteristics of members of the equilibrative nucleoside transporter family have been identified. These transport system are reported to be present in various cell types (Podgorska *et al*, 2005). In some cases the number of these transport systems present is determined by the cell and tissue type (Podgorska *et al*, 2005). Although all the transporters are capable of adenosine salvage, however, their ability to transport the other nucleosides and nucleobases varies (Baldwin *et al*, 2004;Kong *et al*, 2004).

The first two of these transporters, designated hENT1 and hENT2, showed different sensitivities to the classical inhibitor, nitrobenzylmercaptapurine ribonucleoside (NBMPR) [(Baldwin *et al*, 2004;Kong *et al*, 2004)]. Although hENT1 and hENT2 salvage a broad variety of nucleoside permeants, reports indicate that hENT2 exhibits relatively lower

affinity for most of the permeants (Baldwin *et al*, 2004; Kong *et al*, 2004). Additionally Yao and her colleagues have shown that unlike hENT1, hENT2 can transport nucleobases (Yao *et al*, 2002). hENT1 have been reported to be equilibrative-sensitive (es) to the NBMPR whilst hENT2 was insensitive (ei) (Crawford *et al*, 1998)).

A study by Baldwin and his colleagues indicated that the ‘topology of hENT3 is slightly different from the other member of the ENT family’ (Baldwin *et al*, 2005). This transporter has a long (51 residue) hydrophilic N-terminal region preceding TM1 that possesses a putative dileucine-based endosomal/lysosomal targeting motif (Baldwin *et al*, 2005). Apart from being a low affinity nucleoside transporter, hENT3 also mediates the uptake of adenine (Baldwin *et al*, 2005).

hENT4 was discovered quite recently and hence its transporting characteristics have not been fully determined. However, indications are that hENT4 has a relatively low affinity for adenosine (Kong *et al*, 2004). Concentrations of exogenous purines in mammalian cells are shown in Table 1.1

Compounds	Purine	Compound	Pyrimidine
	Concentrations (μM)		Concentrations (μM)
Adenine	0.4	Cytosine	15
Adenosine	0.5	Cytidine	0.6
Guanine	97	Uracil	13
Guanosine	0.9	Uridine	52
Hypoxanthine	172	Orotate	<5
Inosine	168	Orotidine	13
Xanthine	20	Thymine	NA
		Deoxythymidine	0.5

Table 1.1: Physiological average concentrations of salvageable purines in mammalian cells or tissues.

(Reproduced from (Traut, 1994).

## 1.14 Purine metabolism in mature uninfected human erythrocytes

Since mature erythrocytes lack a functional nucleus, they have a limited requirement for nucleotides. The mature erythrocyte lacks the enzymes for *de novo* purine and pyrimidine biosynthesis pathways (Gero & O'Sullivan, 1990). However they possess the ability to take up these nutrients from the external environment. The mature non-infected erythrocytes take up nucleosides through the NBMPR-sensitive equilibrative nucleoside transporter (*es*, ENT1)(Plagemann *et al*, 1988), and purine nucleobases through the facilitative nucleobase transporter (FNT1) (Domin *et al*, 1988). Both transporters are located on the plasma membrane of the cell. Hypoxanthine is rapidly transported across the red cell membrane by facilitated diffusion, so that equilibrium is reached rapidly even at millimolar concentrations of the oxypurine (Lassen, 1967). It has been documented that within the cytosol of the matured erythrocyte hypoxanthine is converted to inosine 5-monophosphate (IMP). However this conversion depends on the concentration of inorganic phosphate (Pi) present in the medium (Giacomello & Salerno, 1979): stimulation of 5-phosphoribosyl- 1-pyrophosphate (PRPP), a co-substrate of and rate-limiting step in the phosphoribosylation of hypoxanthine to IMP needs organic phosphate (Giacomello & Salerno, 1979).

Domin and his colleagues used the inhibitor-stop method (using cold 19 mM papaverine as stop solution) to study the transport of purine nucleobase into mature erythrocytes (Domin *et al*, 1988). They reported that adenine ( $K_i = 13 \pm 1 \mu\text{M}$ ), guanine ( $K_i = 37 \pm 2 \mu\text{M}$ ), and hypoxanthine ( $K_i = 180 \pm 12 \mu\text{M}$ ) were mutually competitive substrates for the transporter. They further revealed that transport of the purine nucleobases was not inhibited by nucleosides (uridine, inosine) or by inhibitors of nucleoside transport (6-[(4-nitrobenzyl)thio]-9- $\beta$ -D-ribofuranosylpurine, dilazep, dipyridamole). They therefore concluded that 'all three purine nucleobases share a common facilitated transport system in human erythrocytes which is functionally distinct from the nucleoside transporter'.

Since human erythrocytes lack the ability to convert IMP to AMP, adenosine or adenine have to be converted to adenine nucleotides in order to maintain ATP level within the erythrocyte. There is, therefore, a rapid uptake of adenosine from the extracellular fluid and this probably explains the observation of a low level adenosine concentrations in human blood (generally reported to be less than 1 pM) [(Schrader *et al*, 1983)]. Uptake of adenosine into matured erythrocyte is reported to be predominantly through the equilibrative nucleoside transporter (Plagemann *et al*, 1988). In matured human

erythrocytes, adenosine is usually used as a substrate for adenylate synthesis (Perrett, 1976). The nucleoside can either be phosphorylated to AMP by adenosine kinase, or deaminated to inosine by adenosine deaminase (see Figure 1.11)[(Paglia *et al*, 1986;Rapoport *et al*, 1987)]. Due to the presence of high adenylate kinase activity within the cytosol of the erythrocytes, AMP is rapidly phosphorylated to ATP (Mohrenweiser *et al*, 1981;Beutler, 1983). The physiological concentrations of salvageable purines in mammalian cells or tissues are shown in Table 1.1.

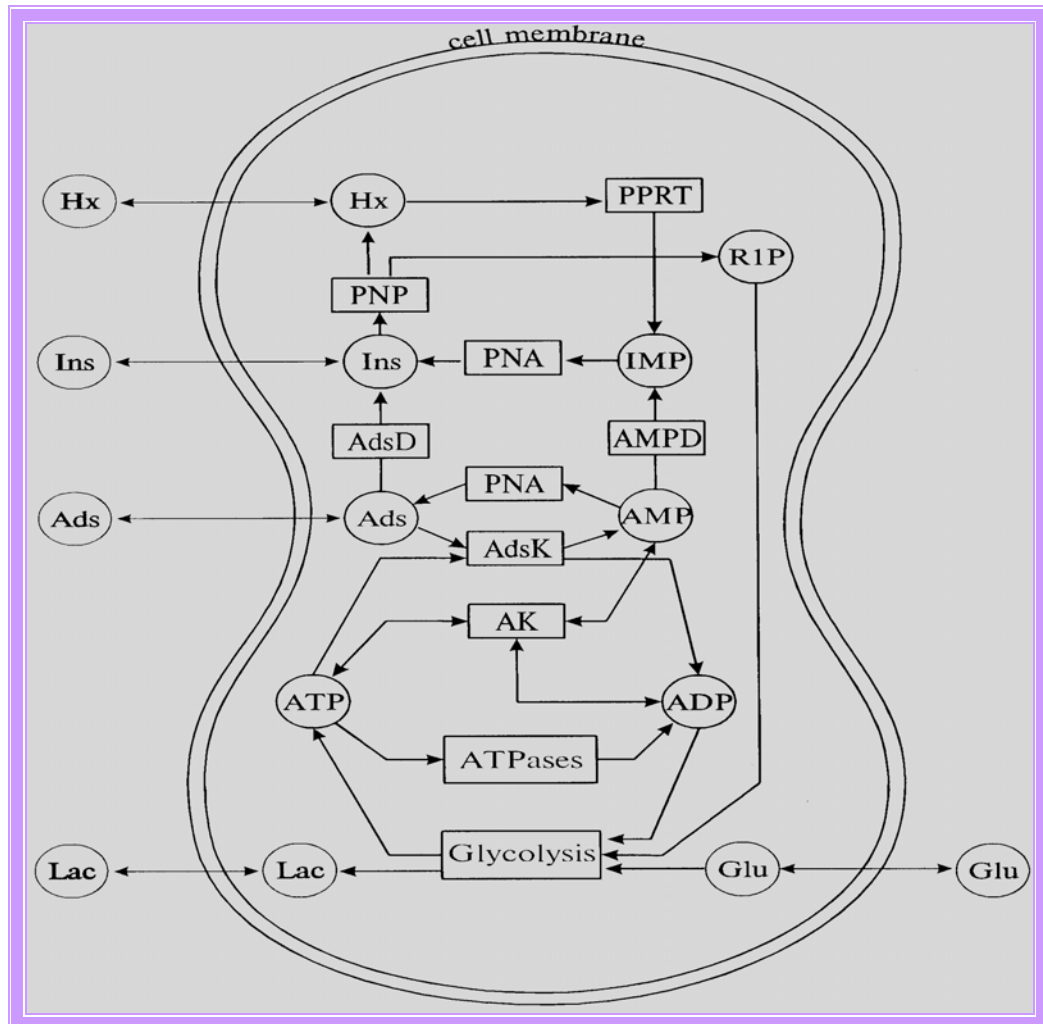


Figure 1.11: Schematic representation of adenosine metabolism in human erythrocytes.

It also shows the relation between metabolism of adenosine and energy. Abbreviations: Ads, adenosine; AMP, adenosine monophosphate; ADP, adenosine diphosphate; ATP, adenosine triphosphate; Glu, glucose; Hx, hypoxanthine; IMP, inosine monophosphate; Ins, inosine; Lac, lactic acid; R1P, ribose-1-phosphate; AK, adenylate kinase; AdsK, adenosine kinase; AdsD, adenosine deaminase; AMPD, AMP deaminase; PNA, purine-5'-nucleotidase; PNP, purine nucleoside phosphorylase; PPRT, purine phosphorybosyl transferase; ATPases, sum of ATP consuming processes. (Reproduced with permission from (Komarova *et al*, 1999).

## 1.15      **Transportation systems in infected erythrocytes**

Invasion of the erythrocyte by the malaria parasite poses another form of challenge to the parasite. Within the erythrocytes, the malaria parasite is faced with the problem of obtaining the nutrients needed for synthesis of required biomolecules. To reach the cytosol of the parasite, nutrients from exogenous sources have to cross the host plasma membrane, the parasitophorous vacuole membrane and finally the parasite's own plasma membrane (Figure 1.12). Each of these membranes possesses unique properties, which influence the movement of compounds across them (Kirk, 2001). To facilitate the parasite's access to an exogenous source of these essential nutrients, transporters for different groups of compounds are located in the membrane barriers. In order to increase parasite's nutrient acquisition after invasion, there occurs formation of a broad specificity channel-like system on the host plasma membrane for the uptake of various kinds of nutrients (Cabantchik, 1989; Elford *et al*, 1990; Cabantchik, 1990). The induced pathway (shown schematically in Figure 1.12), which results in an increased ability of parasite-infected erythrocytes to take up nutrients, is referred to as the New Permeation Pathway, NPP (Kirk, 2001). Details of the channel are discussed in the next section of this thesis. Currently no evidence exists to suggest that the parasite introduces other salvage mechanisms in addition to the NPP on the erythrocyte membrane to maximize the uptake of essential nutrients.



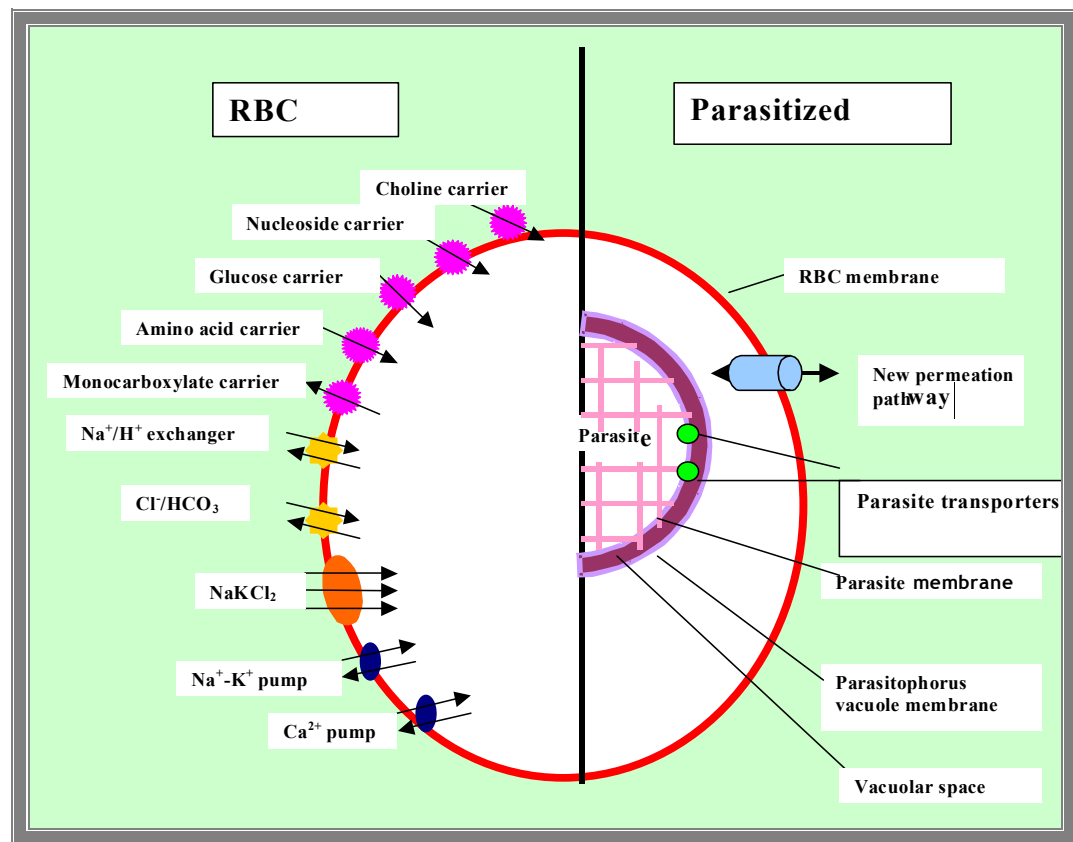


Figure 1.12: Transport systems before and after parasite invasion of the erythrocyte

 =antiport    
  =Pumps    
  =parasite transporters    
  =Carrier    
  =Cotransporter

(Redrawn from Kirk (2001); <http://sites.huji.ac.il/malaria/maps/prbc.html>).

### 1.15.1 The New Permeation Pathway

The NPP is induced in the host plasma membrane of the malaria parasite at about 10-20 hours post invasion (Kirk, 2001). The NPP has been shown to be a non-saturable channel-like system with preference for anionic compounds (Desai *et al*, 2000). According to reports the pathway is responsible for the uptake of nucleosides, amino acids and sugars among others (Desai *et al*, 2000; Kirk, 2001; Krishna *et al*, 2002). However as will be shown later in this thesis the NPP plays at best a minor role in the uptake of purine nucleoside into *P. falciparum* infected erythrocytes.

Classical anion channel inhibitors such as furosemide and 5-nitro-2- (3-phenylpropylamino) benzoic acid (NPPB) have been demonstrated to block the uptake of permeant through the NPP (Kirk *et al*, 1994; Kirk & Horner, 1995; Kirk, 2001). Using the

patch-clamp technique, it was demonstrated that the NPP is localised in the host plasma membrane of *P. falciparum* infected human erythrocytes (Desai *et al*, 2000; Egee *et al*, 2002; Huber *et al*, 2002).

Various models speculating on the origin of the NPP have been published (Figure 1.13). Whilst one model suggests that the NPP is a single channel type, another model depicts it as originating from at least three separate channel types (Huber *et al*, 2002; Duranton *et al*, 2003). Others have also suggested that the NPP originates from an upregulation and/or a modification of endogenous pathways

Until analysis of the NPP is performed at the molecular level, it will remain unclear whether it is an upregulated/modified endogenous membrane transporter or whether it originates from proteins synthesized by the parasite and inserted into the host plasma membrane.

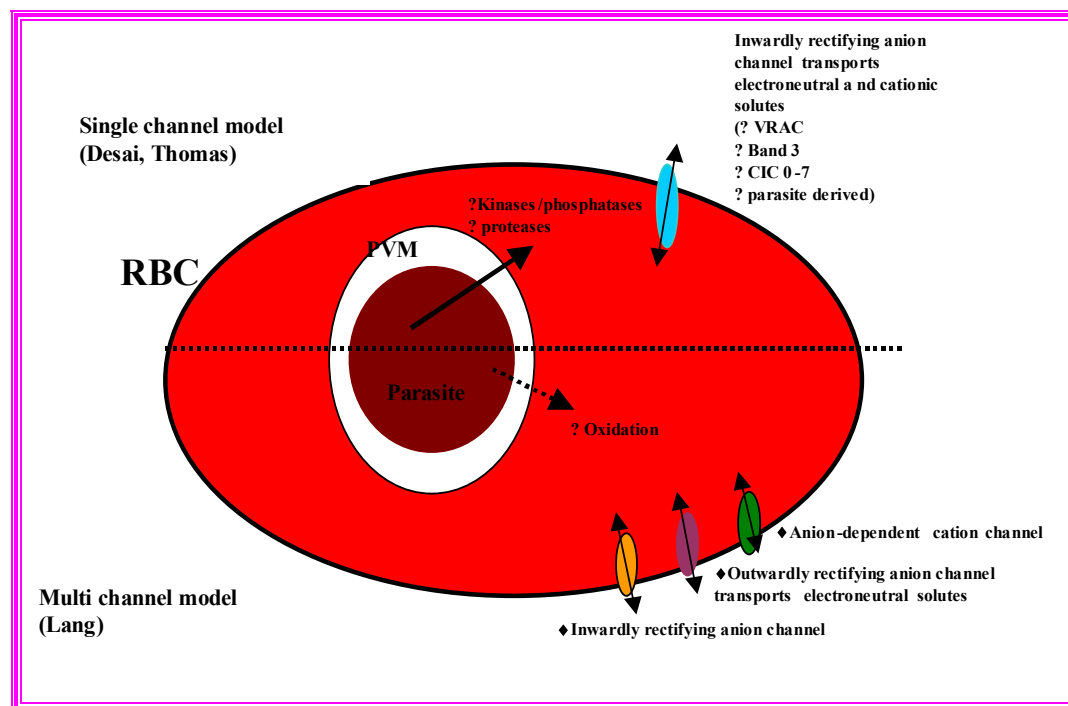


**Figure 1.13: Models for the formation and induction of the new permeability pathway (NPP) in *P. falciparum*-infected human RBCs.**

Abbreviations; cystic fibrosis transmembrane regulator, CFTR; volume-regulated anion channel, VRAC; chloride channel family, CIC; the anion exchanger, Band 3. Re-drawn from (Staines *et al*, 2004).

### 1.15.2 The Parasitophorous Vacuole Membrane

During parasite invasion of the erythrocyte, the indentation created at the meeting points of the two cells continues to develop as the parasite moves inward into the erythrocyte (Ward *et al*, 1993). Eventually the parasite becomes completely enveloped by a membrane referred to as the parasitophorous vacuole membrane (PVM) (Ward *et al*, 1993). The parasite therefore has its own plasma membrane and sits within a parasitophorous vacuole enclosed by the PVM.

Using fluorescent probes, it has been demonstrated that the PVM is derived from the host cell membrane ((Ward *et al*, 1993). Desai and colleagues used the cell-attached patch-clamp method to demonstrate that pores existing in the PVM allow low molecular weight compounds to move freely through the membrane (Desai *et al*, 1993). ‘These channels were open more than 98% of the time at the resting potential of the PVM’ (Desai *et al*, 1993).

## 1.16 Chemical structures of purines

Purines can be grouped as oxy-purine or amino purine depending on which chemical group is present at position 6 of the purine ring. Adenine is a 6-amino purine whilst hypoxanthine is 6-oxy purine. Guanine is 2-amino-6-oxy purine and xanthine is a 2, 6-dioxy purine. Nucleosides consist of a purine base attached to a ribose sugar (Figure 1.14).

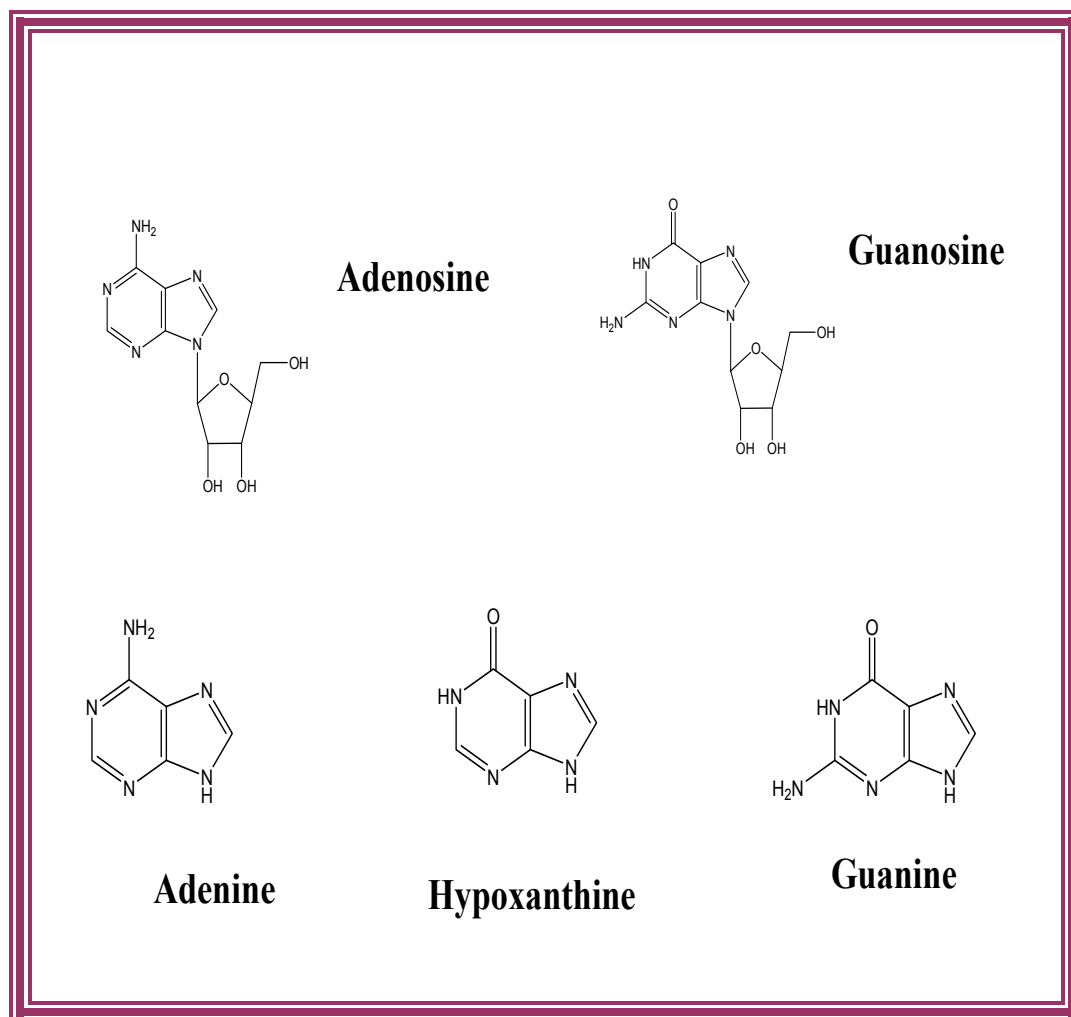


Figure 1.14: Chemical structures of purines.

## 1.17 Salvage and metabolism of purine in parasitic protozoa

Purine nucleosides are important requirement for the growth and development of all protozoans. The compounds are necessary for the synthesis of biomolecules such as the hereditary material, DNA (Gherardi & Sarciron, 2007). Purines are also constituents of co-enzymes, such as nicotinamide adenine dinucleotide (NAD), which play significant roles in the modulation of enzymatic reactions. Purines also constitute the backbone for the synthesis of ATP during energy metabolism in most organisms.

Nucleoside and nucleobase being hydrophilic compounds cannot easily diffuse across the lipid bilayer of the plasma membrane of the protozoan parasite. Specialised transport system therefore exist in the parasite for their translocation (Cohn & Gottlieb, 1997; Carter *et al*, 2000). Salvage of purine nucleobases or nucleosides in protozoa is mediated by various transporters, which are localised in the plasma membrane of the parasites (Landfear *et al*, 2004). Some protozoans have been shown to possess two nucleoside transporters in addition to one or more transporters for the salvage of nucleobase' (de Koning *et al*, 2003). All the nucleoside transporter genes identified in protozoa up to date have been found to belong to the equilibrative nucleoside transporter family, which is described in detail in section 1.19. Studies of these transporters at the molecular level have allowed for a better understanding of the physiology of the parasites. The purine metabolic pathway for *P. falciparum* is shown in Figure 1.15.

## 1.18 Purine metabolism in *P. falciparum*

An estimated 80% of the purine content of erythrocytes exists in the form of ATP, which could be a good source of purine for the growing parasite. However, work done *in vitro* has revealed that the parasites are unable to incorporate this form of nucleotides directly (Tracy & Sherman, 1972). Berman and co-workers reported that no more than 2% of the purine required by *P. falciparum* could be met by the intracellular stores of purine nucleotides, implying that most of this essential nutrient should come from exogenous source (Berman *et al*, 1991).

Although it has been documented that any of the purines, including hypoxanthine, guanine, adenine, inosine and adenosine can satisfy the purine requirement of the growing *P.*

*falciparum* parasite (Marr *et al*, 2003), available evidence indicates that hypoxanthine is the preferred purine required by the malaria parasite for nucleotide synthesis (Berman *et al*, 1991). Adenosine can be converted to hypoxanthine through deamination by adenosine deaminase and dephosphorylation by purine nucleoside phosphorylase (Daddona *et al*, 1984). Details of interconversion of the purines in *P. falciparum* and the enzymes involved are shown in Figure 1.15. The important contribution of hypoxanthine to the growth and development of the malaria parasites had been demonstrated *in vitro*. By making hypoxanthine unavailable to the parasite, through the addition of xanthine oxidase to the culture medium, it was shown that parasite growth was retarded (Berman & Human, 1990; Berman *et al*, 1991). Asahi and colleagues also demonstrated that addition of 15-150 $\mu$ M hypoxanthine into culture medium enhance growth of malaria parasites (Asahi *et al*, 1996).

The malaria parasites have been shown to be able to metabolise adenosine, guanosine, and guanine. However, there is much controversy with regard to utilisation of adenine in the parasite. Some reports have shown the absence of the gene encoding adenine phosphoribosyltransferase (APRT) and methylthioadenosine phosphorylase in any of the *Plasmodium spp* (Chaudhary *et al*, 2004; Ting *et al*, 2005), suggesting that the nucleobase cannot be metabolised in the parasite's cytosol. Additionally absence of the activity of adenine deaminase in the parasite has been reported. These reports raises the question of whether *Plasmodium spp* is capable of utilising adenine in biomolecule synthesis. However, the characterisation of APRT from *P. chabaudi* and *P. falciparum* reported by Walter and konigk, (1974) and Queen, (1989) respectively heightens the aforementioned controversy (Walter & Konigk, 1974; Queen *et al*, 1989). Other reports indicating that *P. falciparum* is able to grow *in vitro* with adenine as sole purine source (Geary *et al*, 1985) and that *P. knowlesi* incorporated adenine into nucleic acids (Gutteridge & Trigg, 1970) must be taken with caution. This is because adenine is easily converted to hypoxanthine in the erythrocyte cytosol and the growth observed could be due to the utilisation of the formed hypxanthine rather than adenine. Van Dyke has demonstrated that the parasite can incorporate adenine into nucleic acids but only at 1% of the efficiency by which hypoxanthine is incorporated into free parasites and 2% at parasitized cell level (Van Dyke, 1975).

During purine metabolism in the cytosol of the parasite, hypoxanthine is converted to inosine monophosphate through the action of hypoxanthine phosphoribosyltransferase

(Berman *et al*, 1991). The compound is finally converted to ATP and GTP, which are used in the synthesis of RNA or DNA (Figure 1.15).

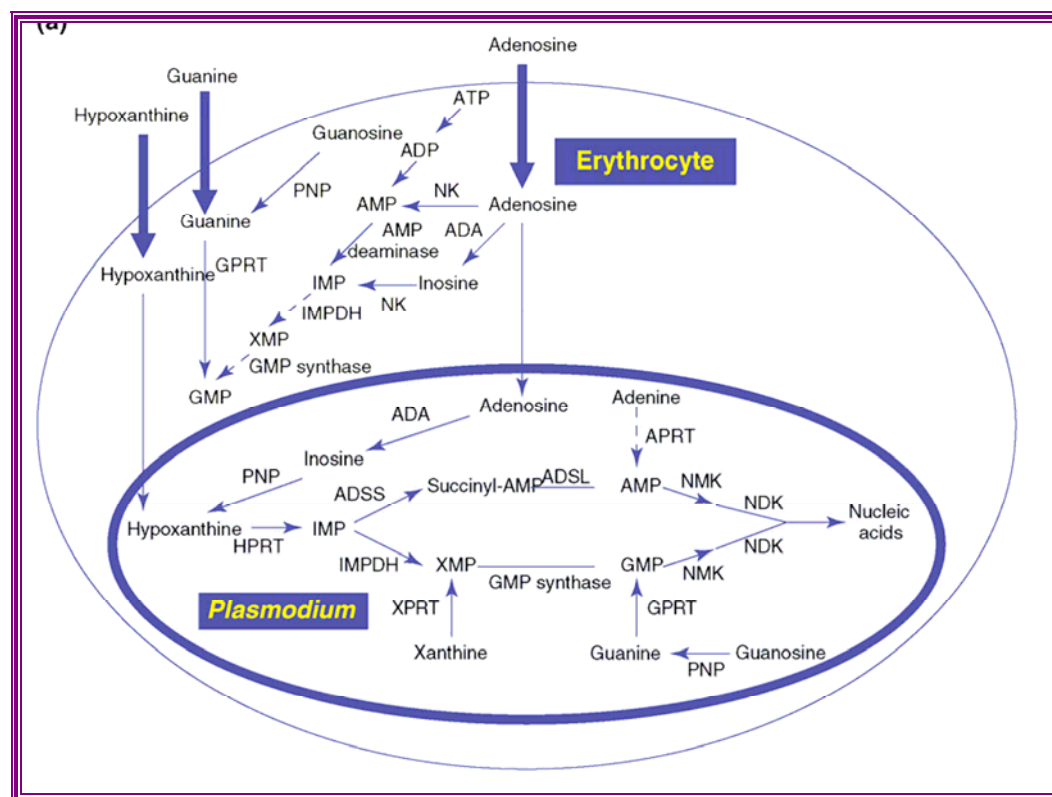


Figure 1.15: The purine pathway in *P. falciparum*.

Abbreviations: ADSS, adenylosuccinate synthase; ADSL, adenylosuccinate lyase; GMP, guanosine monophosphate; NMK, nucleoside monophosphate kinase; NDK, nucleoside diphosphate kinase; NK, nucleoside kinase; APRT, adenine phosphoribosyltransferase; HPRT, hypoxanthine phosphoribosyltransferase; GPRT, guanine phosphoribosyltransferase; IMP, inosine 50-monophosphate; XPRP, xanthine phosphoribosyltransferase; ADA, adenosine deaminase; and PNP, purine nucleoside phosphorylase; XMP, xanthosine monophosphate. Although literature report the conversion of adenine to AMP current evidence is not supportive of this. Reproduced with permission from: (Gherardi & Sarciron, 2007).

## 1.19 The Equilibrative Nucleoside Transporters

The equilibrative nucleoside transporter are a family of protein which allows facilitated diffusion of nucleosides, such as adenosine, down their concentration gradients across cell membranes (Hyde *et al*, 2001). However some report suggest they can act as proton-dependent, concentrative transporters.

Members belonging to the ENT family possess 11 transmembrane (TM) spanning segments with a cytoplasmic N-terminus and extracellular C-terminus (Figure 1.16) (Baldwin *et al.*, 2000 [<http://www.astbury.leeds.ac.uk/Report/2000/Baldwin.2.htm>]). TM 3-6 region in the mammalian ENT is implicated in solute recognition (Hyde *et al.*, 2001; de Koning *et al.*, 2005). Apart from transportation of nucleoside, ENT can also transport nucleobases (Parker *et al.*, 2000). Additionally they have been reported to be targets for coronary vasodilator drugs and can also act as a route for the uptake of cytotoxic drugs into human and protozoan cells (Molina-Arcas *et al.*, 2006). The ENT family has been reported in mammals, plants, yeast, insects, nematodes and protozoa among others (Hyde *et al.*, 2001; Acimovic & Coe, 2002; Martin *et al.*, 2005).

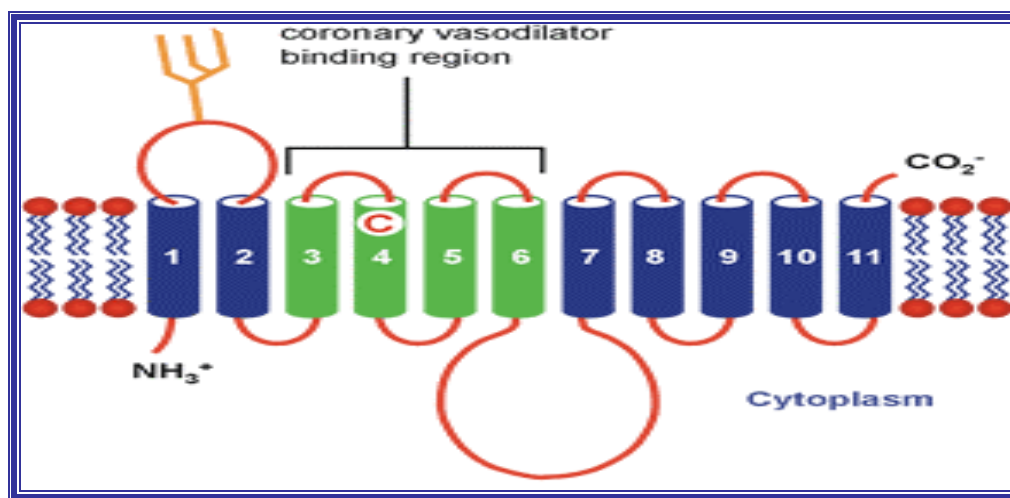


Figure 1.16: Topology of mammalian members of the ENT family.

Reproduced with permission from Baldwin *et al.*, 2000;  
<http://www.astbury.leeds.ac.uk/report/2000/baldwin.2.htm>).

Transport through the ENT, which was first identified at the molecular level in 1997 (Griffiths *et al.*, 1997) is reported to be equilibrative (Parker *et al.*, 2000). On the basis of their sensitivity to nitrobenzylthioinosine (Nitrobenzylmercaptapurine riboside; NBMPR), members of the ENT family can be either equilibrative sensitive (es) or equilibrative insensitive (ei). The es subclass is inhibited by nanomolar concentrations of NBMPR ( $K_i$ : 0.1-10 nM) whilst the ei subclass, are insensitive to NBMPR at micromolar concentrations (Baldwin *et al.*, 2005). Additionally, transporters of the es-type are inhibited by the coronary vasodilators such as dipyridamole (see Figure 1.17 for structure) and dilazep while ei-type transporters are not affected by these compounds.



In 1997 Griffiths and his colleagues reported the cloning from human placenta of es and ei transporters, which they named hENT1 and hENT2 respectively (Griffiths *et al*, 1997). Both hENT 1 and hENT2 were observed to transport a broad range of purine and pyrimidine nucleosides, while hENT2 is also capable of transporting nucleobases (Baldwin *et al*, 2004; Baldwin *et al*, 2005). Two other human nucleoside transporters, designated hENT3 and hENT4 have also been identified (Kong *et al*, 2004; Baldwin *et al*, 2005).

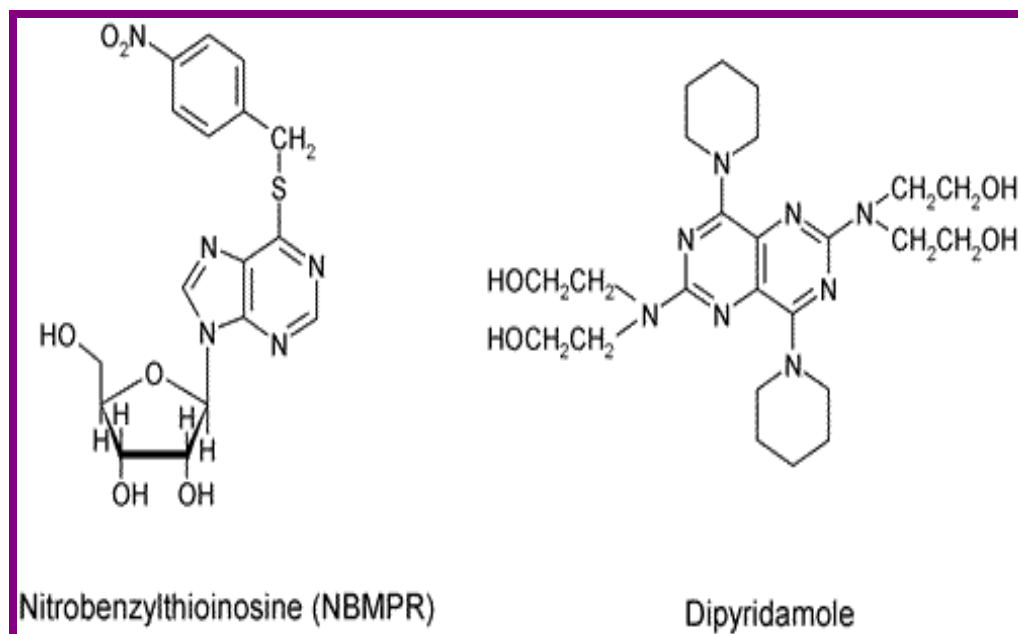


Figure 1.17: Structures of some of the inhibitors of the exogenous purine transporters.

## 1.20 Identification of ENT transporter genes in *Plasmodium falciparum*

In 2000, Baldwin and his group did data-mining of the malaria-genome database for homologues of mammalian nucleoside transporters that could be responsible for purine salvage in *P. falciparum* (Parker *et al*, 2000). They identified a gene that is homologous to the mammalian ENT family. The gene, which was later isolated and cloned, encodes a protein of 422 amino acids with 11 predicted trans membrane domains. The gene was originally named *PfENT1* with an accession number, PF13\_0252.

Oocytes of *Xenopus laevis* were injected with *PfENT1* RNA transcript and maintained in a modified Barth's medium supplemented with 5% horse serum, for two days for the

expression of the protein. The kinetic properties of the expressed purine transporters were then investigated. *PfENT1*, was found to be capable of transporting 3'-deoxynucleoside analogues such as the antiviral drug 3'-azido-2', 3'-dideoxythymidine (AZT). Unlike the mammalian ENT transporters, *PfENT1* was not inhibited by NBMPR and by coronary vasodilators such as dipyridamole, which are known to inhibit members of the mammalian ENT family (Parker *et al*, 2000). *PfENT1* was found to be a saturable transporter of nucleosides and nucleobases (Parker *et al*, 2000). A similar protein was reported simultaneously by a different group (Carter *et al*, 2000). The gene, which they named *PfNT1*, was found to be identical to that reported by Parker and colleagues (*PfENT1*), except for a single nucleotide difference at codon 385: with leucine reported by Parker and co and Phenylalanine by Carter and his colleagues. Kinetic data presented on the transport activities of the two proteins also differed markedly. Detailed comparison of the two studies is presented elsewhere in this thesis.

Further data mining of the malaria genome database revealed the presence of additional members of the ENT family. A gene denoted MAL8P1.32, is annotated in the genome database as a putative nucleoside transporter (Martin *et al*, 2005). The genes with accession numbers PFA0160c and PF14\_0662 respectively have also be found to belong to the ENT family (Martin *et al*, 2005). Detailed analysis of each gene indicates that they probably encode for proteins with secondary structure similar to that of the ENT family (Martin *et al*, 2005).

The genes denoted PFA0160c, MAL8P1.32 and PF13\_0252 were reported to have similar expression profiles, with an increasing abundance of the mRNA between 16 and 24 hours after merozoite invasion of the erythrocyte, and reaching a peak in 32 hours post invasion (Martin *et al*, 2005). PF14\_0662 was shown to differ slightly, with mRNA levels increasing in abundance between 8-20 hours, reaching a peak around 36 hours post-invasion.

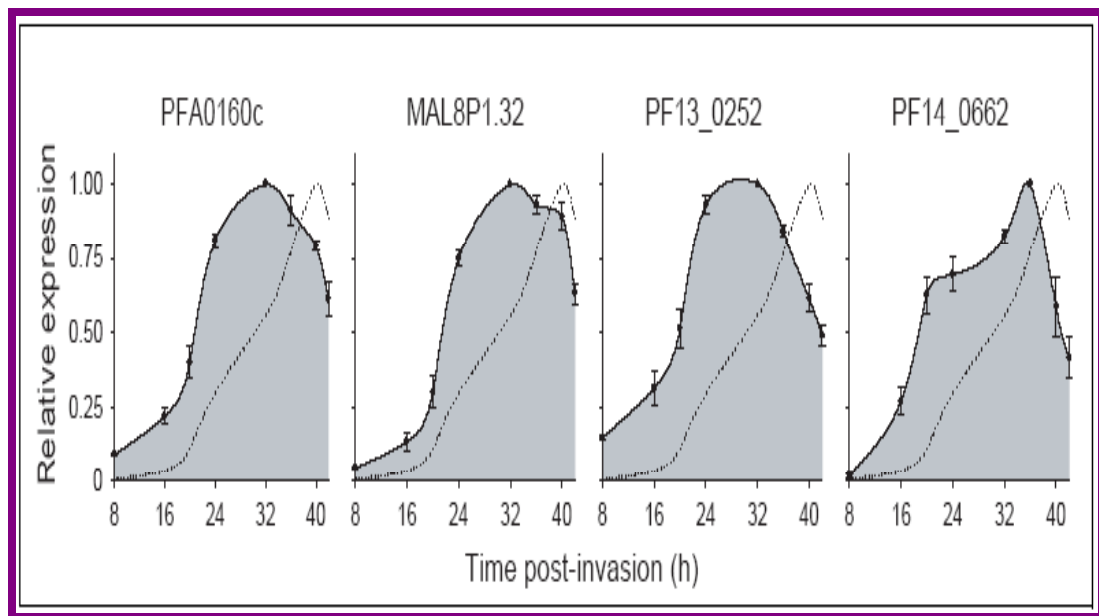


Figure 1.18: Stage-dependent gene expression of the four *P. falciparum* members of the equilibrative nucleoside transporter family, throughout the intraerythrocytic cycle of the parasite.

RT-PCR was conducted to semi-quantify the level of gene expression in  $\sim 1.5 \times 10^4$  parasitized cells at each growth stage. Relative expression (y-axis) is the ratio of the density of the band from the PCR product at each time point in the life cycle relative to that at the time point giving the largest yield of PCR product. Ratios calculated from replicate gels from the same PCR were averaged before the data from the two time courses (carried out approximately 4 months apart and each consisting of  $\geq 2$  PCRs) were combined to give the mean  $\pm$  S.E. For comparison, the relative amount of total RNA in the parasitized cell over the same growth stages is also presented (dotted line). Reproduced with permission from (Martin *et al*, 2005).

## 1.21 Cellular location of *P. falciparum* purine transporters

The location of ENT designated *PfNT1* in the malaria parasite has been determined through the application of techniques such as deconvolution immuno-fluorescence and immuno-electron microscopy (Rager *et al*, 2001). The procedure involves the initial stimulation of the production of polyclonal antisera against the NH<sub>2</sub>-terminal 36 amino acids of *PfNT1* in rabbits. Western blot analysis of parasite lysates revealed that the antibodies were specific for *PfNT1* and that 'the level of *PfNT1* protein in the infected erythrocyte was regulated in a stage-specific fashion' (Rager *et al*, 2001). Additionally, the amount of *PfNT1* polypeptide was reported to increase dramatically during the early trophozoite stage reaching its maximal level in the late trophozoite and schizont stages. Following up with a deconvolution and immuno-electron microscopy using the prepared

monospecific antibodies, the group of Ullman concluded that '*PfNT1* is localized predominantly, if not exclusively, to the plasma membrane of the parasite and not to the parasitophorous vacuolar or erythrocyte membranes' (Rager *et al*, 2001). The locations of the transporters encoded by the three other putative ENT genes in *P. falciparum* have not yet been elucidated.

## 1.22 Purine antimetabolites as antimalarial drugs

Depriving malaria parasites of their purine requirements, through controlled blockage of the salvage pathways is certain to cause parasite death, as shown by (El Bissati *et al*, 2006). Additionally, the purine salvage system present in the parasite could be utilized to deliver cytotoxic compounds into the parasite to cause its death. Compounds that mimic purine in structure (analogues) and in other chemical properties could be used to block components of the purine salvage pathways in the parasite. Alternatively, nucleotide analogues may be built into nucleic acids, or interact with the binding sites of enzymes using ATP or GTP as substrates, and thus disrupt cellular functions and/or replication. In the light of this, purine analogues have become the focus of intense study in the search for novel antimalarial drugs.

In 1994, Coomber and his colleagues investigated the antiplasmodial activities of some adenosine analogues (Coomber *et al*, 1994). They reported that alterations of the purine ring at the 7 or 8 positions significantly increased the toxicity of the compound against *P. falciparum*: sangivamycin (7-deaza-7-amido-adenosine), tubercidin (7 deaza-adenosine), 6-methylamino-deoxyadenosine, 8-aza-2-amino-deoxy-adenosine and 2-chloro-adenosine (Figure 1.19) were found to inhibit parasite growth within IC<sub>37</sub> range of 0.3-11 μM.

Smeijsters and his colleagues (1999) evaluated forty-eight acyclic nucleoside phosphonates for *in vitro* antiplasmodial activities (Smeijsters *et al*, 1999). They reported that only the derivatives with a hydroxyl group attached to the acyclic sugar moiety were potent inhibitors of growth. The two most active analogues were (*S*)-9-(3-hydroxy-2-phosphonylmethoxypropyl) adenine ((*S*)-HPMPA, and (*S*)-3-deaza-HPMPA (Figure 1.20).

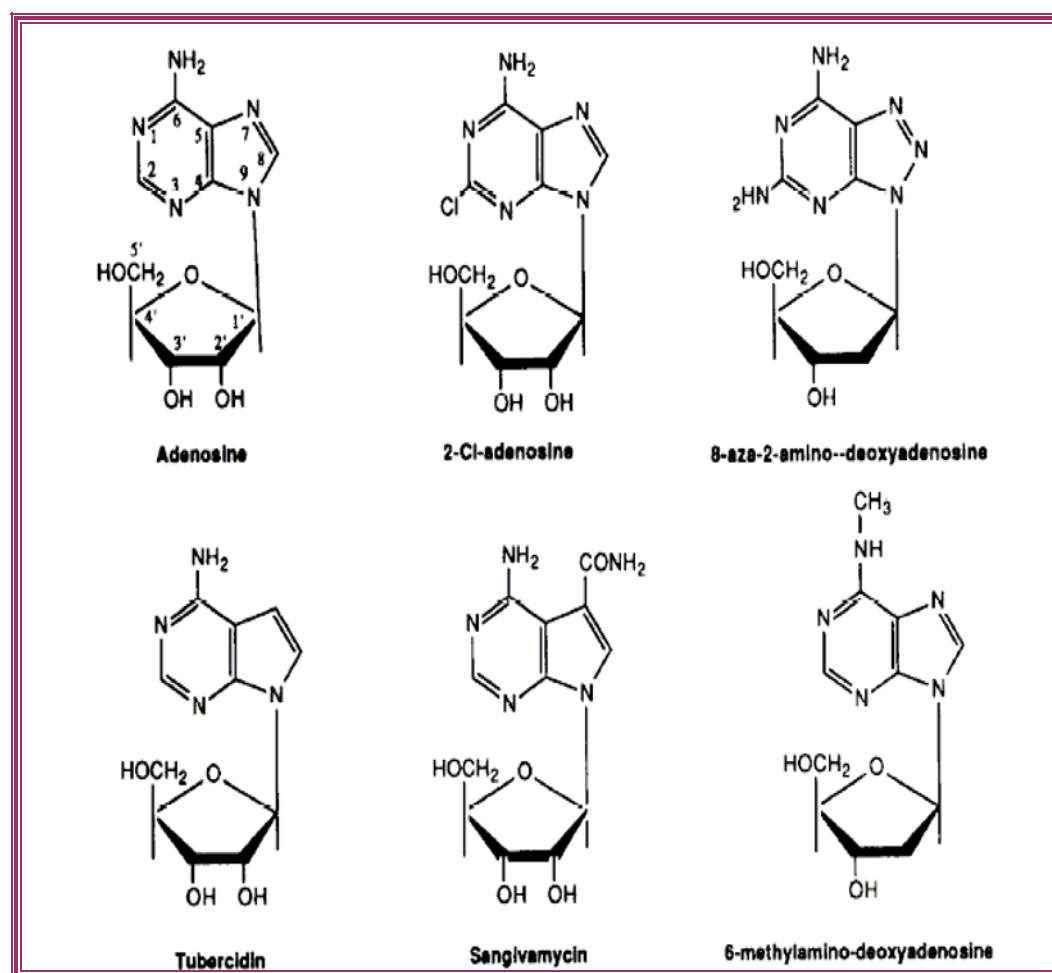


Figure 1.19: Chemical structures of adenosine analogues.

Source: (Coomber *et al*, 1994).

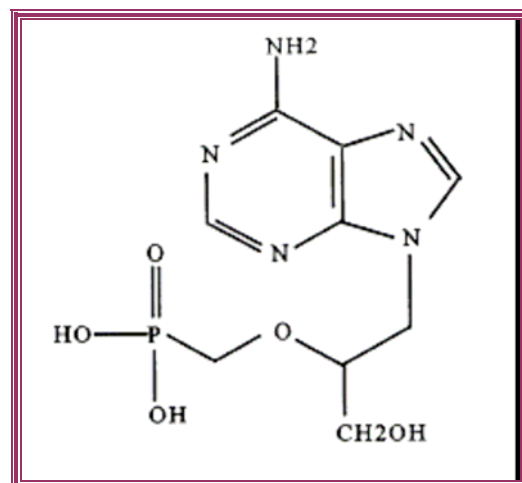


Figure 1.20: Structural formula of HPMPA, an acyclic purine nucleoside phosphonate.

Source: (Smeijsters *et al*, 1999).

Queen and her colleagues also determined the susceptibility of *P. falciparum* to 64 purine and pyrimidine analogues *in vitro*. Twenty two of the analogues produced an IC<sub>50</sub> of 50  $\mu$ M or less (Queen *et al*, 1990).

Recently, Rodenko and his colleagues tested 2,N6-disubstituted adenosine analogues *in vitro* for their antiprotozoal activities (Rodenko *et al*, 2007). They reported that those with promising antiplasmodial activity have large aromatic substitutions, such as N6-2,2-diphenylethyl and naphthylmethyl. This observation suggest that the mode of action of the compounds was through aromatic stacking with haeme in the digestive vacuole of *Plasmodium* (Rodenko *et al*, 2007).

The cyclin-dependent kinases (CDKs), which are essential for the regulation of the eukaryotic cell cycle were the target of a group of purine-derived kinase inhibitors tested by Harmse and his colleagues (Harmse *et al*, 2001). The group reported that 'subfamilies of purines with moderate to poor activity against CDK1/cyclin B activity showed submicromolar activity against *P. falciparum*'.

Studies by Brown and co also show that L-stereoisomer analogues of D-coformycin selectively inhibited *P. falciparum* adenosine deaminase (ADA) in the picomolar range (Brown *et al*, 1999). They further demonstrated that L-nucleoside analogues, L-adenosine, 2,6-diamino-9-(L-ribofuranosyl)purine and 4-amino-1-(L-ribofuranosyl)pyrazolo[3,4-d]-pyrimidine were selectively deaminated by *P. falciparum* ADA, whilst L-thioinosine and L-thioguanosine were not.

### **1.23 Nucleoside and Nucleobase transport in other apicomplexa**

*Toxoplasma gondii*, which causes toxoplasmosis, is an obligate intracellular parasite belonging to the apicomplexan of which *P. falciparum* is also a member. Like *P. falciparum*, *T. gondii* parasites obtain their supply of purine from exogenous sources because they are incapable of *de novo* synthesis (Schwartzman & Pfefferkorn, 1982; Krug *et al*, 1989). Since *Toxoplasma* lives in nucleated cells it obtains free purines from the host

cell cytoplasm by diffusion through pores in the parasitophorous vacuole membrane (Schwab *et al*, 1994).

It has been shown that adenosine is the major purine salvaged by *T. gondii*. Adenosine enters the cytoplasm through transporters (Krug *et al*, 1989): a low affinity, saturable adenosine transporter was identified in experiments performed with isolated tachyzoites (Schwab *et al*, 1995). This transporter, with a  $K_m$  of 230  $\mu$ M, was reported to be inhibited by dipyridamole with an  $IC_{50}$  of 0.7  $\mu$ M. Uptake of hypoxanthine, adenine and inosine through this transporter was also reported to be inhibited at 10  $\mu$ M. This transporter is encoded by the *TgAT1* gene, which belongs to the ENT family, and was the first purine transporter gene to be cloned from among the members of the apicomplexan group (Chiang *et al*, 1999). When expressed in *Xenopus* oocytes, the transporter was found to have broad substrate specificity for purines.

De Koning and colleagues identified a nucleobase transporter in *T. gondii*, which was denoted TgNBT1 and observed to transport hypoxanthine with  $K_m$  of 0.91  $\mu$ M. This transporter is reported to be inhibited by guanine and xanthine. This was the first high affinity nucleobase transporter to be identified in apicomplexan parasites. De Koning and co-workers also identified a nucleoside transporter named TgAT2, with higher affinity than TgAT1 ( $K_m$  value of 0.28  $\mu$ M) [(de Koning *et al*, 2003)]. TgAT2 was found to recognise several nucleoside analogues, making it a good target for novel drugs ((de Koning *et al*, 2003).

Very little is known about purine transporters of other apicomplexan parasites.

*Plasmodium berghei* reportedly expresses a high affinity adenosine/hypoxanthine transporter with relatively low affinity for inosine, and a separate adenine transporter (Hansen *et al*, 1980). Purine uptake in the avian malaria parasite, *P. lophurae* is reported to be similar to that reported for *P. berghei*, although the report provides few details (Tracy & Sherman, 1972). An adenosine transporter has also been reported in *Babesia bovis*, but again few details are known (Matias *et al*, 1990).

## **1.24 Studies on *P. falciparum* purine transport published after conclusion of our own characterisation of purine salvage in isolated trophozoites.**

In the course of the studies reported in this thesis, two reports on purine transport were published. In the first, El Bissati and co-workers disrupted the gene encoding the nucleoside transporter *PfNT1* in *P. falciparum* and studied the characteristics of the resultant phenotype (El Bissati *et al*, 2006). They demonstrated that parasite clones with a disrupted *PfNT1* were auxotrophic for hypoxanthine, inosine, and adenosine under physiological conditions, and could only survive when the growing medium was supplemented with high levels of purine. Parental cells with an intact *PfNT1* gene were able to survive on much lower purine concentrations. Uptake of hypoxanthine into parasite clones with a disrupted *PfNT1* was observed to be significantly reduced, whereas adenosine and inosine transport were only partially affected. The study by El Bissati and co-workers provided evidence for conversion of exogenous purine into hypoxanthine using host enzymes followed by *PfNT1*-mediated transport into the parasite.

In the second publication, Downie and his colleagues investigated the kinetic characteristic of isolated *P. falciparum* parasites (Downie *et al*, 2006). They reported that the transport of nucleosides into the parasite was, in the case of adenosine, inosine and thymidine, very fast, and saturable. A Michaelis-Menten plot revealed that the transporter has a low affinity for these purines. For example, the  $K_m$  for adenosine was calculated as  $1.45 \pm 0.25$  mM. There was also a report of cross-competition for adenosine, inosine and thymidine, but not cytidine. They concluded that the transporter is a major route for the uptake of nucleosides across the parasite plasma membrane. This conclusion, that *PfNT1* was responsible for the low affinity adenosine transport, was backed up by an expression of this gene in *Xenopus* oocytes (Downie *et al*, 2006).



## 1.25 Aims and objectives of study

The main aim of this study is to investigate the mechanism of purine transport in the intraerythrocytic stage of *P. falciparum* parasites.

The specific objectives include:

- (i) To identify purine transporters in the plasma membrane of saponin-freed *P. falciparum* trophozoites (isolated *P. falciparum* parasites)
- (ii) To investigate the mechanism of purine transport in Percoll-concentrated intact *P. falciparum* infected erythrocytes
- (iii) To investigate the interaction between substrate and transporter binding sites that affect their affinity ( $K_m$ ) and selectivity, and the role they play in the salvage of purine from the host
- (iv) To test purine analogues for antiparasmodial activities against *P. falciparum*
- (v) To disrupt the genes encoding the equilibrative nucleoside transporter (ENT) and study the kinetic characteristics of the resultant parasites

## **CHAPTER TWO**

### **2 Materials and methods**

## **2.1 *In vitro* cultivation of *P. falciparum***

### **2.1.1 Parasite lines/clones**

All transport experiments were performed with the standard 3D7 drug-sensitive laboratory clone of *P. falciparum* at the University of Glasgow, Glasgow. The parasites were originally obtained from David Walliker, University of Edinburgh, UK. Clone 3D7 is known to be sensitive to chloroquine and pyrimethamine (Walliker *et al*, 1987). The K1 line of parasites was also used in the drug sensitivity assays; this line is reported to be resistant to chloroquine and pyrimethamine (Lambros & Vanderberg, 1979; Thaithong & Beale, 1981).

### **2.1.2 Preparation of culture media**

Parasites were cultured in RPMI 1640 medium supplemented with 5.94g/L HEPES (Sigma) and 50mg/L hypoxanthine (Sigma) (incomplete medium) to which 0.21% NaHCO<sub>3</sub> (w/v) and 10% heat-activated normal human serum were added (complete medium). Human serum of group AB was obtained from the Glasgow and West Scotland Blood Transfusion Service. The serum was pooled from several donors, heat-inactivated at 56°C for 1 hour to remove complement prior to use.

### **2.1.3 Processing of red blood cells for parasite culture**

Fresh human whole blood used for the parasite cultures and uptake experiments was obtained from the Glasgow and West of Scotland Blood Transfusion Service. Blood of any group was supplied, although the most common was from donors with blood group O, rhesus positive. The blood was washed to remove the plasma, buffy coat and anticoagulant by centrifugation at 630 × g, 10 min, followed by removal of the supernatant and re-suspension of the pellet in an equal volume of incomplete RPMI 1640. The washing was repeated twice more, and then the erythrocytes were finally re-suspended in an equal volume of incomplete RPMI 1640 (approx 50% packed cell volume (PCV)).

### **2.1.4 Culturing of malaria parasites**

Human erythrocytes infected with *P. falciparum* were maintained in continuous culture using standard method (Trager & Jensen, 1976; Haynes *et al*, 1976). The culture consisted of 5% suspension of human erythrocytes in complete RPMI 1640 medium. The culture was

kept at 37°C under a gas mixture of 1% O<sub>2</sub>, 3% CO<sub>2</sub>, and 96% N<sub>2</sub>. Determination of parasitaemia and changing of the medium was done daily. The culture was kept below 5% parasitaemia at all times.

### 2.1.5 Synchronization of culture

Using the method described by (Lambros & Vanderberg, 1979), a predominantly ring stage culture was synchronised by incubation with 5% w/v D-sorbitol (Sigma) for ten minutes. While the uninfected erythrocytes are impermeable to sorbitol, the changes caused in the erythrocyte permeability by the developing parasites allow sorbitol to enter the erythrocytes causing lysis of the cells. Therefore, incubation of parasite pellets with sorbitol results in cell suspensions having only ring stage parasites estimated to be up to 18 hours old (Jensen, 1988). It has been demonstrated that intraerythrocytic parasites growth is not affected by their exposure to sorbitol (Lambros & Vanderberg, 1979; Ginsburg & Stein, 1987; Nakazawa *et al*, 1995). Briefly, the culture was centrifuged for 5 minutes at 700 × g and the supernatant removed and discarded. The parasite pellet was then treated with ten pellet volumes of 5% D-sorbitol (w/v) and incubated at room temperature for 10 minutes. After incubation, the culture was centrifuged at 630 × g for 5 min to pellet the cells and the supernatant removed and discarded. The cells were washed three times in incomplete RPMI 1640 to remove traces of the sorbitol. Thin blood films were prepared, stained with 5% Giemsa's stains and examined under the light microscope to determine the parasitaemia. The pellets were finally resuspended in complete RPMI 1640 and washed blood was added to give a PCV of 5% and about 1% parasitaemia, in a total volume of 25ml. Incubation of the synchronised culture was resumed at 37°C under conditions previously described. A second round of synchronisation was performed if examination of the culture, 24 hours post-synchronisation, showed the presence of a high percentage of ring-stage parasites. This two-stage procedure results in an almost completely synchronised culture, although synchronisation breaks down after 1-2 cycles.

### 2.1.6 Staining of malaria parasites

Parasitaemia was estimated from methanol-fixed, Giemsa-stained blood smears. A thin film was prepared on a microscope slide and allowed to air dry. The film was fixed by brief contact with absolute methanol. The alcohol was allowed to evaporate and the slide put in a staining jar containing freshly prepared 5% Giemsa's stain (v/v) in Giemsa's

buffer, pH 7.4. After staining for 40 minutes at room temperature, the slide was rinsed with tap water, air-dried and examined under the light microscope with 1000× magnification. Parasitaemia was determined by counting both uninfected and parasite-infected erythrocytes in at least ten microscopic fields and expressing the parasite-infected erythrocytes as a percentage of the total erythrocytes.

### **2.1.7 Cryopreservation of malaria parasites**

Parasite material was stored by cryopreservation using the method described by Jensen and colleagues (Jensen *et al*, 1979). A culture with a predominantly ring stage *P. falciparum* parasites (parasitaemia > 2%) was centrifuged at  $630 \times g$  for 5 minutes to pellet the cells. The supernatant was carefully removed and discarded. A volume equal to the volume of the pellet, of deep freezing solution (28% glycerol, 3% sorbitol, 0.65% NaCl) was added drop wise, whilst mixing gently with a Pasteur pipette. A volume of 0.3-0.5 ml of the mixture was aliquoted into cryo-ampoules (Nunc), labelled with pencil or waterproof pen and stored in liquid nitrogen immediately.

### **2.1.8 Thawing of cryopreserved malaria parasites**

The method used to thaw cryopreserved malaria parasites was as described by Aley and co (Aley *et al*, 1984). Briefly, the frozen ampoule was rapidly thawed at 37°C and the contents transferred to a 15 ml centrifuge tube, and the cell volume, V, noted. A fifth of the cell volume V of thawing solution I (12% NaCl solution) was added drop-wise and mixed well with a Pasteur pipette. The mixture was left to stand for 2 minutes at room temperature to enable the freezing mix to be drawn out. Ten times the volume V of thawing solution II (1.6% NaCl solution) was added. The mixture was centrifuged at  $630 \times g$  for 5 min and the supernatant removed and discarded. Ten times the volume V of thawing solution III (0.9% NaCl plus 0.2% glucose solution) was then added with gentle mixing, and after centrifugation at  $630 \times g$ , 5 min, the cells were finally resuspended in 3ml of complete RPMI 1640. This was transferred into a culture flask and a drop of blood was added and the flask was gassed and incubated as previously described.

### 2.1.9 Red blood cell counts using Improved Neubauer haemocytometer

A counting chamber and cover slip were cleaned with ethanol to remove the presence of any grease. The cover slip was then aligned over the counting chamber and a gently downward pressure applied till “Newton’s rings” are produced between the cover slip and the chamber. The chamber was filled with the diluted sample by capillary action. Cells were counted under the light microscope using the  $\times 10$  objective ( $100\times$  magnification). Each square in the counting chamber is  $1\text{mm}^2$  and the chamber depth is  $0.1\text{mm}$ ; therefore the volume overlying each square is  $0.1\text{mm}^3$  (or  $0.0001\text{ml} = 0.1\mu\text{l}$ ).

Therefore, cell count per ml (Cells/ml) = total count  $\times$  1000  $\times$  dilution factor

## 2.2 Purine transport assays

### 2.2.1 Chemicals used in the transport assays

[2,8- $^3\text{H}$ ] Adenine was purchased from Moravsek (USA). [2,8- $^3\text{H}$ ] adenosine and [8- $^3\text{H}$ ] hypoxanthine were obtained from Amersham Pharmacia Biotech (UK). Unlabelled adenine, guanine, hypoxanthine, xanthine, inosine, adenosine, guanosine, uracil and thymine were obtained from Sigma. The chemicals used are of the highest purity available.

The JA- and NA-compounds (purine analogues) used in the experiments described in chapter six are gifts to Harry de Koning from Dan Brown, the MRC Laboratory of Molecular Biology, Cambridge, UK and Gerrit-Jan Koomen, University of Amsterdam, The Netherlands

### 2.2.2 Preparation of saponin-freed *P. falciparum* trophozoites for transport assays

Permeabilised *P. falciparum*-infected erythrocytes were prepared by incubating the culture with 0.15% w/v saponin (Sigma). Saponin, a plant-derived detergent, renders cholesterol-containing membranes freely permeable to macromolecules (Ansorge *et al*, 1996). Saponin interacts with cholesterol in the erythrocyte membrane to form lytic pores, but leaves the parasite plasma membrane (which lacks cholesterol) intact. Therefore treatment of parasitized erythrocytes with saponin permeabilised both the plasma membrane (PM) of the host erythrocyte and parasitophorous vacuole membrane (PVM) in which the

intracellular parasite is enclosed, thereby allowing solutes present in the extracellular medium unimpeded access to the parasite plasma membrane (Ansorge *et al*, 1996).

The culture was first centrifuged  $700 \times g$  for 5 min and the supernatant removed and discarded. The cell pellets were resuspended in 5 cell volumes of 0.15% (w/v) saponin made up in phosphate-buffered saline (137 mM NaCl, 27mM KCl, 1.76mM  $K_2HPO_4$ , and 8mM  $Na_2HPO_4$ ) for up to 2 min at room temperature. The cells were washed three times with incomplete RPMI 1640 to remove all traces of saponin and re-suspended in the same medium for the uptake experiments. Success of permeabilisation of the infected erythrocytes was checked by examining a wet smear of the suspension: a drop of the suspension was put on a microscope slide, covered with a slip and examine under the  $\times 100$  oil immersion.

### 2.2.3 Percoll enrichment of infected erythrocytes

Concentrated trophozoite-infected erythrocytes (60-90% parasitaemia) were obtained by density gradient sedimentation on Percoll (Amersham Biotech) using previously described methods (Gero *et al*, 1988; Kirk & Horner, 1995). Percoll consists of colloidal silica particles of 15-30 nM diameter (23% w/w in water), which have been coated with polyvinylpyrrolidone (PVP). Due to the heterogeneity in particle size, sedimentation occurs at different rates. This occurs spontaneously creating very smooth, isometric gradients in the range of 1.0-1.3 g/ml. Most biological particles having sedimentation coefficient values greater than 60 S can, therefore, be successfully isolated on Percoll gradients (<http://www.sigmaaldrich.com>). By following the manufacturer's instructions, isotonic Percoll solution was prepared.

A working solution of density 1.090 and osmolality  $320 \text{ mosm (kg H}_2\text{O)}^{-1}$  was prepared. Concentration of the late stage parasitized red blood cells (PRBC) was achieved by layering an equal volume of culture at 10% PCV on top of the isotonic Percoll solution and centrifuging at  $1000 \times g$  for 12 minutes. The trophozoite-enriched red blood cells were harvested from the interface. The harvested cells were washed three times with incomplete RPMI1640 and left to stand for 30 minutes in incomplete RPMI1640 supplemented with glucose (0.2%) to allow for full recovery of the parasites, prior to use in uptake experiments.

### 2.2.4 Measurement of purine uptake in saponin-freed *P. falciparum* trophozoites

The amount of radiolabeled permeant transported into *P. falciparum* parasites was measured using the rapid-stop/oil spin method (Figure 2.1) previously described by de Koning and Jarvis (de Koning & Jarvis, 1997). Time/dose dependent uptake described in detail in sections 2.2.5 and 2.2.6 were performed.

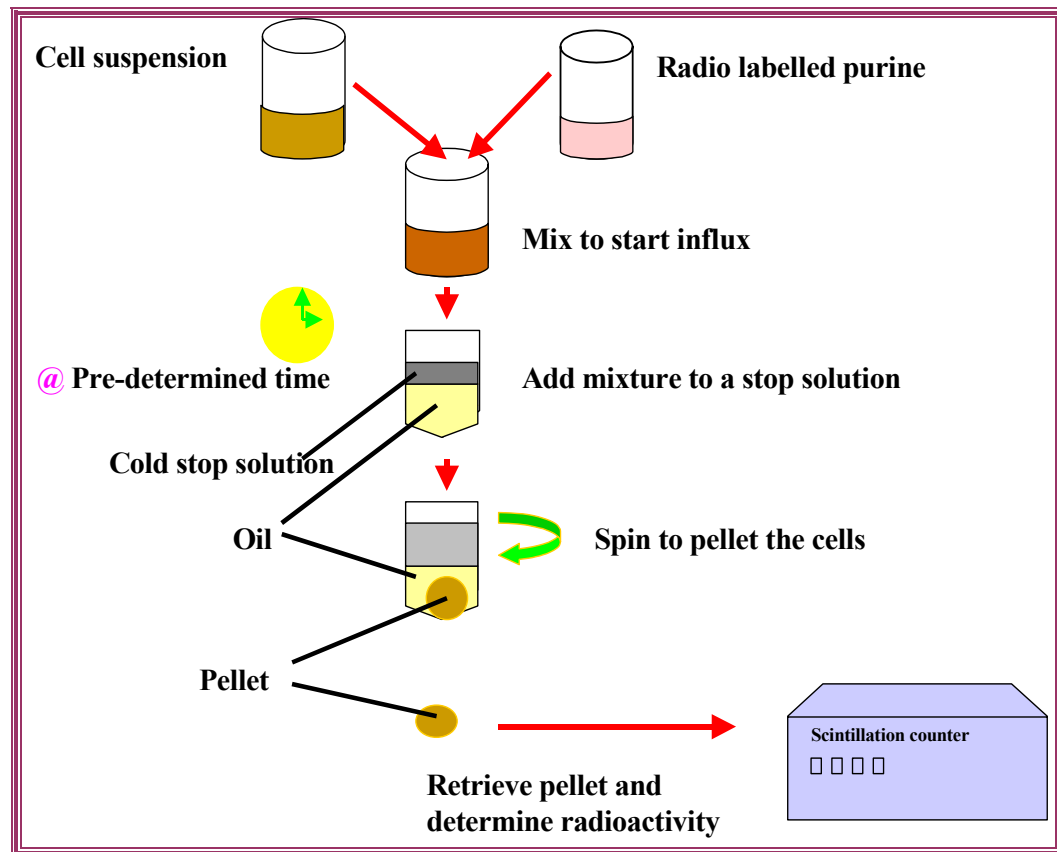


Figure 2.1: Classical uptake technique.

### 2.2.5 Time-dependent uptake of permeant

A time course uptake experiment measures the rate of movement of permeant across a biological membrane. Uptake of [ $^3\text{H}$ ]-hypoxanthine, [ $^3\text{H}$ ]-adenosine or [ $^3\text{H}$ ]-adenine by saponin-freed trophozoite-stage *P. falciparum* parasites were measured at various time intervals to generate plots of uptake rate versus time. Briefly, equal volumes of a suspension of permeabilised-infected erythrocytes (usually at a concentration of  $2-6 \times 10^7$



cells/assay) and a radiolabeled permeant at twice its final concentration were mixed for a predetermined times. Influx of permeant into the cells was terminated by adding 1 ml ice-cold stop solution (usually unlabelled permeant at saturating concentrations) and quickly spinning the cells at 13,000 x g in a microfuge through an oil-mix (300µl of 5 parts dibutylphthalate [Aldrich]: 4 parts dioctyl phthalate [Aldrich], v/v), thus preventing further uptake of permeant which remains in the aqueous layer. The pellets were retrieved and processed for scintillation counting of radiolabel incorporated into the cells using the protocol described below (section 2.2.7).

Non-mediated uptake of the respective permeant was assessed by determining the rate of uptake of the radiolabeled permeant in the presence of 1mM unlabelled permeant as well as with cells and permeant at 0 °C. The rate of uptake of the permeant was obtained from a plot of permeant concentration against time using Prism 4, GraphPad computer program. Using correlation coefficients the linear phase of the uptake was determined from the plot.

### 2.2.6 Dose-dependent uptake of permeant

Dose dependent uptake experiments allowed for the determination of  $IC_{50}$  and  $K_i$  values. Four times the required final concentration of radiolabeled permeant was mixed with an equal volume of an inhibitor also at 4× its final concentration. Two hundred micro litres of the mixture were carefully layered on top of 300 µl oil-mix in a 1.5 ml microfuge tube. The tube was centrifuged briefly at 13000 × g to collect the permeant/inhibitor mix into a single bubble at the top of the oil layer. An equal volume of a suspension of saponin-freed *P. falciparum* parasites was added to the microfuge tube so that it mixed with the radiolabel/inhibitor, and incubated for a predetermined time. The flux of radiolabel was terminated by the addition of 1 ml cold stop solution (1 mM of unlabelled permeant) and centrifuged at 13000 × g for 30 s. The cell pellets were retrieved and processed as described in section 2.2.7 and the amount of radiolabel incorporated was determined using a scintillation counter.

Inhibition and kinetic constants ( $IC_{50}$ ,  $K_i$  and  $K_m$ ) were generated by nonlinear curve fit using GraphPad Prism version 3.0 or 4.0.  $K_i$  values were calculated from the equation  $K_i = IC_{50} / (1 + (L/K_m))$ , where L is the permeant concentration. The  $K_m$  and  $V_{max}$  values were obtained for the transporter using the Michaelis-Menten plot.

### 2.2.7 Processing of sample after uptake assay

The parasite pellets were processed after the uptake using the method previously described by Saliba and colleagues (1998), with a slight modification (Saliba *et al*, 1998). The aqueous phase (which contained the un-incorporated radiolabel) was removed by aspiration and the inside walls of the tube carefully washed with distilled water. The water was aspirated out followed by the oil-mix. Any radioactive material remaining on the walls of the tube was removed by carefully wiping the tube walls with a piece of folded tissue. The cells were resuspended in 200µl of 1% Triton X-100 in distilled water for 10 minutes at room temperature (for the cells to lyse). Proteins in the mixture were precipitated with 200 µl of 5% trichloroacetic acid (TCA). The mixture was finally centrifuged for 7 minutes at  $13000 \times g$  and the supernatant transferred into a scintillation vial. 3ml scintillation fluid (OptiPhase 'HiSafe (Perkin Elmer)) was added and the radioactivity determined with the Perkin-Elmer 1450 Microbeta Wallac Trilux liquid scintillation and luminescence counter. All uptake experiments were performed in triplicate.

## 2.3 Molecular Techniques

### 2.3.1 Extraction of parasite DNA using InstaGene

*P. falciparum* DNA was extracted from infected erythrocytes using the InstaGene™ matrix (BioRad). 'InstaGene™ matrix is a specially formulated, 6% weight to volume Chelex® resin for the rapid isolation of small amounts of genomic DNA of sufficient purity for PCR' (<http://discover.bio-rad.com>). Five hundred microliters of culture material was centrifuged at  $4000 \times g$ , 5 min in a 1.5ml microfuge tube to pellet the cells. After discarding the supernatant, the cells were resuspended in 1ml autoclaved distilled water and incubated at room temperature for 30 minutes to lyse the erythrocytes. The suspension was centrifuged ( $10000 \times g$ , 2 min) and the supernatant removed and discarded. The pellets were incubated with 200 µl of InstaGene™ matrix at 56°C for 30 minutes. The mixture was vortexed at high speed for 10 seconds and put into a heating block at 100°C for 8 minutes. After a brief vortex, the mixture was centrifuged again at  $10000 \times g$  for a minute. The supernatant containing genomic DNA was transferred into a fresh tube and stored at -20°C until required. DNA prepared using this method is suitable for amplification using PCR.

### 2.3.2 DNA extraction using the phenol-chloroform method

The phenol-chloroform method described by Sambrook and co, is another DNA extraction method employed in this study, producing DNA of a higher purity, which is suitable for restriction digestion (Sambrook *et al*, 1989). Five milliliters of parasite culture at 5-10% parasitaemia were centrifuged at  $630 \times g$  for 10 minutes and the supernatant removed and discarded. The pellet was resuspended in equal volume of 0.15% saponin (w/v) and left to stand at room temperature for 20 minutes to lyse the erythrocytes. The mixture was centrifuged at  $3112 \times g$  for 10 minutes and the supernatant removed and discarded. The pellet was resuspended in equal volume of Buffer A (150mM NaCl, 25mM EDTA) and incubated for 30 minutes at room temperature. After centrifugation  $4000 \times g$ , 5 min, the pellet was washed 3 times with ice cold PBS and finally resuspended in 0.4ml of Buffer A. Next, 10 $\mu$ l of 10% SDS (sigma) and 50 $\mu$ g of proteinase K were added to the suspension and incubated overnight at 55°C. DNA was extracted by adding an equal volume of a 1:1 mixture of phenol and chloroform followed by gentle inversion of the tube. The mixture was centrifuged for 2 minutes at  $4000 \times g$  and the top aqueous layer transferred into a fresh tube. The phenol/chloroform extraction was repeated three more times on the supernatant. Finally, 400 $\mu$ l of ether were added, and after centrifugation the top layer (the ether phase) was removed and discarded. The tube was left opened to allow for the remaining traces of ether to evaporate. Eight hundred microliter of ice-cold absolute ethanol and 120  $\mu$ l of 3M sodium acetate were added and the mixture placed in a freezer at -70°C or in liquid nitrogen for 15-30 minutes. After centrifugation at  $4000 \times g$ , 5 min the ethanol was carefully removed and discarded and the tube left with its lid opened in a sterile flow to ensure complete evaporation of the ethanol. Finally, the residue (DNA) was resuspended in 50  $\mu$ l of distilled water or TE and stored at -20°C until required.

### 2.3.3 Purification of DNA using a mini-, midi- and max-prep kit

The QIAprep kits (QIAGEN) were used for purification of small to large amounts of DNA from plasmids. In all cases, the manufacturer's instructions from the product handbook were followed.

### 2.3.4 Polymerase chain reaction (PCR)

Polymerase Chain Reactions (PCR) were performed to amplify the DNA of interest from an appropriate template (mostly DNA extracted from *P. falciparum* clone 3D7). PCR reactions were performed in volumes of 20, 25 or 50 µl containing up to 500ng of genomic DNA template, 1.5mM of MgCl<sub>2</sub>, 0.2 mM dNTP mix, 100nM of forward and backward primers (specifically designed for the gene of interest and 1 Unit Taq polymerase (Roche). The mixture was made up to the required volume with DNase and RNase-free deionised water treated with 0.001% DEPC filtered through 0.2 micron filter and autoclaved (MP Biomedicals inc, Ohio). Thermal cycling was performed on a DNA Engine PTC – 200 Peltier Thermal Cycler (MJ Research Incorporated, USA). The annealing and extension temperatures chosen in this study were in most cases dependent on the average T<sub>m</sub> of the two primers used. Details of the cycling conditions are given elsewhere in this thesis.

### 2.3.5 Determination of DNA concentrations by spectrophotometry

The DNA concentrations of samples were determined using the standard spectrophotometric method. This method takes advantage of the UV light absorption property of the purines and pyrimidines rings present in DNA to measure the amount of DNA present in a sample. 1 µl of the DNA was added to 99 µl of DNase/ RNase-free deionised water. Absorbance at 260 or 280 was first blanked using DNase/ RNase-free deionised water in a cuvette. Absorbance of the mixture containing the DNA was then measured at 260 and 280nm. DNA concentration was calculated based on an OD of 1 corresponding to approximately 50 mg/ml for double-stranded DNA:

DNA concentration of the sample (mg/ml) = 50 mg/ml × Measured A<sub>260</sub> × dilution factor.

The OD<sub>260</sub>/OD<sub>280</sub> ratio for pure DNA is 1.8. Contamination by protein (which has an absorbance maximum of 280 nm) or phenol will cause the ratio to be significantly lower.

### 2.3.6 Agarose electrophoresis of DNA

DNA was separated on the basis of differences in molecular weight by electrophoresis on an agarose gel. The agarose gels (1.5%) were made in 1× Tris-Acetate-EDTA (TAE) with final solute concentrations of 40 mM Tris acetate and 1 mM EDTA, pH 8.0). The buffer contains 0.5 µg/ml of ethidium bromide for visualisation of the dsDNA under ultraviolet (UV) light. The gel was prepared using a standard gel apparatus (Horizon® Gibco BRL). DNA samples were mixed with ×6 Blue/orange loading buffer (15% Ficoll® 400, 0.03%

bromophenol blue, 0.03% xylene cyanol FF, 0.4% orange G, 10mM Tris-HCl (pH 7.5) and 50mM EDTA) supplied by Promega and ran at 120 mV. Voltage was obtained using the Whatman Biometra power supply model 250 supplied by Life technologies. A 100bp DNA ladder (Promega) was run in one of the wells to allow an estimation of the size of the DNA fragments.

### 2.3.7 Amplification of ENT DNA fragments

Primers were designed for amplification of fragments of the four genes (PF13\_0252, MAL8pl.32, PFa0160c and PF14\_0662), which are predicted to encode the equilibrative nucleoside transporter proteins of *P. falciparum*. The designed primer pair for each *ENT* gene (see Table 2.1) was purchased from MWG Biotech, Germany. The forward and reverse oligonucleotides primers for amplifying each fragment contained the restriction site for either *Bam*H1 or *Sac*II at the 5' end to facilitate cloning of insert (ENT fragment) into pCAM/BSL. Lyophilised primers received from suppliers were diluted appropriately as instructed by the manufacturers and stored at -20°C until required. DNA fragments from each of the four ENT genes were amplified by polymerase chain reaction (PCR), with a final reaction volume of 50µl, as described in section 2.3.7. The cycling conditions for each reaction are shown in Table 2.2. The size of each DNA fragment was verified by electrophoresis of 5µl amplicon on 1.5% agarose gel with the aid of a 1kb molecular weight maker (Invitrogen, UK) run alongside as described in section 2.3.4. The expected PCR product sizes are shown in Table 2.1.

About 40µl of each amplicon were purified using the Wizard<sup>®</sup> PCR Preps DNA Purification System (Promega, USA), following the supplier's instructions. The purification was necessary in order to remove excess nucleotides, enzymes, magnesium, buffer, DNA template and primers. The concentration of the purified DNA was then estimated by running an aliquot of the product on 1.5% agarose gel as usual using a SMART<sup>®</sup> DNA ladder (Eurogentec, Belgium) as a molecular weight marker. The colour intensity of the bands in the SMART DNA ladder is associated with the concentration of the DNA loaded. This therefore allows for the concentration of DNA product to be estimated by comparison of the intensity of the bands. By this means the concentration of each ENT DNA fragment amplified was obtained.

Since the DNA fragment is to be used in a gene disruption strategy, it was carefully chosen to remove the central transmembrane domains that are believed to be responsible for the translocation of purine permeant (reviewed by (de Koning *et al*, 2005). The size of the fragment was also chosen to maximise the probability of homologous recombination with the genomic copy of the gene following transfection. The sizes of the four fragments amplified in this study ranged between 675bp and 938bp. The sequences of the four fragments are shown in Figure 2.2 - Figure 2.5.

```

ATGAGTACCGGTAAAGAGTCATCTAAAGCTTATGCTGATATAGAATCCAGGGGTGATTATAAGGA
CGATGGAAAAGAAAGGATCTACATTAAGCAGTAAACAACATTTTCATGTTATCTTTAACCTTTATAT
TAATAGGTTTAAAGTTCTTTGAATGTATGGAATACAGCCTTAGGATTAAATATAAATTTTAAATAT
AATACCTTTTCAGAT TACAGGTTTAGTATGTTCCCTC AATTGTAGCTTTATTTGTTGAGATTCCCAA
AATAATGTTACCATTTCTTTTGGGTGGTTTATCAATTTTATGTGCAGGTTTTCAAATATCTCACA
GTTTTTTTACAGATACACAATTTGATACATATTGTTTAGTAGCTTTTATTGTTATTGGTGTAGTG
GCAGGATTAGCTCAAACCATTCATTTAATATAGGATCAACCATGGAAGATAATATGGGTGGTTA
TATGTCAGCAGGTATTGGTATATCAGGAGTATTTATTTTTGTTATTAATTTATTACTTGATCAAT
TCGTATCTCCCGAAAAACATTATGGTGTTAATAAAGCAAAGTTATTATATTTATATATAATCTGT
GAACTTTGTTAATATTAGCTATAGTATTTTGTGTATGTAATTTAGATTTAACAAACAAGAATAA
TAAAAAAGATGAAGAAAATAAAGAAAACAATGCCACATTATCTTATATGGAATTATTTAAAGATA
GTTACAAAGCTATATTAATCTATGTTTCTTGTAAGTGGTTAACTTTACAATTATTTCCAGGTGTT
GGACACAAAAAATGGCAAGAAAGTCATAATATCTCCGATTATAATGTTACCATTATTGTTGGTAT
GTTTCAAGTTTTTGATTTTCTCAGTAGATATCCACCAAAAT CTTACACATATTAAATCTTTAAAA
ATTTTACTTTCTCTTTAAATAAATTATTGGTTGCCAATTCATTGAGATTATTATTCATTCCATGG
TTTATTTTAAATGCATGTGTTGATCATCCATTTTCAAAAACATTGTACAACAATGTGTATGTAT
GGCTATGTTAGCTTTTACAAATGGTTGGTTTAATACTGTACCATTCTTGTATTTGTTAAAGAAT
TAAAAAAGCCAAGAAAAAGAAAGAAATCGAAATTATATCCACATTCTTAGTTATTGCTATGTTT
GTTGGATTATTCTGTGGTATATGGACTACATACATTTATAACTTATTCAATATAGTTTTACCAAA
GCCAGATTTACCACCCATCGATGTAACACAATAA

```

Figure 2.2: DNA sequence of gene encoding for ENT in *P. falciparum*. This is the gene with plasmidDB accession number PF13\_0252 (designated *PfNT1*).

Total size of the gene is 1269bp and the size of fragment prepared for disruption of the gene was 676 bp (shown in pink). Primers (including restriction sites, underlined) used to amplify the fragment are: *PfNT1* F: GGGGGATCCTACAGGTTTAGTATGTTCCCTC and *PfNT1* R: GGGCCGCGGATTTGGTGGATATCTACTGAG. These are highlighted in light blue in the figure. There were no introns present.

```

ATGAGTGACAGTCAGAGTAAGGATACGTTTCATACAACAGTGGGTGGATTATATGAGAAG
CCTAACAAAGTTTCGAGATATTGAATGTTTATATCCTTGTGATATTGAAAAAGTAGATACT
TTTGAAGAAGATAGGTATAAGAAGTTATTATGTGCAGCATATGCATTAATGGCTATAATA
GCTGATGCTCCATATTTTATGATTGTATCGATGGCTGATTATTTTAAAAGTACTTTTAAT
GTAAATGACGTTATGATAAATGAATTTGCCTTAATGGAAAGTTTAATATTGATTGTTGTT
TGTTCAATTATTACATTTAATTGGAAGTTATCGTTTAAAATGGAATTTACTTATGCCTATA
TTTATGACGATGATATTAGTTGTGTTAAATTTTGTGTTTATTTTAACTTGACTACATT
GGACATAAGATTATCATCTTCAGTGCTATACCTTTAGGTTTAGTATCTTGTATATCTAAA
ATGACTACTATGAAAATATGTGTTTTGTTTAAAAACGCCTATTGTAGTGCTTATGTATGT
GGATTATCTTTTTCAGGTTTTATAGTGTTTATAATATATATGTTAGGGGCATATGTGTTT
TTTCCGAATGATGAAATGAAATTTTTTAAGATGTTTACTTTTTTTTGTGTTGATTATTTGT
TCATTAGCATTAACATGTTTTTCTATCCTATACCGACTATACAAAAACGATTTGTGAAA
ATATTGGAAGAAAAGTATAAAGATAAAGGATTAAAAATTAATAGAAAAATATTTTATGAC
TCTATAAAATCAATGAAAATATTGTGGCCATATATGTTGATTTCATATTTTACAAGTTTA
TTGACTTATCAAATATATCCATCTATATTTCCAACCTTTTATGGATGTTAGTAAAGAATTA
AAAGGAACACTAGCTGGATTTTTATTATTTGGTGATTCTATGGCTCACTTATTAGTTCAT
TATAGAAGAAACGAATTTTTTAAAAACAGATTTTCTACATTAGTCTTTTGCACATTGTTC
GAATATTTTTTTGTACCTATATTTTTATTCTTGCCAAAGCTTCATTATATATATAACTTTA
GTTATTTTTATGTTGACTAGCTTTTCATTTTTATTTCGGACTAATGAATGGATTGGTGAATA
ATTTAATTTTTTTTGAAGCACCAGAAACGTGTAAAGAAAAAAGCAAATATGAATATATTC
AATTAACTCCAAATATACTTTACTTATGTTTAATTTTTTGAATAACCAGTGGGTGTTTAA
TATCCAAGGTTTCATGTAAGAATTGTGAATATAATTGCAGTTATTTTAAATAA

```

**Figure 2.3: DNA sequence of genes encoding for ENT in *P. falciparum*. This is the gene with plasmODB accession number, PF14\_0662 (designated: *PfNT2*).**

Total size of the gene is 1314 bp. Size of DNA segment amplified for disruption of ENT was 778 bp (shown in pink). Primers (including restriction sites, underlined) are: PfNT2 F: GGGGGGATCCGGCTATAATAGCTGATGC, PfNT2 R: GGGGCCGCGGGTGAGCCATGAATCACC. These are highlighted in yellow in the figure. There are no introns present.

```

ATGAGCAATTCTAATAGCAAGGAGCACTACAGAATGGACGGAATTACAGAAAATAAAATA
ATTAATGAAGATGATGAAAGTCTCTTGAACATGAAAAAGAAGAAATAATTTTAAATGGA
AAATTTGAAGAAGAGCCAAAGCTTGATTTAACGAAAAACAAATTGATATTGAAGAGAAG
AATAATAACATGAGTGAGTTTACAAATATTTTCCAAATATAACATTATGTTAATGGGA
ATGTCATCTGTATTAAATGTATAATTGTGTATTAAATACAAACACCTCATATACATGCATTA
TTAAATAAGAATATAGTAGTATCTTCAACCTTTTTTCTATATTTTTCTATTTTAGTTATT
GTATCATTGTTAAGTTCCTTATTTATAGAAGTAAAGACAAGACATATGATGTGTGTTTT
ATATTATCATTCATATTACAAATGATATATCCATTTATTATAAAATATTTTTATGATAAA
ACCGTTTTTTTTTATGTACTAGTAGCATTAAATTGGTGCTACGTGCTCTATGATGAAAACC
ATGATATTTTCCATATCTTCCATTGTTGTAAATGATTCAAAAGTTATTTGTTTATCATAT
GGTTTGACTGGGATATATTCTTTATTTATAACATCCACATTTTTTTATTTTGTTATTTAA
ATAAATAAAGATATACAAAAGTTGATGTTATCATTATTTATAACATCAGCCATCAATTGT
ATATTTATATTAGTGTCTTTTCTATGTTACACTGTATTAAAGAGAACAAATAATTTTAA
GAAAAATTTAAATTTTATACAGAAGAGAGAAAAAATAATAAAATTCACGTGATGATTCT
TATAAATATTATGAAAGTATAACTGAAAAAAATCACAAATATATCATATCCAATAAAT
ATTAATAGTATAATATATGAAAGTAAACAGAAAATACGGAATCCAAATATTCATTAACA
AAAAATGATTCTAACTCAGTTGGTATAAAAAGTAGTAGTAATAATACTAATAATATGACT
AGTAATGAAATAGGAGATCATAAAATATTACAAGAATCTCATTCAAAAATAAAAAATTT
AATGACATACTTCTTAATGAAATAAAACATTATCACTTACTCATAGTAAAAAGAAGAT
AACATAGATGACGAAAATAAAATCATAAAATCAATTCTTTCTATTTAATATAAAATAAA
AAAAATTTAATAAAACAAGCCAAATTAAGCATTCCTTATATAAAAAATCGTTCATATTT
TTATTTTGTAGCTTTTATAATATTTTTCTCAAAATATTATTATTCCTCGGTTGTTTGCCA
GAAATGTGGACTAATAATGTTGATGAAAGATATATATTAATTGGAATTGTGCAATTTGCT
GATTGTATAAGTCGTGTTCCTCCATCCCTTCCAGGAACATTTCCAGTATTTAAATTTTC
CTCTTGACACAAAAAAAAGTATTAATTTATTCTTTATTAAGAACTATCTTATCTGTAATA
GGATTGATAATACCATTAACACAAGATACATTTATTAATAATTTCTTTTTTAAATGTGCA
CTCATTTTTTTAAATATATATTTAAATGGTTGGTTTGTATCATGTCTTTTATTAATGTT
CCAGAAATTCCTCAAACCTATTAATTCATGAGTAATGTTGCAATAGTTAGTAGTTTTGGT
TCAACACTCCTTCGAGTTGGCTTGTTAACAGGCTATGGATGTTCCACACTATATAAATAT
ATCATATCAAAAATGTGA

```

Figure 2.4: DNA sequence of genes encoding for ENT in *P. falciparum*. The is the gene with plasmODB accession number MAL8P1.32 (designated *PfNT3*).

Total size of the gene is 1758 bp and the size of fragment prepared for disruption of the gene was 913 bp (indicated in pink). Primers (including restriction sites underlined) used to amplify the fragment are: *PfNT3* F: GGGGGGATCCTAGTAGCATTAAATTGGTGC and *PfNT3* R: GGGGCCGCGGCAAGGGATGGGAAACACG. The two primers are highlighted in green in the figure. There are no introns present.



```

ATGTTGAAGAAAAGCGAGGAGATCCAGATAAAGGTTATCTTTTTTTTTTATAGGTTTGCTTTT
GAGTTTACCCTCCCATATTTTAATAAATGTATCTTTTTTTGATTAATCACATATACAAGGAAG
AGATAGCTATAACGGTTATGGGTTTTTTATCAGGATTTATGATAATATCATCATTTTTTACAA
TTAACTTTTGAATTTACATCTTTTAAATGGATTATGATATGTAACGGATTAAATGTTTTTAA
TTTATTATTATTATTAAATTTTTGTATGTGTAATGAAATGTTCAAAATATTATATATATGGTA
TATCCGGGATTATCGGTTTTTTTTATTGGTTATTTGTATTTCATCGTGTACAAAATATTCTTTG
CTATTTCCCTTTAAAAGTCAATGGTTATATGGTTACAGGAATTAGTTTCTCTTCATTATTTTT
TTTTGCTATAAAATTTAATAATGTCGTATTTTTCTATCGAAGATGGTAATATAAGTTCATATT
ACAACACAATATATTTATCCATAGGAAGTATAGTTCATTATACTTGTTTGTATAATTTTTTAT
ACAATATAATTTCTCCATATTTCAAGGAGCAAAAAGAGAAAATAGAAAGTGCACAGAACAAAA
AATGTATTGAATATAATGGATCGAATGATTTATGTGAAGTTGAAAAAGGAAAAAACAAATCA
TCAGAAAATATCCAGAGTAATAATGTCTCTATGATAAGTAAATGTAAAAATAAAATTAATAA
TGTTGGAAAAATGTTTAATTGTGCTAATAATAATTGAGGGAGCTTGTTTAATAAGATATTATT
ATTTATGTTTAATACCTATATTCTTTTCATTTTTTCGTGACCTCTATAATATATCCTCACATG
AGTAAGCAAAAAAAAAAAAAAAAAAATAAAGGAAAATGAAACAAGTCTATAAATATTTAATATATT
ATATATATAGATAGATATATGTATGTATGTATGTTTATGTTTATGTTTATGTTTGTGTTTAT
GTTTATGTTTATGTTTATGTTTGTGTTTATGTTTATGTTTATGTTTATGTTTGTGTTTATGTT
TTGTGTTTATGTTTATGTTTATGTTTGTGTTTATGTTTATGTTTATGTTTATGTTTATGTTTAT
TTTTAGTTCCGAATAAGCTGAAGAAGAACGTATATTACAAATACCTGTTTATGTTTCTTTAC
CAACTCAGTGATCTTATATTCATATCATTGTGACTGTTTATTATAGTGCTTTTAACTTTTT
TAAACAAAAATATGTTGCCATATTATGTTTAAAGCAGAATCCTTCTTTTGCTATTATCCTTTA
AAATTAAGAATTTAACTGAAGCATCCTTTTTATATTCTAATACTTTTTTGTCAATTCCTAATA
TTTGTAATAGGAGGTACGAATGGTTCTTTGATCAATATTAGTTATGCCAGAATATCAGACTG
TTTTGAAGAATCAAATAAGAAAACCAACAAATCGCTGTGGCATCATCCTTCTGTGCTTTAT
GTCTATTAATGAGTTTTTGCATTAGCACCATGGTTTTGTAATGCAATAATTCATTTGTAA

```

Figure 2.5: Unspliced DNA sequence of genes encoding for ENT in *P. falciparum*. This is the gene with plasmid DB accession number PFA0160C (designated *PfNT4*).

Total size of the gene is 1558 bp and the size of fragment prepared for disruption of the gene is 938 bp, (shown in pink). Primers (including restriction sites, underlined) used to amplify the fragment are PfNT4 F: GGGGGGATCCGAAGAGATAGCTATAACGG, PfNT4 R: GGGGCCGCGGCTTATTCGAATCATGTGA. The primers are highlighted in blue in the figure. A 253bp intron is present and is highlighted in bright green.

Gene	Size of DNA (bp)	Fragment amplified (bp)	Product size (bp)	Primer sequence
<b>PF13_0252</b> ( <i>PfNT1</i> )	1269	210-885	676	<i>PfNT1</i> F=TACAGGTTTAGTATGTTCTC <i>PfNT1</i> R=ATTTGGTGGATATCTACTGAG
<b>PF14_0662</b> ( <i>PfNT2</i> )	1314	170-948	778	<i>PfNT2</i> F=GGCTATAATAGCTGATG <i>PfNT2</i> R=GTGAGCCATAGAATCAC
<b>MAL8pl.3 2</b> ( <i>PfNT3</i> )	1758	498-1411	913	<i>PfNT3</i> F=CTAGTAGCATTAAATTGGTGC <i>PfNT3</i> R=CAAGGGATGGGAAAACACG
<b>PFA0160c</b> ( <i>PfNT4</i> )	1558	270-955	938*	<i>PfNT4</i> F=GTATGTGTAATGAAATGTCC <i>PfNT4</i> R=ATATAAGATCACTGAGTTGG

Table 2.1: A table showing the size of each of the four *P. falciparum* equilibrative nucleoside transporter genes, the size of each fragment cloned into pCAM/BSL and the primer pairs used to amplify each of the DNA fragments.

\*Presence of 243 bp intron

Gene	Cycling conditions
<b>PF13_0252</b> ( <i>PfNT1</i> )	94°C, 3 min/ 94°C, 30 s/ 48°C, 1 min/ 70°C, 1 min/ ×35cycles/ 70°C, 5 min
<b>PF14_0662</b> ( <i>PfNT2</i> )	94°C, 3 min/ 94°C, 30 s/ 53°C, 1 min/ 65°C, 2 min/ ×30 cycles/ 65°C, 5 min
<b>MAL8pl.32</b> ( <i>PfNT3</i> )	94°C, 3 min/ 94°C, 30 s/ 53°C, 1 min/ 65°C, 2 min/ 30 cycles/ 65°C, 5 min
<b>PFA0160</b> ( <i>PfNT4</i> )	94°C, 3 min/ 94°C, 30 s/ 53°C, 1 min/ 65°C, 2 min/ ×30 cycles/ 65°C, 5 min

Table 2.2: Cycling condition for the amplification of the four *P. falciparum* equilibrative nucleoside transporter genes.

Order of events: Initial denaturation/ denaturation/ annealing/ extension/ number of cycles/ final extension.

### 2.3.8 Purification of the ENT DNA fragments

The ENT amplicons prepared above were purified using the Wizard<sup>®</sup> PCR Preps DNA Purification kit (Promega). This process ensures removal of PCR enzyme, buffer, excess nucleotides, magnesium, template DNA and primers. 100µl of amplicon were prepared for each gene, and purified using the kit. Two micro litres of the purified product obtained were loaded and run on a 1.5% agarose gel to confirm the size as well as to estimate the DNA concentration. A SMART<sup>®</sup> DNA ladder (EUROGENTEC) was used as a molecular weight marker and to allow for an estimation of DNA concentration, as the 1000bp band contains a known quantity of DNA (100ng).

### 2.3.9 Plasmid used in preparing DNA construct

PCAM/BSD was the plasmid chosen for the preparation of the construct that would be used to disrupt the *ENT* gene in *P. falciparum*. The initial plasmid was a gift from the group of Christian Doering (INSERM U609, Wellcome Centre for Molecular Parasitology, Anderson College, Glasgow). pCAM-BSD is a 4519bp vector which expresses the blasticidin-S-deaminase (BSD) selectable marker that is under the control of a 0.6-kb *P. falciparum* calmodulin 5' untranslated region (UTR) and a 0.6-kb hrp2 3' UTR (Sidhu *et al.*, 2005). Transformed cells can be selected with 100mg/ml ampicillin in *E. coli* culture and with 2.5 µg/ml blasticidin in cultures containing *P. falciparum*. The plasmid has restriction site for numerous enzymes including *Bam* H1 and *Sac* II.

A larger quantity of the plasmid was prepared from the gift received using the procedure described below. DH5-α chemically competent cells (Invitrogen, UK) were transformed with the plasmid as described in section 2.3.12. After propagation of the bacteria overnight, the plasmid was retrieved and purified using the method described in section 2.3.13. Plasmid was store at -80°C until required. Stablate of the transformed cells was also prepared by mixing 500µl of the transformed bacteria culture with 250 µl sterile glycerol. The mixture was allowed to stand for one hour at room temperature and stored at -80°C.

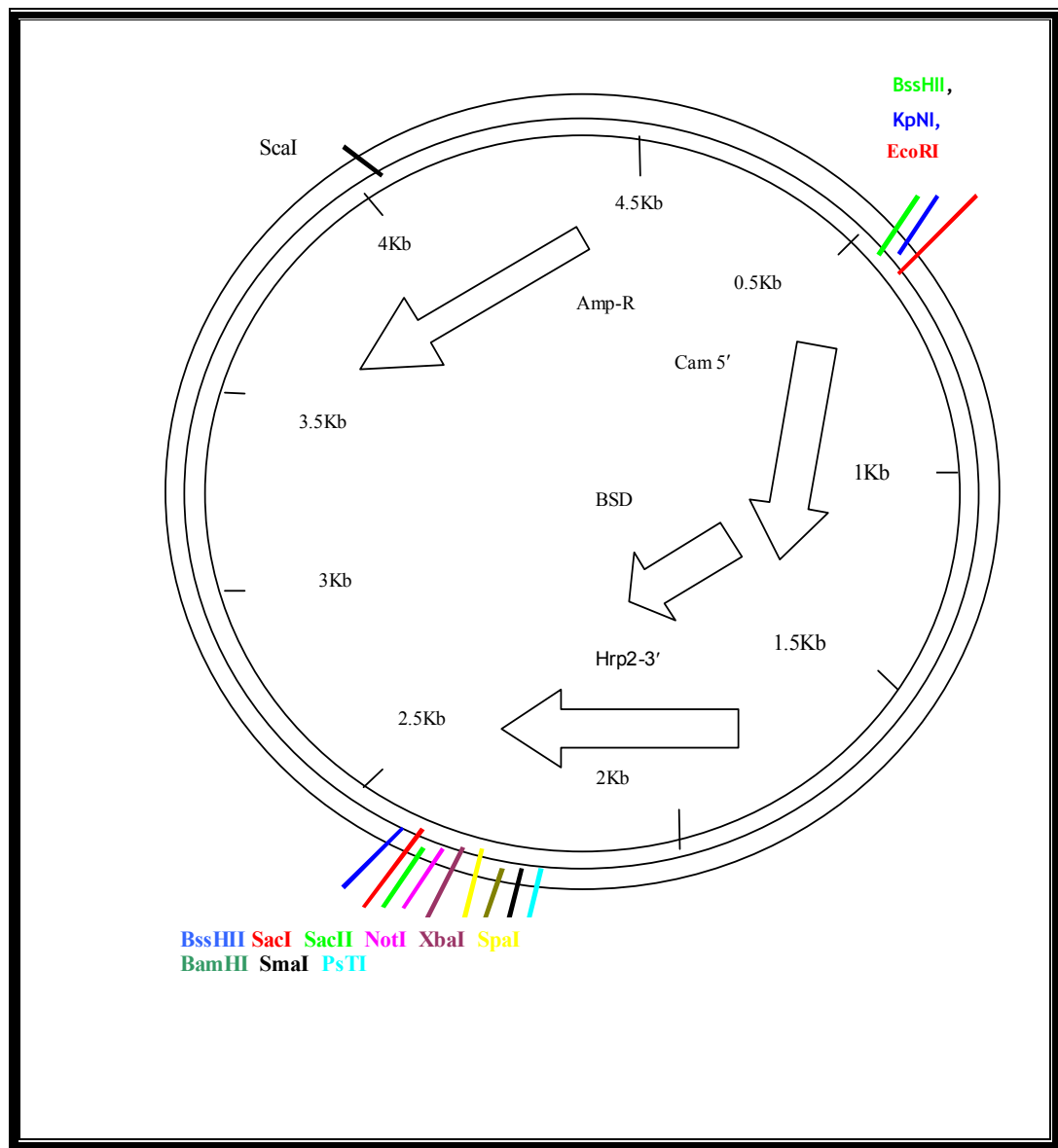


Figure 2.6: Schematic presentation of the vector pCAM-BSD.

The plasmid has a total length of 4519 bp with ampicillin (AMP-R) resistance genes. Transformed cells can therefore be selected with 100 µg/ml ampicillin in *E. coli* culture. The figure also shows the *Bam*HI and *Sac*II restriction site where the cloning of the ENT fragment was done. This transfection plasmid also expresses the blasticidin-S-deaminase (BSD) selectable marker, which is under the control of a 0.6-kb *P. falciparum* calmodulin 5' untranslated region (UTR) and a 0.6-kb hrp2 3' (UTR). Re drawn from (Sidhu *et al*, 2005).

```

CTAAATTGTAAGCGTTAATATTTTGTAAAATTGCGTTAAATTTTGTAAATCAGCTCATTTTTTAACCAATAG
GCCGAAATCGGCAAAATCCCTTATAAATCAAAAGAATAGACCGAGATAGGGTTGAGTGTGTTCCAGTTTGGAAACA
AGAGTCCACTATTAAAGAACGTGGACTCCAACGTCAAAGGGCGAAAAACCGTCTATCAGGGCGATGGCCCACTACG
TGAACCATCACCTTAATCAAGTTTTTTGGGGTCGAGGTGCCGTAAAGCACTAAATCGGAACCTAAAGGGAGCCCC
CGATTTAGAGCTTGACGGGGAAAGCCGGCGAACGTGGCGAGAAAGGAAGGGAAGAAAGCGAAAGGAGCGGGCGCTA
GGGCGCTGGCAAGTATAGCGTACAGTGTGCGCGTAACCAACACCCGCGCGCTTAATGCGCCGCTACAGGGCGC
GTCCCATTCGCCATTAGGCTGCGCAACTGTTGGAAGGGCGATCGGTGCGGGCTCTTCGCTATTACGCCAGCTG
GCGAAAGGGGATGTGCTGCAAGGCGATTAAGTTGGGTAAAGCCAGGGTTTTCCAGTCACGACGTTGTAAACGA
CGGCCAGTGAGCGCGCGTAATACGACTCACTATAGGGCGAATTGGGTACCCCATGGGAATCTATATGTGATTAAT
TTTATATATTATCAATTTATATATTTTTTAAATGCTTACTTAATTATCTTTTTTTTTTTTTTTTTTTTTTTTTCC
TCTTTTTATATTAAATTTATTTTGAATAATTTGATATATATATATATATAATAATATATATATACATGTAGTAGT
ATTAAACAATGTATAATATATAATAAATATATTTATATATTTTCATTTCAATTTTAATTTTTTTTGGTTTTTTTT
TTTTTCTTTTTGTTCATATTTAAAAAAATTTATATTCATATAAGTTATGCATTTTTTATAAACATTATTCAATATA
TGTATAATATAATATATATATATATATTAATGTATTATTTCAATGTGCATGATAAAGAAAAAAATTAATATTATA
AAAAAAGAAAAATAAAACAAAAAAGAAAAAAGAAAAAAGAAAAAATACAAAAATAAATAATATAATTT
ATAATTATATATTTCTGTCAATAAAAAATATATATATATATATATATATATATTTATAATATGTATATTTTAACTAGA
AAAGGAATAACTAATATTTTATTTATTTATCATTTCAAGATTTATATTTTATAATAATAAATACCTAATAGAAATATA
TCAATGGTGCATGCCAAGCCTTTGTCTCAAGAAGAAATCCACCTCATTTGAAAGAGCAACGGCTACAATCAACAGCA
TCCCCATCTCTGAAGACTACAGCGTCGCCAGCGCAGCTCTCTCTAGCGACGGCCGCATCTTCACTGGTGTCAATGT
ATATCATTTTACTGGGGGACCTTGTGCAAGCTCGTGGTGTCTGGGCACTGCTGCTGCTGCGGAGCTGGCAACCTG
ACTTGTATCTGCGCATCGGAAATGAGAAGCAGGGGCACTTTGAGCCCTGCGGACGGTGACGACAGCTGCTTCG
ATCTGCATCCTGGGATCAAAGCGATAGTGAAGGACAGTGATGGACAGCCGACGGCAGTTGGGATTCTGTAATTGCT
GCCCTCTGGTTATGTGTGGGAGGGCTAAGCTTTAATAATAGATTAAAAATATTATAAAAAATAAACATAAACACA
GAAATTACAAAAAATACATATGAATTTTTTTTTTGTAACTCTTCCTTATAAATATAGAATAATGAATCATATAAA
ACATATCATTATTTTATTTACATTTAAATTTATTTTGTTCAGTATCTTTAATTTATTTATGTATATAAAAAATA
ACTTACAAATTTTATTTAATAAACAATATATGTTTATTAATTTTGTAAATTTATGGGATAGCATTTTTTTTTTA
CTGTCTGTATTTTTCTTTTTTAATTATGTTTTAATTGTATTTTATTTTATTATTTGTTCTTTTTATAGTATTATTT
TAAACAAAATGTATTTCTAAGAACTTATAATAATAATAAATATAAATTTTAAATAAAATTTATTTATCTTTTA
CAATATGAACATAAAGTACAACATTAATATATAGCTTTTAAATTTTATTTCTCAATCATGTAAATCTTAAATTTT
TCTTTTTTAAACATATGTTAAATATTTTATTTCTCATTTATATAAGAACATATTTTAACTGCAGCCCGGGGAT
CCACTAGTTCTAGACGGCGCCGCCCGCTGGAGCTCCAGCTTTTGTTCCTTTAGTGAGGGTTAATTGCGCGCT
TGGCGTATCATGGTCATAGCTGTTTCTGTGTGAAATTTGTTATCCGCTCACAAATCCACACAACATACGAGCCGG
AAGCATAAAGTGTAAGCCTGGGGTGCCTAATGAGTGAGCTAACTCACATTAATTGCGTTGCGCTCACTGCCCGCT
TTCCAGTCGGGAAACCTGTCTGTCAGCTGCATTAATGAATCGGCCAACGCGCGGGGAGAGGCGGTTTGCCTATTG
GGCGCTCTTCCGCTTCTCGCTCACTGACTCGCTGCGCTCGGTGCTTCCGCTGCGGCGAGCGGTATCAGTCACTC
AAAGCGGTAAATACCGTTATCCACAGAATCAGGGGATAACAGCAGGAAAGAACATGTGAGCAAAAGGCCAGCAAAAG
GCCAGAACCGTAAAAAGGCCGCGTTGCTGGCGTTTTTCCATAGGCTCCGCCCCCTGACGAGCATCACAAAAATC
GACGCTCAAGTCAGAGGTGGCGAAACCCGACAGGACTATAAAGATACAGGCGTTTCCCCCTGGAAGCTCCCTCGT
GCGCTCTCTGTTCCGACCTGCGCGTTACCGGATACCTGTCCGCTTCTCCTTCCGGAGCGTGGCGCTTTCT
CATAGCTCAGCTGTAGGTATCTCAGTTCCGTTAGGTGCTTCCGCTCAAGCTGGGCTGTGTGCACGAACCCCCG
TTCAGCCCGTATACCGTGTGCGCTTATCCGTTAACTATCTGCTTTGAGTCCAACCCGTTAAGACACGACTTATCGCCACT
GGCAGCAGCCACTGGTAACAGGATTAGCAGAGCGAGGTATGTAGGCGGTGCTACAGAGTTCTTGAAGTGGTGGCCT
AACTACGGCTACACTAGAAGGACAGTATTTGGTATCTGCGCTCTGCTGAAGCCAGTTACCTTCGAAAAAGAGTTG
TAGCTCTTGATCCGGCAACAAACCCGCTGGTAGCGGTGGTTTTTTTGTGTTGCAAGCAGCAGATTACGCGCAG
AAAAAAGGATCTCAAGAAGATCCTTTGATCTTTTACGGGGTCTGACGCTCAGTGGAACGAAAACTCACGTTAA
GGGATTTTGGTCATGAGATTATCAAAAAGGATCTTCACTTAGATCTTTTAAATTAATAAATGAAGTTTAAATCAA
TCTAAAGTATATATGAGTAACTTGGTCTGACAGTTACCAATGCTTAATCAGTGAGGCACCTATCTCAGCGATCTG
TCTATTTCTGTTTATCCATAGTTGCTGACTCCCCGTCGTGTAGATAACTACGATACGGGAGGGCTTACCATCTGGC
CCCAGTGTGCAATGATACCGGAGACCCACGCTCACCGGCTCCAGATTTATCAGCAATAAACAGCCAGCCGGA
GGGCCGAGCGCAGAAGTGGTCTGCACTTTATCCGCTCCATCCAGTCTATTAATTGTTGCGGGGAAGCTAGAGT
AAGTAGTTCGCCAGTTAATAGTTTGGCAACGTTGTTGCCATTGCTACAGGCATCGTGGTGTACGCTCGTCTGTTT
GGTATGGCTTCATTCAGCTCCGTTCCCAACGATCAAGGCGAGTTACATGATCCCCATGTTGTGCAAAAAAGCGG
TTAGCTCTTCCGTCCTCCGATCGTTGTGCAAGTAAGTTGGCCGAGTGTATCACTCATGGTTATGGCAGCACT
GCATAATCTCTTACTGTATGCCATCCGTAAGATGCTTTTCTGTGACTGGTGAGTACTCAACCAAGTCATTCTGA
GAATAGTGTATGCGGCGACCGAGTTGCTCTTGCCCGGCTCAATACGGGATAAATACCGCGCCACATAGCAGAACTT
TAAAGTGTCTCATCATTTGAAAAACGTTCTCGGGCGAAAACTCTCAAGGATCTTACCGCTGTTGAGATCCAGTTT
GATGTAACCCACTCGTGACCCAACCTGATCTTCAAGCATCTTTACTTTTACCAGCGTTTCTGGGTGAGCAAAAAACA
GGAAGGCAAAATGCCGCAAAAAAGGAATAAGGGCGACACGGAAATGTTGAATACTCATACTCTTCTTTTCAAT
ATTATTGAAGCATTATCAGGGTATTGTCTCATGAGCGGATACATATTTGAATGTATTAGAAAAATAAACAAAT
AGGGGTTCGCGCACATTTCCCGAAAAAGTGCCAC

```

Figure 2.7: DNA sequence of the 4519bp pCAM-BSD.

The figure shows the restriction site for *Bam*H1 (underlined bold blue colour), *Sac*II (underlined red colour) and the forward (pCAM-BSD\_ F2) and reverse primers (pCAM-BSD\_ R2) that are highlighted purple and light green respectively.

### 2.3.10 Restriction digestion of ENT DNA or pCAM-BSD plasmid

In order to create sticky ends, the plasmid and ENT fragments were digested with *Bam*H1 and *Sac*II (Promega, USA). A 20µl digestion-mix was prepared containing 1µl of either 1µg/µl plasmid (pCAM-BSD) or the purified DNA fragment of the *ENT* gene, 2µl ×10 buffer C [100 mM Tris-HCl, (pH 7.9), 500 mM NaCl, 100 mM MgCl, and 10 mM DTT], 0.5 µl *Bam* H1 (10u/µl), 0.5 µl *Sac* II (10u/µl) and 16.0 µl DNase/ RNase-free water.

*Sac* II recognises the restriction site: 5' ...CC GC▼GG...3'  
3' ...GG▲CG CC...5'

*Bam* H1 recognises: 5'...G▼GATC C...3'  
3'...C CTAG▲G...5'.

Digestion was performed overnight at 37°C for 5-6 hours and was terminated by heat inactivation of the enzyme at 70°C for 10 minutes. To confirm that digestion of both plasmid and the *ENT* fragment was successful, 2 µl of the digested product were run on 1.5% agarose gel alongside the uncut DNA using the procedure described in section 2.3.6.

### 2.3.11 Ligation of ENT fragment into pCAM-BSD

The DNA fragments of *ENT* were subcloned into pCAM-BSD plasmid at the *Bam* HI and *Sac* II restriction sites (Figure 2.6) using T4 DNA ligase (Invitrogen). The T4 DNA ligase which was originally isolated from *E. coli* lambda lysogen can join DNA fragments with staggered or blunt ends (Invitrogen). Three different reaction-mixes containing the following ratio of insert and vector were set up:

<b>Tube A</b>	1 part insert: 1 part vector
<b>Tube B</b>	2.5 part insert: 1 part vector
<b>Tube C (control)</b>	0 part insert: 1 part vector

Each tube contains a 20 µl reaction mix made up of, vector: insert ratio (as stated above, with a total DNA concentration of 500 ng), 4 µl of ×5 ligase buffer (250mM Tris-HCl [pH 7.6], 50 mM MgCl<sub>2</sub>, 5 mM ATP, 5 mM DTT and 25% [w/v] polyethylene glycol-8000), 1U ligase (1U/µl) and top up with Dnase/RNase-free deionised water. The digest was incubated at 14°C overnight. The resultant DNA construct was denoted pCAM-BSD/*ENT*

### 2.3.12 Transforming DH5 $\alpha$ cells with (pCAM-BSD/ENT)

DH5- $\alpha$  chemically competent cells (Invitrogen) were transformed with the constructed plasmid (pCAM-BSD/ENT) using the heat-shock method (Sambrook *et al.*, 1989). Briefly, 50  $\mu$ l of the stock DH5- $\alpha$  chemically competent cells were pre-incubated with 50 ng of pCAM-BSD/ENT construct on ice for 30 minutes followed by heat shock at 42°C for 45 seconds. The suspension was placed on ice immediately for two minutes for the bacteria cells to recover. Two hundred and fifty micro litres of Super Optimal broth (SOC) medium (0.5% Yeast Extract, 2% Tryptone, 10 mM NaCl, 2.5 mM KCl, 10 mM MgCl<sub>2</sub>, 10 mM MgSO<sub>4</sub>, 20 mM Glucose) were added to the transformed bacterial cells. The transformants were incubated at 37°C for one hour in order for the antibiotic (ampicillin) resistance gene to be expressed. 100  $\mu$ l of the transformed cells was spread under sterile condition on Luria-Bertani (LB) agar containing 1% bacto tryptone, 0.5% yeast extract, 1%NaCl 1 per cent, 0.1% glucose. The plate also contains ampicillin (100 $\mu$ g/ml) to allow for selection of transformed cells. The inoculated plate was incubated overnight at 37°C. A plate with untransformed bacteria cells was set up as a control.

Success of the transformation was checked by PCR using the ENT-forward and reverse primers shown in Table 2.2. Single bacteria colonies were picked into 1 $\times$  sterile PBS. The mixture was used as the DNA template in a PCR reaction set up using the method and cycling conditions described in section 2.3.7. 2  $\mu$ l of the PCR product were run on 1.5% agarose gel along side a molecular size marker. The expected band sizes are as shown in Table 2.1.

To obtain large copies of the pCAM-BSD/ENT construct, a single colony of the transformed bacteria cells on the plate was picked into 500ml liquid LB (containing 100 $\mu$ g/ml ampicillin). The culture was incubated in a shaking incubator at 37°C, 225 rpm. Incubation was terminated when the OD<sub>600</sub> of the culture reaches 0.5-0.75.

### 2.3.13 Retrieval and purification of pCAM-BSD/ENT

Following propagation of the bacteria cells containing the pCAM-BSD/ENT construct, the culture was centrifuged at  $6000 \times g$  for 15 minutes (at  $4^{\circ}\text{C}$ ) to pellet the cells. The construct was retrieved from the pellet and purified using a maxi DNA purification kit (Qiagen) following the manufacturer's instructions. The purified DNA was re-dissolved in  $150 \mu\text{l}$  of DNase/RNase-free deionised water. The concentration of pCAM-BSD/ENT DNA was estimated using the spectrophotometric method described in section 2.3.5. The purified plasmid DNA was stored at  $-70^{\circ}\text{C}$  until required. The presence of the ENT fragment within the construct was confirmed by PCR and restriction digest of pCAM-BSD/ENT. Using the ENT forward and reverse primers shown in Table 2.2, the ENT insert was amplified by PCR. The PCR method used is as described in section 2.3.7. The PCR amplification was followed by gel electrophoresis of the PCR product. The expected band sizes are as shown in Table 2.1.

A  $10 \mu\text{l}$  enzyme digest-mix was also set up in order to confirm the presence of the ENT fragment in the construct. The digestion-mix consisted of  $1 \mu\text{l}$  of  $10\times$  buffer C,  $2 \mu\text{l}$  purified pCAM-BSD/ENT construct,  $0.2 \mu\text{l}$  *Bam* H1,  $2 \mu\text{l}$  *Sac* II and  $6.6 \mu\text{l}$  with DNase/RNase-free deionised water. Digest-mix was incubated at  $37^{\circ}\text{C}$  for 3 hours followed by electrophoresis of  $5\text{--}8 \mu\text{l}$  of the digest-product on 1.5% agarose gel.

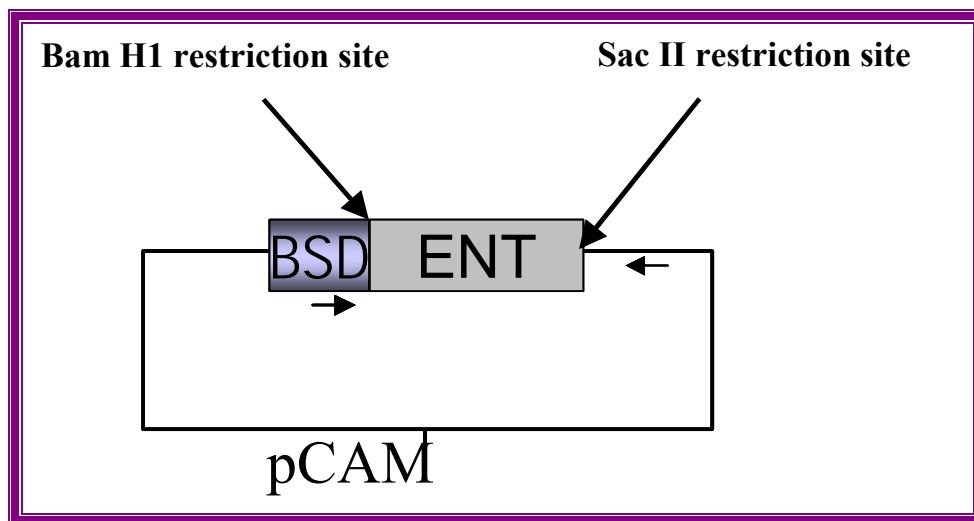


Figure 2.8: PCAM-BSD/ENT construct showing the restriction sites for *Sac* II and *Bam* H1.



### 2.3.14 Sequencing of pCAM-BSD/ENT

In order to confirm the presence of the entire coding region of the *ENT* fragment in the construct and also to verify whether the sequences matches that enlisted in the PlasmoDB for the gene, an aliquot of the purified pCAM/BSD-*ENT* construct was sent for sequencing at the University of Dundee Sequencing Service (DSS). Purified pCAM/BSD-*ENT* construct at a concentration of 600 ng/30 µl H<sub>2</sub>O and 3.2 µM of the pCAM/BSD forward primer were sent.

## 2.4 Transfection of *P. falciparum* by electroporation

*P. falciparum* parasite, clone 3D7, was transfected with the PCAM-BSD/*ENT* construct using previously described methods (Sidhu and Fidock, 2005). Briefly, a 3 ml culture at around 5-6% parasitaemia (predominantly of ring-stage parasites) was washed with an incomplete cytomix (120 mM KCl, 0.15 mM CaCl<sub>2</sub>, 2 mM EGTA, 5 mM MgCl<sub>2</sub>, 10 mM K<sub>2</sub>HPO<sub>4</sub>/ KH<sub>2</sub>PO<sub>4</sub>, 25 mM Hepes, pH 7.6). The parasite pellets were then re-suspended to a final volume of 400µl in an incomplete cytomix containing 100 µg of the purified DNA construct. Electroporation of the parasites was performed in a 0.2 cm cuvette using a GenePulser (Bio-Rad) set at 0.33 kv and 950 µF. Control cells were treated similarly except that the cytomix did not contain any DNA construct. After electroporation, samples were mixed with fresh erythrocytes to give a 5% haematocrit in normal complete culture medium RPMI1640 with 10% human serum, supplemented with 1mM adenosine, hypoxanthine and inosine. The culture was maintained under standard conditions as described in section 2.1.4.

### 2.4.1 Selection of transfected *P. falciparum* parasites

Forty-eight hours after transfection, blasticidin (CALBIOCHEM, Merck Biosciences Ltd, Nottingham) was added to the culture to a final concentration of 2.5µg/ml in order to select for transfected cells containing the construct (PCAM-BSD/*ENT*). The culture was maintained under constant 2.5 µg/ml blasticidin drug pressures. The pCAM-BSD vector contains a cassette conferring resistance to blasticidin (BSD) as a positive selectable marker (Sidhu *et al.*, 2005). As the parasite is haploid and *ENT* is a single copy gene, only one round of drug selection is necessary to obtain a null-mutant. Blasticidin-resistant parasites appeared after 3-4 weeks of selective culture.

### 2.4.2 Verification of integration by PCR

Integration of the episome through homologous recombination into the parasite's genome was verified by PCR examination of the genotype of blasticidin-resistant parasite populations at the *ENT* locus. This was done using different combinations of primers (see Table 2.4) which allow to distinguish between: (i) the wild-type locus, (ii) the 5' integration event, (iii) the 3' integration event, and (iv) the episomal form of the transfected plasmid (Figure 2.9).

Genomic DNA from the control parasites (3D7 clones of *P. falciparum*) and the transfectant was extracted using previously published method (2.3.2). The DNA was subjected to amplification using the following PCR primer pairs: *PfNT* UP and *PfNT* DOWN; pCAM-BSD F2 and PCAM-BSD R2. Primers *PfNT* UP and *PfNT* DOWN correspond to *PfNT* sequences up and down stream the *ENT* gene respectively, while primers pCAM-BSD F2 and pCAM-BSD R2 correspond to pCAM-BSD vector sequences flanking the insertion site. Primers for the four *ENT* genes were designated with the prefix *PfNT1*, *PfNT2*, *PfNT3* and *PfNT4* corresponding to Pf13\_0252, Pf14\_0662, MAL8pl.32 and Pfa0160c respectively. Parasites with disrupted *ENT* gene were designated 3D7Δ*PfNT1*, 3D7Δ*PfNT2*, 3D7Δ*PfNT3* and 3D7Δ*PfNT4* for the corresponding Pf13\_0252, Pf14\_0662, MAL8pl.32 and Pfa0160c genes respectively.

Primer	Sequence
<i>PfNT1</i> Up	5' TATGGAATACAGCCTTAGG 3'
<i>PfNT1</i> Down	5' CTAACATAGCCATACATACAC 3'
<i>PfNT2</i> Up	5' GGATACGTTTCATACAACAG 3'
<i>PfNT2</i> Down	5' CACAATTCTTACATGAACC 3'
<i>PfNT3</i> Up	5'CACTACAGAATGGACGGAATTACA3'
<i>PfNT3</i> Down	5'ATCCATAGCCTGTTAACAAGCCAA3'
<i>PfNT4</i> Up	5' GAGGAGATCCAGATAAAGGTTA'
<i>PfNT4</i> Down	5' TCTGATATTCTGGCATAACTAATA3'
pCAM-BSD_F2	5' ATTTATTAAACTGCAGCCC 3'
pCAM-BSD_R2	5' AAGCTGGAGCTCCACCGC 3'

**Table 2.3:** Primers used to check integration of the episomes: *PfNT1*, *PfNT2*, *PfNT3* and *PfNT4*.

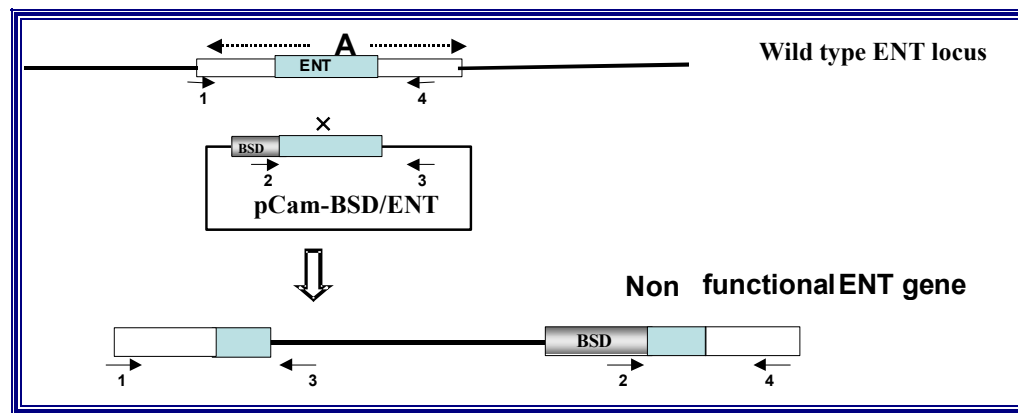


Figure 2.9: Confirmation of integration in *P. falciparum* transfectant lacking the *ENT* gene. 'A' is the entire *ENT* gene and the part in light blue colour (labelled ENT) represent the fragment used in preparing the construct. The primers for checking the various integration events are marked 1-4. Combination of 1 + 3: indicate integration at 5' end; 2 + 4: indicate integration at 3' end; 2 + 3: indicate the presence of the episome; 1 + 4: indicate the presence of the ENT Wild type locus. NB: 1 = *PfNT* Up; 2 = pCAM F2; 3 = pCAM R2; 4 = *PfNT* Down.

Primer combination	Cycling condition	Expected product size (bp)
<i>PfNT1</i> UP+pCAM R2 (1+3)	94°C, 3min/ 94°C, 30sec/ 55°C, 1min/ 62°C, 2min/ 25 cycles/ 62°C, 5min	731
<i>PfNT1</i> Down+pCAM F2 (2+4)		840
pCAM F2+pCAM R2 (2+3)		712
<i>PfNT1</i> Up+NT1 Down (1+4)		895
<i>PfNT2</i> UP+pCAM R2 (1+3)	94°C, 3min/ 94°C, 30sec/ 55°C, 1min/ 62°C, 2min/ 25 cycles/ 62°C, 5min	942
<i>PfNT2</i> Down+pCAM F2 (2+4)		1138
pCAM F2+pCAM R2 (2+3)		818
<i>PfNT2</i> Up+NT2 Down (1+4)		1266
<i>PfNT3</i> UP+pCAM R2 (1+3)	94°C, 3min/ 94°C, 30sec/ 55°C, 1min/ 62°C, 2min/ 25 cycles/ 62°C, 5min	1401
<i>PfNT3</i> Down+pCAM F2 (2+4)		1244
pCAM F2+pCAM R2 (2+3)		949
<i>PfNT3</i> Up+NT3 Down (1+4)		1696
<i>PfNT4</i> UP+pCAM R2 (1+3)	94°C, 3min/ 94°C, 30sec/ 55°C, 1min/ 62°C, 2min/ 25 cycles/ 62°C, 5min	1196
<i>PfNT4</i> Down+pCAM F2 (2+4)		1173
pCAM F2+pCAM R2 (2+3)		963
<i>PfNT4</i> Up+ <i>PfNT4</i> Down (1+4)		1408

Table 2.4: Primer combinations used to check integration of the episome.

The expected product size of the amplicons and the cycling conditions for their amplification is shown. The primer pair combinations represent the following: *PfNT* UP+pCAM R2 = integration at 5' end; *PfNT* Down+pCAM F2 = integration at the 3' end; pCAM F2+pCAM R2 = presence of the episome; *PfNT* Up+*PfNT* Down = presence of the wild type.

### 2.4.3 Cloning of 3D7 $\Delta$ PfNT1 parasites

Cloning of 3D7 $\Delta$ PfNT1 (parasites with disrupted Pf13\_0252) was performed in a 96 well plate using the limited dilution method previously described (Rosario, 1981). A culture of about 1% parasitaemia was incubated in a shaking incubator at 37°C for 48 hours to ensure single parasite invasion of the erythrocytes. An accurate count of parasitaemia (by microscopy of Giemsa-stained thin films, section 2.1.6) and red blood cell densities (using a haemocytometer, section 2.1.9) were performed. The number of parasites per microlitre of culture was calculated by multiplying the red cell density by the parasitaemia. The culture was diluted with 5% blood suspension in complete RPMI 1640 to obtain a concentration range of 10000-0.5 parasites/0.1 ml aliquot. Twenty cultures of 0.5 parasites/0.1ml in alternative wells of a 96-well plate were set up. Five other wells containing cultures with parasitaemia of 10000 parasites/0.1ml or 100 parasites /0.1 ml respectively were also set up on the plate.

The culture medium contains blasticidin (2.5 µg/ml) and was supplemented with additional purines to a final concentration of 1mM hypoxanthine, 1mM adenosine and 1mM inosine. The plate with the cultures was placed in a Modular incubator chamber (MP, Cambridge, UK) and gassed with a gas mixture containing 1% O<sub>2</sub>, 3% CO<sub>2</sub>, and 96% N<sub>2</sub>. The chamber was placed in an incubator set at 37°C.

Medium was changed every 48 hours until day 4 when smears were prepared from the wells with parasitaemia at 10000 parasites/ 0.1ml. The smears were processed using the method described in section 2.1.6 and the presence of parasites verified. Once parasites were present, culturing was resumed otherwise plates were discarded. 0.1ml blood suspension (5% PVC) was added to each culture on day 6 and the culture split into two wells. Microscopic examination of the culture initially at 100 parasite/ 100ml was done on day 7 to determine the presence of parasites. If parasites were absent from these cultures till day 12 then the plate was discarded. Otherwise, culturing was continued. From day 12, cultures from wells with the starting parasitaemia of 0.5 parasites /100 ml were microscopically examined for the presence of parasites.

Once parasites were seen in a well, the entire content of the well was transferred into a culture flask and made up to 2ml with blood/RPMI 1640 medium at 5% PCV containing blasticidin (100ug/ml) and cultured as previously described (section 2.1). Fresh

blood/RPMI 1640 mixture (5% PCV) was added to each well on day 12 and thereafter the medium was changed every 24 hours. Once the parasitaemia of the cultures in the flask has reached 5%, PCR analysis was carried out using the method described in section 2.4.2 in order to verify disruption of the *ENT* gene. Southern blot analysis was also carried out to confirm integration. Once integration is confirmed stabilates were prepared: parasite clones from the culture flask were cryopreserved as described in section 2.1.7.

#### 2.4.4 Confirmation of Integration by Southern blot analysis

Southern blotting was performed as described by Fidock and Wellems to independently confirm homologous integration at the *PfNT1* locus in the parasite clones and the absence of the wild type (Fidock & Wellems, 1997). Genomic DNA from the wild type and the clones was extracted using previously described method (section 2.3.2). 5 µg DNA was digested with *Xmn*I. A 20 µl digestion mix consisting of 1× NEBuffer 2 (50 mM NaCl, 10 mM Tris-HCl, 10 mM MgCl<sub>2</sub>, 1mM DTT), 1U *Xmn* I, 0.2 µl and 100 µg/ml BSA was set up. The Digest-mix was incubated at 37°C overnight. 12 µl, of the digest-mix were loaded on 0.8% agarose gel and run at low voltage (22 V) overnight. After electrophoresis, the gel was photographed.

The DNA was partially depurinated by immersing the gel in 0.25 M HCl for 15 minutes. Alkaline denaturation of nucleic acid was performed by agitating the gel in denaturation solution: (0.2 mM and 0.5 M NaCl). This was followed by neutralisation of the gel at room temperature for 1 hour in a solution containing, 0.025 M NaHPO<sub>4</sub>/NaH<sub>2</sub>PO<sub>4</sub> (pH=6.5).

Denatured DNA was transferred from the gel onto a positively charged nylon membrane (Hybond N<sup>+</sup>, Amersham Biosciences) by capillary action using 20× SSC (17.5% NaCl, 8.8% sodium trisodium citrate, pH 7). The transfer was allowed to continue for up to 24 hours at room temperature. The membrane containing the DNA was washed in 2 × SSC to remove residual agarose by placing it in a tray containing the solution and shaking it gently for 10 minutes at room temperature. The membrane was then air-dried at room temperature. The DNA was cross-linked to the membrane by exposure to UV illumination using the StrataLinker™ 2400 UV Crosslinker (Stratagene) set at optimum crosslink.

A *PfNT1* fragment was used as fluorescein- labelled ENT probe using the 'Gene Images™ Random Prime Labeling Kit' (Amersham Biosciences, USA,). The kit is designed to label nucleic acid by random prime labelling (Amersham Hand book). Nonamers of random sequence are used to prime DNA synthesis on a denatured DNA template in a reaction catalysed by the klenow fragment of *E coli* DNA polymerase. Fluorescein-11-dUTP (F1-dUTP) partially replaces dTTP in the reaction so that a fluorescein labelled probe is generated ([http://www.gelifesciences.co.jp/tech\\_support/manual/pdf/nadna/RPN3520.pdf](http://www.gelifesciences.co.jp/tech_support/manual/pdf/nadna/RPN3520.pdf)). There is net synthesis of probe in this reaction, with up to 350ng probe synthesised from 50ng template. The probe can be denatured and used directly in hybridisation.

Detection of the hybridised gene of interest was done with the Gene Images CDP star detection module. Following hybridisation this detection module allows detection of hybrids by incubation with anti fluorescein alkaline phosphatase (AP) conjugate. After washing off the excess conjugate, probe-bound AP is used to catalyse light production by enzymatic decomposition of a stabilised dioxetane substrate (Amersham Handbook).

Following the instructions in the manufacturer's handbook 50ng *PfNT1* DNA was denatured by heating for 5 minutes in boiling water and used to prepare the probe. A 50 µl reaction-mix was prepared in 1.5ml microcentrifuge tube placed on ice bath. The reaction-mix consist of the following: 50ng denatured *PfNT1* DNA, 10 µl nucleotide mix (5× F1-dUTP, dATP, dCTP, dGTP and dTTP in Tris-HCl, pH 7.8, mercaptoethanol and MgCl<sub>2</sub>), 5 µl primers (random monomers in an aqueous solution), enzyme solution (5 units/µl exonuclease free Klenow in buffer, pH 6.5), top up to the final volume with water. The reaction-mix was gently pipetted up and down followed by brief spin to ensure uniform mixture. The reaction-mix was incubated at 37°C for 1 hour.

Following the manufacturer's instructions the Southern blot was hybridized to the probe representing the same region of *PfNT1* present in the plasmid pCAM/BSD-NT1. The probe hybridized to a 7.9kb fragment in wild type 3D7 parasites, representing the genomic copy of *PfNT1*. This was followed by detection using the Gene Images CDP-Star detection module.

## 2.5 Isotopic method for testing sensitivity to antimalarial drugs.

Cultures used for the drug sensitivity assays contained predominantly ring forms of the parasites. In some cases cultures were naturally synchronous; otherwise they were synchronized by brief incubation with 5% aqueous D-sorbitol using standard method (Lambros & Vanderberg, 1979) [Section 2.1.5]. All drug sensitivity assays were performed in 96-well microtitre plates using the method described by Rieckmann and others (Rieckmann *et al*, 1978). Briefly, stocks of drugs were prepared by dissolving in DMSO. Chloroquine was prepared from chloroquine sulphate supplied by May and Baker, England. The Pyrimethamine used was a gift from Prof. David Walliker (University of Edinburgh, UK) to Dr Lisa Randford Cartwright (University of Glasgow, UK). Serial dilutions of the dissolved drugs were made with incomplete RPMI1640 medium to obtain five times the required final concentration range. Each well of a microtitre plate, except for the outermost rows and columns, was pre-dosed with 50 µl of the appropriate drug solution. Parasite cultures were diluted appropriately with fresh uninfected erythrocytes and RPMI 1640 culture medium to achieve a final parasitaemia in the wells of 0.5-1.0% and PCV of 2%. Two hundred microlitres of the diluted parasite culture were added to each well of the pre-dosed plates. Positive control wells consisted of: 50 µl culture medium without drug (but containing the same amount of DMSO as in drug wells) and 200 µl infected erythrocytes. Negative control wells contained 50 µl culture medium without drug (but containing the same amount of DMSO as in drug wells) and 200 µl uninfected erythrocytes respectively. Each assay point was done in triplicate on the same plate and each experiment was performed three times.

The plates were incubated at 37°C for 42-48 hours in a modular incubator chamber (MP, Cambridge, UK), gassed with a mixture of 3% CO<sub>2</sub>, 1% O<sub>2</sub>, 96% N<sub>2</sub>. Cultures were incubated for an initial period of 24 hours followed by the addition of 10 µl of incomplete RPMI1640 medium containing 1.87 µM [<sup>3</sup>H]-hypoxanthine with a specific activity of 37 GBq/mmol (Amersham Biosciences) to each well. Incubation was resumed under the same conditions for a further 24 hours. At the end of incubation, cells were harvested from each well onto a single fibreglass filter paper using a Filtermate Harvester (Packard Instruments). The filter paper was dried, sealed in a plastic bag and 3 ml scintillation fluid

(OptiPhase HiSafe, Perkin Elmer) was added. Radioactivity incorporated into the parasites was counted with a Microbeta Wallac Trilux liquid scintillation and luminescence counter.

The IC<sub>50</sub> value, representing 50% inhibition of uptake of [<sup>3</sup>H]-hypoxanthine, was determined from a non-linear regression analysis of log drug concentration against radiolabel incorporated into the parasites using Prism version 4.0, using the equation for a sigmoidal dose-response curve with variable slope. Mean IC<sub>50</sub> values and standard errors of the mean (s.e.m.) for each drug were determined from three independent drug sensitivity assays performed in triplicate on each plate.

## 2.6 PicoGreen<sup>®</sup> Method for drug sensitivity assays

PicoGreen<sup>®</sup> (Invitrogen-Molecular Probes) is a fluorochrome which selectively binds dsDNA by intercalation, resulting in an exceptionally high increase in fluorescence emission. PicoGreen<sup>®</sup> has been shown to detect as little as 25 pg/ml of dsDNA in the presence of ssDNA, RNA, and free nucleotides (Corbett *et al*, 2004). Corbett and co-workers also demonstrated that replication of malaria parasites was directly proportional to the amount of PicoGreen<sup>®</sup> fluorescence, with a linear relationship between parasitaemia of 0.1% and 15%. This property of PicoGreen<sup>®</sup> was used in this study to determine the susceptibility of malaria parasites to antimalarial drugs.

*P. falciparum* parasites were cultured in the presence of different concentrations of test compounds. After 48 hours incubation in a 96-well microtitre plate, 150 µl of the culture from each well were transferred into a new, opaque, 96-well plate and centrifuged at 630 × g, 5 min to pellet the cells. The supernatant was removed and the cells resuspended in saponin (0.15%, w/v) to lyse the erythrocytes. Following centrifugation of the plate, the supernatant was removed and the plate washed with 200 µl of PBS. Freed parasite pellets in the wells were re-suspended in 150 µl of PBS.

Fifty microlitres of lysis/fluorescence-mix consisting of PicoGreen<sup>®</sup> (1:200 in TE buffer, pH 7.5) and Triton X-100 (final concentration, 2%) in nucleic acid- and DNase-free water were added to each well. Plates were incubated in the dark at room temperature for between 5-30 minutes and fluorescence intensity measured at 485 nM (Excitation) and 528 nM (Emission) using a Perkin Elmer LS 55 Luminescence Spectrophotometer. Positive



control wells consisted of parasites without drugs whilst the negative controls contained uninfected blood. Control wells were treated similarly. The mean background reading from the two control wells was subtracted from the test fluorescence reading to give the final fluorescence measurement. Fluorescence (arbitrary units ranging from 1 to 1000 units) was plotted against drug concentrations in a non-linear sigmoid plot using Prism version 4.0. All experiments were performed in triplicate for each drug concentration.

## 2.7 Data analysis

For any given permeant, the linear phase of uptake was first determined using the described time dependent assay. Linearity was assessed using linear regression, defined as a correlation coefficient  $>0.95$  and significant difference from zero uptake (F-test; GraphPad Prism version 4). A graph of the initial rate of uptake of a permeant plotted against substrate concentration results in a curve that becomes asymptotic to a horizontal line, which represents “maximum rate of uptake” referred to as the  $V_{\max}$  (Figure 2.10). . The  $K_m$  is the concentration of substrate that gives "half-maximal activity" i.e.  $0.5 \times V_{\max}$ . The relationship between  $K_m$  and  $V_{\max}$  is defined by the Michaelis-Menten equation:

$$v = V_{\max} / (1 + (K_m/[S])),$$

where  $[S]$  is the concentration of substrate and  $v$  = the rate of uptake at concentration  $S$

The  $K_m$  denotes the affinity of the transporter for the permeant. A relatively low  $K_m$  value signifies a high affinity of the transporter for the substrate and vice versa.

The effects of different inhibitors on the uptake of radiolabeled permeants in this study were compared using the  $IC_{50}$  values. The  $IC_{50}$  value is the concentration of the inhibitor required to reduce the influx of the permeant by half (50%). A relatively low  $IC_{50}$  value will therefore mean a relatively strong inhibitor, but the  $IC_{50}$  is a function of the permeant concentration. The inhibition constant  $K_i$ , which is independent of the permeant concentration, was calculated from the equation  $K_i = IC_{50} / (1+(L/K_m))$ , where  $L$  is the permeant concentration.

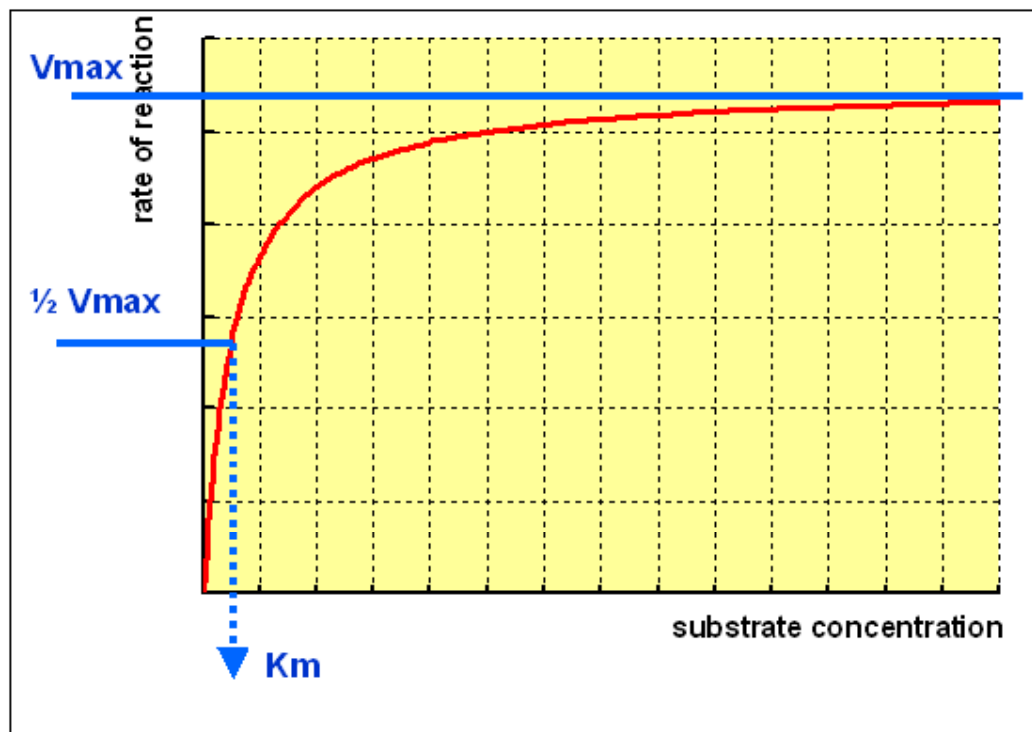


Figure 2.10: A typical Michaelis-Menten plot.

Dependence of initial velocity on substrate concentration for a reaction obeying Michaelis-Menten kinetics. The  $K_m$  is the concentration of substrate that gives "half-maximal activity" whilst  $V_{max}$  is the maximum rate of uptake (<http://www.ucl.ac.uk/~ucbcdab/enzass/substrate.htm>).

## **CHAPTER THREE**

### **3 Purine transport into uninfected and *P. falciparum* infected human erythrocytes**

### 3.1 Summary

Transport of purine from an exogenous source into *P. falciparum* infected erythrocyte is an important event, necessary for the growth and development of the parasite. Up to now, three routes of purine transport into the infected erythrocyte have been identified: the human equilibrative nucleoside transporter (hENT1), the human facilitative nucleobase transporter (hFNT1), and the New Permeation Pathway (NPP). Although detailed studies of the hENT1, hFNT1 and NPP have been carried out, there is no information on the relative contribution of each of these salvage mechanisms to the overall uptake of purine into the *P. falciparum* infected erythrocytes. The effect of classical inhibitors, such as furosemide, on hFNT1 and hENT1 has not been studied although it has been demonstrated for the NPP. Using a standard uptake technique, the transport of adenosine, hypoxanthine and adenine into uninfected and *P. falciparum*-infected human erythrocytes in the presence or absence of inhibitors was measured. Kinetic values obtained from such experiments allowed for the assessment of the contribution of each of these transporters to the overall purine salvage in parasitized erythrocytes. Results from these investigations indicate that transport of exogenous purines into infected or uninfected erythrocytes occurred primarily through equilibrative transporters, rather than the NPP, which is non-saturable.

Hypoxanthine and adenine appeared to enter erythrocytes mainly through the hFNT1 whereas adenosine entered predominantly through the hENT1 nucleoside transporter. The rate of purine uptake was approximately doubled in infected cells compared to uninfected erythrocytes. Additionally, the rate of adenosine uptake into infected hRBC was comparably higher than that of hypoxanthine uptake. It was also observed that furosemide has similar inhibitory effects on purine transport through the hFNT1 and the NPP. This observation gives support to the hypothesis that the NPP evolved out of endogenous proteins. From observations made in this study, it can be firmly concluded that endogenous transporters are the major means of purine uptake into infected erythrocytes.

### 3.2 Introduction

The mature non-infected human erythrocytes have numerous membrane transport systems, which are responsible for the uptake of essential nutrients and other compounds from external sources (Kirk, 2001). Though the importance of some of these transport systems is not clear at the moment, they are thought to have evolved from the cell from which the erythrocyte originated (Kirk, 2001). Most of these endogenous transport systems, especially those responsible for purine salvage, have been characterized with regard to their kinetic properties (Kirk, 2001). It has been shown that hypoxanthine is rapidly transported across the non-infected red cell membrane by a facilitated diffusion through the human facilitative nucleobase transporter (Domin *et al*, 1988; de Koning *et al*, 2005). Similarly, Kraupp and colleagues reported that the transport of adenine and hypoxanthine in human erythrocytes occurs through two mechanisms (Kraupp *et al*, 1991). The first mechanism involves a common carrier for both nucleobases and the second is through an unsaturable permeation pathway in which uptake is 4–5-fold faster for adenine than for hypoxanthine (Kraupp *et al*, 1991). The group further demonstrated that adenine and hypoxanthine ‘share a common transporter and that their membrane transport is adequately described by the alternating conformation model of carrier-mediated transport’. In terms of nucleoside transport, it has also been shown that the non-infected erythrocyte takes up these nutrients through the equilibrative nucleoside transporter (hENT1), which is located in the erythrocyte membrane (Plagemann *et al*, 1988). While hENT1 is inhibited by papaverin (Domin *et al*, 1988), hENT1 is potently blocked by 6-[(nitrobenzyl)-thio] 9- $\beta$ -D-ribofuranosylpurine (NBMPR) (Plagemann *et al*, 1988; Plagemann & Woffendin, 1988).

During the intraerythrocytic stage of the parasite lifecycle, which involves a repeated cycle of red blood cell invasion by the parasite, followed by multiplication and release of merozoites (daughter cells), there is an increased demand for nutrients, particularly purines. Unlike pyrimidines, the malaria parasite is incapable of *de novo* synthesis of purines and therefore has to depend on exogenous sources for the supply of this essential nutrient (Divo *et al*, 1985). Despite the abundance of adenosine triphosphate (ATP) in the host erythrocyte cytosol, hypoxanthine rather than adenosine is the main purine precursor utilized by parasite (Webster & Whaun, 1981; Scheibel & Sherman, 1988). Indeed, it has been shown that supplementation of culture medium with 100–400  $\mu$ M hypoxanthine increases parasite yields three- to fourfold (Zoig *et al*, 1982; Divo & Jensen, 1982; Freese *et*

*al*, 1988). Further evidence indicating that hypoxanthine is the preferred purine source was provided by Berman and colleagues (Berman *et al*, 1991). By depleting hypoxanthine in a parasite culture through the addition of xanthine oxidase, *P. falciparum* growth was reduced by about 90% (Berman *et al*, 1991). Based on this evidence and others, Berman and co-workers devised a model for the metabolism of purine in non-infected and infected erythrocytes, which is shown in figure 3.1 (Berman *et al*, 1991). In the model, hypoxanthine may enter or diffuse out of the erythrocyte through a non-concentrative purine base transporter located in the RBC membrane.

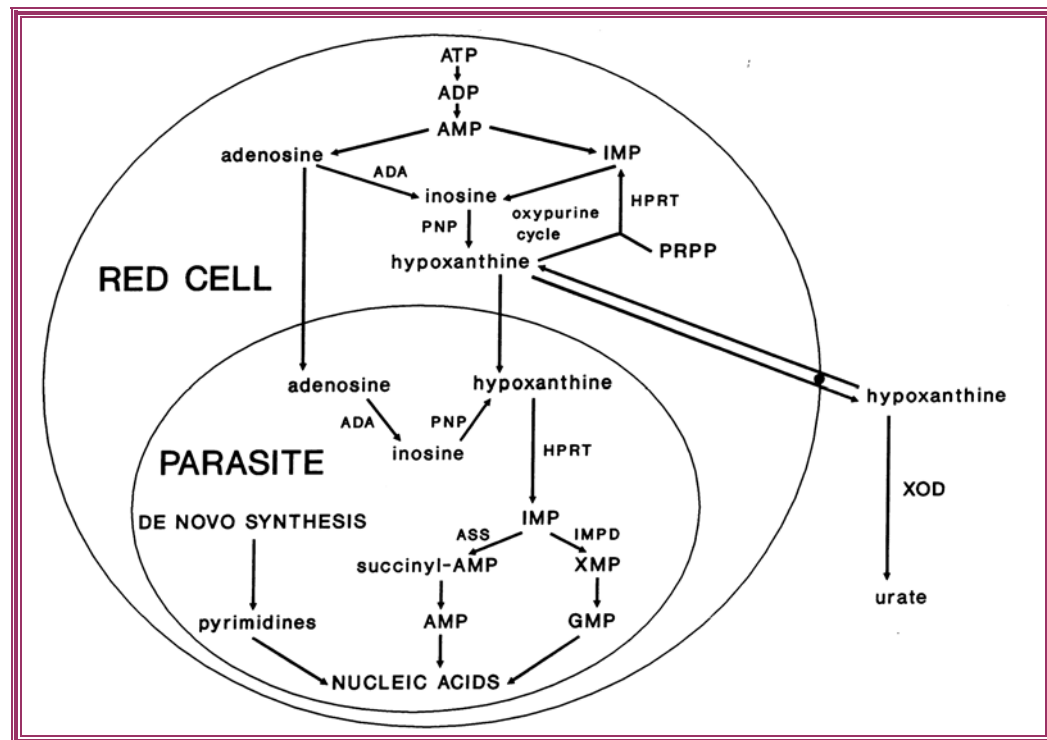
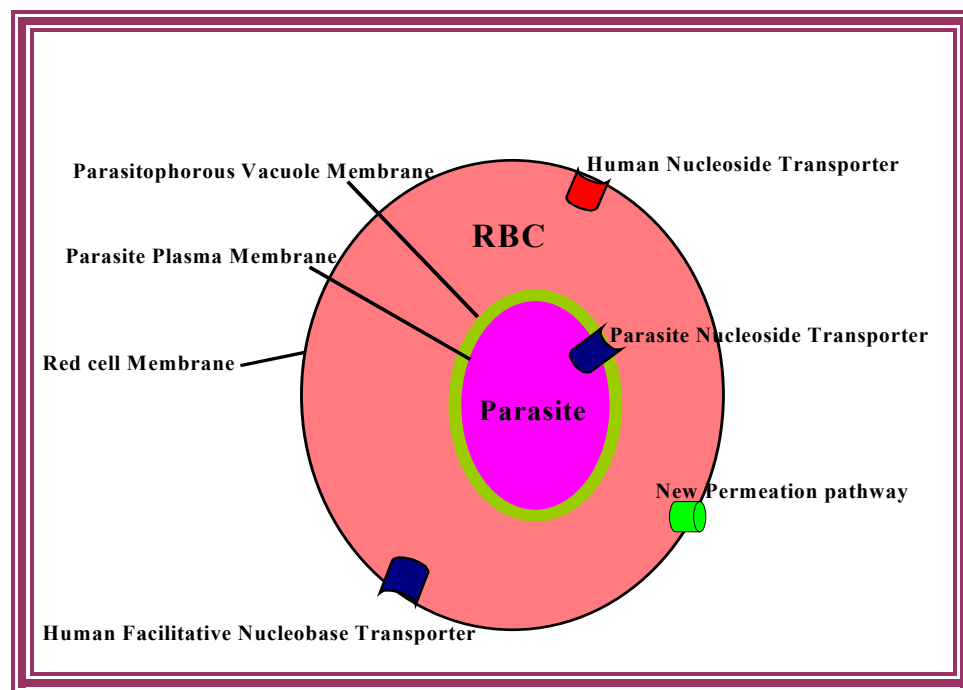


Figure 3.1: The sources of hypoxanthine in infected erythrocyte, proposed by Berman and colleagues (Berman *et al*, 1991).

Abbreviations: ADA, adenosine deaminase; PNP, purine nucleoside phosphorylase; HPRT, hypoxanthine phosphoribosyl transferase; XOD, xanthine oxidase; PRPP, 5-phosphoribosyl-l-pyrophosphate; ASS, adenylosuccinate synthase; IMPD, inosine monophosphate dehydrogenase. (Reproduced with permission from (Berman *et al*, 1991).

For nutrients to reach the parasite from an exogenous source they have to cross numerous membranes barriers including the host RBC membrane, the parasitophorus vacuole membrane and the parasite's plasma membrane (Figure 3.2). In order to facilitate the rapid movement of nutrient from exogenous sources into the infected cell, the parasite induces an additional, NBMPR-insensitive uptake system in the host plasma membrane (Gero *et al*, 1988). The induced uptake system, referred to as the New Permeation Pathway has been described in detailed in section 1.15.1. The pathway, which does not distinguish between

the D and L-enantiomers of nucleosides, particularly adenosine (Upston & Gero, 1995), exhibits the characteristic of an anionic channel, mediating the uptake of some anions. It is, therefore, inhibited by a range of anionic channel blockers such as furosemide and 5-nitro-2- (3-phenylpropylamino) benzoic acid (NPPB) (Kirk *et al*, 1994).



**Figure 3.2: Schematic presentation of an infected human erythrocyte showing location of purine transporters and the new permeation pathway.**

Given the continued presence of the hFNT1 and hENT1 in the infected erythrocyte, it is not completely clear what function the NPP plays with regard to purine salvage. Although the purine-mediating role of the NPP as well as the other endogenous transporters has been studied, the relative contribution of each component to the overall purine salvage in an infected cell has not been clearly elucidated. The current study therefore sought to investigate the degree to which the overall purine salvage by the intraerythrocytic-stage *P. falciparum*-infected erythrocyte is attributable to the NPP. Using classical inhibitors that block the NPP and the endogenous transporter, hENT1, the kinetics of purine transport into infected and non-infected RBC was studied. Transport of 0.5  $\mu\text{M}$  [ $^3\text{H}$ ]-adenosine or 1.0  $\mu\text{M}$  [ $^3\text{H}$ ]-hypoxanthine into *P. falciparum*-infected erythrocytes and uninfected erythrocytes in the presence of NBMPR, furosemide, and 1mM of unlabelled adenosine or hypoxanthine was investigated. The inhibitory effect of increasing concentrations of furosemide and unlabelled adenine on the uptake of 1.0  $\mu\text{M}$  [ $^3\text{H}$ ]-adenine into uninfected erythrocytes was also investigated.

### **3.3 Adenosine uptake into Percoll™-enriched *P. falciparum* infected erythrocytes is not consistent with salvage through the NPP**

The extent to which the new permeation pathway contributes to adenosine salvage in *P. falciparum*-infected erythrocytes was investigated in this study. All experiments were carried out using the 3D7 clone of *P. falciparum* at the trophozoite-stage. The parasites were maintained in complete RPMI 1640 using the Trager and Jensen method, described in section 2.1.4 of this thesis. Prior to an experiment the culture was synchronized using standard method (Lambros & Vanderberg, 1979) (section 2.1.5). Cell counts of the culture were made using an improved Neubauer counting chamber and the parasitaemia was determined on methanol-fixed, Giemsa-stained blood smears (section 2.1.6).

Concentrated trophozoite-stage infected erythrocytes (60-90% parasitaemia) were obtained by density gradient sedimentation on Percoll™ (Amersham Biosciences) using previously described method (Gero *et al*, 1988; Kirk & Horner, 1995). Briefly, isotonic Percoll™ solution was prepared by mixing the stock Percoll™ solution (100%) with PBS and distilled water to give a working solution of density 1.090 and osmolality 320 mosm (kg H<sub>2</sub>O)<sup>-1</sup>. Concentration of the trophozoite-stage parasitized erythrocytes was achieved by layering an equal volume of culture at 10% haematocrit on top of the isotonic Percoll solution and centrifuging at 650 × g for 12 minutes. The trophozoite-enriched red blood cells were harvested from the interface. Pellets with up to 80% infected erythrocytes were obtained using this method. The concentrated cells were washed three times with incomplete RPMI 1640 and incubated in the same medium containing glucose (0.2%) for 30 minute to allow for full recovery of the parasites before their use in uptake experiments. Results were similar when erythrocyte medium (140mM NaCl, 5mM KCl, 20mM Tris/HCl, (pH 7.4), 2mM MgCl<sub>2</sub>, and 0.1mM EDTA) was used as the assay buffer instead of incomplete RPMI 1640.

Transport of 0.5 μM [<sup>3</sup>H]-adenosine into uninfected and *P. falciparum* infected erythrocytes was investigated using the uptake technique described in section 2.2. Briefly, a solution of radiolabeled adenosine at twice the intended final concentration was prepared in the presence (also at twice the final concentration) or absence of NBMPR or furosemide. An equal volume of the radio-labelled adenosine/inhibitor mixture and the Percoll-concentrated parasitized erythrocytes were mixed together and at predetermined time



interval 200  $\mu$ l of the mixture was dispensed into an ice-cold stop solution which had been carefully layered on an oil-mix (300  $\mu$ l of 5 parts dibutylphthalate: 4 parts dioctyl phthalate, v/v) in a 1.5 ml microcentrifuge tube. The influx of the permeant was terminated by sedimenting the parasites below the oil using centrifugation at  $13000 \times g$  for 60 s. The stop solution used in this experiment contains 10  $\mu$ M dilazep and 200  $\mu$ M furosemide in erythrocyte medium (140 mM NaCl, 5 mM KCl, 20 mM Tris/HCl, (pH 7.4), 2 mM  $MgCl_2$ , and 0.1 mM EDTA). Furosemide in the stop solution inhibits the parasite-induced new permeation pathway whilst dilazep is an inhibitor of the exogenous (erythrocyte) nucleoside transporter (Kirk, 2001). Uninfected erythrocytes were incubated in parallel with the infected erythrocyte culture under identical conditions for at least 24 hours before the start of the experiment and were also centrifuged through isotonic Percoll™. The uptake of permeant into these cells was investigated using the same procedure described for the infected cells. The samples were processed for scintillation counting using the procedure described in section 2.2.7.

Non-mediated influx of adenosine into the cells was assessed by measuring the rate of uptake of the radiolabeled permeant in the presence of 1 mM unlabeled permeant. The rate of uptake of adenosine was obtained from a plot of permeant concentration against time. Experiments were performed in triplicate at room temperature.

Observations made in these experiments indicate that 0.5  $\mu$ M [ $^3H$ ]-adenosine was transported very rapidly into both *P. falciparum*-infected and uninfected human erythrocytes. A plot of permeant concentration against time indicates that the uptake was linear for at least 10 seconds, thus allowing for the determination of uptake rates by linear regression over this period. The results shows that [ $^3H$ ]-adenosine was taken up by uninfected human erythrocytes with a rate of  $0.032 \pm 0.006$  pmol  $(10^7 \text{ cells})^{-1} \text{ s}^{-1}$  with complete inhibition of uptake in the presence of 1 mM unlabelled permeant (Figure 3.3). Uptake of 0.5  $\mu$ M [ $^3H$ ]-adenosine by the uninfected erythrocyte was 95% inhibited by 100 nM NBMPR (Figure 3.3). This observation is in line with the well-documented presence of the NBMPR-sensitive es/hENT1 adenosine transporter in human erythrocytes (Plagemann 1988). An important observation made in this study is that adenosine uptake into infected or uninfected human red blood cells (hRBC) was not noticeably inhibited by 100  $\mu$ M furosemide (Figure 3.4), suggesting that the NPP plays at best a limited role in the salvage of this purine.

The uptake rate of 0.5  $\mu$ M [ $^3H$ ]-adenosine into infected human erythrocytes ( $0.070 \pm 0.005$ ) was observed to be more than twice as fast than into uninfected erythrocytes and

adenosine also accumulated two fold higher in *P. falciparum*-infected erythrocytes than in uninfected cells (Figure 3.4). This observation is consistent with a generally higher level of nutrient uptake in infected cells as discussed by Kirk and colleagues (Kirk *et al*, 1999).

Since the uptake of this nucleoside, as observed in this study, was almost completely inhibited by NBMPR and also the salvage mechanism involved was fully saturable (which are inconsistent with the properties of the NPP), it may be concluded that the NPP plays only a minor role in the salvage of adenosine in infected erythrocytes.

This conclusion was further strengthened by the observation that the rate of adenosine uptake in infected hRBC was identical in the presence or absence of 100  $\mu\text{M}$  of the NPP-inhibitor furosemide ( $0.054 \pm 0.006$  and  $0.059 \pm 0.003$   $\text{pmol} (10^7 \text{ cells})^{-1} \text{s}^{-1}$ , respectively), which indicates that hENT1 was not sensitive to furosemide (Figure 3.4).

In conclusion, evidence gathered from these experiments indicates that adenosine transport in *P. falciparum* infected erythrocyte is overwhelmingly through hENT1.

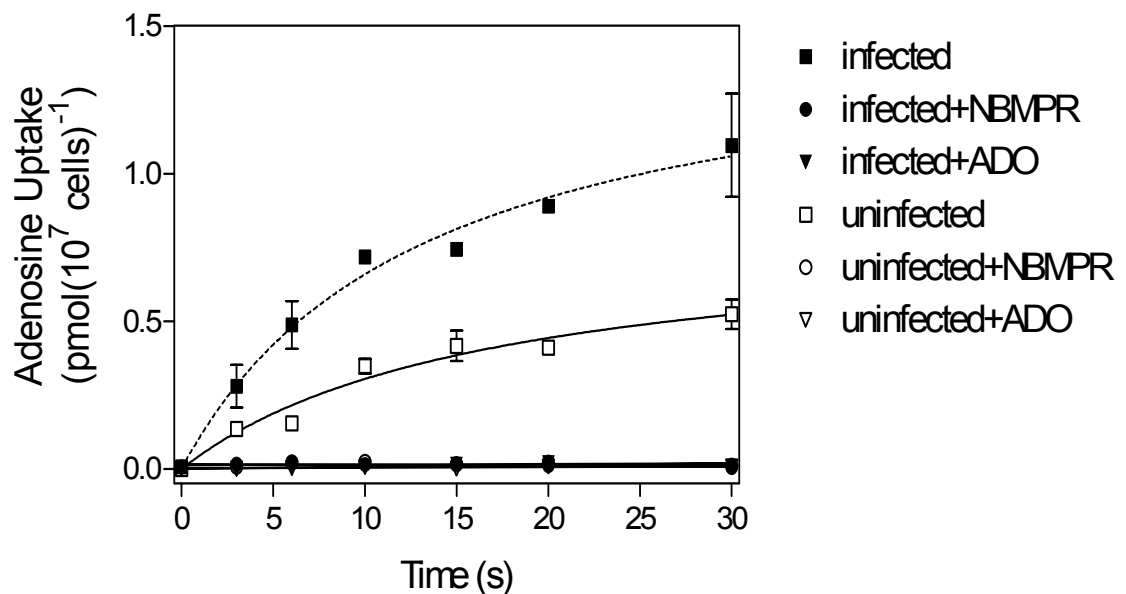


Figure 3.3: Adenosine transport in *P. falciparum*-infected and uninfected human erythrocytes with inhibition by NBMPR.

Uptake of 0.5  $\mu\text{M}$  [<sup>3</sup>H]-adenosine in Percoll-enriched infected (closed symbols, dashed lines) and uninfected (open symbols, solid lines) erythrocytes without inhibitor (squares), in the presence of 0.1  $\mu\text{M}$  NBMPR (circles) or 1 mM unlabelled adenosine (ADO) (triangles).

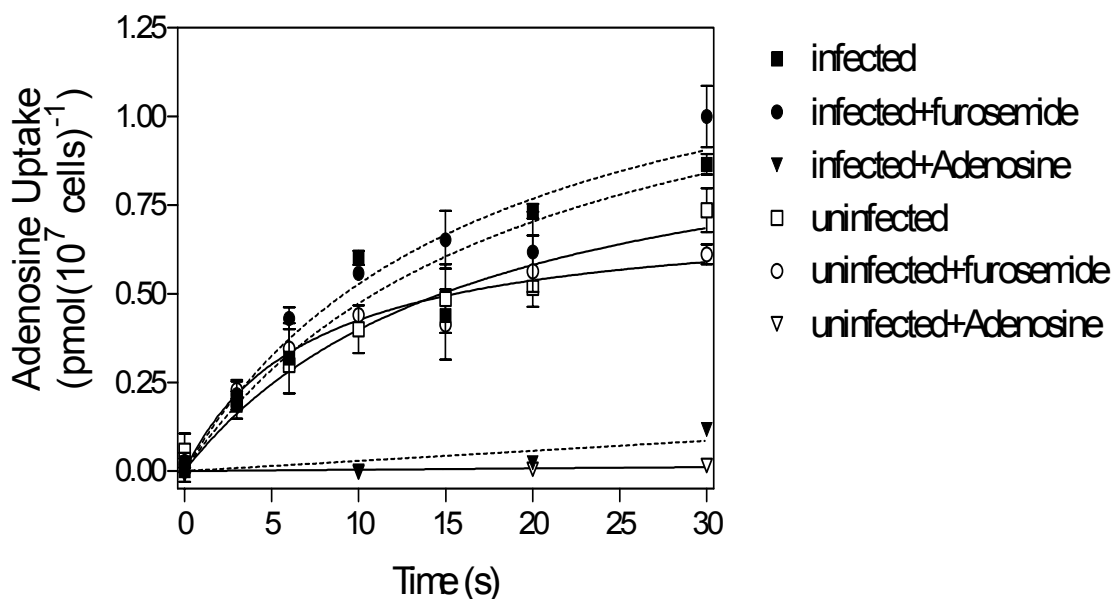


Figure 3.4: Adenosine transport in *P. falciparum*-infected and uninfected human erythrocytes with inhibition by furosemide.

Uptake of  $0.5 \mu\text{M}$  [ $^3\text{H}$ ]-adenosine in Percoll-enriched infected (closed symbols, dashed lines) and uninfected (open symbols, solid lines) erythrocytes without inhibitor (squares), in the presence of  $100 \mu\text{M}$  furosemide (circles) or  $1 \text{ mM}$  unlabelled adenosine (triangles).

### 3.4 Hypoxanthine uptake into uninfected erythrocytes and Percoll-enriched *P. falciparum*-infected erythrocytes occurs mainly through hFNT1 and is inhibited by furosemide

Transport of hypoxanthine through hFNT1 following the blocking of the NPP with furosemide was investigated. Uptake of  $1 \mu\text{M}$  [ $^3\text{H}$ ]-hypoxanthine into uninfected erythrocytes and into Percoll-enriched *P. falciparum* infected erythrocytes was performed in the presence or absence of  $250 \mu\text{M}$  furosemide. The cell preparation and uptake techniques employed were as described for the experiment with adenosine (section 3.3). The stop solution used in these experiments consisted of  $19 \text{ mM}$  Papaverine (in  $165 \text{ mM}$  NaCl), which inhibits the exogenous nucleobase transporter, hFNT1 (Domin *et al*, 1988). Assessment of the non-mediated influx of permeant into the cells was performed by measuring the rate of uptake of the radiolabeled permeant in the presence of  $1 \text{ mM}$  unlabelled permeant, as well as with cells and permeant at  $0^\circ\text{C}$ . Since increased phosphoribosylation of nucleobases occurs in phosphate-containing buffers (Capuozzo *et al*, 1986; Plagemann, 1986), a phosphate-free buffer was used in these transport experiments in order to minimize metabolism of the purine nucleobases that might

otherwise complicate the interpretation of the results. The rate of uptake of hypoxanthine was obtained from a plot of permeant concentration against time. Transport of 1  $\mu\text{M}$  [ $^3\text{H}$ ]-hypoxanthine into uninfected erythrocytes and into Percoll-enriched *P. falciparum* infected erythrocytes was saturable and linear for up to 10 seconds. Uptake of 1  $\mu\text{M}$  [ $^3\text{H}$ ]-hypoxanthine into uninfected erythrocytes hFNT1 was observed to occur at a rate of  $0.012 \pm 0.005 \text{ pmol } (10^7 \text{ cells})^{-1} \text{ s}^{-1}$  and involved a fully saturable transporter (Figure 3.5). This rate was considerably lower than the uptake of 0.5  $\mu\text{M}$  [ $^3\text{H}$ ]-adenosine. Transport of 1  $\mu\text{M}$  [ $^3\text{H}$ ]-hypoxanthine was also saturable in Percoll-enriched *P. falciparum*-infected erythrocytes, at  $0.029 \pm 0.005 \text{ pmol } (10^7 \text{ cells})^{-1} \text{ s}^{-1}$  (Figure 3.5). This represents a very similar increase in transport rates, of 2.3-fold and 2.1-fold, respectively, for hypoxanthine and adenosine in parasite-infected hRBC compared to uninfected hRBC. Hypoxanthine uptake by the uninfected and *P. falciparum*-infected hRBC was inhibited 65% and 67%, respectively, by 250  $\mu\text{M}$  furosemide (Figure 3.5). The inhibition of hFNT1 by furosemide has not been reported previously. To further investigate the effect of furosemide on the hFNT1, hypoxanthine was replaced with adenine as the substrate (see section 3.5 below). The choice of adenine was based on the fact that it is reported to be the preferred substrate for this transporter and it is also stable after uptake (Wallace *et al*, 2002).

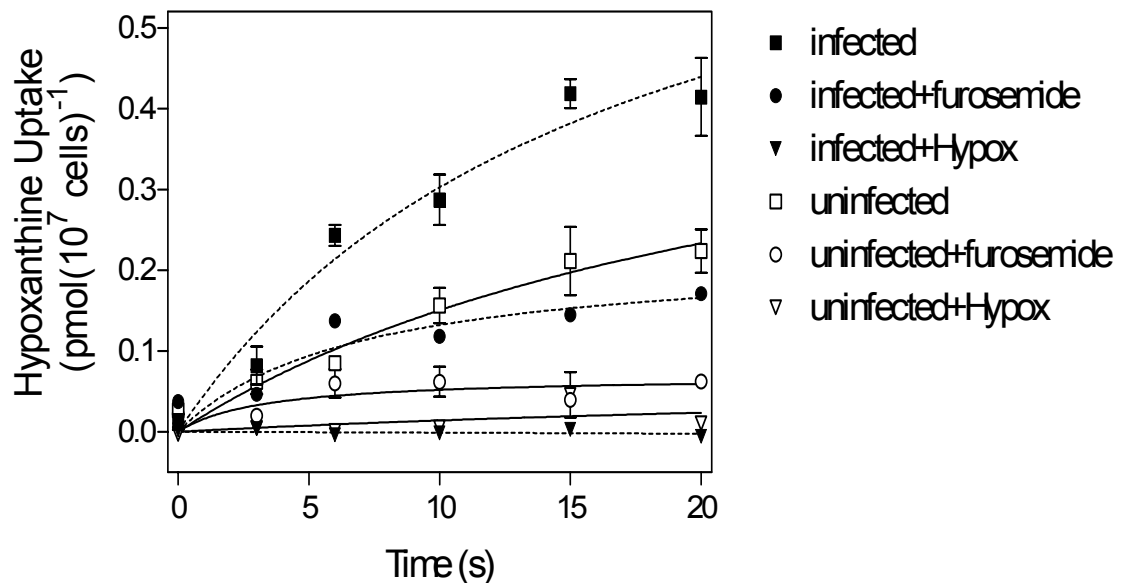


Figure 3.5: Transport of 1  $\mu\text{M}$  [ $^3\text{H}$ ]-Hypoxanthine in *P. falciparum*-infected and uninfected human erythrocytes with inhibition by furosemide. Uptake of 1  $\mu\text{M}$  [ $^3\text{H}$ ]-hypoxanthine (Hypox) in Percoll-enriched infected (closed symbols, dashed lines) and uninfected (open symbols, solid lines) erythrocytes without inhibitor (squares), in the presence of 250  $\mu\text{M}$  furosemide (circles) or 1 mM unlabelled hypoxanthine (triangles).

### 3.5 Adenine transport into uninfected human erythrocytes is inhibited by furosemide

To further investigate the inhibitory effect of furosemide on transport of nucleobases through hFNT1, the dose-dependent inhibition of uptake of [ $^3\text{H}$ ]-adenine into uninfected erythrocytes was investigated. Dose-dependent inhibition of uptake was investigated as described in section 2.2.6. Briefly, mature human erythrocytes were washed three times with erythrocyte medium (section 3.2) and re-suspended in the same medium to achieve a haematocrit of 25%. The cell suspension was allowed to equilibrate at room temperature for approximately ten minutes. The RBC concentration of the suspension was determined with the improved Neubauer counting chamber, to allow uptake to be expressed in terms of cell number. The cell suspension and different concentrations of furosemide or unlabelled adenine, containing [ $^3\text{H}$ ]-adenine at a final concentration of 1  $\mu\text{M}$  were incubated on top of an oil-mix for 5 seconds. The concentration range for unlabelled adenine and furosemide was 0 – 1000  $\mu\text{M}$  and 0 – 500  $\mu\text{M}$  respectively. The flux of [ $^3\text{H}$ ]-adenine into the cells was terminated by the addition of 1 ml cold stop solution (19 mM Papaverine in 165 mM NaCl) followed by centrifugation at  $13000 \times g$  to pellet the cells and separate them from the aqueous layer through the oil-mix, thus preventing further uptake of radiolabeled permeant. The cell pellets were retrieved as previously described (Section 2.2.7) and the amount of radiolabeled adenine taken up into the cells was determined by scintillation counting. The  $\text{IC}_{50}$  value for the inhibition of uptake of 1  $\mu\text{M}$  [ $^3\text{H}$ ]-adenine by unlabelled adenine and by furosemide was determined from a non-linear plot of [ $^3\text{H}$ ]-adenine uptake against log concentration of the inhibitor.

The results of the dose-dependent uptake of 1  $\mu\text{M}$  [ $^3\text{H}$ ]-adenine into uninfected erythrocytes in the presence of unlabelled adenine and furosemide are shown in Figure 3.6. Furosemide was observed to competitively inhibit the uptake of [ $^3\text{H}$ ]-adenine into uninfected erythrocytes with a mean  $\text{IC}_{50}$  value of  $5.6 \pm 2.2 \mu\text{M}$ . High extracellular concentrations of unlabelled adenine similarly inhibited uptake of [ $^3\text{H}$ ]-adenine into the uninfected cells with a mean  $\text{IC}_{50}$  value of  $3.7 \pm 0.9 \mu\text{M}$ .

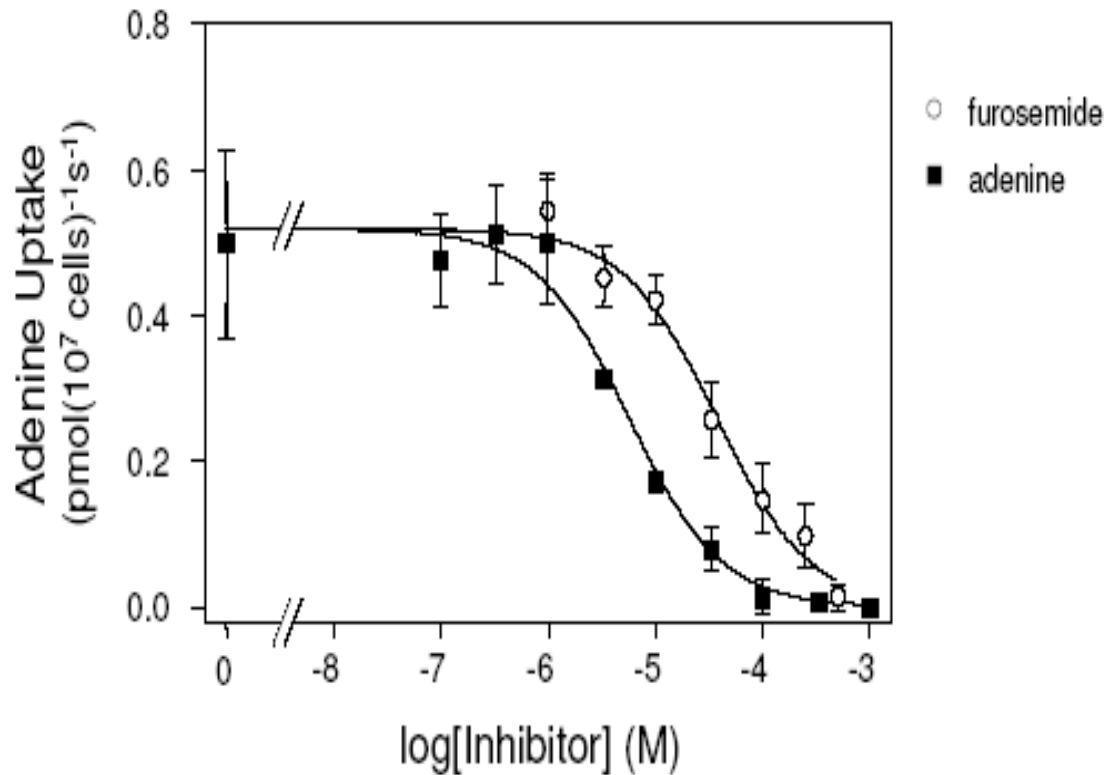


Figure 3.6: Adenine transport in uninfected human erythrocytes with inhibition by furosemide.

Uptake of 1  $\mu\text{M}$  [<sup>3</sup>H]-adenine by uninfected human erythrocytes over 5 seconds, in the presence or absence of various concentrations of unlabelled adenine (closed squares) or furosemide (open circles), as indicated. The experiment shown is representative of four independent experiments and was conducted in triplicate. Data points represent the mean of three samples and error bars for each point represent the standard errors of the mean.

### 3.6 Discussion

The observations reported in this chapter provide compelling evidence that purine salvage in the trophozoite stage of *P. falciparum* infected erythrocyte occurs mainly through the hFNT1 and hENT1 endogenous transporters on the red cell surface. These observations contradict reports implicating the NPP as the main channel of purine uptake into *P. falciparum* trophozoite-stage infected erythrocytes. The results reported here clearly demonstrate that in *P. falciparum* infected erythrocytes, purine uptake occurs primarily through saturable transporters: adenosine appeared to be transported from exogenous sources into the cell through hENT1 whilst hypoxanthine uptake was through hFNT1. The equilibrative nature of the transporters observed here clearly suggests that the NPP, which is non-saturable and not inhibited by NBMPR, plays only a minor role in purine salvage and uptake into infected erythrocytes. Although the NPP is doubtless capable of mediating purine transport, our results show that this channel is not as important to purine uptake into infected cells as previously thought. However, there is strong evidence to show that the NPP generally plays a major role in the salvage of other nutrients such as pantothenic acid into the infected cells (Saliba *et al*, 1998). Not only are hFNT1 and hENT1 present in malaria parasite-infected erythrocytes, their activity appears to be increased and this can not be attributed solely to increased purine utilisation as initial transport rates and total uptake over 30 s were both increased. A similarly increased rate of uptake up into infected erythrocytes compared with the uninfected cell has also been reported for other compounds. The activity of the Na-K pump in uninfected erythrocytes was increased two-fold after infection with *P. falciparum* (Staines *et al*, 2001). A significant increase in the rate of uptake of tryptophan (Ginsburg & Krugliak, 1983) and choline (Elford *et al*, 1990) into infected erythrocytes, compared to uninfected cells, has also been reported. The regulatory mechanism behind this general increase in transporter efficiency is not known.

Notwithstanding our observation that the majority of adenosine and hypoxanthine uptake into infected erythrocytes was mediated by the hENT1 and hFNT1, others (Upston & Gero, 1995; Gero & Hall, 1997) have reported that nucleosides, at least, can be transported by the furosemide-sensitive New Permeation Pathways (NPP). Gero and co-workers clearly demonstrated the uptake of L-adenosine, which is not a substrate of hENT1, through the NPP (Upston & Gero, 1995; Gero & Hall, 1997). Our observations place some doubt on the pharmacological importance of the NPP as a conduit for selective entry of

toxic enantiomers into the infected erythrocytes only (Gero *et al*, 1999), although the selective uptake of even small amounts of the L-enantiomer, comparative to D-adenosine, could affect parasite viability.

In line with findings from this study, it is being proposed that inhibition of the hENT1 may cause parasite death, most likely through purine starvation. This assertion is supported by reports showing that nucleoside transport inhibitors, such as NBMPR, dilazep and dipyridamole, all display intrinsic activity against *P. falciparum in vitro* (Plagemann, 1986). It is therefore most likely that inhibitors of hENT1 would have at least a growth-delaying effect on *P. falciparum*, and perhaps more so if used in combination with an inhibitor of the hFNT1. However, it must be emphasised that blocking both endogenous transporters would also deprive the uninfected erythrocytes of a purine source. While erythrocytes, unlike the *Plasmodium* parasites that infect them, do not need purines for nucleic acid synthesis, their energy balance would be affected as they require adenosine for synthesis of ATP (Komarova *et al*, 1999). However, it is anticipated that infected erythrocytes will be far more quickly affected as their intracellular purine stores would be rapidly depleted by the highly efficient *P. falciparum* purine salvage system.

A further observation made in this study is that the rate of adenosine uptake is considerably higher than the rate of hypoxanthine uptake in infected hRBC even though hypoxanthine is the preferred purine for *P. falciparum* (Berman *et al*, 1991; Berman & Human, 1991). An explanation for this observation could be that due to the presence of adenosine deaminase, adenosine is rapidly converted to hypoxanthine in the cytosol of the infected erythrocyte, as reviewed by De Koning and colleagues (de Koning *et al*, 2005).

A final notable observation made in this study is the inhibition of transport through hFNT1 by furosemide. The inhibition by furosemide of [<sup>3</sup>H]-hypoxanthine and [<sup>3</sup>H]-adenine uptake reported here was definitely not through inhibition of the NPP, as it was observed equally in infected and uninfected hRBC. The similar inhibitory effect of furosemide on hFNT1 and NPP increase the suspicion that the NPP is a modification of endogenous protein as suggested by (Egee *et al*, 2002) and (Verloo *et al*, 2004). However it must be emphasised that furosemide is not a very specific agent, as it blocks several other transporters and channels in the host erythrocytes including the Na<sup>+</sup>/K<sup>+</sup> co-transporter (Dunham *et al*, 1980; Garcia-Romeu *et al*, 1991).



### 3.7 Conclusions

Nucleobases and nucleosides present at very low levels in the host plasma gain entry into the parasite-infected erythrocyte predominantly through equilibrative transporters rather than the parasite-induced New Permeation Pathway, which is reported not to be saturable. The process of uptake is efficiently driven by the rapid salvage of purines from the cytosol by the intracellular parasite, which maintains a concentration gradient across the hRBC plasma membrane. This study also showed a faster uptake rate of adenosine into parasite-infected cells compared with hypoxanthine. The rate of purine uptake was also found to be approximately doubled in parasite-infected cells compared to uninfected cells.

## **CHAPTER FOUR**

### **4 Purine transport in saponin-freed *P. falciparum* trophozoites**

## 4.1 Summary

The malaria parasite *P. falciparum* lacks the capability to synthesise the purine ring *de novo* and has to salvage this important nutrient from the host milieu through transporters. Although the potential of these transporters as target for novel antiplasmodial compounds has been recognised, compared to other protozoa such as *Trypanosoma brucei* and *Leishmania donovani* little is known about their kinetic properties. Yet such knowledge would inform any rational design strategy for purine-based antimalarial drugs. It was therefore an objective of this study to systematically investigate and characterise the parasite's purine transporters in terms of their substrate affinity, selectivity, and the role they play in the salvage of purine from the host. Using classical uptake techniques, four transporters were identified in saponin-freed *P. falciparum*-infected erythrocytes. Three separate and novel transport activities were identified: a high affinity hypoxanthine transporter with a secondary capacity for purine nucleosides, which was named PfNT1, a separate high affinity transporter for uptake of adenine (named PfADET1) and a low affinity/high capacity adenine carrier (denoted PfADET2). Additionally, a low affinity adenosine transporter with kinetic properties similar to that previously reported by other research groups was also characterised. The kinetic data obtained in this study demonstrated that hypoxanthine was taken up with 12-fold higher efficiency than adenosine, confirming assertions that hypoxanthine is the preferred source of purine for the growing parasite. A hypoxanthine analogue, JA-32, was found to exhibit promising antimalarial activity. These findings re-emphasise the importance of purine transporters as targets for novel antimalarial drugs. A new model for purine salvage in *P. falciparum* is presented, based predominantly on the highly efficient uptake of hypoxanthine by PfNT1 and a high capacity for purine nucleoside uptake by a lower affinity carrier.

## 4.2 Background

*P. falciparum* parasites require purine for the synthesis of DNA and other important biomolecules needed to sustain life, growth and reproduction. Like the other members of the parasitic protozoa studied to date, *P. falciparum* are unable to synthesize purine *de novo* and have to depend on salvage mechanisms for the supply of this essential nutrient from the host. To date, all transporters of purine nucleosides in protozoa have been found to belong to the Equilibrative Nucleoside Transporters (ENT) family. The characteristics of ENT transporters have been described in detail in section 1.20 of this thesis.

Four putative Equilibrative Nucleoside Transporters (ENT) genes, denoted PFA0160c, MAL8P1.32, PF14\_0662 and PF13\_0252 have been identified within the *P. falciparum* genome database (Martin *et al*, 2005). However, only one gene PF13\_0252, has been characterised and was believed to encode a moderate to low affinity adenosine transporter (Parker *et al*, 2000; Carter *et al*, 2000). The two groups independently cloned a *P. falciparum* gene of the equilibrative nucleoside transporter family, which they termed PfENT1 or PfNT1. The protein was expressed in *Xenopus laevis* oocytes and the kinetics of transport was assessed. However, the two groups reported significantly different kinetic properties for the same protein. Carter and colleagues described PfNT1 as a broad specificity nucleoside transporter with  $K_m$  values of 13.2  $\mu\text{M}$  and 253  $\mu\text{M}$  for adenosine and inosine, respectively, and no affinity for nucleobases (Carter *et al*, 2000). In contrast, Parker and co-workers reported a purine nucleoside/nucleobase transporter with a similar, but low, affinity for adenosine, adenine and hypoxanthine ( $K_m$  values 320 – 410  $\mu\text{M}$ ) [(Parker *et al*, 2000)].

One reason for the observed difference could be linked to the type of system in which the protein was expressed. It has been documented that endogenous proteins present in vectors such as *Xenopus laevis* are able to interact with foreign expressed proteins, which affect their functional properties and thereby confound the results obtained from studies using such proteins (Wagner *et al*, 2000).

The work presented in this chapter was designed to address the large discrepancy observed in the two available studies of purine transport, both of which used exogenous expression systems. To avoid the potential problems of variable expression levels associated with *Xenopus oocytes*, purine transport was studied in the parasite itself, using saponin-freed *P.*

*falciparum* parasites. This work was started in 2004, and was in the process of finalisation when a third group, led by Kirk, published data on the kinetic properties of a purine transporter in the parasite, similarly using saponin-freed *P. falciparum* parasites (Downie *et al*, 2006). The outcome of their investigation showed the presence of a low affinity adenosine transporter, similar to that described by (Parker and Carter) with  $K_m$  estimates of 13 and 320  $\mu\text{M}$  (Parker *et al*, 2000; Carter *et al*, 2000). However, despite using the same system as that presented here, the conclusions reported were completely different. A major short coming of the published studies is that they all used micromolar concentrations of radiolabelled substrate in their assays, which would result in the saturation of any transporters with sub- or lower-micromolar  $K_m$  values. Thus the presence of high affinity purine transporters could not be detected. The current studies used radiolabeled substrate concentrations in the sub-micromolar range (0.1-0.5  $\mu\text{M}$ ), allowing detection of any high affinity transporters if present.

#### **4.2.1 Mechanism of permeabilisation of *P. falciparum* infected erythrocytes**

*P. falciparum* parasites with a permeabilised red cell membrane were prepared using the saponin permeabilisation method. The plant-derived detergent, saponin, interacts with cholesterol in the cell membrane, causing ‘disruption of the barrier properties of cholesterol-containing membranes’ (Ansorge *et al*, 1996). Although the ghost of the red cell membrane remains present (Figure 4.1), it no longer acts as barrier to the entry of compounds from external sources (Siddiqui *et al*, 1979).

The parasitophorous vacuole membrane is also not a barrier to the inward movement of nutrients as studies show that it is permeable to small solutes (Desai *et al*, 1993). Since the parasite plasma membrane is not significantly affected by the saponin treatment (Saliba *et al*, 1998; Allen & Kirk, 2004), initial rates of transport measured in this system reflect uptake by the Plasmodium- encoded transporters located in the parasite’s plasma membrane.

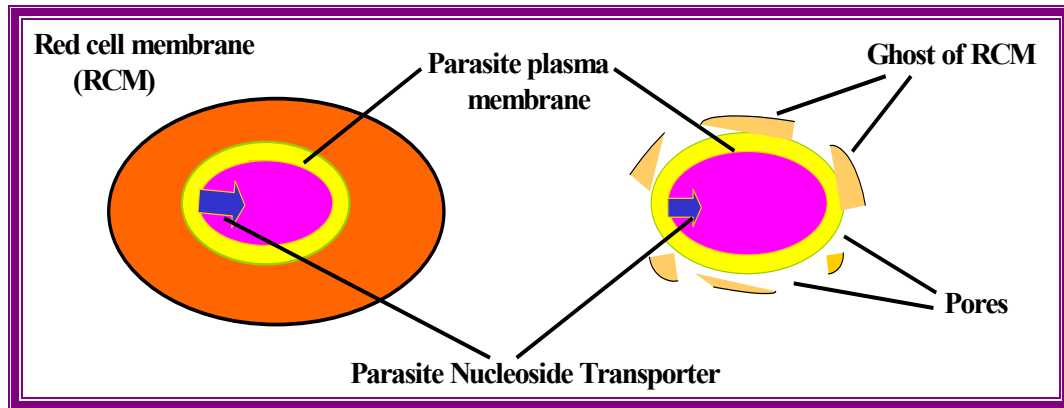


Figure 4.1: A *P. falciparum*-infected erythrocyte showing the presence of the different membranes before and after saponin permeabilisation of the RBC.

The blue arrows represent the purine transporter. Although fragments of the RBCM are present, they do not hinder the movement of nutrients into the parasite.

#### 4.2.2 Hypoxanthine, the preferred purine source for *P. falciparum*

It is well documented that hypoxanthine is the preferred purine source for the malaria parasites. For example, very high activities of hypoxanthine-guanine phosphoribosyltransferase and inosine phosphorylase have been measured in the parasite, whereas adenine phosphoribosyltransferase and adenosine kinase activities were low or absent (Reyes *et al*, 1982). Adenosine is metabolised through rapid deamination to inosine and thence to hypoxanthine (Reyes *et al*, 1982), and this process mostly occurs extracellularly, as discussed in chapter three of this thesis. This explains the observation of Hansen and co that inhibition of adenosine deaminase with deoxycoformycin potently reduced [ $^3\text{H}$ ]-adenosine uptake by *P. berghei* (Hansen *et al*, 1980). The importance of hypoxanthine in the growth and development of *Plasmodium* was also shown in the study of Berman and his colleagues (Berman *et al*, 1991).

While it is clear that hypoxanthine is fundamental for the survival and multiplication of the malaria parasite, most of the available information on *Plasmodium* purine transporters has been concerned with the uptake of adenosine. It was, therefore, an objective of this study to investigate the salvage of purines in saponin-isolated *P. falciparum* trophozoites with particular emphasis on the uptake of hypoxanthine.

### 4.3 Preparation of saponin-freed *P. falciparum* (clone 3D7) trophozoites for uptake studies

*P. falciparum* (clone 3D7) was maintained in continuous culture using standard methods, described in section 2.1.4. Synchronised *P. falciparum* culture was obtained by treatment of the cultured parasites with sorbitol (section 2.1.5). Permeabilised *P. falciparum* infected erythrocytes were prepared by incubating the synchronised culture (trophozoite stage) with 0.15% saponin as described in section 2.2.2. The classical uptake method described in section 2.2.4 was used to study the flux of radiolabeled purine compounds into saponin-permeabilised *P. falciparum* trophozoites. The permeants studied were hypoxanthine, adenine and adenosine. The inhibitory effect of guanine, guanosine, inosine, the pyrimidines (cytosine, cytidine, uridine, uracil, thymidine, thymine) and some purine analogues on the transport of hypoxanthine, adenine and adenosine was also investigated.

Two types of assays were conducted in this part of the study: (i) the time dependent uptake assay, which allows the linear phase of the uptake and thus the transport rate to be determined, and (ii) the concentration-dependent assay that assesses the ability of a non-radiolabeled compound to inhibit uptake of a radiolabeled purine.

For the time course, 200 µl of a suspension of saponin-permeabilised, parasite-infected erythrocytes (usually at  $2-6 \times 10^7$  cell/assay) were mixed with the same volume of radiolabeled permeant which was at twice the final intended concentration. At pre-determined times, uptake was terminated by adding 1 ml ice-cold, 2 mM stop solution (unlabelled permeant at saturating concentrations). The mixture was immediately centrifuged at  $13000 \times g$  for 30 s through an oil-mix (300 µl of 5 parts dibutylphthalate: 4 parts dioctyl phthalate, v/v) to pellet the cells and separate them from the aqueous radiolabeled permeant.

When uptake was too rapid to provide a reliable linearity of transport at room temperature, it was reassessed at 6 °C, using a ThermoStat plus (Eppendorf, Germany) temperature controlled microfuge rack to maintain a reduced temperature during the incubation, thus reducing the uptake rate.

For the dose dependent assay, radiolabeled permeant was mixed with the same volume and concentration of an inhibitor. Two hundred microlitres of the mixture were carefully layered onto 300  $\mu$ l oil-mix in a 1.5 ml microfuge tube. The tube was centrifuged briefly at  $13000 \times g$  to collect the mixture into a single bubble on top of the oil layer. An equal volume of saponin-freed *P. falciparum* trophozoites (isolated parasites), suspended in hypoxanthine-free, RPMI 1640 usually at about  $3\text{--}6 \times 10^7$  parasites/assay, was incubated with the radio-labelled/inhibitor mixture on top of the oil-mix for a pre-determined time. The uptake of radiolabel was terminated by adding 1 ml cold stop solution (2 mM of unlabelled permeant) prior to centrifugation at  $13000 \times g$  for 30 s.

Inhibition studies were always performed within the linear phase of uptake, and thus reflect true initial rates of transport across the *P. falciparum* plasma membrane rather than rates of metabolism or sequestration.

After uptake, the samples were processed for scintillation counting using the method described in section 2.2.7 of this thesis. Non-mediated influx of the respective permeant was assessed by determining the rate of uptake of the radiolabeled permeant in the presence of 1 mM unlabelled permeant as well as with cells and permeant at 0°C.

## 4.4 Data analysis

For any given permeant, the linear phase of uptake was first determined using the described time dependent assay. The curve of best fit through the points was assessed for linearity using linear regression. Linearity is defined as a correlation coefficient  $>0.95$  and significant difference from zero uptake (F-test; GraphPad Prism version 4).



## 4.5 High affinity hypoxanthine transport in saponin-freed *P. falciparum* trophozoites

Studies of the uptake of hypoxanthine into saponin-permeabilised *P. falciparum* infected erythrocytes were performed at room temperature.

### 4.5.1 Time dependent uptake of hypoxanthine into saponin-freed *P. falciparum* trophozoites

The time dependent assays revealed that uptake of 0.25 or 0.1  $\mu\text{M}$  [ $^3\text{H}$ ]-hypoxanthine was rapid and followed a hyperbolic curve, which was linear up to 120 s at both permeant concentrations (Figure 4.2). The correlation coefficients ( $r^2$ ) determined by linear regression over the first 120 s were 0.99 and 0.98 for permeant concentrations at 0.25  $\mu\text{M}$  and 0.1  $\mu\text{M}$  respectively. Rates of  $0.62 \pm 0.04$  and  $0.40 \pm 0.03$   $\text{pmol} (10^7 \text{ cells})^{-1} \text{s}^{-1}$  were determined at permeant concentrations of 0.25  $\mu\text{M}$  and 0.1  $\mu\text{M}$  respectively, and the uptake was completely inhibited by 1 mM unlabelled hypoxanthine (Figure 4.2(A and B)).

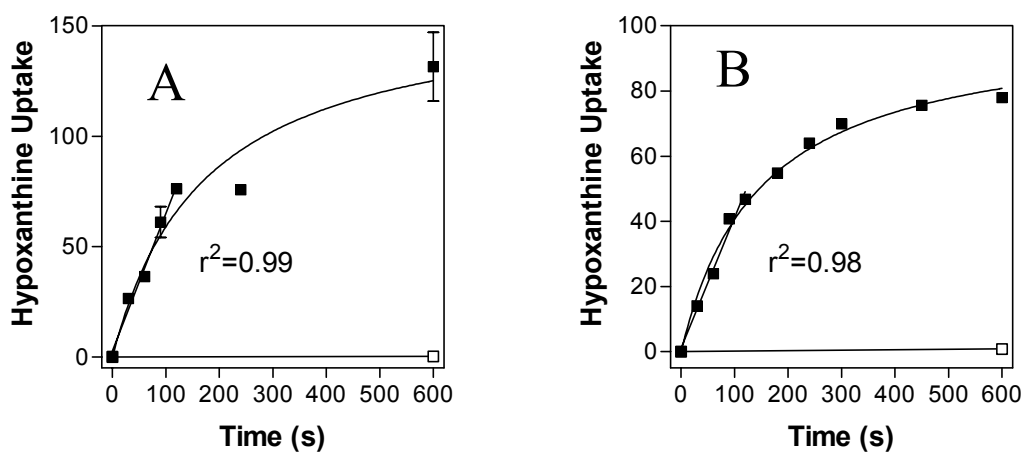


Figure 4.2: Hypoxanthine transport in saponin-freed *P. falciparum* trophozoites.

Representative graphs showing uptake of (A) 0.25  $\mu\text{M}$  [ $^3\text{H}$ ]-hypoxanthine and (B) 0.10  $\mu\text{M}$  [ $^3\text{H}$ ]-hypoxanthine into saponin-freed *P. falciparum* trophozoites in the presence (closed squares) or absence (open squares) of 1 mM unlabeled hypoxanthine at 20  $^{\circ}\text{C}$ . Data points are the mean of 3 experiments and error bars indicate SEM. Uptake was expressed as  $\text{pmol}(10^7 \text{ cells})^{-1}$

### 4.5.2 Determination of $K_m$ and $V_{max}$ values for the high affinity hypoxanthine transporter

Analysis of the results from the dose-dependent uptake of [ $^3$ H]-hypoxanthine at sub-micromolar concentrations revealed the presence of a very high affinity transporter for oxopurines, with a mean  $K_m$  value for hypoxanthine of  $0.34 \pm 0.05 \mu\text{M}$ , a  $V_{max}$  of  $0.36 \pm 0.12 \text{ pmol}(10^7 \text{ cells})^{-1} \text{ s}^{-1}$  ( $n = 6$ ; Figure 4.3) and a mean  $K_i$  value of  $0.11 \pm 0.01 \mu\text{M}$  for guanine ( $n=3$ ); inosine also displayed affinity in the low micromolar range for this transporter ( $K_i = 1.99 \pm 0.20 \mu\text{M}$ ;  $n=3$ ) (Figure 4.3).

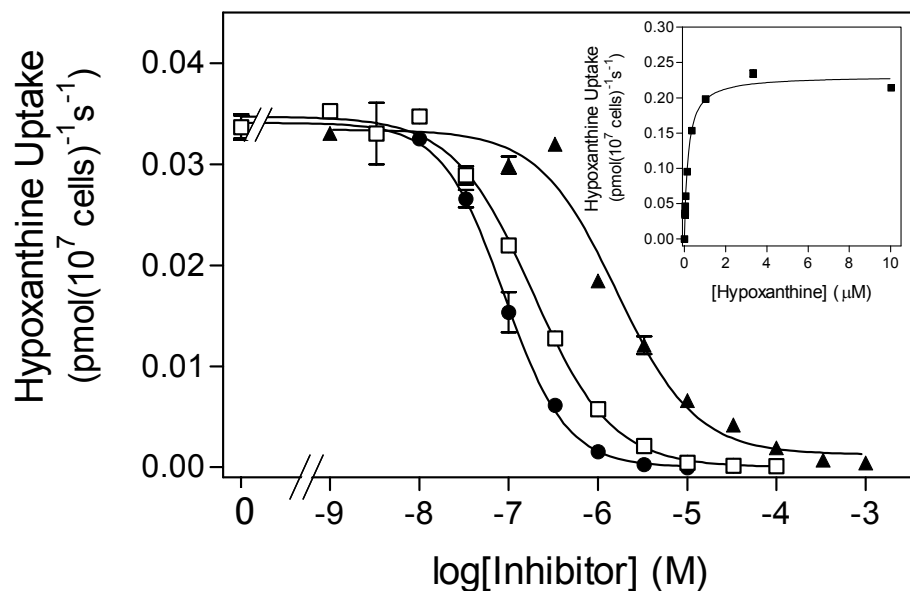


Figure 4.3: Characterization of a high affinity *P. falciparum* hypoxanthine transporter.

Uptake of 30 nM [ $^3$ H]-hypoxanthine in the presence or absence of various concentrations of unlabelled hypoxanthine ( $\square$ ), guanine ( $\bullet$ ) or inosine ( $\blacktriangle$ ). Inset: conversion of hypoxanthine inhibition data to Michaelis-Menten plot for determination of  $K_m$  and  $V_{max}$ . Data points are the mean of triplicate determinations and error bars show the standard error of the mean (SEM).

### 4.5.3 Inhibitory effect of other purines on the high affinity hypoxanthine transporter

Adenosine and guanosine (Figure 4.4) displayed affinity in the low micromolar range for the hypoxanthine transporter (Table 4.1). However, adenine did not inhibit the transport of 0.03  $\mu\text{M}$  [ $^3\text{H}$ ]-hypoxanthine into the saponin-freed trophozoites at concentrations close to 1 mM (Figure 4.4).

In order to avoid confusion later on, this high affinity purine transporter will hereafter be referred to as the *P. falciparum* Nucleoside Transporter 1 (PfNT1) in this thesis.

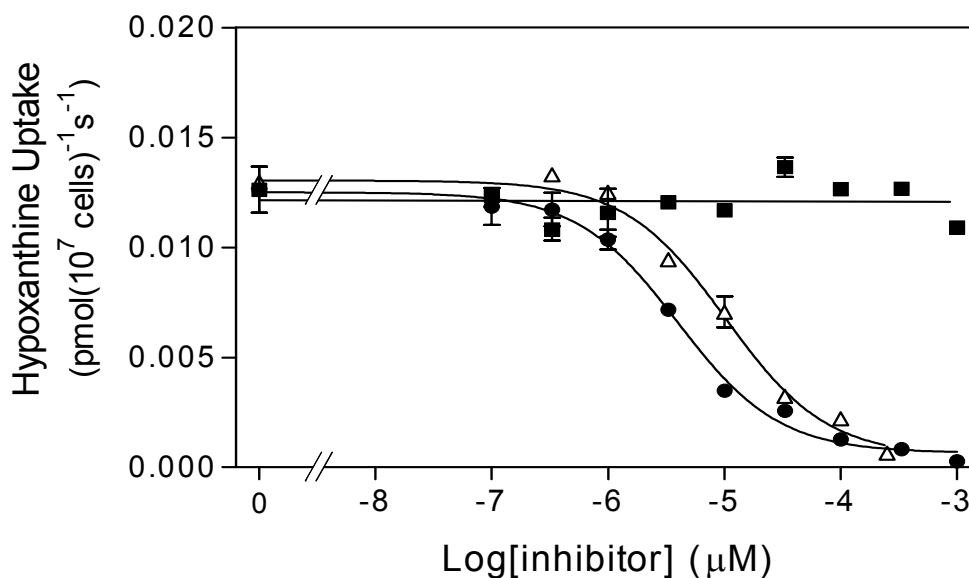


Figure 4.4: Characterization of a high affinity *P. falciparum* hypoxanthine transporter.

Uptake of 30 nM [ $^3\text{H}$ ]-hypoxanthine in the presence or absence of various concentrations of unlabelled adenine (■), guanosine ( $\Delta$ ) or adenosine ( $\bullet$ ). Representative experiments are shown, conducted in triplicate. Data points are the mean of triplicate determinations and error bars indicate SEM.

In summary this work has demonstrated the presence of a transporter with a high affinity for hypoxanthine ( $K_m = 0.34 \pm 0.05 \mu\text{M}$ ) which also has affinity for guanine, adenosine and guanosine in the low micromolar range, but which does not bind adenine.

## 4.6 Inhibitory effect of purine analogues on the high affinity hypoxanthine transporter

The effect of purine analogues received from Dr. Daniel Brown (MRC, Cambridge, UK) was tested against the uptake of [ $^3\text{H}$ ]-hypoxanthine through PfNT1. It was observed that the uptake of 0.30 nM [ $^3\text{H}$ ]-hypoxanthine into saponin permeabilised *P. falciparum* infected erythrocyte was inhibited by the purine analogue, JA-32 with a  $K_i$  of  $14 \pm 3 \mu\text{M}$  (Figure 4.6). Two other analogues, JA-23 and JA-24, had little ( $K_i = 320 \pm 80 \mu\text{M}$  for JA-24) or no effect (JA23) on high affinity hypoxanthine transport (Figure 4.5). From the chemical structures of the analogues shown in figure 4.6, it can be deduced that the strong inhibitory effect of JA-32 was probably due to its 'hypoxanthine-like' conformation. Apparently, the amino substitution at the N<sup>6</sup> position prevents proper binding of the adenosine analogues, the amine substitution at position 2 is shared with guanosine and thus unlikely to prevent high affinity binding.

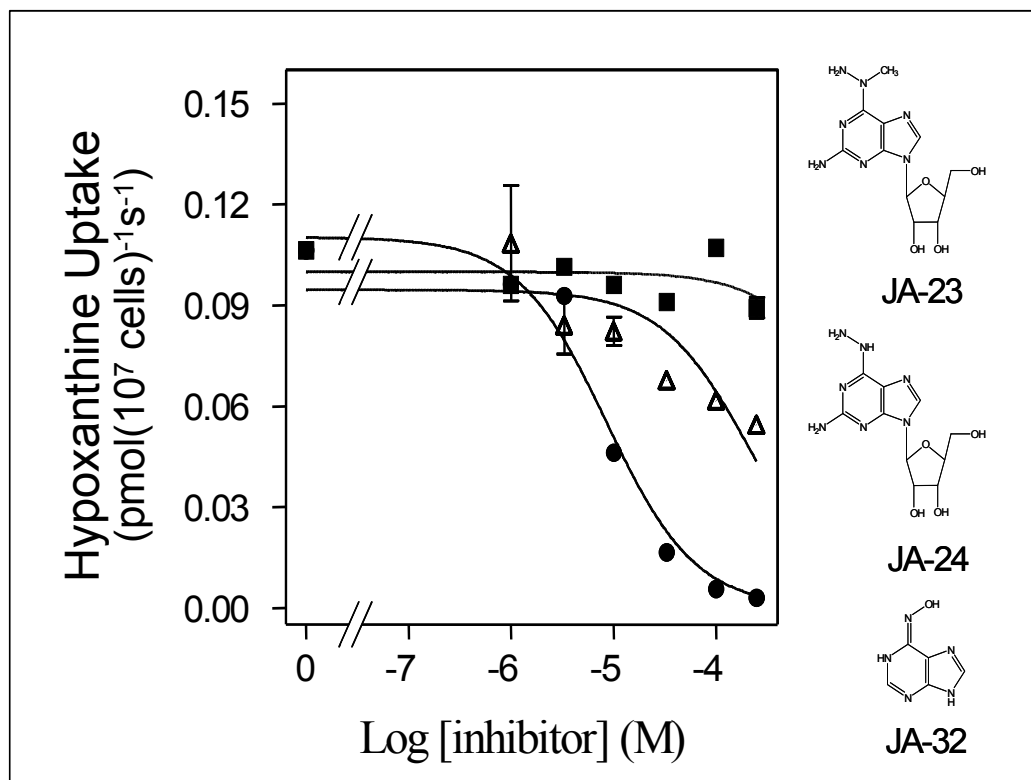


Figure 4.5: Uptake of 30 nM [ $^3\text{H}$ ]-hypoxanthine in the presence or absence of purine analogues JA-23, JA-24 and JA 32.

The figure shows the uptake of 30 nM [ $^3\text{H}$ ]-hypoxanthine in the presence or absence of JA23 (■), JA24 (Δ), JA32 (●). Data points are the mean of 3 experiments and error bars indicate SEM. Chemical structures of the JA-compounds are also shown.

## 4.7 Inhibition of high affinity hypoxanthine transport by Pyrimidines

In general, pyrimidines had little effect on the uptake of sub micromolar concentrations of [ $^3\text{H}$ ]- hypoxanthine. Only uridine, uracil and thymidine, at a concentration of 1 mM inhibitor, appreciably inhibited transport of 30 nM [ $^3\text{H}$ ]-hypoxanthine by  $36 \pm 9\%$  ( $P < 0.03$ ),  $49 \pm 6\%$  ( $P < 0.005$ ) and  $57 \pm 6\%$  ( $P < 0.02$ ) respectively (Paired Student's t-test against no-inhibitor control, based on four independent experiments in duplicate). Cytosine, thymine and cytidine did not significantly inhibit the transport of 30 nM [ $^3\text{H}$ ]-hypoxanthine.

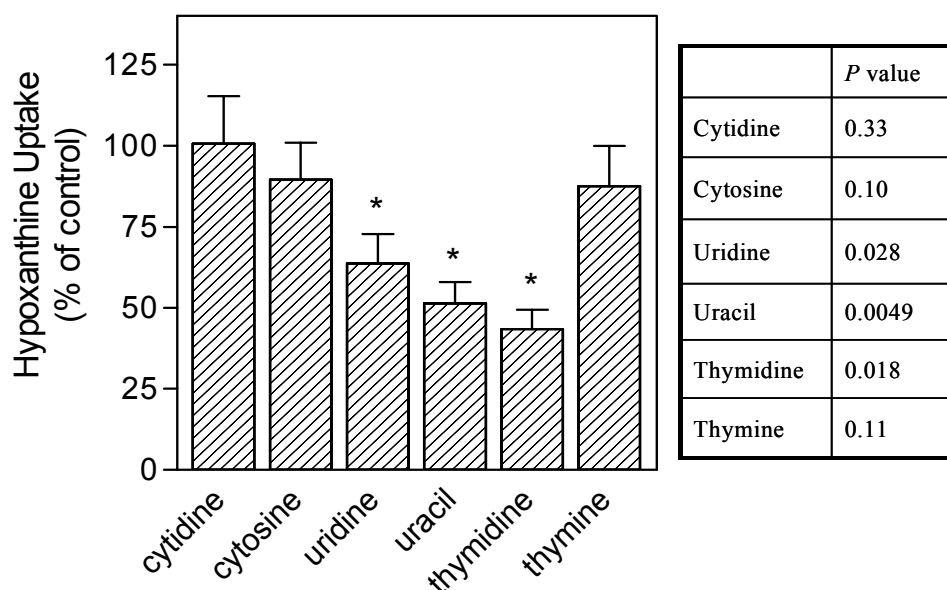


Figure 4.6: Effect of pyrimidines on the transport of 30 nM [ $^3\text{H}$ ]-hypoxanthine by saponin-freed *P. falciparum* trophozoites.

Inhibitor concentrations were 1 mM and transport was measured at 20 °C over 60 s. Data shown are the means and SEM of four independent experiments, each performed in duplicate. Control values (100%) were taken as the uptake of [ $^3\text{H}$ ]-hypoxanthine in the absence of inhibitor. Statistical significance was determined using a paired Student T-test with the mean rate of uptake in the presence of each inhibitor paired with the mean control rate of uptake of the same experiment. \*, indicates significant inhibition,  $P < 0.05$ . Shown in the table on the right are the p-values of the paired student's t-test against no-inhibitor control, based on four independent experiments in duplicate.

## 4.8 High affinity adenosine transport into saponin-freed *P. falciparum* trophozoites

Observations made in the current studies indicate that the transport of [ $^3\text{H}$ ]-hypoxanthine through PfNT1 was inhibited by adenosine with a  $K_i$  of  $4.0 \pm 0.67 \mu\text{M}$ . To investigate whether adenosine is a true ligand for the high affinity hypoxanthine transporter, rather than an inhibitor, high affinity uptake of [ $^3\text{H}$ ]-adenosine in saponin-freed trophozoites was investigated using the uptake techniques described earlier (section 2.2). All the experiments were performed at room temperature. The results of these investigations are shown in section 4.8.1 to section 4.8.2.

### 4.8.1 Time dependent uptake of adenosine

Uptake of  $0.25 \mu\text{M}$  [ $^3\text{H}$ ]-adenosine proceeded with a rate of  $0.015 \pm 0.002 \text{ pmol}(10^7 \text{ cells})^{-1} \text{ s}^{-1}$  over the linear phase (at least 30 s), and was completely inhibited by 1 mM adenosine (Figure 4.7). At the end of linear phase, cells had transported approx.  $0.55 \text{ pmol}$  [ $^3\text{H}$ ]-adenosine/ $10^7$  cells, which would correspond to  $\sim 8$ -fold the extracellular concentration if unmetabolised [based on intracellular volume of  $2.8 \times 10^{-7} \text{ l}/10^7$  parasites isolated by saponin treatment; (Saliba *et al*, 1998)].

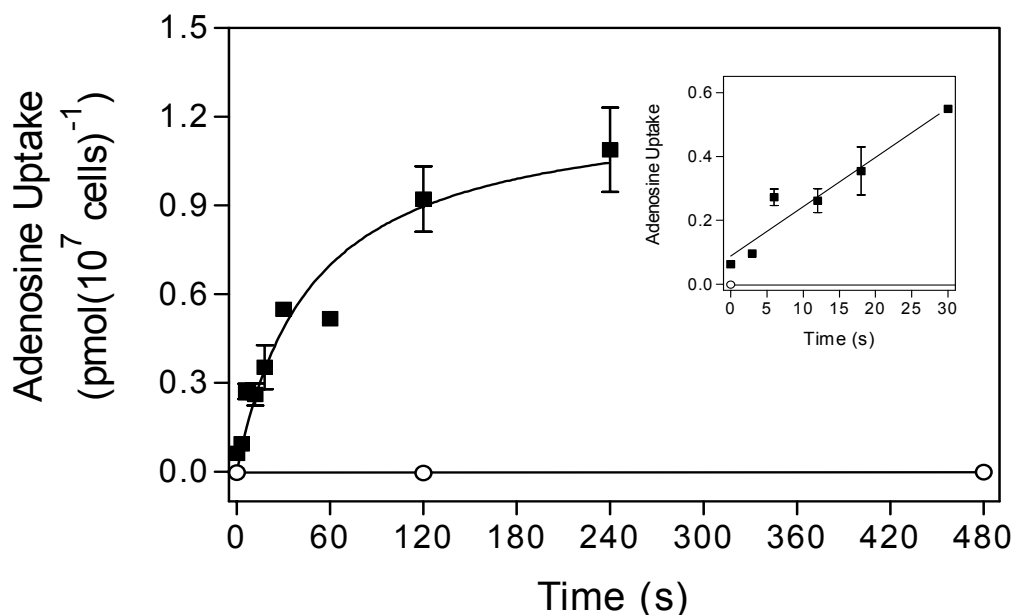


Figure 4.7: Uptake of low concentrations of [ $^3\text{H}$ ]-adenosine in isolated *P. falciparum* trophozoites.

Uptake of  $0.25 \mu\text{M}$  [ $^3\text{H}$ ]-adenosine ( $\square$ ) was linear over 30 s ( $r^2 > 0.99$ ; inset). Uptake in the presence of 1 mM adenosine ( $\square$ ) was not significantly different from zero (F-test,  $P = 0.67$ ). Data points are the mean of 3 experiments and error bars show the standard error of the mean (SEM).

### 4.8.2 Determination of the $K_m$ and inhibition profile for the high affinity adenosine transport

When kinetic values obtained from the uptake of  $0.25 \mu\text{M}$  [ $^3\text{H}$ ]-adenosine were fitted into a Michaelis-Menten plot, a mean  $K_m$  value of  $2.0 \pm 0.2 \mu\text{M}$  and  $V_{\max}$   $0.18 \pm 0.08 (10^7 \text{ cells})^{-1} \text{s}^{-1}$  ( $n=3$ ; Figure 4.8, inset) were obtained. From the dose-response uptake assay it was clear that transport of  $0.25 \mu\text{M}$  [ $^3\text{H}$ ]-adenosine was inhibited by unlabelled adenosine as well as by hypoxanthine (mean  $K_i = 0.75 \pm 0.18 \mu\text{M}$ ;  $n=3$ ), but not by adenine (Figure 4.8). An important observation made in this experiment is that the inhibition by hypoxanthine in three independent assays was not quite complete at  $100 \mu\text{M}$  ( $6.1 \pm 0.2\%$ ;  $P<0.05$ , paired Student's t-test). A possible reason for this observation could be that there is a minor contribution to the  $0.25 \mu\text{M}$  [ $^3\text{H}$ ]-adenosine flux from a second, low affinity adenosine transporter that is insensitive to hypoxanthine.

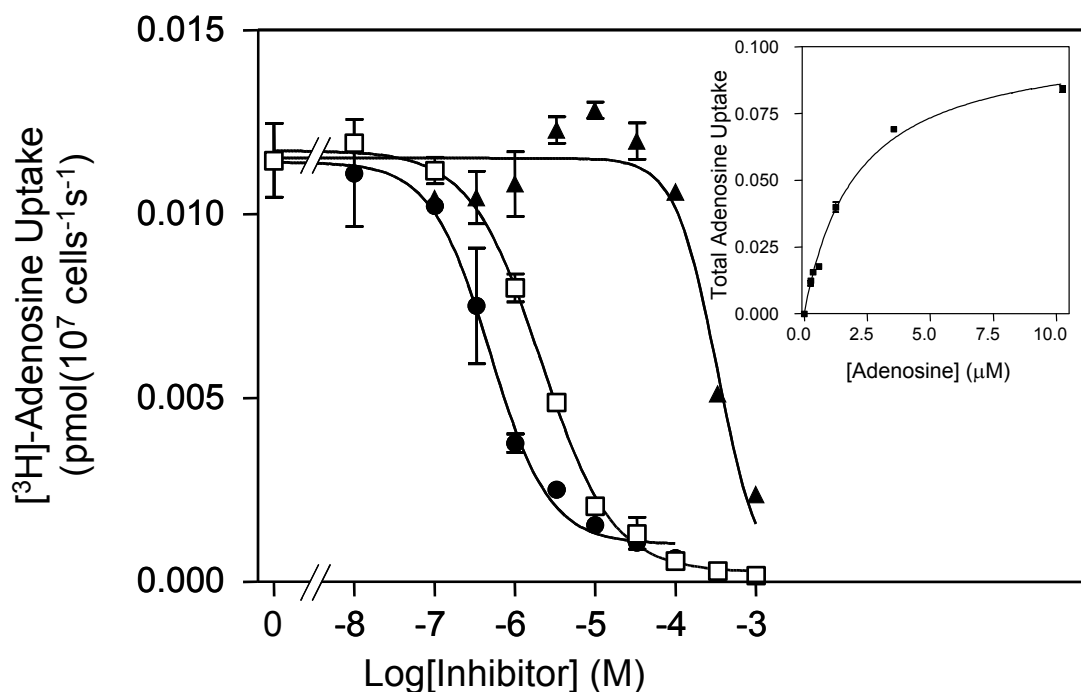


Figure 4.8: Uptake of low concentrations of [ $^3\text{H}$ ]-adenosine in saponin-free *P. falciparum* trophozoites.

Transport of  $0.25 \mu\text{M}$  [ $^3\text{H}$ ]-adenosine was measured over 30 s in the presence or absence of various concentrations of unlabelled adenosine ( $\square$ ), adenine ( $\blacktriangle$ ) and hypoxanthine ( $\bullet$ ). Inset: conversion of the adenosine inhibition data to a Michaelis-Menten plot. The adenine  $\text{IC}_{50}$  value was obtained by extrapolation to 100% inhibition. Data points are the mean values from representative experiments performed in triplicate; error bars represent SEM.

Combining results from this experiment with that from the uptake of hypoxanthine (section 4.5.3), it can be concluded that PfNT1 took up both adenosine and hypoxanthine. Meaning that hypoxanthine and adenosine have reciprocal inhibition on the high affinity transporter. This assertion is based on the fact that the  $K_i$  value for adenosine on hypoxanthine transport is similar to the  $K_m$  for adenosine; and the  $K_m$  for hypoxanthine is similar to the  $K_i$  value for hypoxanthine with [ $^3\text{H}$ ]-adenosine transport.

## **4.9 Transport of adenine into saponin-freed *P. falciparum* trophozoites**

Since adenine did not appear to be transported by PfNT1, further investigations were conducted to assess whether a separate transporter exists for the uptake of adenine into saponin-permeabilised parasites. Time course and dose dependent uptake experiments of 1  $\mu\text{M}$  of [ $^3\text{H}$ ]-adenine were therefore performed using the procedure described in section 2.2.4.

### **4.9.1 Uptake of adenine is mediated by a separate high affinity transporter**

Uptake of 1  $\mu\text{M}$  of [ $^3\text{H}$ ]-adenine was rapid and was almost completely saturated by 1 mM unlabelled adenine. This observation was suggestive of an uptake process mediated by a high-affinity transporter (Figure 4.9). The rate of transport was estimated as  $0.0091 \pm 0.0025 \text{ pmol } (10^7 \text{ cells})^{-1} \text{ s}^{-1}$  by linear regression over the linear phase (6 s;  $r^2 = 0.93$ ).

Comparatively, the measured rate of uptake of [ $^3\text{H}$ ]-adenine was two orders of magnitude lower than for [ $^3\text{H}$ ]-hypoxanthine, again confirming hypoxanthine as the preferred purine source by the growing malaria parasites. The novel adenine transport activity observed here was designated *P. falciparum* adenine transporter 1 (PfADET1).



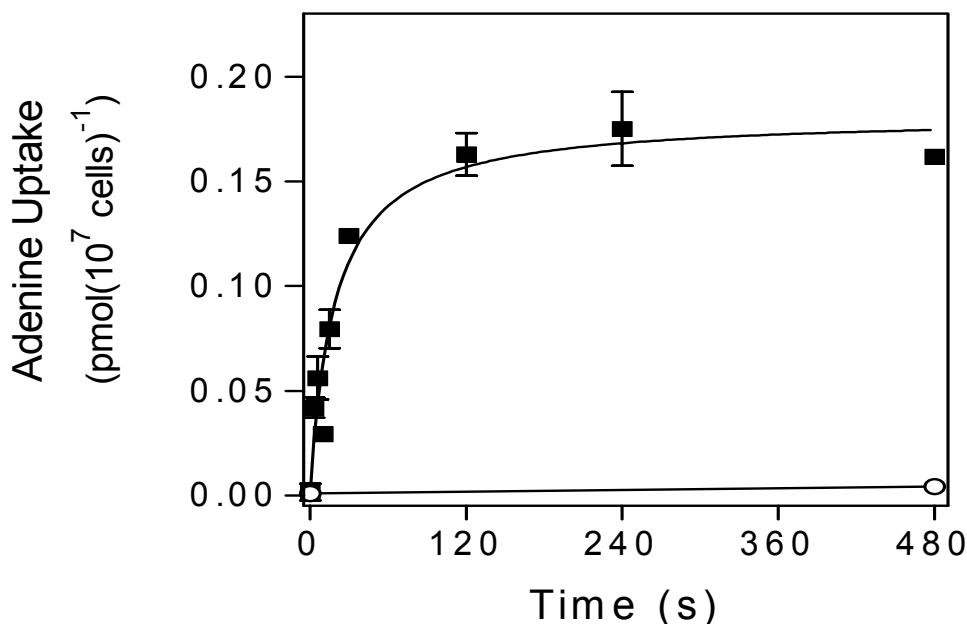


Figure 4.9: Characterization of a high affinity adenine transporter in *P. falciparum* trophozoites (Transport of 1  $\mu\text{M}$  [ $^3\text{H}$ ]-adenine).

Transport of 1  $\mu\text{M}$  [ $^3\text{H}$ ]-adenine in saponin-freed *P. falciparum* trophozoites over a period of 8 minutes, in the presence (○) or absence (■) of 1 mM unlabelled adenine. Data points are the mean of 3 experiments and error bars indicate SEM.

#### 4.9.2 Determination of $K_m$ and $V_{max}$ for PfADET1

The  $K_m$  value for the high affinity adenine transporter was estimated through uptake of 50 nM [ $^3\text{H}$ ]-adenine. The results, shown in Figure 4.10, indicate that uptake was linear for up to 240 s, allowing inhibition experiments at an incubation time of 150 s. In the absence of inhibitor the transport rate was estimated as  $3.9 \pm 0.2 \times 10^{-5} \text{ pmol (10}^7 \text{ cells)}^{-1} \text{ s}^{-1}$  as calculated by linear regression ( $r^2 = 0.98$ ). At 240 s, uptake was inhibited 70% by 1 mM adenine.

Using a Michaelis-Menten plot, a  $K_m$  of  $0.23 \pm 0.07$  and  $V_{max}$  of  $0.0004 \text{ pmol (10}^7 \text{ cells)}^{-1} \text{ s}^{-1}$  was estimated for this transporter (Figure 4.11). Combining the high  $K_m$  value, which was similar to the hypoxanthine  $K_m$  for PfNT1 with the very low  $V_{max}$  measured here, PfADET1 can be said to be a high affinity/low capacity transport system (see Table 4.1 for  $V_{max}/K_m$  ratio).

Analysis of the results clearly show that there was a substantial uptake component that was not sensitive to 1mM adenine, as indicated by the positive gradient of uptake observed in the presence of 1mM unlabelled adenine in Figure 4.10. Uptake through PfADET1 represents approximately 70-80% of total uptake at this [ $^3\text{H}$ ]-adenine concentration, leaving approximately 20-30% of adenine uptake through an alternative pathway. One explanation for this observation could be that this proportion of adenine uptake is occurring by diffusion: adenine is known to have the highest diffusion component among all the purine compounds, and is accumulated by the related parasite *T. gondii* solely through passive diffusion (de Koning *et al*, 2003). An alternative explanation may be the presence of a second, as yet uncharacterised, adenine transporter (see section 4.9).

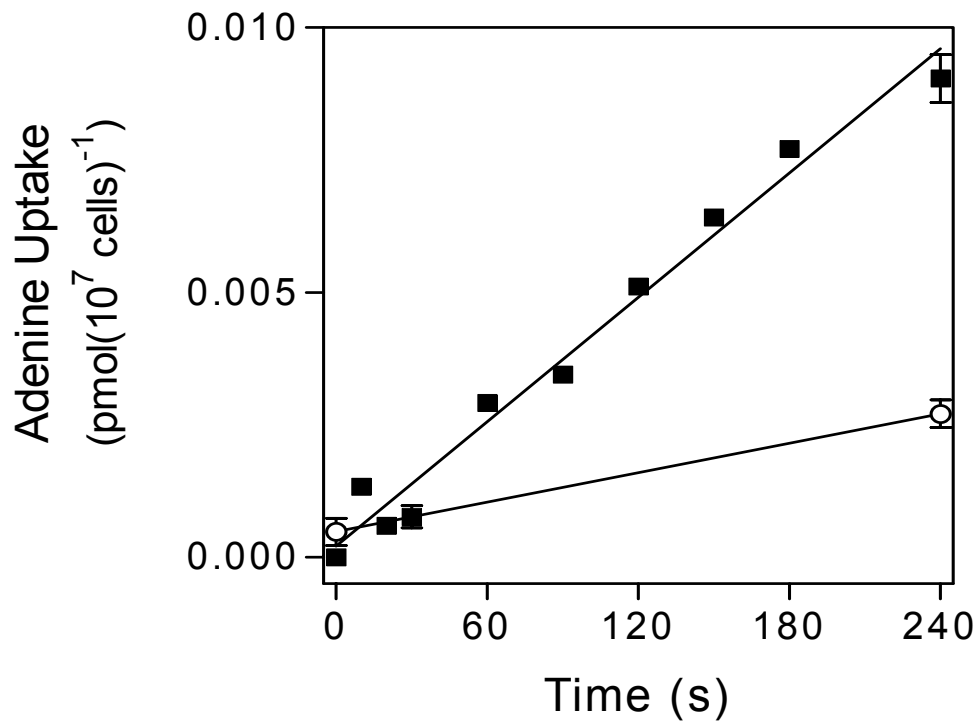


Figure 4.10: Characterization of a high affinity adenine transporter in saponin-free *P. falciparum* trophozoites (Transport of 0.05  $\mu\text{M}$  [ $^3\text{H}$ ]-adenine).

Transport of 0.05  $\mu\text{M}$  [ $^3\text{H}$ ]-adenine over 240 s, in the presence (○) or absence (■) of 1 mM unlabelled adenine. Data points are the mean of 3 experiments and error bars indicate SEM.

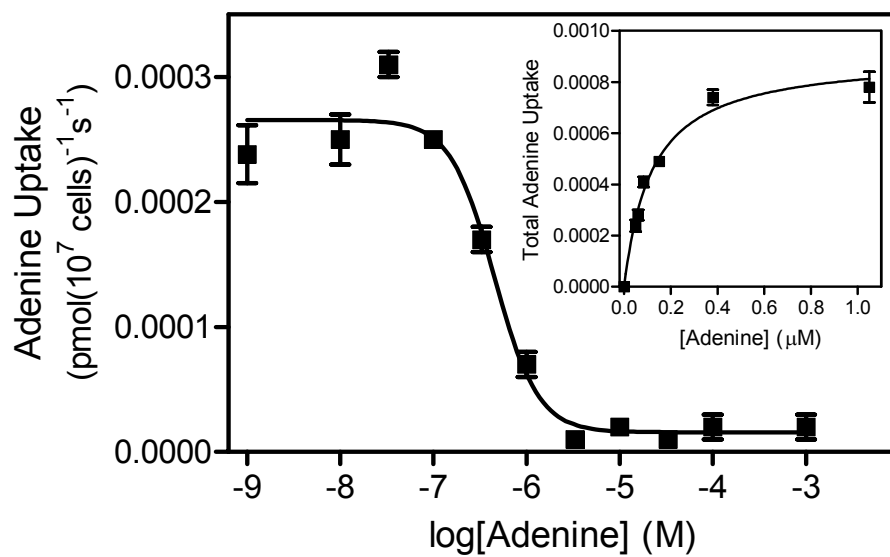


Figure 4.11: Characterization of a high affinity adenine transporter in *P. falciparum* trophozoites (Michaelis-Menten plot).

Transport of 0.05 μM [<sup>3</sup>H]-adenine was inhibited by increasing concentrations of unlabelled adenine. Inset: conversion of the inhibition data to a Michaelis-Menten plot. Data points are the mean of 3 replicates and error bars indicate SEM.

### 4.9.3 Inhibition profile of PfADET 1

Observations made in this study indicate that, unlike PfNT1, the adenine carrier (PfADET1) detected here was not inhibited by the oxopurines, hypoxanthine (Figure 4.12), guanine (data not shown) and inosine (data not shown), though it was sensitive to adenosine, with a  $K_i$  value of  $2.0 \pm 0.2 \mu\text{M}$  (Figure 4.12).

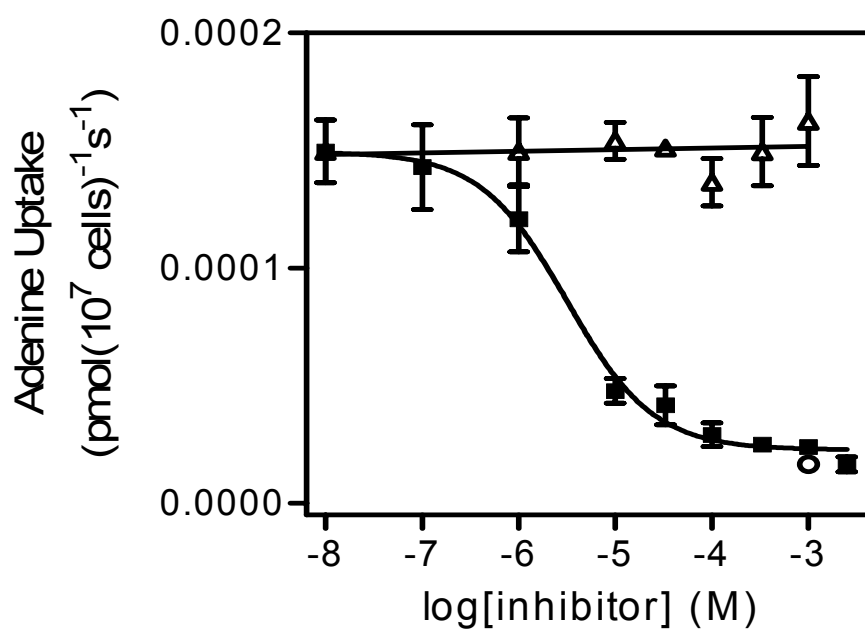


Figure 4.12: Uptake of  $0.05 \mu\text{M}$  [ $^3\text{H}$ ]-adenine into saponin-freed *P. falciparum* trophozoites in the presence of varying concentrations of other purines.

The figure shows the uptake of  $0.05 \mu\text{M}$  [ $^3\text{H}$ ]-adenine in the presence of hypoxanthine ( $\Delta$ ), adenosine ( $\blacksquare$ ) or 1 mM adenine ( $\circ$ ). Data points are the mean of 3 experiments and error bars indicate SEM.

#### 4.10 A very low affinity/high capacity transporter of adenine exists in saponin-freed *P. falciparum* trophozoites

Since the uptake of  $0.05\ \mu\text{M}$  [ $^3\text{H}$ ]-adenine was not fully inhibited by  $1\ \text{mM}$  unlabelled adenine, the possible presence of a low-affinity adenine transport activity in *P. falciparum* trophozoites was investigated. The uptake of adenine described above was repeated using a higher concentration of radiolabeled permeant ( $10\ \mu\text{M}$  [ $^3\text{H}$ ]-adenine). As shown in Figure 4.13, uptake of  $10\ \mu\text{M}$  [ $^3\text{H}$ ]-adenine was linear for up to  $12\ \text{s}$ , with a rate of  $0.13 \pm 0.01\ \text{pmol}\ (10^7\ \text{cells})^{-1}\text{s}^{-1}$  ( $r^2 = 0.96$ ). This could not be entirely attributed to simple diffusion as it was partly inhibited ( $\sim 60\%$ ) by  $1\ \text{mM}$  adenine. Attempts to establish a  $K_m$  value for [ $^3\text{H}$ ]-adenine uptake on this transporter were unsuccessful due in part to the high rate of diffusion of adenine at high concentrations, and also because the limitations of adenine solubility prevented the determination of a complete inhibition curve. However, the  $K_m$  for adenine was estimated to be in excess of  $1\ \text{mM}$ , and the  $K_i$  value for adenosine on this transporter was observed to be  $>2.5\ \text{mM}$ . There was no clear inhibition by up to  $1\ \text{mM}$  hypoxanthine. This low affinity but high capacity transport activity was provisionally designated PfADET2.

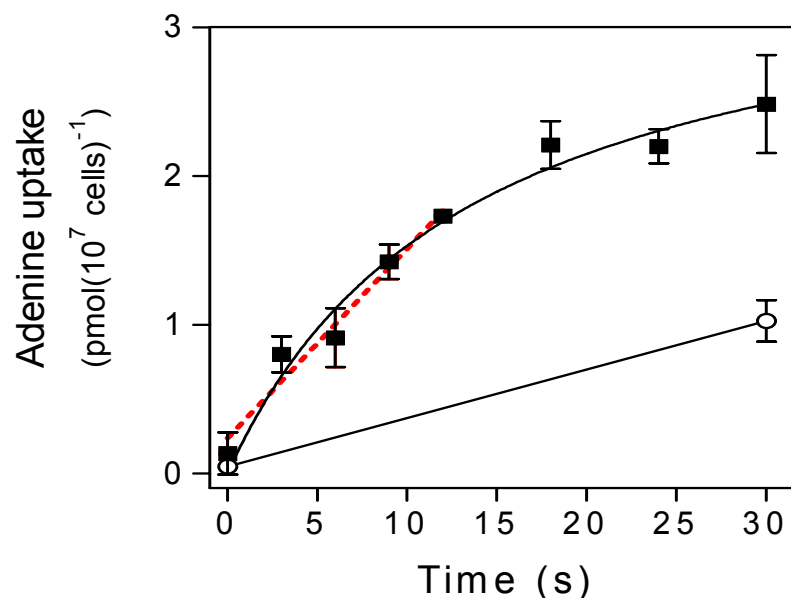


Figure 4.13: Uptake of  $10\ \mu\text{M}$  [ $^3\text{H}$ ]-adenine by *P. falciparum* trophozoites.

Saponin-freed trophozoites were incubated for up to 30 seconds with  $10\ \mu\text{M}$  [ $^3\text{H}$ ]-adenine, in the presence (○) or absence (■) of  $1\ \text{mM}$  unlabelled adenine. Data points are the mean of 3 experiments and error bars indicate SEM. The straight dotted red line shows the linear regression line fitted over the first 15 seconds of uptake.

## 4.11 Low affinity transport of adenosine in saponin-freed *P. falciparum* trophozoites

The low affinity adenosine transport activity in *P. falciparum*, which was previously described by the groups of Ullman and Baldwin (Parker *et al*, 2000;Carter *et al*, 2000), was re-investigated in the current study using concentrations of the radiolabeled permeant that would saturate the high affinity transporter. The outcome is reported in sections 4.11.1-4.11.2.

### 4.11.1 Existence of a low affinity adenosine transporter in *P. falciparum* trophozoites confirmed

At room temperature (22 °C) 25 µM [<sup>3</sup>H]-adenosine was rapidly taken up by saponin-freed *P. falciparum* trophozoites (Figure 4.14). This observation is consistent with the report of Downie and colleagues (Downie *et al*, 2006). In order to slow down the uptake rate and allow for accurate determination of the linear phase of uptake, the experiment was repeated at 6 °C. It was consistently observed that uptake of 25 µM [<sup>3</sup>H] - adenosine at this temperature was linear over a period of 4 – 6 s (Figure 4.15), and that initial rates of transport could therefore be assessed over a three second interval. Whether uptake was conducted at 22 °C or 6 °C, it was observed that the transporter was almost completely saturated by the presence of 1 mM unlabelled adenosine, although this never inhibited 100% of transport (Figure 4.14 and Figure 4.15). This clearly confirms the presence of a low affinity transporter for adenosine. At 6 °C the rate of uptake of 25 µM [<sup>3</sup>H]-adenosine was  $0.041 \pm 0.004$  pmol ( $10^7$  cells)<sup>-1</sup>s<sup>-1</sup>, less than 10% of the estimated rate at room temperature. The transport activity was designated *P. falciparum* Low Affinity Adenosine Transporter (PfLAAT).

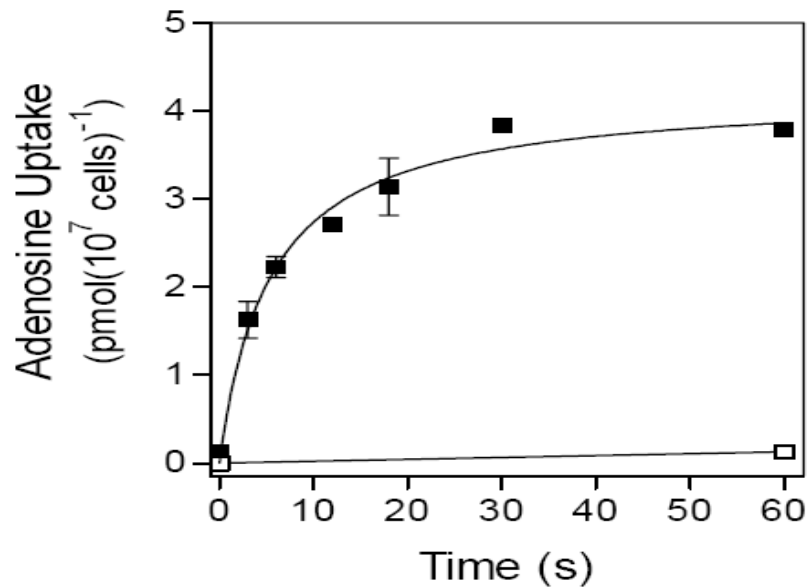


Figure 4.14: Low affinity transport of adenosine in saponin-freed *P. falciparum* trophozoites (at room temperature).

Uptake of 25  $\mu\text{M}$  [3H]-adenosine (at room temperature) was determined at various time points in the presence (□) or absence (■) of 1 mM unlabelled adenosine. Curves were calculated by non-linear regression using a hyperbolic fit. Data points are the mean of 3 experiments and error bars indicate SEM.

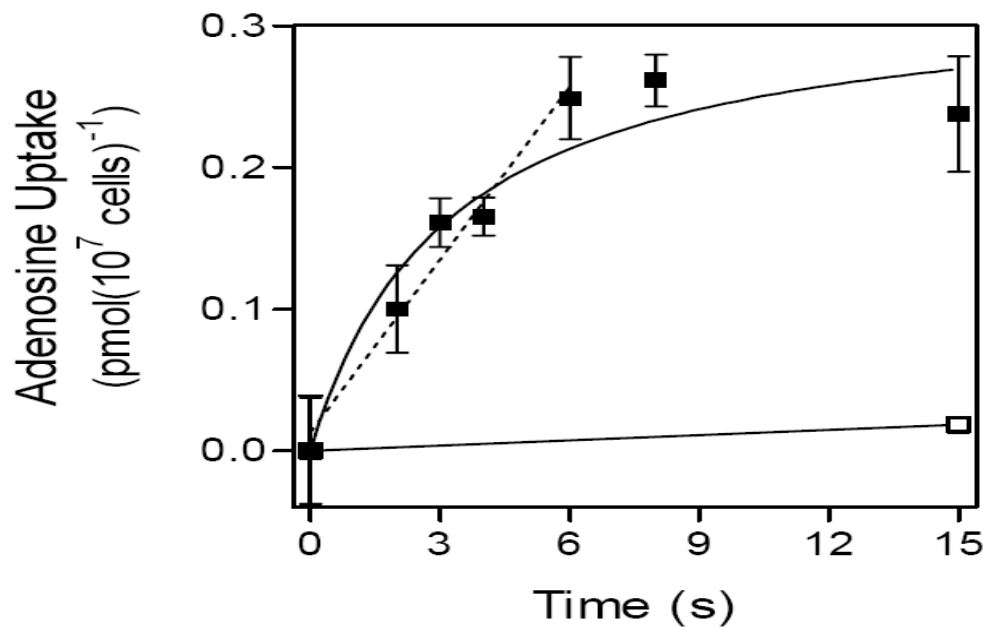


Figure 4.15: Low affinity transport of adenosine in saponin-freed *P. falciparum* trophozoites (at 6 °C).

Uptake of 25  $\mu\text{M}$  [3H]-adenosine (at 6 °C) was determined at various time points in the presence (□) or absence (■) of 1 mM unlabelled adenosine. Curves were calculated by non-linear regression using a hyperbolic fit. The dotted line was calculated by linear regression ( $r^2 = 0.97$ ). Data points are the mean of 3 experiments and error bars indicate SEM.

#### 4.11.2 Determination of $K_m$ and $V_{max}$ of PfLAAT

The  $K_m$  and  $V_{max}$  values were measured at 6 °C for the flux of 25  $\mu\text{M}$  [ $^3\text{H}$ ]-adenosine over a three second interval (Figure 4.16). The mean  $K_m$  value under these conditions was  $197 \pm 20 \mu\text{M}$ , with a  $V_{max}$  of  $0.19 \pm 0.03 \text{ pmol } (10^7 \text{ cells})^{-1} \text{ s}^{-1}$  ( $n=3$ ). The  $K_m$  value obtained here confirms the presence of a transporter with low affinity for adenosine as reported by others (Parker *et al*, 2000; Carter *et al*, 2000; Downie *et al*, 2006).

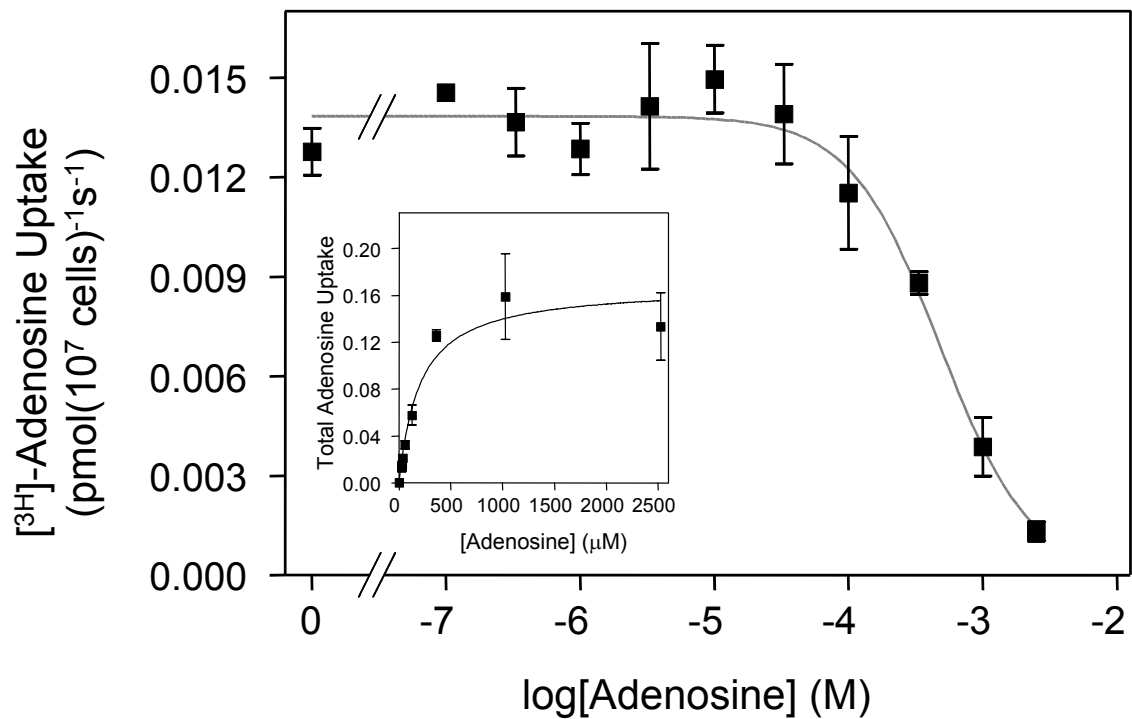


Figure 4.16: Transport of 25  $\mu\text{M}$  [ $^3\text{H}$ ]-adenosine into saponin-freed *P. falciparum* trophozoites (Michaelis-Menten plot).

Transport of 25  $\mu\text{M}$  [ $^3\text{H}$ ]-adenosine was determined over a three second interval at 6 °C, in the presence of various concentrations of unlabelled adenosine as indicated. Inset: conversion to a Michaelis-Menten plot. Data points are the mean of 3 experiments and error bars indicate SEM.



## 4.12 Effect of dipyridamol on the low affinity adenosine transporter

Dipyridamol (N, N' (4, 8-Dipiperidinopyrimido [5,4-d] pyrimidine) [Figure 4.7], a cardiovascular agent reported to be a potent inhibitor of nucleoside transport (Shi & Young, 1986), was tested for its inhibitory effect on the low affinity adenosine transporter. A dose dependent uptake of 1-25  $\mu\text{M}$  dipyridamol on the transport of 25  $\mu\text{M}$  [ $^3\text{H}$ ]-adenosine into saponin-freed *P. falciparum* trophozoites was performed at 6 °C using previously described method (section 2.2.6). Incubation time for the uptake was 3 seconds.

Result (Figure 4.18) indicates that dipyridamol at up to 25  $\mu\text{M}$  has little effect on the uptake of high concentrations of adenosine (low affinity adenosine transporter). This observation is consistent with the report of Parker and co workers (Parker *et al*, 2000). However, it contrasts that of Carter and colleagues, who showed that adenosine uptake was inhibited (up to 85%) by 10  $\mu\text{M}$  dipyridamole [(Carter *et al*, 2000)].

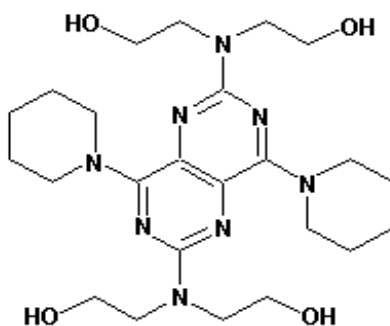


Figure 4.17: Structure of Dipyridamol.

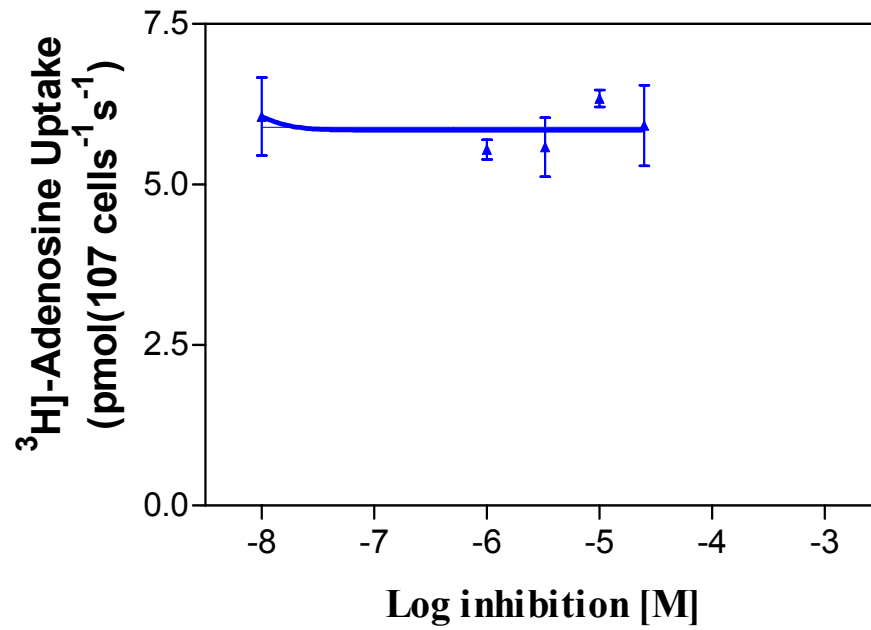


Figure 4.18: Effect of dipyridamole (1-25  $\mu\text{M}$ ) on the uptake of 25  $\mu\text{M}$  [ $^3\text{H}$ ]-adenosine at 6  $^{\circ}\text{C}$  by saponin-freed *P. falciparum* trophozoites.

Incubation time was 3 seconds. Dipyridamole was used from a stock solution in ethanol - the solvent did not exceed 1% during the final incubation with the parasites. This experiment is representative of three identical experiments each performed in triplicate. Data shown are means and SEM.

### 4.13 Summary of results: Profile of purine transport in *P. falciparum* trophozoites.

Findings from this part of the study strongly suggest that isolated trophozoites express:

- (i) a high affinity hypoxanthine transporter with a secondary capacity for purine nucleosides (designated PfNT1),
- (ii) a separate high affinity transporter for adenine (designated PfADET1)
- (iii) a low affinity adenosine transporter (designated PfLAAT) and
- (iv) a low affinity/high capacity adenine carrier (designated PfADET2).

Summary of the kinetic properties of PfNT1, PfADET1 and PfLAAT is shown in Table 4.1. For technical reasons (see section 4.10) the kinetic properties of PfADET2 could not be measured. It was clear that the high affinity transport activity observed here is encoded by the previously reported PfNT1, which by the kinetic properties reported by the group of Kirk (Downie *et al*, 2006) suggests that it is a low rather than a high affinity transporter.

	High affinity [ <sup>3</sup> H]-hypoxanthine uptake (PfNT1)		High affinity [ <sup>3</sup> H]-adenosine uptake (PfNT1)		Low affinity [ <sup>3</sup> H]-adenosine uptake (PfLAAT)		Affinity [ <sup>3</sup> H]-adenine uptake (PfADET1)	
	K <sub>i</sub> or K <sub>m</sub> value (at 22°C, μM, SE)	N	K <sub>i</sub> or K <sub>m</sub> value (at 22°C, μM, SE)	N	K <sub>i</sub> or K <sub>m</sub> value (at 6°C, μM, SE)	N	K <sub>i</sub> or K <sub>m</sub> value (at 22°C, μM, SE)	N
V <sub>max</sub>	0.36 ± 0.12	6	0.18 ± 0.08	3	0.19 ± 0.03	3	.0004 ± .0002	3
V <sub>max</sub> /K <sub>m</sub>	1.1		0.090		0.00096		0.0019	
Hypoxanthine	<b>0.34 ± 0.05</b>	6	<b>0.75 ± 0.18</b>	3	ND		>1000	3
Guanine	0.11 ± 0.01	3	ND		ND		>50	3
Inosine	2.0 ± 0.2	3	ND		ND		>1000	3
adenosine	4.0 ± 0.67	3	<b>2.0 ± .02</b>	3	<b>197 ± 20</b>	3	2.0 ± 0.2	3
Guanosine	11.6 ± 2.7	3	ND		ND		ND	
Adenine	>500	3	240 ± 70	3	ND		<b>0.23 ± 0.07</b>	3

Table 4.1: Summary of the kinetic studies of saponin-freed *P. falciparum* trophozoites.

Values in bold are K<sub>m</sub> values obtained with radiolabeled substrate; other values are K<sub>i</sub> values, obtained from dose-dependent inhibition of radiolabeled substrate. All values were determined using non-linear regression from experiments in duplicate or triplicate with a minimum of 8 points over the relevant range. Zero values were taken to be radiolabel associated with the cell pellet in the presence of saturating concentrations of unlabelled permeant. Units for V<sub>max</sub> are pmol (10<sup>7</sup> cells)<sup>-1</sup>s<sup>-1</sup>. ND= not determined.

#### 4.14 Proposed model for purine transport in saponin-freed *P. falciparum* trophozoites

From evidence gathered in this study a new model for transport of purine in isolated *P. falciparum* trophozoites is proposed (Figure 4.19), where uptake is predominantly reliant on a high affinity nucleoside transport activity, designated PfNT1. This transporter, which has a high affinity for hypoxanthine, also salvages adenosine, guanosine, inosine and guanine. The model also includes a low affinity/high capacity PfLAAT, which presumably contributes significantly to adenosine uptake only when high levels of extracellular purine are present. The two adenine transporters proposed in this model, PFADET1 and PFADET2 may not be important in the salvage of the parasite's purine requirement for synthesis of bio-molecules as adenine is not believed to be an important purine source for the parasite due to the reported absence of the genes encoding adenine phosphoribosyltransferase (APRT) and methylthioadenosine phosphorylase in any of the *Plasmodium* spp (Chaudhary *et al*, 2004; Ting *et al*, 2005). Whilst the capacity of PFADET2 may be high, it is unlikely that sufficiently high adenine concentrations are present at the parasite plasma membrane to allow much uptake by this low affinity transporter. Conversely, the affinity of PFADET1 is high enough to salvage traces of adenine undoubtedly present in the infected erythrocytes (because of the presence of hFNT1 on the red cell plasma membrane, see Chapter 3), but its capacity is so low that its contribution to purine uptake, compared to PfNT1, is almost negligible. It is certainly conceivable that these transporters have a more prominent role in other parts of the complex *Plasmodium* life cycle.

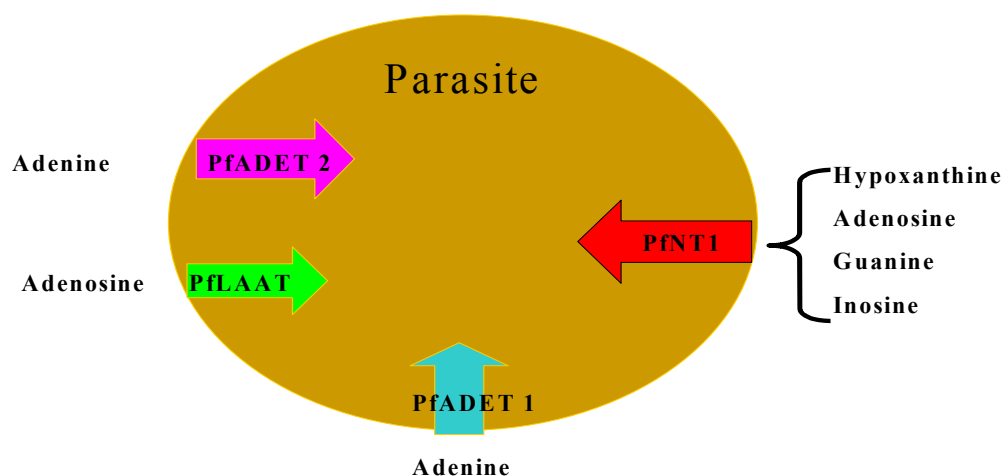


Figure 4.19: Proposed model of purine transport systems in *P. falciparum* trophozoites.

The substrates for each transporter are indicated. PfNT1=High affinity hypoxanthine/nucleoside transporter; PFADET1=adenine transporter 1 (high affinity); PfLAAT= low affinity adenosine transporter; PFADET 2=adenine transporter 2 (low affinity).

## 4.15 Discussion

From observations made in this study, it can be concluded that saponin-freed *P. falciparum* trophozoites exhibit four transport activities for the uptake of purines. These are; (i) PfNT1 for the uptake of predominantly hypoxanthine and also guanosine, adenosine, inosine, guanine but not adenine (ii) PfADET1 for the uptake of adenine at low concentrations of the nutrient, (iii) PfADET2 for the uptake of adenine when levels of adenine are high (iv) PfLAAT for uptake of adenosine when the exogenous concentration of the purine is high.

Homology searches of the *P. falciparum* genome database have shown four genes encoding transporters of the equilibrative nucleoside transporters family in the parasite, each of which is expressed during the intraerythrocytic stage of the parasite's life cycle (Martin *et al.*, 2005). It is very tempting to conclude that each of the transporters identified in this study is encoded for by one of the identified genes. However until each of these genes has been investigated using a gene disruption strategy followed by kinetic study of the resultant phenotype it would be erroneous to draw conclusions on this issue. At present, only one of the four genes encoding for an ENT homologue in *P. falciparum* has been cloned and characterized: PfNT1 (PF13\_0252) mRNA was expressed in the oocytes of *Xenopus laevis* by two groups of researchers working independently (Parker *et al.*, 2000; Carter *et al.*, 2000). The kinetic properties and other characteristics described by the two groups clearly fit a low affinity transporter. Recently, a follow up to these studies using saponin-freed *P. falciparum* trophozoites, carried out by the group of Kirk (Downie *et al.*, 2006), also showed the presence of a low affinity adenosine transporter.

When the kinetic data obtained in this study was compared with that obtained by the group of Kirk in saponin-freed trophozoites, it was clear that the transporter designated PfLAAT in this study is the closest to that described by that group. Apart from the slightly lower  $K_m$  value of  $197 \pm 20 \mu\text{M}$  obtained in this study, other observations such as the rapidity of equilibration and insensitivity to dipyrindamole were very similar to that reported by the group of Kirk. On the basis of the earlier studies by groups of Carter and Parker (Parker *et al.*, 2000; Carter *et al.*, 2000), as well as their own analysis of *PfNT1* in *Xenopus* oocytes, Kirk's group (Downie *et al.*, 2006) concluded, that PfNT1 encodes the low affinity adenosine transporter. Data presented in the current chapter do not corroborate or disprove this assertion, but it will be demonstrated in Chapter 6 that PfLAAT activity is completely unaltered after disruption of the *PfNT1* gene.

Since hypoxanthine is the preferred purine source for *P. falciparum*. (Berman *et al*, 1991), an efficient transporter for its uptake during the intraerythrocytic stages of the parasite was expected. A high affinity hypoxanthine transporter, was identified in this study, and designated PfNT1 on the basis of gene disruption studies (Chapter 5) and kinetic studies (chapter 6). This transporter demonstrated the highest affinity for the oxopurine nucleobases, guanine and hypoxanthine, with low, if any, affinity for adenine. This transporter also showed high affinity for purine nucleosides, apparently not discriminating between aminopurine and oxopurine nucleosides. The transporter appeared to display a preference for oxopurine nucleobases over aminopurine bases. It is possible that the selectivity of PfNT1 relies on the sugar moiety present in nucleosides, but not in the nucleobases (i.e. a different orientation for the two classes of purines within the transporter binding pocket). Alternatively, the nucleobases or nucleosides may not be true substrates for PfNT1 and may act to inhibit hypoxanthine transport allosterically.

In order to practically address this last issue, transport of micro-molar concentrations of [<sup>3</sup>H]-adenosine into isolated *P. falciparum* trophozoites was investigated (section 4.8). A high affinity adenosine transporter that was inhibited by hypoxanthine but not adenine with compellingly similar reciprocal  $K_m$  and  $K_i$  values was observed (i.e.  $K_i$  value for adenosine on hypoxanthine transport was similar to the  $K_m$  for adenosine; and the  $K_m$  for hypoxanthine was similar to the  $K_i$  value for hypoxanthine with [<sup>3</sup>H]-adenosine transport). This strongly suggests that PfNT1 is able to transport hypoxanthine and adenosine. However, the value of the calculated  $V_{max}/K_m$  ratio suggests an 11.9-fold higher efficiency of translocation for hypoxanthine compared to adenosine, which gives further support to the assertion that hypoxanthine is the preferred purine source to the parasite. The basis for the selectivity of hypoxanthine over, for example, inosine, may indeed be a different orientation in the transporter-binding pocket, or limited steric hindrance of the ribose moiety within the translocation pathway. A combination of the two factors would account for both the selectivity profile and the reduced translocation efficiency for nucleosides.

Adenine did not appear to be a substrate for PfNT1, suggesting that a separate transporter may exist for its uptake. Further investigation revealed the presence of a separate saturable adenine transporter, designated PfADET1, which is distinguishable from PfNT1 by its insensitivity to inhibition by the oxopurines hypoxanthine, guanine and inosine. PfADET1 displayed very high affinity for adenosine and adenine, though the  $V_{max}$  was two to three orders of magnitude lower than that measured for the high affinity transport of

hypoxanthine and adenosine through PfNT1. This observation implies that adenine is a far less important purine source for Plasmodium compared to hypoxanthine or adenosine. A second adenine transporter, PfADET2, with low affinity for the nucleobase, was also demonstrated in this study. The role of this transporter is not immediately known but can be postulated to play at best a limited role in purine salvage, at least in the intraerythrocytic stages of *P. falciparum* investigated here, as argued above. Some of the transporters characterised in the trophozoite stages of the parasite, and thought to play limited role in the uptake of purine, could be important at a different stage of the life-cycle, when purine uptake is required from a different external milieu.

A compound with the ability to prevent or reduce the replication of deoxyribonucleic acid (DNA) and the synthesis of ribonucleic acid (RNA) in the nucleus of the malaria parasite should be a good antimalarial drug. Since DNA replication requires purine and pyrimidine nucleotides, blockage of their supply may prevent parasite multiplication, as shown by El Bissati and colleagues (El Bissati *et al*, 2006). Purine antimetabolites have thus received consideration in the search for novel antimalarial drug to combat the surge in drug resistance parasites. In this study, purine analogues JA-23 (2-Amino-N<sup>6</sup>-amino-N<sup>6</sup>-methyladenosine), JA-24 (2-Amino-N<sup>6</sup>-amino-adenosine) and JA-32 (N<sup>6</sup>-Hydroxy-9H-purin-6-amine), donated by Daniel Brown and David Loakes of the MRC Laboratory of Molecular Biology, Cambridge, UK, were tested for their antiplasmodial activities. These compounds showed moderate antiplasmodial activity *in vitro* and *in vivo* (Too *et al*, 2007). The compound with the chemical structure closest to hypoxanthine, JA-32, displayed moderately high affinity for PfNT1, whereas JA-23 and JA-24 had very low affinity for PfNT1, indicating that, for nucleosides, substitutions at N<sup>6</sup> result in low affinity for this carrier. However, it is possible that these analogues are accumulated instead through PfLAAT, as this was not tested.

## 4.16 Conclusions

This study identified four transporters for the uptake of purine nucleobases and nucleosides in saponin-freed *P. falciparum*-infected erythrocytes. The transporters and their substrate according to the test performed in this study is listed below:

PfNT1 - hypoxanthine, adenosine, guanine, inosine

PfLAAT - adenosine

PfADET1 - adenine

PfADET2 - adenine.

Finding from this study is consistent with studies involving other *Plasmodium* species which show a transport system for hypoxanthine with secondary capacity for purine nucleosides and a separate uptake system for adenine [reviewed by de koning and co (de Koning *et al*, 2005)]. The high affinity purine transporter, PfNT1 in the parasite's plasma membrane could be a target for anti-purine based drugs. Inhibition of the uptake of hypoxanthine through the PfNT1 transporter by an antiplasmodial purine analogue, JA-32, provides support for the further investigation of purine analogues as potential antimalarial drugs.



## **CHAPTER FIVE**

### **5 Generation of *P. falciparum* clones with disrupted Equilibrative Nucleoside Transporter- encoding genes**

## 5.1 Summary

Four genes with homology to the Equilibrative Nucleoside Transporter (ENT) family are present in the *P. falciparum* genome. In order to gain proper understanding of the exact role played by each of these genes in purine salvage by the parasites, clones of *P. falciparum* with a disrupted *ENT* locus were generated for each of the four genes using the insertion-gene disruption method. *P. falciparum* malaria parasites were transfected by electroporation with plasmids containing a fragment of each of the genes encoding the putative ENT proteins. Transfected parasites, selected using the selectable marker blasticidin, emerged in culture approximately 21 days post-transfection. A single crossover homologous recombination at the *ENT* locus was expected to generate a pseudo diploid configuration, with both truncated copies lacking some of the transmembrane domains of the protein predicted to be essential for the function of the protein. Parasites with the disrupted genes were designated  $\Delta PfNT1$ ,  $\Delta PfNT2$ ,  $\Delta PfNT3$  and  $\Delta PfNT4$ ; corresponding to genes listed in PlasmoDB as PF13\_0252, MAL8P1.32, PFA0160c and PF14\_0662 respectively. Parasites with  $\Delta ENT$  were observed to grow relatively better when the culture medium was supplemented with extra purine such as adenosine inosine and hypoxanthine. A clone designated 3D7 $\Delta PfNT1$  (locus listed as PF13\_0252 in PlasmoDB) was generated using the limiting dilution method from parasites transformed with a plasmid containing the central region of this gene. Molecular analysis of the clone using PCR and southern blot confirmed that the *ENT* gene *PfNT1* had indeed been disrupted. Generation of 3D7 $\Delta ENT$  clones for each of the four genes combined with kinetic assessment should pave the way for proper understanding of the functions of these transporter proteins.

## 5.2 Introduction

Earlier in this study, four separate transporter activities were observed to be responsible for purine salvage in saponin-freed *P. falciparum* infected erythrocytes (see chapter four). Homology searching of the *P. falciparum* genome database by Martin and co-workers had revealed the existence of four genes with homology to the equilibrative nucleoside transporter protein family in the parasite (Martin *et al*, 2005). It was therefore speculated that a link exists between the four genes listed in the genome database and the four purine transporters found in the current study. In order to verify this, parasite lines with a disrupted locus for each of the four putative *ENT* genes were generated using a previously described gene targeting strategy (Fidock *et al*, 2000). The kinetic characteristics of the generated phenotypes lacking the genes encoding the ENTs were then determined using the classical uptake techniques (see chapter six).

Gene targeting in *P. falciparum* involves the alteration of a chosen gene in a predetermined way by homologous recombination (Menard & Janse, 1997). Two commonly used methods are the replacement and insertion methods. In this study, the insertion method was employed to disrupt genes encoding ENT-family proteins in *P. falciparum*. The method involves homologous recombination between the gene of interest (listed as PF13\_0252 in the genome database) and a DNA construct comprising the target DNA that had been subcloned into a plasmid. The plasmid, pCAM/BSD, used in this study to prepare the construct, contains a cassette that confers resistance to blasticidin (BSD) as a positive selectable marker (Sidhu *et al*, 2005). *P. falciparum* can support the replication of circular plasmid DNA molecules. It was anticipated that a single crossover homologous recombination at the *ENT* locus would generate a pseudo-diploid configuration, with both truncated copies lacking some of the transmembrane domains of the protein predicted to be essential for the function of the transporter (Figure 5.1). As the parasite is haploid and each *ENT* gene is present as single copy gene, only one round of drug selection is necessary to produce a null-mutant.

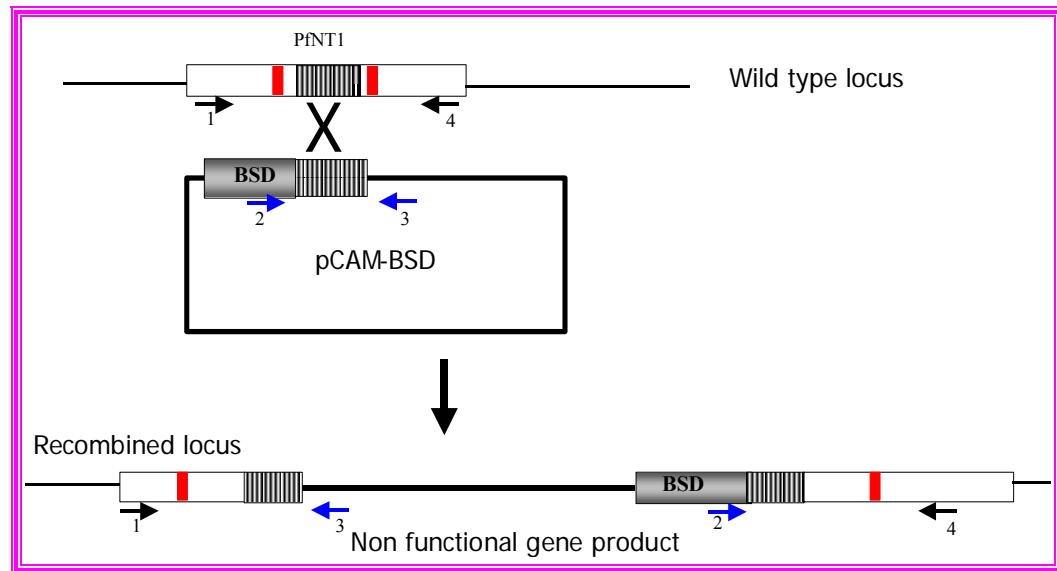


Figure 5.1: Strategy for disruption of the ENT locus.

The wild-type *PfNT1* chromosomal locus is shown at the top including the construct pCAM-BSD/ENT used to disrupt the ENT gene. The insert excludes the transmembrane domains, considered to be essential for the functioning of the transporter. Single crossover homologous recombination results in a pseudo-diploid configuration with two truncated copies, each of which lacks some of the essential transmembrane domains, shown at the bottom. Adapted from (Fidock *et al*, 2000).

### 5.2.1 Four genes encode Equilibrative Nucleoside Transporters in *P. falciparum*

Martin and his colleagues identified numerous genes in the *P. falciparum* genome database encoding proteins involved in membrane permeability (Martin *et al*, 2005). The principle was ‘based on the theory that polypeptides comprising transporter proteins typically possess multiple hydrophobic transmembrane domains (TMDs) and hydrophilic extra-membrane loops that are detected as peaks and troughs respectively in a plot of the hydrophobicity index of the polypeptide’ (Martin *et al*, 2005). Four genes were identified that putatively encode for nucleoside and/or nucleobase transporters in *P. falciparum*. One of the four genes had been isolated and cloned earlier on by the groups of Ullman and of Baldwin (Parker *et al*, 2000; Carter *et al*, 2000). The four genes identified are listed in PlasmoDB with the accession numbers PF13\_0252, MAL8P1.32, PFA0160c and PF14\_0662 (Martin *et al*, 2005). Search of the GeneDB indicate that, PF13\_0252, MAL8P1.32, PF14\_0662 and PFA0160c are on chromosomes 13, 8, 14 and 1 respectively of the *P. falciparum* genome.

Despite their conserved structure, ‘the four *ENT* genes share limited sequence similarities with each other and are only weakly related to ENT proteins from other organisms’ (Martin *et al*, 2005). Details of their expression during the parasite’s asexual lifecycle, reported in the same study, revealed that the genes listed as PFA0160c, MAL8P1.32 and PF13\_0252 had similar expression profiles. Transcription was observed to start early during the parasite development in the erythrocyte, increasing rapidly in abundance between 16 and 24 hours post invasion. The level of transcript reached a maximum 32 hours after invasion and then declined slowly (Figure 1.18). Transcription of the gene identified as PF14\_0662 was reported to start between 8-20 hours and peaked at approximately 36 h post invasion.

### 5.2.2 Alignment of amino acids of the four ENT proteins

Before disruption of the four genes encoding equilibrative nucleoside transporters in *P. falciparum* was performed, multiple alignments of the predicted amino acid sequences of the four genes encoding for ENT were performed using ClustalX program. The alignment revealed limited similarities in the predicted amino acid sequences for the four genes (see Figure 5.2) and only six amino acids conserved in all four genes. The predicted amino acid sequences of the *Pf(E)NT1* clones used by Parker and colleagues (Parker *et al*, 2000) and Carter and colleagues (Carter *et al*, 2000) respectively were also compared. The alignment of the sequences indicated a single amino acid difference at position 385; with leucine reported for Parker and co (Parker *et al*, 2000) and Phenylalanine for Carter and co (Carter *et al*, 2000). It is possible that this small difference could explain some of the discrepancies observed in the two studies. The Phe385 polymorphism is unusual: in a multiple alignment of 28 protozoan ENT family genes plus the four human ENT sequences, the equivalent amino acid residue was conserved in so far as it was never aromatic, amide, charged, cysteine or proline (alignment not shown).

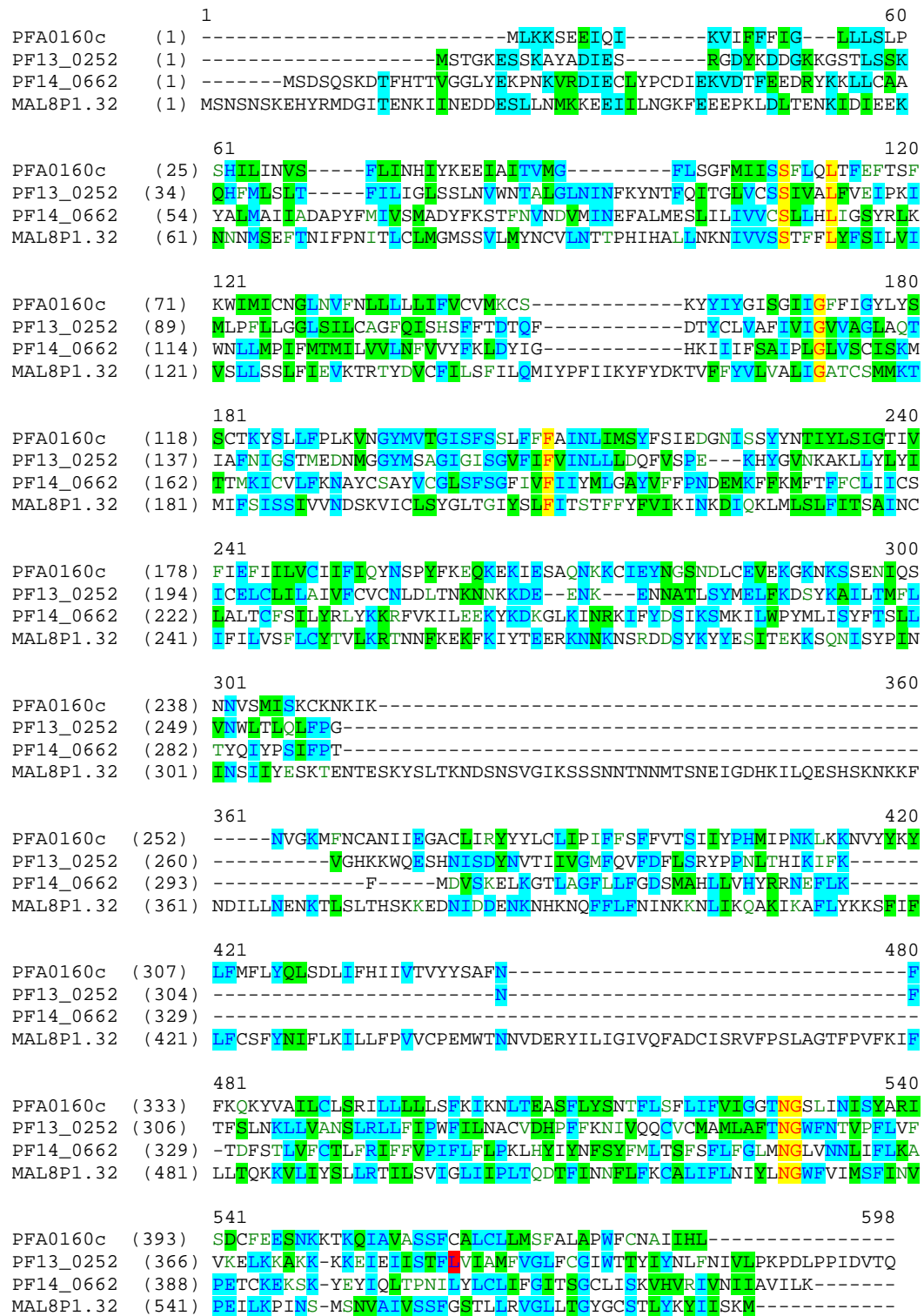


Figure 5.2: Alignment of the predicted amino acid sequences from the four ENT encoding genes in *P. falciparum*.

Similarity in all four genes is highlighted in yellow. Similarity in two or three of the sequences is shown in bright blue. The point where the difference between sequence reported by (Parker *et al*, 2000) and (Carter *et al*, 2000) (i.e. Leucine 385) is highlighted with a red box.

### 5.3 Alignment of the nucleotides of the four genes encoding for ENT in *P. falciparum*

To ascertain similarity between the four genes encoding for equilibrative nucleoside transporter in *P. falciparum*, multiples alignment of the genes was performed using the ClustalX program. The outcome of the alignment shown in Figure 5.3 indicates limited similarity between the four genes.

```

PfNT1 -----
PfNT2 -----
PfNT3 ATGAGCAATTCTAATAGCAAGGAGCACTACAGAATGGACGGAATTACAGAAAATAAAATA 60
PfNT4 -----

PfNT1 -----
PfNT2 -----
PfNT3 ATTAATGAAGATGATGAAAGTCTCTTGAACATGAAAAAGAAGAAATAATTTTAAATGGA 120
PfNT4 -----

PfNT1 -----
PfNT2 -----
PfNT3 AAATTTGAAGAAGAGCCAAAGCTTGATTTAACCGAAAACAAAATTGATATTGAAGAGAAG 180
PfNT4 -----

PfNT1 -----
PfNT2 -----
PfNT3 AATAATAACATGAGTGAGTTTACAAATATTTTCCAAATATAACATTATGTTTAAATGGGA 240
PfNT4 -----

PfNT1 -----ATG-AGTACCGGTAAAGAGTC-ATCTAAAGC--TT 31
PfNT2 -----ATGAGTGACAG----TC-AGAGTAAGG--AT 24
PfNT3 ATGTCATCTGTATTAAATGTATAATTGTGTATTAATAACAACACCTC-ATATACATGCATT 299
PfNT4 -----ATGTTGAAGAAAAGCGAGGAGATCCAGATAAAGG--TT 36

PfNT1 ATGCTGATATAGAATCCAGGGTGATTATAAGGACGATGGAAAGAAAGGATCTACATTAA 91
PfNT2 A--CGTTTC-ATACAACAGTGGG---T-GGA---TTATATGAGAAGCCTAACAAAGTTC 73
PfNT3 AT-TAAATA-AGAATATAGTAGTATCT-TCAAC-CTTTTTTCTATATTTTTC--TATTTT 353
PfNT4 AT-CTTTTT-TTT-TATAG--GT---T-TG---CTTTTGAGTTTACCCTCCCATATTTT 83

PfNT1 GCAGTAAAC-AACATTTTCATGTTATCTTTAACCTTTTATAT-TAATAGGTTT-AAGTTCT- 147
PfNT2 G-AGATATTGAATGTTTAT--A--TCCTTGATGATATTGAA--AA-AG-TAGATACTTTTG 124
PfNT3 --AGTTATTGTATCATTGTTAAGTTCCTTAT-TTATAGAAGTAA-AGACAAGAACATATG 409
PfNT4 --AATAAATGTATCTTTTGA-TTAATCAC-ATATACAAGGAAGAGATAGCTATAACGG 139

PfNT1 TTGAATGTATGGAATACAGCCTTAGGATTA-AA-T-ATAAATT--TTAAATATAA--TAC 200
PfNT2 AAGAA-GATAGGTAT-AAGAAGT--TATTATGTGCAGCATATGCATTAATGGCTA--TAA 178
PfNT3 ATGTGTGTTTTATAT-TATCATTATATTACAAATGATATATCCATTTATTATAAAATAT 468
PfNT4 TTATGGGTTTTTAT-CAGGATT--TATGATAA-T-ATC-ATC-ATTT-TTACAAT-TAA 190

PfNT1 CTTTCAGAT--TAC--AGGTTTAGTATG--TTCCTCAATTGTAGCT--T--TATTTG-T- 248
PfNT2 -TAGCTGATGCTCCATATTTTATGATTGTATCGATGGCTGATTATT--TTAAAGTACT- 234
PfNT3 TTTTATGATAAAACCGTTTTTTTTTATGTACTAGTAGCAT-TAATTGGTGCTACGTGCTC 527
PfNT4 CTTT-TGAATTAC--ATCTTTTAAATGGATTA-TGATATGTAACGGAT--TAAATG-TT 243

```

PfNT1 TGAGATTCCCAAAATAATGTTACCATTTCCTTTGGGTGGTTTATCAATTTTATGTGCAGG 308  
 PfNT2 TTTAATGTAAATGACGTTATGATAAATGAATTTGCCT---TAATGGAAAG-TTTAA---- 286  
 PfNT3 TATGATGAAAACCATGATATTTTCCAT-ATCTTCCAT-TGTTGT-AAATGATTCAAAAGT 584  
 PfNT4 TTTAATTTAT--TAT--TATTATTAAT--TTTGTATGTGTAATGAAATG-TTCAAAA-- 294

PfNT1 TTTTCAAATATCTCACAGTTTTTTTACAGATACACAATTTGATACATATTGTTTAGTAGC 368  
 PfNT2 TATTG---AT--TGTTGTTTGTTCAT-TAT-TA-CATTTAATT-GGAA----- 325  
 PfNT3 TATTTGTTTATCATATGGTTTGGACTGG-GATATATTCTTTATTT-ATAACATCCACATTT 642  
 PfNT4 TATTA--TAT-ATATGGTATATCCGG-GAT-TATCGGTT-TTT-TTA-----TT 336

PfNT1 TTTTATT--GTTATTGGTGTAGTGGCAGGATTAGC-----TCAAAC-CAT--TGCATT- 416  
 PfNT2 -GTTATC--GT--TTAAAA-TGGA-----ATTTAC-----TT-ATGCCTAT----ATTTA 364  
 PfNT3 TTTTATTTTGTATTATTAATAA-TAAATAAAGATATACAAAAGTTGATGT-TATCATTATTTA 700  
 PfNT4 GGTTATTT-GT-ATTCATCGGTACAAA-ATATTC-----TT--TGC-TAT--TTCCTT- 382

PfNT1 TAAT-AT-AGG-ATCAACCAT-GGAAGATAATATGGGT--GGTTATATGT--CAGCAGG 467  
 PfNT2 TGACGAT--G--AT-ATTAGT--TGTG-TTAAATTT-TGTTGTTTATTT-T-AAACTTGA 413  
 PfNT3 TAAC-ATCAGCCATCAATTGT-ATAT--TTATATTAGTGTCTTTTCTATGTTACACTGTA 756  
 PfNT4 TAA--A--AG---TCAATGGTTATATGGTTACAGGAAT-TAGTTTCTCT-T--CATTATT 431

PfNT1 T---ATTGG-----TA--TATCA-GGAGTATT-TATT--TTTGT-TATT-AATTTAT--- 508  
 PfNT2 CTACATTGGACATAAGATTATCATCTTCAGTGCTATACCTTTAGGTTTAGTATCTTG--- 470  
 PfNT3 TTAAAGAGAACAAATAATTTTAAAGAAAAATTTAAAA--TTTA--TACAGAAGAGAGAAA 812  
 PfNT4 TTTTTTTG--CTA-TAAATTTAA--TAATGTCGTATT--TTTC--TATCGAAGATGG--- 479

PfNT1 ---TACTTGATCAATTCGTAT--C--TCCCGAAAAACATTATGGT--GTTAA-TAAAGCA 558  
 PfNT2 ---TATAT-CTAAAATGAC-T-ACTATGAAAATATGTGTTTTG---TTTAA--AAACGC 518  
 PfNT3 AAATA-AT-AAAAATTCACGTGATGATTCTTATAAATATTATGAAAGTATAACTGAAAA 870  
 PfNT4 ---TA-AT-ATAAGTTCATATTACAACACA-ATATAT-TTATC---CATAG--GAACATA 526

PfNT1 AAGTTAT----TATATTTATAT--ATAATCTGTGA-ACTTTGTTTAATAT-T-AGC-TAT 608  
 PfNT2 CTATTGTAGTGCTTATGTATGTGGATTATCTTTTTCAGGTTTATAGTGTTT-A---TAA 574  
 PfNT3 AAATCACAAAATATATC-ATATCCAATAAATATT---AATAGTATAATATATGAAAGTAA 926  
 PfNT4 TAGTT-----TTTATC-GAATTCATTATAC-TT---GTTTGTATAATTTT-A---TAC 571

PfNT1 AGTAT---TTTGTGTATGTA-ATTTAGATTTAACAACAAGAA--TAA-----TA- 652  
 PfNT2 TATATATGTTAGGG---GCATATGTGTTTTTCCGA--ATGAT--GAA-----AT 617  
 PfNT3 AACAGAAAATACGGAATCCAAATATTCAATTAACAAAAAATGATTCTAACTCAGTTGGTAT 986  
 PfNT4 AATATA--ATTC---TCCATAT-TTCAAGGAGCAAAAA-GAG---AA---A-----AT 611

PfNT1 AAAAAGATG-A---AGAAAATAAGAAAACAA--TGCCACATTATCTTATATGGA-ATTA 705  
 PfNT2 GAAATTTTTTA---AGATGTTTACTTTTTT---TTGTTGATTATTTGT--TCATTAGCA 669  
 PfNT3 AAAAAGTAGTAGTAATAATACTAATAATATGACTAGTAATGAAATAGGAGATCAT-AAAA 1045  
 PfNT4 AGAAAGT-GCAC--AGA--ACAAAAATGT-A-TTG-AATATAAT-GGA--TCGA-ATGA 659

PfNT1 T-TTA-AAGATAG--TTACAAAGCTATATTA-----ACTATGTTTCTTGT--AAACT 751  
 PfNT2 T-TAACATGTTT---TTCTA---TCCTATA-----C-CGAC-T-ATAC--AAAA- 706  
 PfNT3 TATTACAAGAATCTCATTCAAAAATAAAAAATTTAATGAC-ATACTTCTTAATGAAAAT 1104  
 PfNT4 T-TTATGTGAAG---TTGAAAAAGGAAAAA-----C-AAA--TCATCA-GAAAAT 702

PfNT1 GGTTAACTTTACAATTATTTCCAGGTGTTGGACACAA---AAAATGGCA-A-GAA--AGT 804  
 PfNT2 AACGAT-TTGTGAA--AAT---ATT-GGAAGAAA--AG-TATAA-AGAT-A--AAGGATT 752  
 PfNT3 AAA-ACATTATCACTTACT-C-ATA-GTAAAAAGAAGATAACATAGATGACGAA--AAT 1158  
 PfNT4 ATCCAGAGTAATAATGTCT-CTATG-ATAAGTAA-ATG-TAAAA--AT-A--AA--ATT 750

PfNT1 CATAATATCTCCGATTATAATGTTACCATTATTGTTGGTATGTTTCAAG--TTTTTGATT 862  
 PfNT2 AAAAAATTAATA-GA--AAAATATTTATGACTCTATAAAATCAATGAAA-ATATT--GTG 806  
 PfNT3 AAAAAATCA-T---A--AAAATCAATTCTTTCTATTTAATATAAAATAAAAAAATTTAATA 1212  
 PfNT4 AAAAAATGT-TG-GA--AAAATGT-TTAATTGTGCT-AATATAATTGAGGGAGCTT--GTT 802



```

PfNT1 TTCTCAGTAGATATCCACCAATCTTACACATAT----TAAATCTTTAAAAATTTTACT 918
PfNT2 -----GCC---AT-----AT----ATGTTGA-----TTTCATATTTTACAAGTTTATT 842
PfNT3 AAACAAGCCAAAATTAAAGCATTCTTATATAAAAAATCGTTCATATTTT-TATTTT--GT 1269
PfNT4 TAATAAG--ATATTATT--AT--TTATGTTTAATACCTATATCTTTT-CATTTTTCGT 854

PfNT1 TTCTCTTTAAATAAATT-AT-----TGGTTGCC-----A-ATTCATTG 954
PfNT2 GACTTATCAAATATATCCATCTA----TAT--TTCCAACCTTT-----ATGGATGTTA 889
PfNT3 AGCTTTTATAATATTTTCTCAAAATATTATTATCCCGTTGTTTGTCCAGAAATGTGG 1329
PfNT4 GACCTCTATAATATATC-CTCAC-----ATGATTCC-----G-----A-ATAAGCTG 894

PfNT1 A-GATTATTATTCATTCCA--TG---GTTTATTTTAAATG--C-ATGTGTTGATCATCCA 1005
PfNT2 GTAAAGAATTAAAAGGAACACTAGCTGG--ATTTTTATT-----ATTTGGTGATTCTATG 942
PfNT3 ACTAATAATGTTGATGAAAGATATATTAATTGGAATTGTGCAATTTGCTGATTGTATA 1389
PfNT4 AAGAAGAACGTATATTACAAATACCTGTTTATGTTTCTTTACCAACTCAGTGATCTTATA 954

PfNT1 -----TTTTTCAAAAACATTGTACAACAATGTGTAT--GTA-TGGCTA-TGTTAGCTTT- 1055
PfNT2 -----GCTCACT-TATTAGTTCAT-TAT-AGAAGAAACGAATTTT----TAA 982
PfNT3 AGTCGTGTTTTCCCATCCCT-TGCAGGAACAT-TTCCAGTA-TTAAAATTTTCTCTTTG 1446
PfNT4 -----TTTCATATCATTGTGACTGTTTAT-TAT-AGTGCTTTTAACTTTT----TT- 999

PfNT1 -TACAAATGGTTGGT--TTAATACTGTACCATTCCCTT--GTA-----TT---TGTTAA- 1100
PfNT2 AAACAGATTTTCTACATTAGTCTTTTGCACATTGTTTCAGAA--TATTTT-T-TG-TACC 1037
PfNT3 ACACAAAAAAAAGTA--TTAAT-TTATTC--TTTATTAAGAA-CTATCTTATCTG-TAA- 1498
PfNT4 AAACAAAAATATGTT--GCCATATTATG---TTTAAGCAGAATCCTTCTT-T-TGCTAT- 1051

PfNT1 -AGAATTAaaaaaAGCCAAGAAAAAGAAAGAAATCGAAATTATATCCACATTCTTAGTTA 1159
PfNT2 TAT-ATTTTTATT---C--TT-GCCA-AAG--CTTCATTATATATA-TAACT-TTAGTTA 1085
PfNT3 TAGGATTGATAAT--ACCATT-AACACAAG--ATACATTT-AT-TAATAA-T-TTCCTTT 1549
PfNT4 TATCCTTTTAAATTAAGAATTTAACTGAAGC-ATCCTTTTATATTCTAA-T--ACTTT 1106

PfNT1 TTGCTATGTTTGTT-GGAT--TATTCTGTGGTAT-ATGGACTACATACATTATAACTTA 1215
PfNT2 TTT-TATGTTGACTAGCTTTTCATT-TTTATTCGGACTAATGA-ATGGATTG--GTGA-A 1139
PfNT3 TTA-AATGTGCACT--CAT--TTTT-TTAAATAT-ATATTTAA-ATGG-TTGGTTTGTTA 1600
PfNT4 TT----TGT-CATT--CCTAATATT-TGTAATAGGAGGTACGA-ATGG-TTC-TTTG--A 1153

PfNT1 TTCAATATAGTTTACC-AAAG--CCAGATT--TACCACCC----ATC-GATGT----A- 1260
PfNT2 T-AA-TTTAATTTTTTTGAAAGCACCAGAAACGTGTAAAGAAAAAGCAAATATGAATAT 1197
PfNT3 T-CA-TGT-CTTTTATT-AATGTTCCAGAAAT-TCTCAA-----ACC-TAT-T----A- 1642
PfNT4 T-CA-----ATATTAGT-TATG--CCAGAA--TATCAG-----ACTGTTT-TGAAGA- 1193

PfNT1 ACACAAT-AA----- 1269
PfNT2 ATTCAATTAACCTCAAATATACTTTACTTATGTTTAATTTTGG--AATAACCAGTGGG 1254
PfNT3 ATTCAAT-GAGT--AATGTTGCAATAGTTA-GT--AGTTTTGGTTCAACACTCCTTC-G 1694
PfNT4 ATCAAAT-AAGA--AAAC--CAA-ACA-A-AT--CGCTGTGG--CATCA-TCCTCTCTG 1238

PfNT1 ----- 1269
PfNT2 TG-TTT--AATATCCA-AGGTTTCATGTAA--GAATTGTGA-ATATAATTGCAGTTATTT 1306
PfNT3 AG-TTG--GCTTGTTAACAGGCT-ATGGAT--GTTCCACACTATATAAATATA-TCATAT 1747
PfNT4 TGCTTTATGTCTATTAATGAGTT-TTGCATTAGCACCATGTTTTGTAATGCAATAAT-T 1296

PfNT1 ----- 1269
PfNT2 TAAAA--TAA 1314
PfNT3 CAAAAATGTGA 1758
PfNT4 CATT--TGTA 1305

```

**Figure 5.3: Alignment of the four genes encoding for equilibrative nucleoside transporter in *P. falciparum*.**

## 5.4 Phylogenic tree of the four genes encoding for ENT in *P. falciparum*

Using the ClustalX program, a phylogenetic tree of the four genes encoding for the equilibrative nucleoside transporter was generated. TbAT1, which encodes for the adenosine transporter in *T. brucei* was included for comparison as an outgroup. The tree, which is shown in Figure 5.4 indicates that there is limited similarity between all five genes. However there appears to be a more recent ancestral link between *PfNT1* and *PfNT4*.

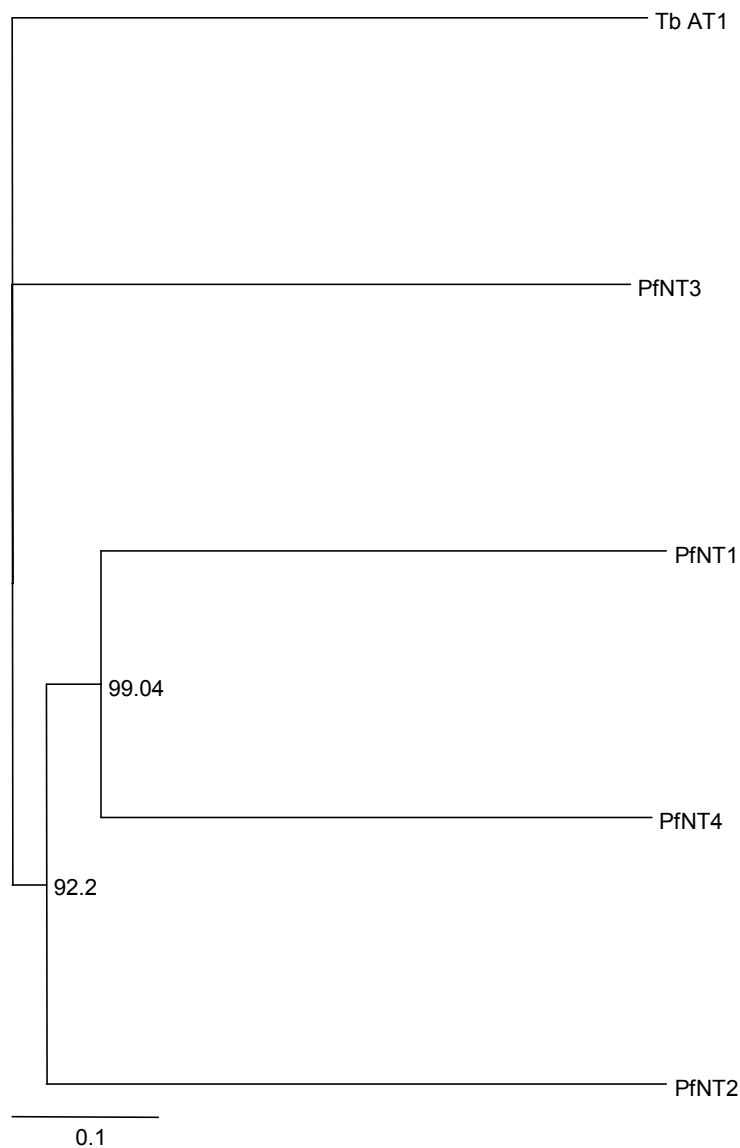


Figure 5.4: Phylogenetic tree, with bootstrap values, of the four genes encoding for ENT in *P. falciparum* and TbAT1 of *T. brucei*.

The scale bar represents the distances as numbers of substitutions per site.

## 5.5 Sequencing of *PfNT1* (PF13\_0252) in *P. falciparum* clone 3D7

To ensure that the sequence of the wild type *PfNT1* is exactly as indicated in the PlasmoDB, a 1254 bp portion of parasite clone 3D7 was amplified and sequenced. This included the entire coding region of PF13\_0252 gene plus regions up- and downstream from this segment. Three sets of primers were designed for amplification of overlapping portions of the gene. The primer sets are:

*PfNT1* SEQ1FOR=5' AATGAGTACCGGTAAAGA 3'  
*PfNT1* SEQ1REV= 5'AATATTAAACAAAGTTCACAG 3';

*PfNT1* SEQ2FOR=5' TATTTCCAGGTGTTGGACAC 3',  
*PfNT1* SEQ2REV= 5' GATGGGTGGTAAATCTGGC 3';

*PfNT1* F=5' TTACAGGTTTAGTATGTTTCCTC 3'  
*PfNT1* R=5' ATTTGGTGGATATCTACTGA G3').

The entire gene and the subgroups are shown in Figure 5.5. The amplicons was then shipped to the University of Dundee for sequencing.

Outcome of the sequencing showed that the *PfNT1* gene from the 3D7 clones of *P. falciparum* used in this study is 100% identical to the entry in PlasmoDB for PF13\_0252.

TATATATATATATATATTTATTTAATAAATATATTTTGTAAAAATTAAAGAATATATATATATTAATATTATG  
TATATATATTATATAATTAATATAGTAAATAAATAAATATACATATAAAATATAATATTATATATATAATATTT  
TTAGGTATTTATAAAATATATATATATATATATATATATATTTATATATATGTGCTGTTTACATATATATTAA  
TAGGTTAATATATATATATATATTTATTTATATTTATATGAATATATAAATATATTATATATTTATTTTGTAT  
TTATCTATTATTTTATAAAGTAAATGAGTACCGGTAAAGAGTCATCTAAAGCTTATGCTGATATAGAA  
TCCAGGGGTGATTATAAGGACGATGGAAAGAAAGGATCTACATTAAGCAGTAAACAACATTTTCATGTTATCTT  
TAACCTTTTATATTAATAGGTTTAAAGTTCTTTGAATGTATGGAATACAGCCTTAGGATTAAATATAAATTTTAA  
ATATAATACCTTTTCAGATTACAGGTTTAGTATGTTCTCAATTGTAGCTTTATTTGTTGAGATTCCCAAAATA  
ATGTTACCATTTCTTTTGGGTGGTTTATCAATTTTATGTGCAGGTTTCAAATATCTCACAGTTTTCACAGT  
ATACACAATTTGATACATATTGTTTAGTAGCTTTTATTGTTATTGTTGAGTGGCAGGATTAGCTCAAACCAT  
TGCATTTAATATAGGATCAACCATGGAAGATAATATGGGTGGTTATATGTGACGAGGTATTGGTATATCAGGA  
GTATTTATTTTGTATTATTAATTTATTACTTGATCAATTCGTATCTCCGAAAAACATTATGGTGTATAATAAG  
CAAAGTTATTATTTATATATAATCTGTGAACCTTTGTTTAAATTTAGCTATAGTATTTTGTGTATGTAATTT  
AGATTTAAACAACAAGAATAATAAAAAAGATGAAGAAAATAAAGAAAACAATGCCACATTATCTTATATGGAA  
TTATTTAAAGATAGTTACAAAGCTATATTAACATATGTTTCTTGTAACCTGGTTAACTTTACAATTAATTTCCAG  
GTGTTGGACACAAAAAATGGCAAGAAAGTCATAATATCTCCGATTATAATGTTACCATTATTGTTGGTATGTT  
TCAAGTTTTTGATTTTCTCAGTAGATATCCACCAAATCTTACACATATTAATAATCTTTAAAAATTTTACTTTC  
TCTTTAAATAAATTATTGGTTGCCAATTCATTGAGATTATTATTCATTCCATGGTTTATTTTAAATGCATGTG  
TTGATCATCCATTTTCAAAAACATTGTACAACAATGTGTATGTATGGCTATGTTAGCTTTTACAAATGGTTG  
GTTTAATACTGTACCATTCTTGTATTTGTTAAAGAATTAAAAAAGCCAAAGAAAAGAAAGAAATCGAAATT  
ATATCCACATTCTTAGTTATTGCTATGTTTGTGGATTATCTGTGGTATATGGACTACATACATTTATAACT  
TATTCAATATAGTTTACCAAAGCCAGATTACCACCCATCGATGTAACACAATAAATAAATAAAAAATGAAG  
AGAAATAATGAATAATATATATATATATATATATTTACATATATATATTTATTTATTTATATATTTATTCATT  
TTTACATTTATAAGTATTATGTAAATTTCTGATATATCTCCTCAATTTTCTTAAAAATAAATTTAAAAA  
AAAAAAAAAAAAAAAAAAAAAAAAAATTTATATATATAAATGTGTGTACATATCATTATATGTTGTATT  
AAAATTTTTAAAACTTTTACCATTTTAAAAAATAAAAAAATAAATACAAGTTATAAACTTAATATAT  
AAATATATATATATATATATTTATATATTTATATGTATTATTTATTTTGTATGAGGTTCTCTATATTT  
TATACCAAG

Figure 5.5: Sequencing of *PfNT1*.

The figure is Part of *P. falciparum* genome showing the entire 1269 bp ENT1 (PF13\_0252) in yellow colour. The under lined nucleotides constitute the 676 bp insert that was cloned into pCAM/BSD and used to disrupt the gene. The three pairs of primers used to amplify the entire ENT1 in order to sequence are shown in bold pink, red and blue (*PfNT1* SEQ1FOR=5'AATGAGTACCGGTAAAGA3', *PfNT1* SEQ1REV= 5'AATATTAAACAAGTTCACAG3'; *PfNT1* SEQ2FOR=5'TATTTCCAGGTGTTGGACAC3', *PfNT1* SEQ2REV= 5'GATGGGTGGTAAATCTGGC3'; *PfNT1* F=5'TTACAGGTTTAGTATGTTCCCTC3' *PfNT1* R=5'ATTTGGTGGATATCTACTGAG3'). Three overlapping segments of the gene were amplified and sequenced independently at the university of Dundee sequencing service.

## 5.6 Preparation of plasmid constructs for disruption of the equilibrative nucleoside transporter genes

Four DNA fragments were prepared for insertion into the vector pCAM/BSD for disruption of the genes encoding for the equilibrative nucleoside transporter proteins in *P. falciparum*, as described in section 2.3.7. The DNA sequences of the four genes encoding ENTs in *P. falciparum* and the target DNA chosen for disruption of gene functionality are shown in section 2.3.7. The fragments were chosen to ensure maximum disruption of the portion responsible for solute translocation in the parasite. Generally, the fragments chosen included the sequence encoding the transmembrane domains 3-6, as well as a portion of transmembrane domain 2, that are predicted to be responsible for solute translocation

(Hyde *et al*, 2001;de Koning *et al*, 2005). In order to increase the probability of recombination after integration, particular attention was given to the size of fragment chosen as detailed in section 2.3.7. Fragments sizes of 676 bp, 913 bp, 1171 bp (includes 243 bp intron) and 778 bp were therefore chosen for PF13\_0252, MAL8P1.32, PFA0160c and PF14\_0662 respectively.

Gel electrophoresis (section 2.3.6) confirmed that the expected size of PCR fragment for each gene was obtained with the gene-specific primers used, as shown in section 2.3.7. The PCR product was purified as described in section 2.3.8 and the concentration of the purified PCR product was determined as described in section 2.3.5.

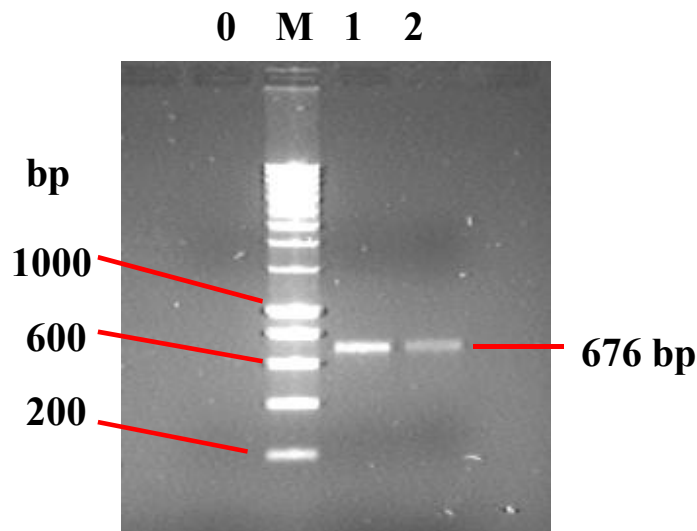


Figure 5.6: Amplification of *PfNT1* (PF13\_0252).

Polymerase chain reaction of *PfNT1* fragment (676 bp) separated on 1.5% agarose gel stained with ethidium bromide. Lanes marked 1 and 2 contain the 676 bp fragment, lane 0 is the blank and Lane M is the SMART molecular weight marker.

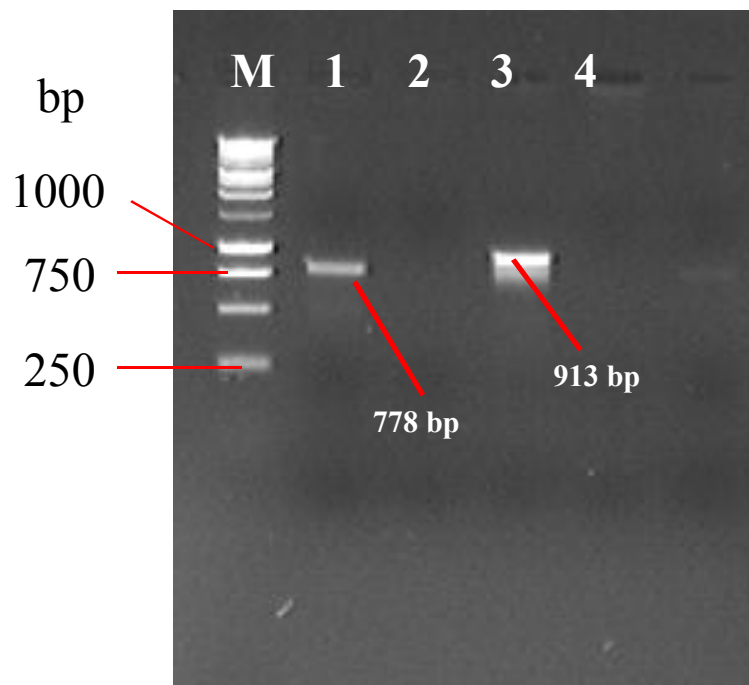


Figure 5.7: Amplification of *PfNT2* and *PfNT3* DNA fragments.

Amplified fragments of *PfNT2* and *PfNT3* separated on 1.5% agarose gel stained with ethidium bromide. *PfNT2* shown in lane 1 had a band size of 778 bp whilst *PfNT3* (lane 3) was 913 bp. Lanes marked 2 and 4 are the negative controls (no DNA) and the lane marked M is the molecular weight marker.

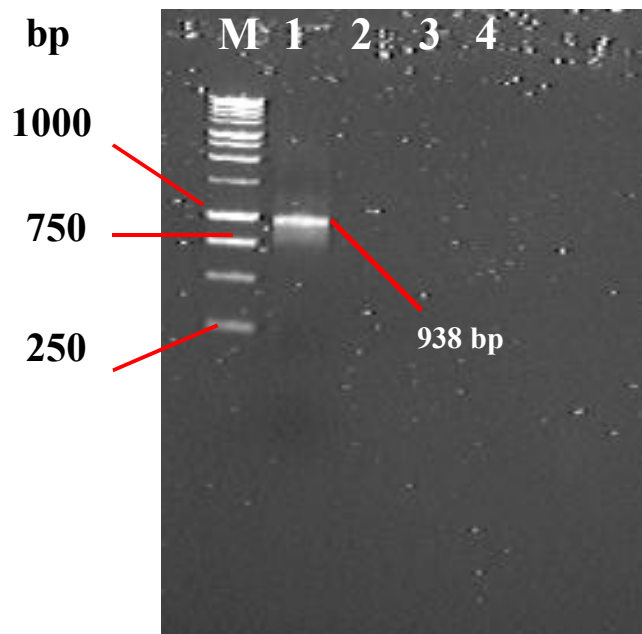


Figure 5.8: Amplification of *PfNT4* DNA fragment.

*PfNT4* amplified fragment was separated on 1.5% agarose gel stained with ethidium bromide. The fragment, which is in lane 1, has a size of 938 bp. Lanes marked 2 and M are negative control and molecular weight markers respectively.

## 5.7 Preparation of pCAM/BSD-ENT construct

Each of the purified PCR products prepared above was ligated into the expression vector, pCAM/BSD, as described in section 2.3.11. The constructs were designated pCAM/BSD-PfNT1, pCAM/BSD-PfNT2, pCAM/BSD-PfNT3 and pCAM/BSD-PfNT4 for fragments targeting the ENT encoding genes, PF13\_0252, PF14\_0662, MAL8P1.32 and PFA0160c and respectively. Plasmids were purified as described in section 2.3.3.

## 5.8 Transformation of DH5 $\alpha$ competent cells with pCAM/BSD-ENT construct

DH5- $\alpha$  chemically competent cells (Invitrogen, UK) were transformed with each of the four constructed plasmids (pCAM-BSD/ENT) using the standard heat-shock methods as described in section 2.3.12. There was an average growth of 30 single bacteria colonies per plate. Single colonies were subcultured into 500ml liquid bacterial culture as described in section 2.3.12. Plasmid was prepared from the liquid overnight bacterial cultures, as described in section 2.3.13 and plasmid DNA was purified using the maxi DNA purification kit (Qiagen, UK).

The presence of the ENT inserts in each of the four pCAM/BSD-ENT constructs was verified by PCR using the forward and reverse primers designed for amplifying the ENT fragments. PCR conditions described in section 2.3.7 were used for the amplifications. Four microlitres of the amplicon were then run on a 1.5% agarose. The insert amplified from each of the four pCAM/BSD NT plasmids was confirmed as being of the expected size (Table 2.1). Figure 5.9 shows verification of PfNT1 in pCAM/BSD-PfNT1 plasmid.

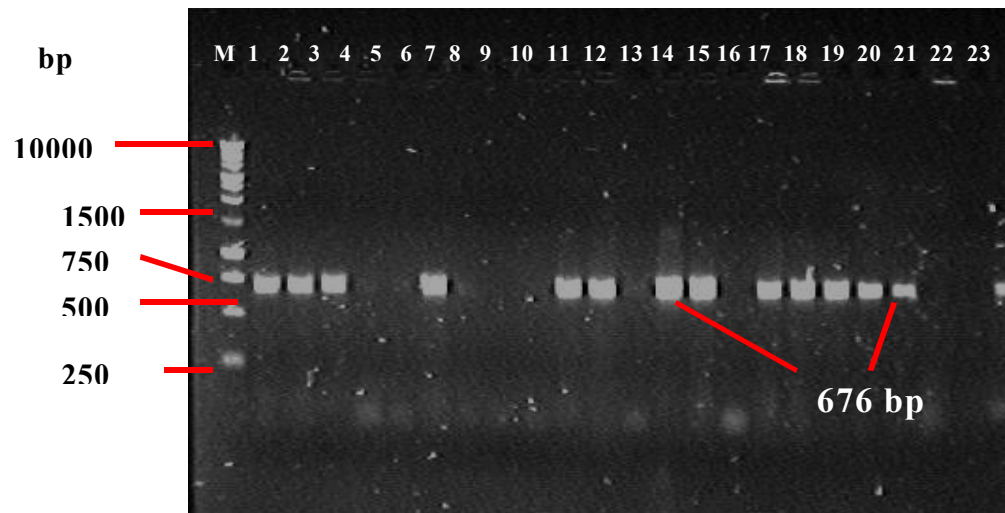


Figure 5.9: Verification of presence of *PfNT1* insert in plasmid pCAM/BSD-PfNT1 by PCR.

Each lane is from a culture prepared with a single colony as discussed above (section 5.5). The construct retrieved from the bacteria cells was subjected to PCR amplification using the forward and reverse primers PfNT1 F and PfNT1 R. The figure shows separation of the amplicon on 1.5% agarose gel stained with ethidium bromide. The lane marked M represents the molecular weight marker. The lanes with the 676 bp band show the colonies from the bacteria that were successful transformed with the construct, pCAM/BSD-NT1.

Presence of the insert in the purified pCAM/BSD-ENT constructs was also verified by restriction digest with *Bam*H1 and *Sac*II. The enzymes are expected to cut the construct at the 5' and 3' end respectively of the insert, resulting in two bands (insert and vector).

The fragments obtained from restriction of the four construct with *Bam*H1 and *Sac*II indicate that ligation of each of the ENT fragments into pCAM/BSD-NT was successful. Figure 5.10 is a picture of the gel showing the resultant fragments after restriction digest of the construct, pCAM/BSD-PfNT1.



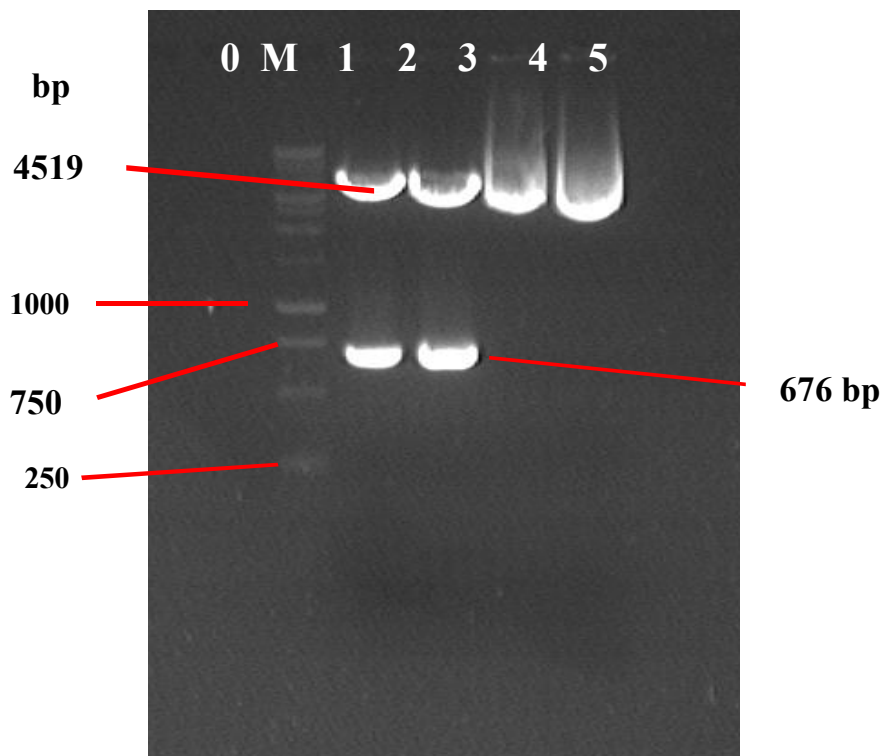


**Figure 5.10: Verification of the presence of *PfNT1* inserts in the plasmid pCAM/BSD-*PfNT1* by restriction digestion with *Bam*HI and *Sac*II.**  
 The digested product was separated on 1.5% agarose gel stained with ethidium bromide. Lane 1: molecular weight marker. Lanes 2 and 3: Digested (cut) product (showing the 676bp *PfNT1* and the 4519 pCAM/BSD fragments). Lanes 4 and 5: undigested (uncut) product.

The sequence of each of the four inserts was verified through sequencing. Each of the four pCAM/BSD-ENT plasmids was purified as described in section 2.3.3 and sequenced using the appropriate pCAM/BSD forward primer at the University of Dundee Sequencing Service (DSS). The results of the sequencing confirmed that each plasmid construct contained the exact sequence of the gene fragments for *PfNT1*, *PfNT2*, *PfNT3*, and *PfNT4*.

## 5.9 Transfection of *P. falciparum* by electroporation

Asexual parasites of *P. falciparum* clone 3D7 were cultured as previously described (section 2.1.4). Predominantly ring stage of the parasites were transfected with each of the purified pCAM/BSD-NT plasmids using the methods described in section 2.4. Blasticidin-resistant parasites appeared in each of the four experiments after 3-4 weeks of selective culture, indicating successful transformation of parasites with the plasmids conferring resistance to Blasticidin. The plasmids could replicate episomally, which would confer blasticidin resistance but would not result in disruption of the *PfNT* loci. Therefore, PCR analysis was used to verify that the episome had integrated into the parasite's genome through homologous recombination.

### 5.10 Confirmation of integration of 3D7 $\Delta$ *PfNT1*, 3D7 $\Delta$ *PfNT2* and 3D7 $\Delta$ *PfNT3* in uncloned parasite cultures

Different combinations of primers (see Table 2.3) specific to the *PfNT* gene allow discrimination of (i) the wild-type locus, (ii) a 5' integration event, (iii) a 3' integration event, and (iv) the episomal form of the transfected plasmid. Pictures of the gels showing integration of the pCAM/BSD-*PfNT* construct, verified with various primer combinations are shown in Figure 5.11 to Figure 5.13. It was clear from the results that integration was achieved for all the four genes under investigation.

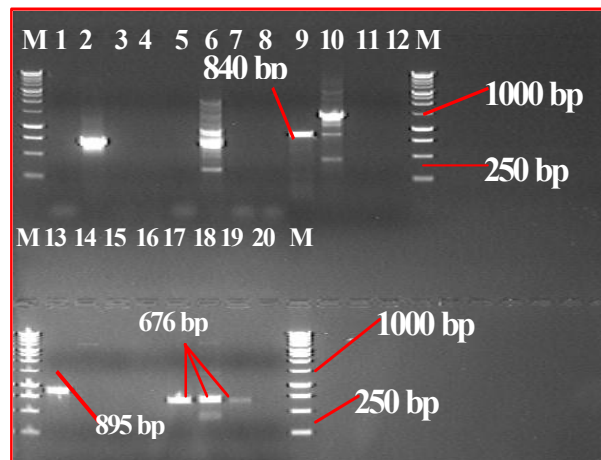


Figure 5.11: PCR analysis of uncloned *PfNT1* transfectants, pCAM/BSD-*PfNT1* and wild type 3D7 parasites.

Genomic DNA from *PfNT1* transfectants, pCAM/BSD-*PfNT1* and wild type 3D7 parasites were subjected to PCR analysis. Primer pairs were used to detect the presence of the episome, using pCAM F2 and pCAM R2 (1-4), integration at the 5' end of the insert using primers *PfNT1* up and pCAM R2 (lanes 5-8), integration at the 3' end of the insert, using *PfNT1* Down+pCAM F2 (9-12), the wild type gene using *PfNT1* Up+*PfNT1* Down (13-16) and presence of the *PfNT1* fragment (lane 17-20) as detailed in section 2.4.2. Lanes 1, 5, 9, 13 and 17: amplifications using DNA from the transfectant. Lanes 2, 6, 10, 14 and 18: amplifications using DNA from pCAM/BSD *PfNT1*; lanes 3, 7, 11, 15 and 19: amplifications using DNA from wild type parasite; lanes 4, 8, 12, 16 and 20: negative control (water as template). Lanes marked M are molecular weight markers. See Table 2.4 for the expected band sizes.

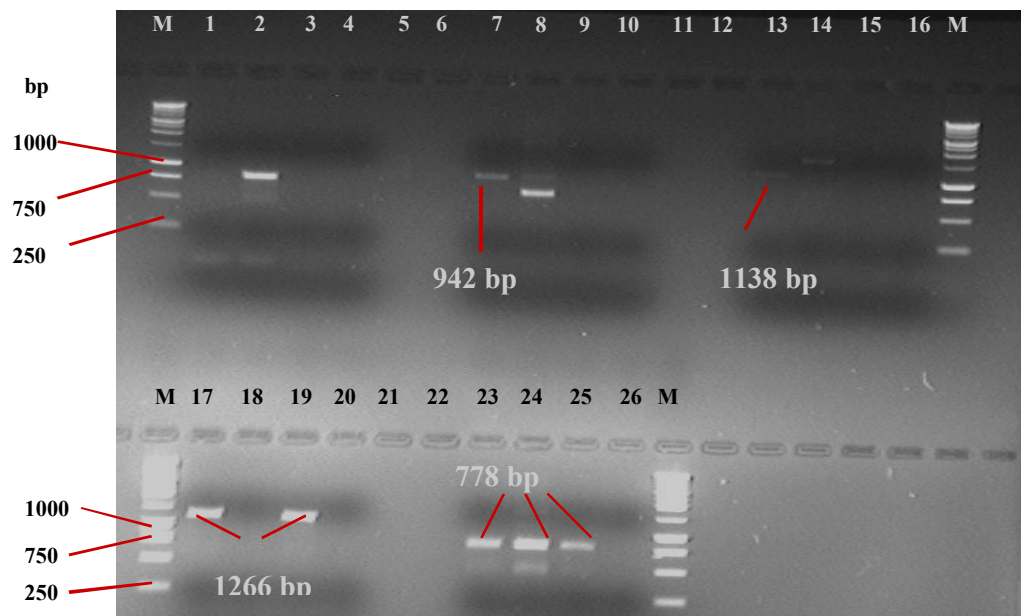


Figure 5.12 PCR analysis of uncloned PfNT2 to verify integration of pCAM/BS-D-PfNT2 into parasite's genome.

Lanes 1, 7, 13, 17 and 23 contain DNA from the transfectant; Lanes 2, 8, 14, 18 and 24 contain DNA from the construct; lanes 3, 9, 15, 19 and 25 contain DNA from wild type parasite; lanes 4, 10, 16, 20 and 26 are negative controls (water as template). Lanes marked M are molecular weight markers. Primer pairs used were pCAM F2 and pCAM R2 (lanes 1-4), primers *PfNT1* up and pCAM R2 (lanes 7-10), *PNT1* Down+pCAM F2 (13-16), *PfNT1* Up+*PfNT1* Down (17-20) and presence of the *PfNT2* fragment (lane 23-26). see Table 2.4 for detail of expected band sizes. The figure shows integration at the 5' end (lane 7) and 3' end (lane 13).

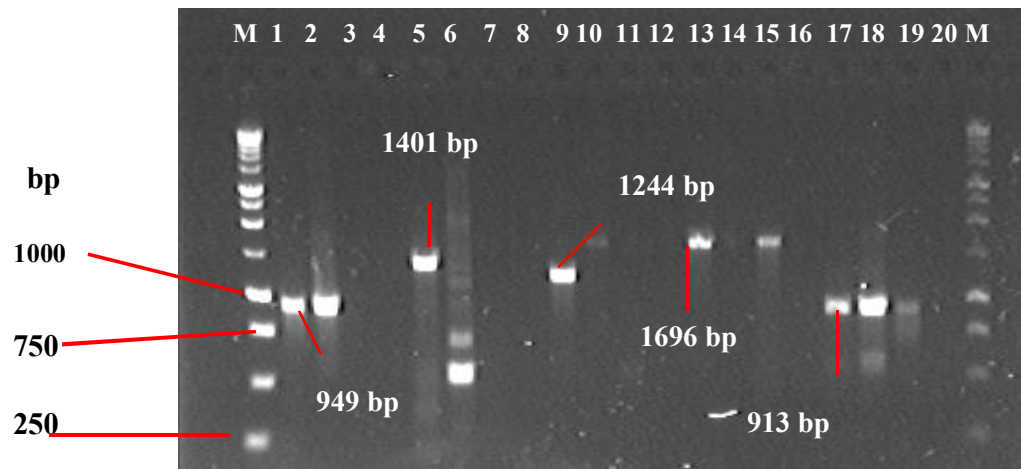


Figure 5.13: PCR analysis of uncloned PfNT3 to verify integration of pCAM/BS-D-PfNT2 into parasite's genome.

Lanes 1, 5, 9, 13 and 17 contain DNA from the transfectant; Lanes 2, 6, 10, 14 and 18 contain DNA from the construct; lanes 3, 7, 11, 15 and 19 contain DNA from wild type parasite; lanes 4, 8, 12, 16 and 20 are negative controls (water as template). Lanes marked M are molecular weight markers. Primer pairs used were pCAM F2 and pCAM R2 (lanes 1-4), primers *PfNT1* up and pCAM R2 (lanes 5-8), *PNT1* Down+pCAM F2 (9-12), *PfNT1* Up+*PfNT1* Down (13-16) and presence of the *PfNT3* fragment (lane 17-20). The figure shows integration at the 5' end (lane 5:1401 bp) and 3' end (lane 9:1244 bp).

## 5.11 Cloning of parasites with disrupted *PfNT1*

Once integration of pCAM/BSD *PfNT* into parasite's genome had been confirmed, the parasites were frozen down into liquid nitrogen (section 2.1.7). To proceed with further characterisation of the gene-disrupted parasites it was necessary to clone the transfected lines to obtain homogeneous parasite populations.

The work presented in this section of the thesis describes the cloning and subsequent analysis of parasite clones with a disrupted *PfNT1* gene. Cloning of the 3D7 parasite line with a disrupted *PfNT1* (Pf13\_0252) was performed in a 96 well plate using the limited dilution method described in section 2.3.19. Four parasite clones were obtained by this method and were designated 3D7  $\Delta$ *PfNT1*-D6, 3D7  $\Delta$ *PfNT1*-B9 and 3D7  $\Delta$ *PfNT1*-B11. PCR confirmation in three of the clones is shown in Figure 5.14.

Due to time constraints, clones could not be prepared for the other three disrupted ENT genes (*PfNT2*, *PfNT3* and *PfNT4*). However, the frozen parasites would be cloned in the future and the kinetic properties of the phenotype lacking the ENT gene determined.

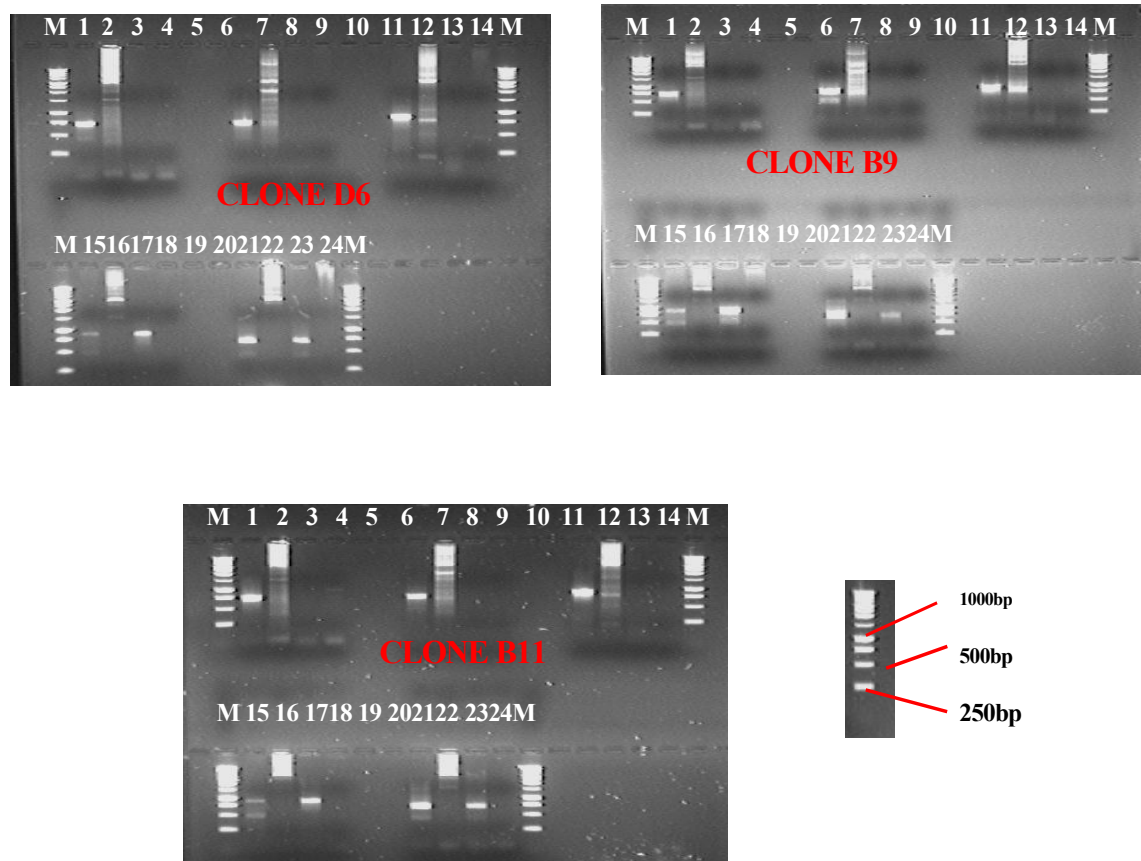


Figure 5.14: PCR analysis of the three clones of *PfNT1* transfectants, pCAM/BSD-*PfNT1* and wild type 3D7 parasites.

Genomic DNA from cloned  $\Delta PfNT1$  transfectants, pCAM/BSD and wild type 3D7 parasites were subjected to PCR analysis. Primer pairs were used to detect the presence of the episome, using pCAM F2 and pCAM R2 (1-4), integration at the 5' end of the insert using primers NT1 up and pCAM R2 (lanes 6-9), integration at the 3' end of the insert, using NT1 Down+pCAM F2 (11-14) and the wild type gene using NT1 Up+NT1 Down, (15-18) and presence of the *PfNT1* fragment (lane 21-24) as detailed in section 2.4.2. Lanes 1, 6, 11, 15 and 21: amplifications using DNA from the transfectant. Lanes 2, 7, 12, 16 and 22: amplifications using DNA from pCAM/BSD; lanes 3, 8, 13, 17 and 23: amplifications using DNA from wild type parasite; lanes 4, 9, 14, 18 and 24: negative control (water as template). Lanes marked M are molecular weight markers. The size of the molecular weight marker is shown at the bottom right corner. Presence of the bands in lanes 6 (731 bp) and 11 (840 bp) confirmed integration at the 5' and 3' end respectively. Integration appears to have occurred in all the three  $\Delta PfNT1$  clones. The episome was still observed to be present (lane 1; 712 bp). See Table 2.4 for the expected band sizes.

## 5.12 Molecular characterisation of 3D7 $\Delta$ *PfNT1* clones

### 5.12.1 PCR characterisation of 3D7 $\Delta$ *PfNT1* clones

The four 3D7 $\Delta$ *PfNT1* parasite clones were characterised by PCR as described in section 2.4.2 using combinations of primers. The outcomes of this analysis for clones 3D7 $\Delta$ *PfNT1*-B11 and 3D7 $\Delta$ *PfNT1*-D6 are shown in Figure 5.15. The results indicate that (i) the parasites have lost their wild-type gene (lane 4) indicating that the *PfNT1* gene has been interrupted, (ii) amplicons with expected sizes for 5' and 3' integration events were recovered (lanes 1 and 2), and (iii) a band arising either from the episome or from an integrated concatemer of the plasmid was still present in the cloned parasites (lane 3). Similar results were obtained with clones 3D7 $\Delta$ *PfNT1*-B7 and 3D7 $\Delta$ *PfNT1*-B9.

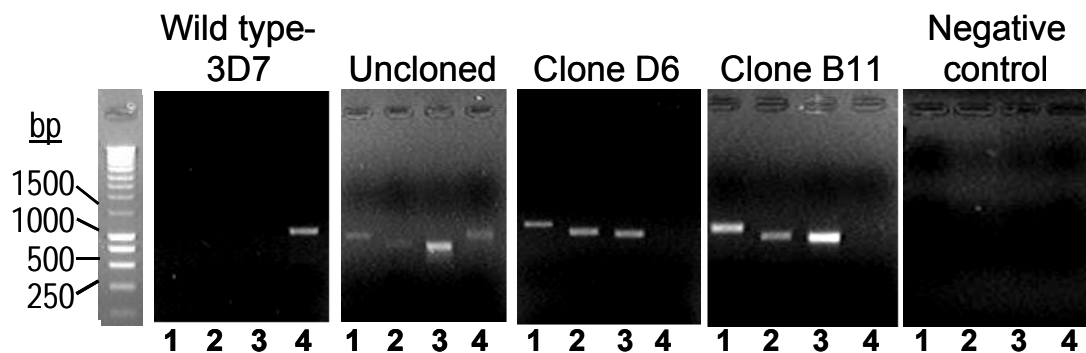


Figure 5.15: PCR analysis of genomic DNA from the wild-type 3D7, uncloned pCAM/BSD-*PfNT1* transfected parasite population and two of the 3D7 $\Delta$ *PfNT1* clones (B11 and D6).

Lane 1 in each box contains the products of amplification with primers I and III, and a product of 1088 bp. indicates integration at 5' end of the locus. Lane 2 contains the products of amplification with primers II and IV, and a product of 908 bp. indicates integration at the 3' end. Lane 3 contains the products of amplification with primers II and III, and a product of 850 bp. indicates the presence of the episome. Lane 4 contains the products of amplification with primers I and IV, and a product of 1174 bp indicates the intact *PfNT1* gene.

### 5.12.2 Southern blot analysis of 3D7 $\Delta$ *PfNT1* clones

Southern blotting was performed as described (Fidock and Wellem, 1997) to confirm homologous integration at *PfNT1* in the 3D7 $\Delta$ *PfNT1* clones and the absence of the wild type intact *PfNT1* in the culture, as detailed in section 2.4.4 and section 2.4.2.

The Southern blot was hybridized to a probe representing the same region of *PfNT1* present in the plasmid pCAM/BSD-*PfNT1* (Fig. 5.20). The probe hybridized to a 7.9kb

fragment in wild type 3D7 parasites, representing the genomic copy of *PfNT1* (Figure 5.17). This fragment was absent in the four 3D7 $\Delta$ *PfNT1* clones B11, B9, B7 and D6, being replaced by two fragments of 7.1kb and 5.9kb, representing the interruption of *PfNT1* by the integrated plasmid sequence. Episomal plasmid with an expected size of 5.2kb was not detected by southern blotting (see Figure 5.16), whereas it was detected by PCR (Figure 5.15). This is likely to be a reflection of the lower sensitivity of southern blotting method compared with PCR for the detection of episomes present in a minority of parasites in the culture. Alternatively, the PCR product observed may represent amplification from multiple copies of the plasmid inserted into the locus. It is not possible to differentiate between multiple copies of the plasmid integrating into a locus and circular episomes by Southern blot analysis, as any of these digests would merely drop out the extra plasmid copies from the locus and appear the same as circular episomes.

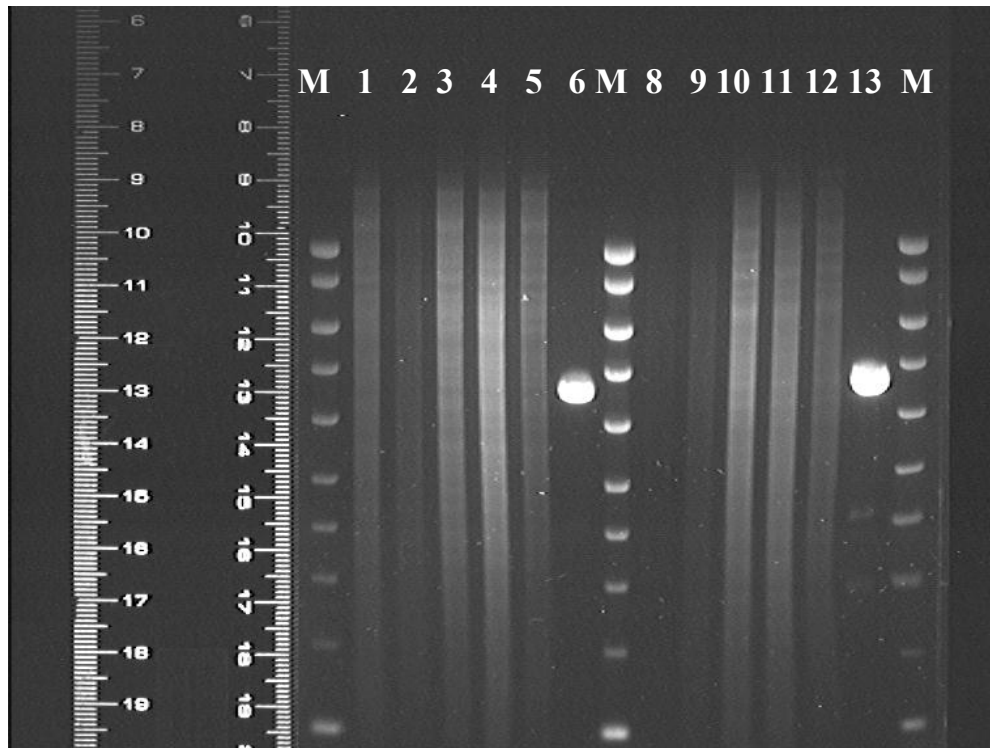


Figure 5.16: Separation of 12  $\mu$ l of restriction digested DNA with *Xmn*I of wild type (3D7 of *P. falciparum*) and DNA from four 3D7 $\Delta$ *PfNT1* clones on 0.8% agarose gel prior to Southern blotting.

Lanes 1 and 8 contain the wild type DNA, lanes 2 and 9 contain 3D7 $\Delta$ *PfNT1*-B11 DNA; Lanes 3 and 10 contain 3D7 $\Delta$ *PfNT1*-B9; lanes 4 and 11 contain 3D7 $\Delta$ *PfNT1*-B7; Lanes 5 and 12 contain 3D7 $\Delta$ *PfNT1*-D6, lanes 6 and 13 contain the plasmid (pCAM/BSD). Lanes marked M contain the SMART DNA ladder.

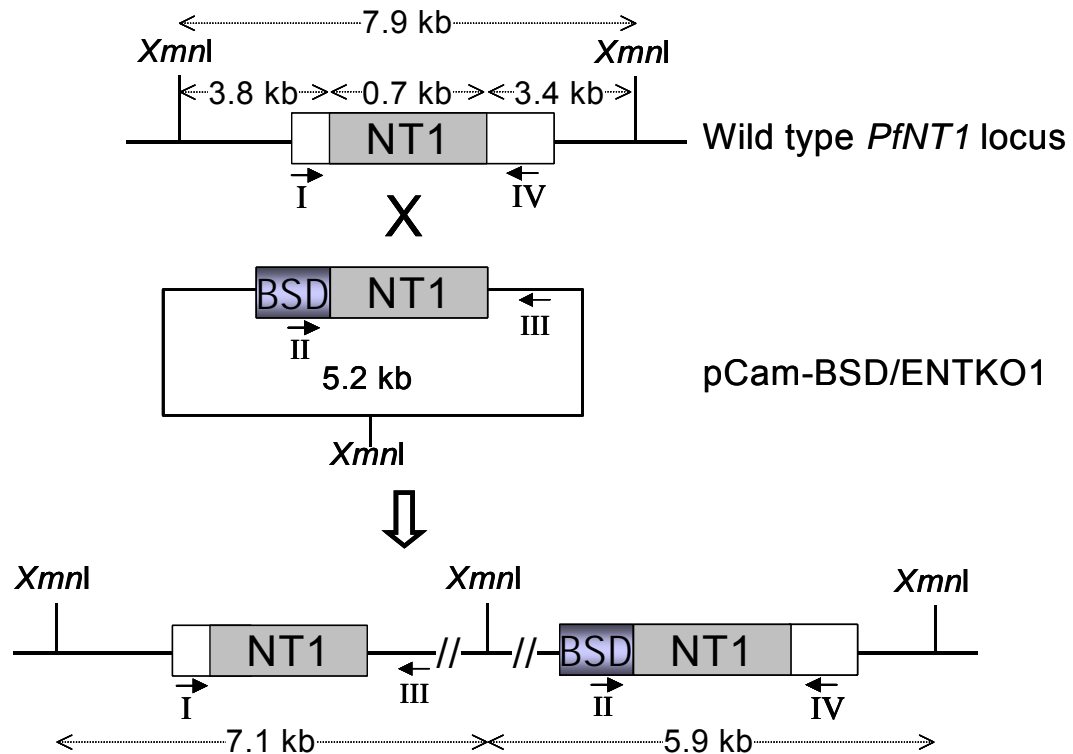


Figure 5.17: Gene disruption strategy.

Primers used to detect integration of the construct into the wild type locus are shown by arrows labeled I, II, III and IV which correspond to the text descriptions as follows: I: *PfNT1\_UP*; II: *pCAM-BSD\_F2*; III: *PCAM-BSD\_R2*; IV: *PfNT1\_DOWN*. The restriction sites of the endonuclease, *XmnI*, in the wild-type locus, construct and the integrants are as indicated.

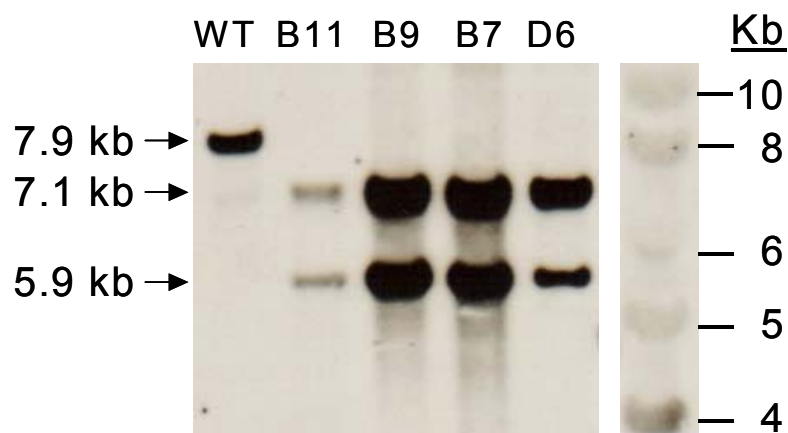


Figure 5.18: Southern blot showing the wild type locus and the digested products of the clones by *XmnI*.

The blot was probed with a fluorescein labeled-PCR product representing nucleotides 210 to 885 of *PfNT1* gene. The sizes of the bands are as shown.



## 5.13 Discussion

Gene targeting by homologous recombination, allows disruption of specific genes and consequently the interruption in the function of the proteins they encode (Menard & Janse, 1997). In this study, the technique was used to disrupt the genes that encode for equilibrative nucleoside transporters (ENT) in *P. falciparum*. Employing the gene manipulation techniques described in this chapter in combination with the classical uptake technique (chapter two), the true kinetic properties of *PfNT1* were uncovered (see chapter six).

All the four genes predicted by Martin and his colleagues (Martin *et al*, 2005) to encode for the equilibrative nucleoside transporters in *P. falciparum* were successfully disrupted by homologous recombination. The four genes targeted and disrupted were designated *PfNT1*, *PfNT2*, *PfNT3* and *PfNT4*, corresponding to the loci with PlasmoDB accession numbers PF13\_0252, PF14\_0662 MAL8P1.32, and PFA0160c respectively. Single crossover homologous recombination at each *PfNT* locus was expected to produce a pseudodiploid configuration, with both truncated copies lacking some of the transmembrane domains of the protein necessary for transport activity. In most cases blasticidin-resistant parasites (transfectants) emerged 21 days post-electroporation. Parasite growth under drug pressure confirmed successful transfection. In the absence of an antibody to confirm changes in the transporter protein, the disruption of the *ENT* genes could only be confirmed through Southern blot and PCR analysis.

The observation that the parasites with a disrupted *PfNT1* gene could only grow normally when the medium was supplemented with extra purines also indicated the loss of transport activity by this protein and emphasized the essentiality of this transporter. This observation also throws the spotlight on purine transporters as a possible target for novel antimalarial drugs.

As the transfected lines went through numerous growth cycles it was expected that the episomal copies of the plasmid would disappear, because replication of the plasmid is not regulated with that of the parasite, and it is likely that some merozoites of a schizont would segregate without any episomal copies. Therefore over time the number of parasites with episomal copies should decrease. It is therefore most likely that the PCR product observed

using primers, which would amplify, an episome, most likely represent multiple copies of the plasmid inserted into the locus. It is well documented that by a single crossover event several copies of the plasmid can integrate into the malaria genome (McCoubrie *et al*, 2007)). While plasmid rescue can be used to rescue episomes from parasites, the presence of rescued plasmids does not necessarily infer the presence of replicating episomes in parasites. This is because homologous plasmid sequences in the genomic DNA of parasites containing multiple plasmid copies will naturally recombine in *E. coli* upon transformation to yield plasmids.

From the Southern blot, no wild type band was observed in any of the 3D7 $\Delta$ *PfNT1* clones, indicating that all parasites after cloning harboured the integration event. This was confirmed by PCR, where only bands representative of integration at 5' and 3' ends were obtained, whereas no band representative of a wild-type locus (as would be the case in parasites that only harbour episomes) was observed.

Taken together, the PCR and the Southern blot analyses confirmed that integration into *PfNT1* had occurred and the *PfNT1* locus had been disrupted. It was not possible to verify whether this gene disruption resulted in the complete loss of the PfNT1 protein, as no antisera were available. It is possible that a truncated form of PfNT1 could be produced, consisting of domain 1 and part of domain two (excluding the domain thought to be responsible for solute translocation). However this truncated protein is highly unlikely to be able to perform the same function of a wild-type PfNT1 with eleven trans-membrane domains. The 3D7 clone (control) was sequenced to confirm that its *PfNT1* sequence was 100% identical to the entry in PlasmoDB as PF13\_0252.

## 5.14 Conclusions

All four of the genes thought to encode for ENT in *P. falciparum* were successfully disrupted by homologous recombination. For each of the four disruptions, parasites with non-functioning ENT gene recovered after transfection and selection, indicating that none of the four ENT genes are essential to asexual *P. falciparum* parasites growing under *in vitro* culture conditions [although it was necessary to supplement the culture medium with additional purines to ensure growth]. Parasite clones were made by limiting dilution from one of the transfectant (*PfNTI*). Uncloned parasites from the other three transfection experiments were stored to await analysis at a later date, since time did not allow their further analysis for this thesis. The resultant 3D7 $\Delta$ *PfNTI* clones were analysed by PCR and Southern blot, confirming the absence of the intact, wild-type *PfNTI* gene and the integration of the pCAM/BSB-*PfNTI* plasmid into the *PfNTI* locus.

## **CHAPTER SIX**

- 6 Characterisation of purine transport parameters in *P. falciparum* parasites lacking the gene encoding the Equilibrative Nucleoside Transporter 1 protein (PfNT1).**

## 6.1 Summary

The kinetic properties of nucleoside and nucleobase transport in parasite clones with a disrupted gene, coding for one of the four Equilibrative Nucleoside Transporter proteins in *P. falciparum* were determined. The technique employed for disruption of *PfNT1* gene was described in chapter five of this thesis. In the present chapter, classical uptake techniques were used to assess the difference in purine salvage between parasites clones lacking the *PfNT1* gene (3D7 $\Delta$ *PfNT1*) and the parental clone 3D7 of *P. falciparum* (wild type). It was clearly demonstrated in this study that in 3D7 $\Delta$ *PfNT1* clones the high affinity hypoxanthine/ nucleoside transport activity observed in the wild type parasites was completely abolished, whereas the low affinity adenosine transport activity remained unchanged. Adenine transport in the 3D7 $\Delta$ *PfNT1* clones appeared to be slightly increased. We conclude that the gene with PlasmoDB accession number PF13\_0252 (*PfNT1*) encodes a high affinity hypoxanthine/nucleoside transport activity in *P. falciparum*.

## 6.2 Introduction

In order to ascertain the link between the four *P. falciparum* genes encoding proteins of the Equilibrative Nucleoside Transporter (ENT) family and the four apparently distinct purine transport activities reported in chapter four of this thesis, an assessment of purine transporters in clones with a disrupted *ENT* gene was performed. The outcome of this investigation is expected to reveal the exact contribution of at least one ENT protein in purine salvage into *P. falciparum* and address some of the controversies surrounding purine uptake in *P. falciparum*. Parasites with a disrupted *PfNT1* gene, whose generation was described in chapter five, were used in this investigation.

A purine uptake profile was prepared for one of the 3D7 $\Delta$ *PfNT1* clones, 3D7 $\Delta$ PfNT1-D6, using the uptake techniques described in chapter two. Non-transformed 3D7 parasites (wild-type) that had undergone the same electroporation process as the genetically modified clones, but were not transfected with the pCAM/BSD-*PfNT1* construct, were used as controls. Transport of hypoxanthine, adenine and adenosine at high or low concentrations was assessed exactly as described in chapter four for the saponin-freed *P. falciparum* trophozoites. For any given permeant, the linear phase of uptake was determined, with a constant permeant concentration incubated with the cells for different time periods to generate a plot of uptake versus time. Linearity was assessed using linear regression and defined as a correlation coefficient >0.95 and significant difference from zero uptake (F-test; GraphPad Prism version 4). When uptake was too rapid to obtain linearity of transport at room temperature, it was reassessed at 6 °C. Only the linear part of the uptake was used for estimation of the uptake rate as it reflects true rates of transport across the *P. falciparum* plasma membrane rather than rates of metabolism or sequestration.

### 6.3 Kinetic characterisation of parasites- summary of procedure

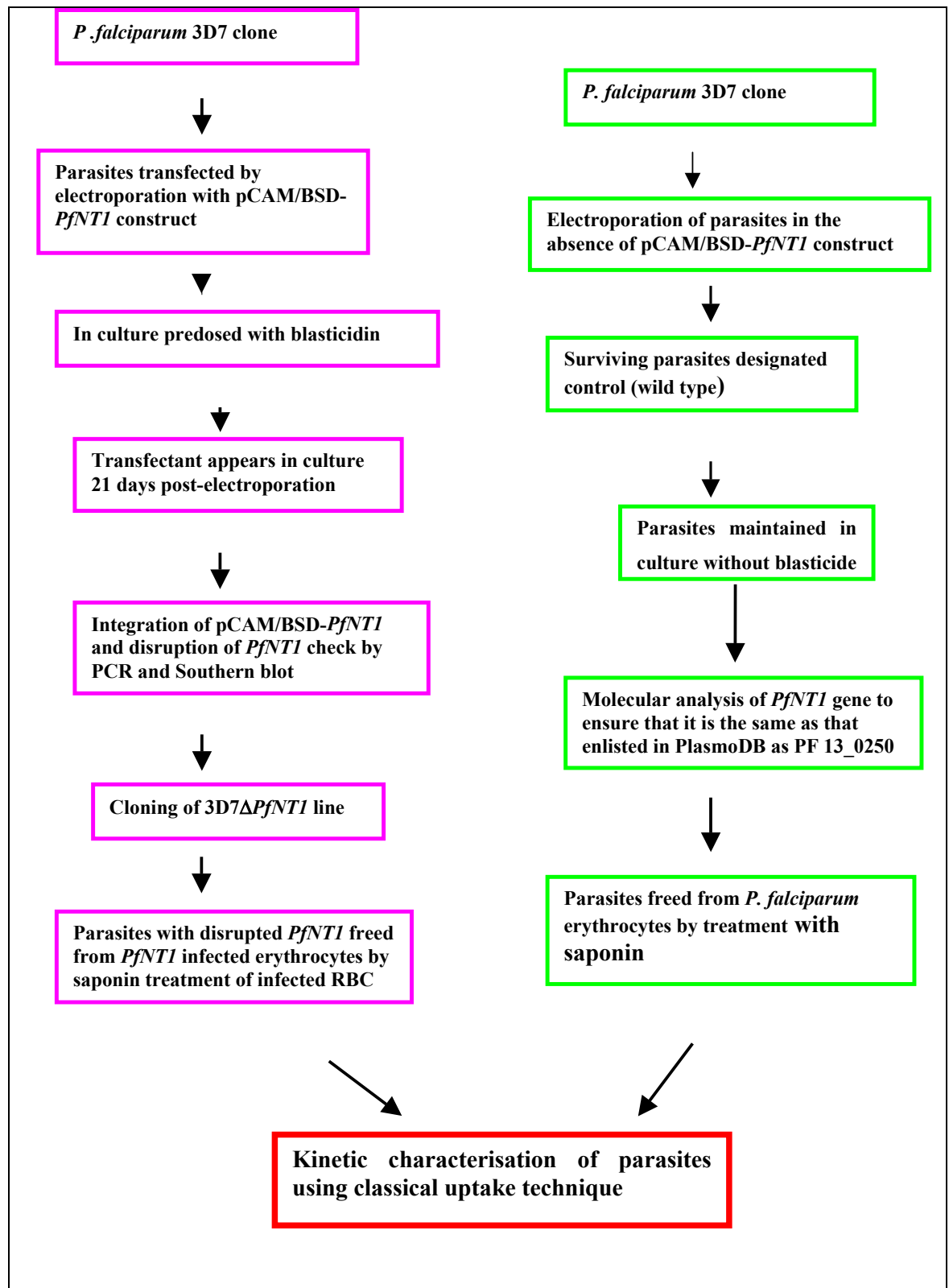


Figure 6.1.: Flow diagram for the production of *3D7ΔPfNT1* clones and wild-type control parasites used to assess purine transport in *P. falciparum*.

## 6.4 High affinity Adenosine transport is abolished in clone 3D7 $\Delta$ PfNT1-D6

Time dependent uptake of 0.25  $\mu$ M [ $^3$ H]-adenosine into saponin-freed *P. falciparum* trophozoites of 3D7 $\Delta$ PfNT1, lacking PfNT1, or wild type clone 3D7 (control) was carried out using the method developed and described in Chapter 4.

Comparison of adenosine transport in control (wild type) parasites and in 3D7 $\Delta$ PfNT1-D6 indicates that uptake of 0.25  $\mu$ M [ $^3$ H]-adenosine was reduced by 97 – 100% in the latter (n = 3; Figure 6.2). This observation clearly demonstrates the loss of high-affinity adenosine transport in the mutant line. The lack of high affinity adenosine transport activity was specific rather than a general reduction in transport rates as demonstrated below.

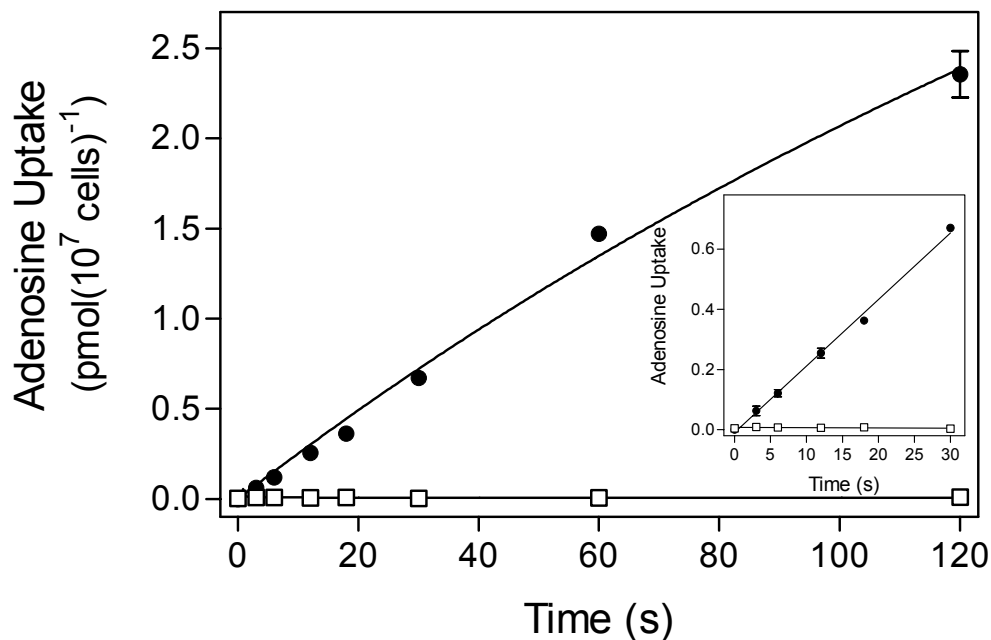


Figure 6.2: Purine transport in *P. falciparum* trophozoites of clone 3D7 $\Delta$ PfNT1-D6 lacking PfNT1 (Transport of 0.25  $\mu$ M [ $^3$ H]-adenosine at 22 °C).

Transport of 0.25 [ $^3$ H]-adenosine at 22 °C in 3D7 $\Delta$ PfNT1-D6 is indicated with open symbols and in wild-type 3D7 parasites with closed symbols. Insert shows the linear phase of the uptake obtained by linear regression. Data points shown are the mean of duplicate determinations and the experiment shown is typical of three identical determinations.



## 6.5 High affinity Hypoxanthine transport in clone 3D7 $\Delta$ PfNT1-D6 is abolished

Uptake of 0.4  $\mu\text{M}$  [ $^3\text{H}$ ]-hypoxanthine into saponin-freed 3D7 $\Delta$ PfNT1 or into wild-type control parasites was also assessed. The result, which is shown in Figure 6.3, indicates a reduction by 82 – 98% in hypoxanthine uptake into 3D7 $\Delta$ PfNT1 when compared with the wild-type ( $n = 3$ ).

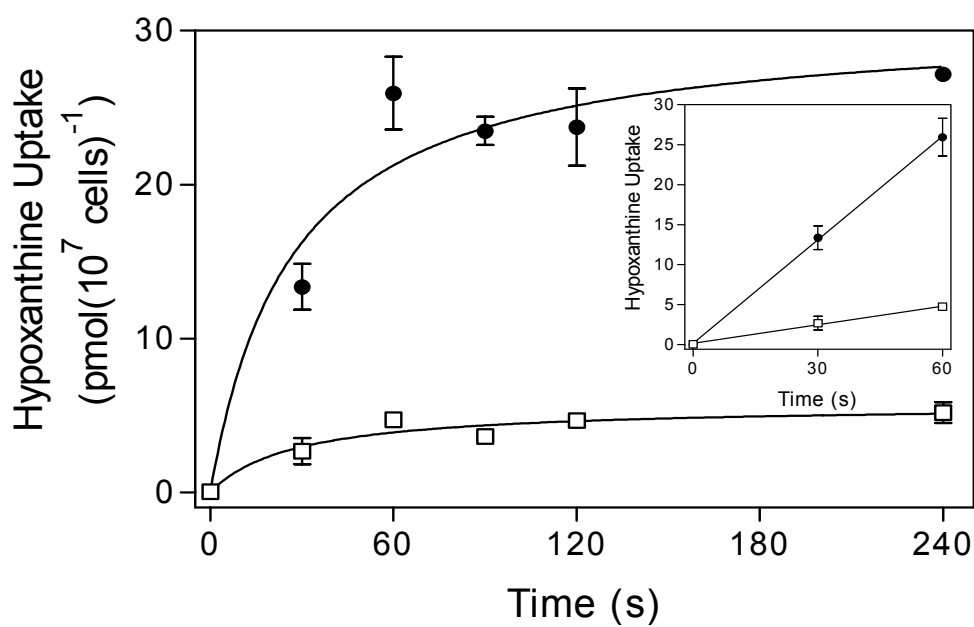


Figure 6.3: Purine transport in *P. falciparum* trophozoites lacking PfNT1 (transport of 0.4  $\mu\text{M}$  [ $^3\text{H}$ ]-hypoxanthine at 22 °C).

Transport of 0.4  $\mu\text{M}$  [ $^3\text{H}$ ]-hypoxanthine at 22 °C in 3D7 $\Delta$ PfNT1-D6 is indicated with open symbols and in wild-type 3D7 parasites with closed symbols. Insert shows the linear phase of the uptake.

## 6.6 High affinity adenine transport is not abolished in clone 3D7 $\Delta$ PfNT1-D6

Uptake of 1  $\mu$ M [ $^3$ H]-adenine was not greatly affected in the 3D7 $\Delta$ PfNT1 parasites (Figure 6.4): the initial rates of transport over 12 s were not significantly different in clone 3D7 $\Delta$ PfNT1-D6 and wild-type 3D7 control parasites (n = 3; Paired t-test). However, in each of three independent experiments the maximum level of [ $^3$ H]-adenine transport in clone 3D7 $\Delta$ PfNT1-D6 was double that of the wild-type control ( $0.16 \pm 0.06$  vs.  $0.077 \pm 0.022$  pmol ( $10^7$  cells) $^{-1}$ s $^{-1}$ ; n=3, non-linear regression).

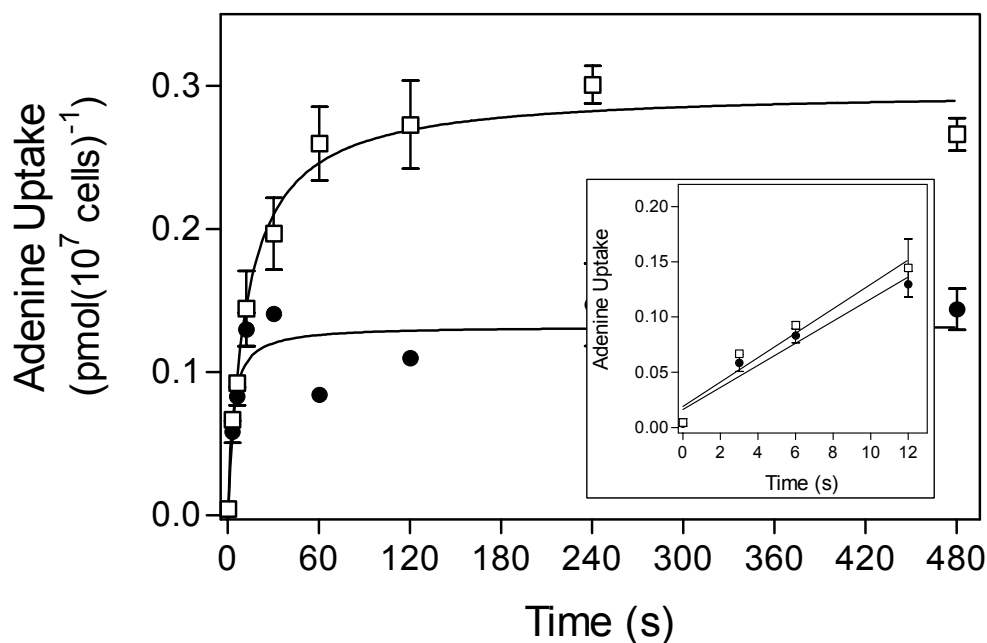


Figure 6.4: Purine transport in *P. falciparum* trophozoites lacking PfNT1 (Transport of 1  $\mu$ M [ $^3$ H]-adenine at 22 °C).

Transport of 1  $\mu$ M [ $^3$ H]-adenine at 22 °C in 3D7 $\Delta$ PfNT1-D6 is indicated with open symbols and in wild-type 3D7 parasites with closed symbols. Insert displays the linear phase of uptake ( $r^2 = 0.99$  for 3D7 $\Delta$ PfNT1-D6 and 0.98 for wild-type 3D7).

## 6.7 Low affinity adenosine transporter is not abolished in clone 3D7 $\Delta$ *PfNT1*-D6

Time dependent uptake of 25  $\mu$ M [ $^3$ H]-adenosine into saponin-freed *P. falciparum* trophozoites of clone 3D7 $\Delta$ *PfNT1*-D6, lacking PfNT1, or into wild-type 3D7 (control) parasites was also investigated. The high concentration of the permeant used in this experiment was supposed to saturate the high affinity transporter and thus permit the uptake rate of the low affinity adenosine transporter to be measured. Since previous experiments with wild-type parasites (chapter four) revealed a very rapid uptake rate of this transporter, and a very short period of linear uptake these experiments were performed at 6°C in order to slow down the rate of uptake and make it measurable.

The outcome of this experiment clearly shows that uptake of 25  $\mu$ M [ $^3$ H]-adenosine at 6 °C was not affected by the disruption of *PfNT1* in the parasite as identical rates of uptake were measured in clone 3D7 $\Delta$ *PfNT1*-D6 and the wild-type 3D7 (Figure 6.4). In contrast to the observations with the high affinity adenine transport activity, very similar overall uptake rates were achieved after 20 seconds in both parasite clones.

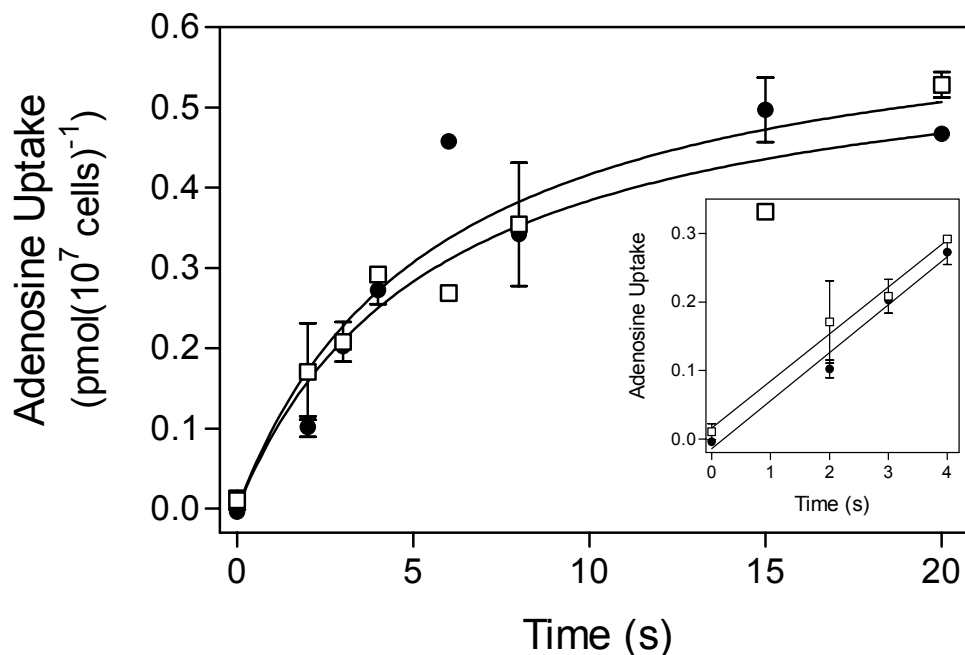


Figure 6.5: Purine transport in *P. falciparum* trophozoites lacking PfNT1 (Transport of 25  $\mu$ M [ $^3$ H]-adenosine at 6 °C).

Transport of 25  $\mu$ M [ $^3$ H]-adenosine at 6 °C in 3D7 $\Delta$ *PfNT1*-D6 is indicated with open symbols and in wild-type 3D7 parasites with closed symbols. Insert shows the linear phase of the uptake.

## 6.8 Sensitivity of parasites lacking PfNT1 to JA- and NA-compounds

Using an improved PicoGreen<sup>®</sup> method (see Chapter seven for details of the method), purine analogues, JA-32, JA-23, NA-130 and NA-137 were tested for activity against parasites of clone 3D7 $\Delta$ *PfNT1*-D6 and wild-type (3D7). Chloroquine was included in the assays as positive control. The assay was performed exactly as described in section 2.6. The compounds were tested over a concentration range of 0-500  $\mu$ M.

The result of the tests, which is presented in Table 6.1, shows apparent differences in sensitivity between wild-type parasites and parasites with a disrupted *PfNT1* for each of the compounds tested; the mean IC<sub>50</sub> values appear to be higher for the 3D7 $\Delta$ *PfNT1* clone, compared to the wild-type 3D7 control. However statistical analysis (unpaired t-test) of the results shows that with the exception of N-130, there was no significant difference between the two parasite types. Thus, the absence of the high affinity hypoxanthine/nucleoside transporter had no effect on the activity of these antiparasmodial purine analogues. Clearly, their activity did not primarily rely on entry through PfNT1. One trivial explanation would be that they are not substrates of the transporter. However, as their hydrophilicity is not compatible with passive trans-membrane diffusion at significant rates, they would have to be transported by one of the lower-affinity transporters. The fact that the *in vitro* antimalarial activity of the compounds is relatively low and, for NA-130 and NA-137, three orders of magnitude less than against *T. brucei*, is indeed consistent with an efficient uptake by *P. falciparum*. Overall, the JA-compounds had lower IC<sub>50</sub> values than the NA-compounds indicating a higher antimalarial activity *in vitro* in the former. There were some variability in the IC<sub>50</sub> values and this may probably account for the failure to observe a significant difference. Though statistical analysis shows a significant difference in the response of 3D7 $\Delta$ *PfNT1* clone and the 3D7 *P. falciparum* control to NA-130, the difference may not be biologically relevant as the difference is small.

Compound	Result	3D7 $\Delta$ PfNT1-D6	3D7 (wild type)	P value (paired student's t-test)
<b>JA-23</b>	Assay 1 ( $\mu$ M)	3.62	0.84	0.300631
	Assay 2 ( $\mu$ M)	2.46	-	
	Assay 3 ( $\mu$ M)	-	-	
	<b>Mean IC<sub>50</sub> (<math>\mu</math>M)</b>	3.0	0.84	
	<b>SEM</b>	0.6	ND	
<b>JA-32</b>	Assay 1 ( $\mu$ M)	1.8	1.72	ND
	Assay 2 ( $\mu$ M)	3.3	4.27	
	Assay 3 ( $\mu$ M)	4.86	1.66	
	<b>Mean IC<sub>50</sub> (<math>\mu</math>M)</b>	3.3	2.6	
	<b>SEM</b>	0.9	0.9	
<b>NA-130</b>	Assay 1 ( $\mu$ M)	102	64	0.041447
	Assay 2 ( $\mu$ M)	93.3	44.2	
	Assay 3 ( $\mu$ M)	169	155	
	<b>Mean IC<sub>50</sub> (<math>\mu</math>M)</b>	121.4	87.7	
	<b>SEM</b>	23.9	34.1	
<b>NA-137</b>	Assay 1 ( $\mu$ M)	98.5	77.5	0.172057
	Assay 2 ( $\mu$ M)	208	91.7	
	Assay 3 ( $\mu$ M)	196	199	
	<b>Mean IC<sub>50</sub> (<math>\mu</math>M)</b>	167.5	122.7	
	<b>SEM</b>	34.7	38.4	
<b>Chloroquine</b>	Assay 1 (nM)	9.8	2.29	0.104576
	Assay 2 (nM)	11.6	11.0	
	Assay 3 (nM)	11.6	12.10	
	Assay 4 (nM)			
	<b>Mean IC<sub>50</sub> (<math>\mu</math>M)</b>		8.5	
	<b>SEM</b>	3.3	2.2	

Table 6.1 : Sensitivity of *P. falciparum* clones 3D7 $\Delta$ PfNT1-D6 and wild type (3D7 clones of *P. falciparum*) to JA- and NA-compounds.

The values shown are the mean IC<sub>50</sub> ( $\mu$ M) from triplicate. The SEM represents standard error of mean, P values shown are from paired t-tests for each compound. ND=not done.

## 6.9 Discussion

The high affinity transport of adenosine and hypoxanthine present in the wild-type parasites was found to be completely absent in 3D7 $\Delta$ *PfNT1* parasites, whereas the low affinity transport of adenosine remained unchanged. Initial rates of transport for [ $^3$ H]-adenine uptake in the clone with a disrupted *PfNT1* and the wild-type 3D7 clone were also similar. These results strongly suggest that the disruption of the *PfNT1* gene only affected the high affinity hypoxanthine/nucleoside transport activities.

This finding is in agreement with a recently published independent report that disruption of the *PfNT1* gene renders the parasite incapable of completing the intraerythrocytic life cycle under standard purine level culture conditions (El Bissati *et al*, 2006). The report states that the  $\Delta$ *PfNT1* parasites (produced independently of this study, but using the same parental clone 3D7) could only grow in a medium supplemented with >10  $\mu$ M hypoxanthine, adenosine or inosine whilst the wild-type *P. falciparum* were able to grow in very low levels of purines (El Bissati *et al*, 2006). Observations reported in that study therefore provided indirect evidence that *PfNT1* is most likely to encode a high affinity purine transporter. Unfortunately, El Bissati and colleagues (El Bissati *et al*, 2006) did not perform studies to determine any kinetic characteristics, or the substrate selectivity profile of this important transporter.

The conclusion from our study, that *PfNT1* encodes a high affinity hypoxanthine/nucleoside transporter, is at odds with the previous reports of others that *PfNT1*, when expressed in *Xenopus laevis* oocytes, is a relatively low affinity transporter of hypoxanthine/nucleoside (Parker *et al*, 2000;Carter *et al*, 2000;Downie *et al*, 2006). It must however be stressed that the previous reports differed substantially from each (the reported  $K_m$  for the uptake of adenosine by the three groups ranges from 13 $\mu$ M to 1860 $\mu$ M) which appears to suggest that the *Xenopus* expression system produces inconsistent results when expressing *Plasmodium* transporters, perhaps as a result of interference by the vector's endogenous proteins, or the extremely high AT-content of the *Plasmodium* genome (Goman *et al*, 1982;Pollack *et al*, 1982;McCutchan *et al*, 1984;Musto *et al*, 1997) and the resultant different codon preferences of *Plasmodium* and *Xenopus*. Having said this, it must be added that the single amino acid difference observed between the two groups (phe vrs leu) could also have contributed to the significant difference in their results and

probably in addition to the difference in clones of parasites used in the two experiment (Carter and co used 3D7 and W2 whilst Parker and co used only 3D7).

In work published subsequent to the findings presented here, Downie and colleagues (Downie *et al*, 2006) studied adenosine transport using saponin-freed *P. falciparum*-parasites, rather than *Xenopus laevis* oocytes. However, they failed to detect the presence of a high affinity transport activity for adenosine. This can be explained if the high level of permeant (more than 10 $\mu$ M) used in the uptake assays saturated the high affinity transporter. Since low affinity transporters are functional even at high permeant concentrations, this became the sole transporter detected in that study.

To avoid making a similar mistake in this study, the concentration of the permeant used in the uptake assays (less than 0.5 $\mu$ M) was carefully chosen to prevent saturation of any high affinity transporter. In addition, to remove all ambiguity surrounding the outcome of investigations conducted in this study, the *PfNT1* gene of clone 3D7 (wild-type) was re-sequenced and was found to be 100% identical to the entry in PlasmoDB (PF13\_0252).

On the basis of the evidence gathered in this study, it is proposed that purine salvage in *P. falciparum* is based predominantly on the highly efficient uptake of hypoxanthine and purine nucleosides by PfNT1.

The related apicomplexan parasite *T. gondii* also expresses a high affinity transporter, TgAT2, with a  $K_m$  value of 0.49  $\mu$ M for adenosine and 0.77  $\mu$ M for inosine (de Koning *et al*, 2003). However unlike *P. falciparum*, *T. gondii* expresses a separate high affinity transporter for oxopurine nucleobases, TgNBT1, which, in direct parallel with *P. falciparum*, does not transport adenine (de Koning *et al*, 2003). For both apicomplexan parasites, the expression of a high affinity purine transporter would seem essential, as their environment, within the host cell, is unlikely to contain a high level of free purine (Ngo *et al*, 2000) and nucleotides cannot be directly salvaged across the parasite plasma membrane.

An interesting observation made in this study is the relatively high uptake of 1  $\mu$ M [ $^3$ H]-adenine into 3D7 $\Delta$ *PfNT1* parasites compared with wild-type 3D7 parasites after the linear phase; the difference in uptake during this phase was approximately doubled in 3D7 $\Delta$ *PfNT1* parasites. This phenomenon may reflect an adaptation by the 3D7 $\Delta$ *PfNT1* parasites to compensate for the loss of the high affinity hypoxanthine/nucleoside transport

activity. As the initial rates of [ $^3\text{H}$ ]-adenine transport were identical in the wild-type and gene-disrupted clones, this would seem to reflect increased metabolism of adenine rather than an upregulation of purine transport activity induced by lack of a purine source, as documented for other protozoan species including *Crithidia fasciculata* and *T. brucei* [reviewed by de Koning and co-workers (de Koning *et al*, 2005)].

## 6.10 Conclusion

Data gathered in this study provide compelling evidence that the protein encoded by *PfNT1* is responsible for the high affinity uptake of hypoxanthine/nucleoside in isolated *P. falciparum* trophozoites. There was an apparent increase in the uptake of adenine into *P. falciparum* clones lacking *PfNT1*, presumably to compensate for the loss of high affinity hypoxanthine salvage.



## **CHAPTER SEVEN**

### **7 Development of an improved microfluorimetric method for *in vitro* assessment of the susceptibility of *P. falciparum* to purine antimetabolites**

## 7.1 Summary

A major objective of this study was the assessment of purine analogues for antiplasmodial activities using an appropriate *in vitro* drug sensitivity method. For various reasons, discussed below, the traditional microscopic assay and the [ $^3\text{H}$ ]-hypoxanthine incorporation methods are unsuitable for use in such experiments. A published microfluorimetric assay that used PicoGreen<sup>®</sup> dye to stain parasite DNA followed by fluorimetric analysis for assessment of parasite growth *in vitro* was thought to be more appropriate for drug sensitivity assays of purine analogues. However, in an attempt to validate the published PicoGreen<sup>®</sup> method, it was discovered that the haemoglobin present in cultures of *P. falciparum*-infected erythrocytes quenched the fluorescence signal, thereby dramatically reducing the sensitivity of the assay and thus limiting its usefulness. In order to resolve this problem, a new procedure was developed, which incorporates additional steps to remove the interfering haemoglobin. Lysing of the red blood cells in the culture with saponin, followed by washes with PBS led to the restoration of PicoGreen<sup>®</sup> fluorescence. Susceptibility to chloroquine and pyrimethamine of 3D7 and K1 laboratory lines of *P. falciparum* were tested using the improved PicoGreen<sup>®</sup> method in parallel with the traditional [ $^3\text{H}$ ]-hypoxanthine incorporation method. The  $\text{IC}_{50}\text{s}$  obtained with both methods were observed to be similar, indicating that the new improved PicoGreen<sup>®</sup> method could be a good substitute for the [ $^3\text{H}$ ]-hypoxanthine uptake method for the assessment of parasite susceptibility to purine antimetabolites. With the improved PicoGreen<sup>®</sup> method, the antimalarial activity of a small library of purine analogues was evaluated. The outcome of this screening suggests that some purine analogues could serve as lead compounds towards the development of a purine-based antimalarial therapy.

## 7.2 Introduction

The recent upsurge in drug resistant *P. falciparum* malaria has necessitated the search for safe and effective antimalarial drugs (Rieckmann, 1983), particularly those that would exploit the unique metabolic pathways of the parasite. In view of this, the purine salvage system in the parasite was considered an important drug target. This is because the parasites lack the ability to synthesise purines *de novo* and have to salvage the nutrients from the host through transporters (Sherman, 1979). It was therefore expected that blockage of purine salvage would adversely affect parasite growth. With the purine salvage activities in *P. falciparum* fully characterized in this study (see chapter four), the available information on the kinetic properties of the transporters should facilitate the development of rational purine-based chemotherapy of malaria. The main objective of this part of the study was therefore to develop a high-throughput *in vitro* method to be used to evaluate purine-based analogues as potential antimalarial drugs.

Various methods exist for screening novel compounds for antimalarial activities. The ‘gold standard’ microscopy method is often laborious and needs an experienced microscopist (WHO, 1990). Another popular method is the radio-isotopic test, which measures the incorporation of  $^3\text{H}$ -hypoxanthine into the nucleic acids of viable parasites (Desjardins *et al*, 1979). The obvious disadvantage of this method is the requirement for the use and disposal of radiolabelled material. Additionally, the isotopic method is not suitable for assessing purine antimetabolites because of the presence of the nucleobase in the radiolabel compound, which may impact directly on purine metabolism in the parasites and thus compromise the results. Due to the shortcomings of these methods other methods for assessing purine-based compounds were considered. This led to the identification of a novel microfluorimetric method using PicoGreen<sup>®</sup> dye to stain parasite DNA (Corbett *et al*, 2004). The authors demonstrated that PicoGreen<sup>®</sup> was able to detect as little as 25 pg/ml of dsDNA in the presence of ssDNA, RNA, and free nucleotides (Corbett *et al*, 2004). Replication of malaria parasites in culture was found to be directly proportional to the amount of PicoGreen<sup>®</sup> fluorescence, with a linear relationship observed between 0.1% and 15% parasitaemia.

The microfluorimetric method was therefore considered as the most appropriate for the evaluation of purine antimetabolites. However, in an attempt to use this method as published (Corbett *et al*, 2004), it was observed that the presence of blood in the parasite

culture quenched the fluorescence of PicoGreen<sup>®</sup>. Even at a low haematocrit of 0.5%, the effect was severe. Haemoglobin is known to absorb light over a very broad range of wavelengths including the emission and excitation wavelengths of PicoGreen<sup>®</sup>.

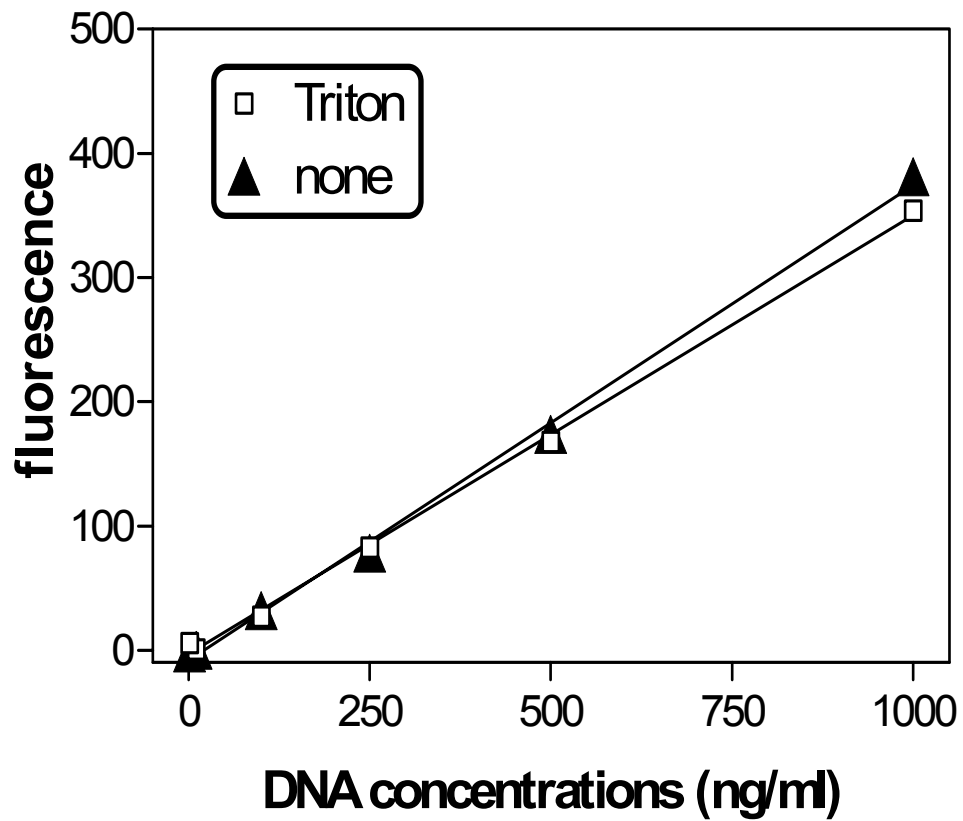
To overcome this problem, additional steps were introduced to remove the probable interfering compound. This was achieved through lysis of the RBC using saponin, followed by a series of washes with 1×PBS. By this process the fluorescence of PicoGreen<sup>®</sup> was easily detectable and the assay became a highly sensitive and reproducible tool for assessing the efficacy of antimalarial drugs. The IC<sub>50</sub> values of some antimalarial drugs obtained with the improved PicoGreen<sup>®</sup> method were compared with that obtained with the traditional [<sup>3</sup>H]-hypoxanthine incorporation method.

Guided by the kinetic information in chapter four of this thesis some purine analogues were carefully selected from the library of Dan Brown, the MRC Laboratory of Molecular Biology, Cambridge, UK and Gerrit-Jan Koomen, University of Amsterdam, The Netherlands. *In vitro* antimalarial potential of the analogues were determined using the improved PicoGreen<sup>®</sup> method.

### 7.3 PicoGreen<sup>®</sup> fluorescence is directly proportional to DNA concentration

In order to confirm the relationship between fluorescence of PicoGreen<sup>®</sup> and the DNA concentration reported in literature (<http://www.probes.com/media/pis/mp07581.pdf>; Corbett *et al.*, 2004), a concentration range of 1 ng/mL to 1000 ng/mL salmon sperm DNA (Sigma-Aldrich, Poole, UK) was prepared by serial dilution with nucleic acid- and DNase-free water (ICN). One hundred and fifty microlitres of each dilution were dispensed into wells of a 96-well microtitre plate (Greiner Bio-One) followed by the addition of 50 µl lysis/fluorescence-mix consisting of PicoGreen<sup>®</sup> (1:200 in TE buffer, pH 7.5) and Triton X-100 (final concentration, 2%) in nucleic acid- and DNase-free water. After incubation of the plate in the dark at room temperature for up to 30 minutes, fluorescence intensity was measured at 485 nm (Excitation) and 528 nm (Emission) using a Perkin Elmer LS 55 Luminescence Spectrophotometer. Control wells were set up on each plate. The control wells consisted of the highest concentration of salmon sperm DNA solution without PicoGreen<sup>®</sup> or lysis/fluorescence-mix alone in nucleic acid- and DNase-free water respectively. The mean background reading from the two control wells was subtracted from the test fluorescence reading to give the final fluorescence measurement. Fluorescence readings, which consisted of arbitrary units ranging from 1 to 1000, were plotted against salmon sperm DNA concentrations. The experiment was repeated in the absence of Triton X-100 from the lysis/fluorescence mix. All experiments were performed in triplicate and repeated in three independent experiments.

Observations made in this experiment showed a linear relationship between PicoGreen<sup>®</sup> fluorescence and salmon sperm DNA concentration (Figure 7.1). This observation is consistent with that reported by Corbett and colleagues in 2004 (Corbett *et al.*, 2004). It was further observed that the presence of 2% Triton X-100 in the fluorescence-mix did not significantly change the slope of the line (P-value from student's t-test = 0.481), implying that the fluorescence signal from the DNA- PicoGreen<sup>®</sup> interaction was not affected by the presence of Triton X-100.



	Triton	none
$r^2$	0.9983	0.9975

Figure 7.1: Relationship between PicoGreen® fluorescence and salmon sperm DNA.

The figure shows the relationship between PicoGreen® fluorescence and salmon sperm DNA in the presence (open squares) or absence (black triangles) of 2% Triton X-100. Background fluorescence, defined as fluorescence detected in the absence of added DNA, was subtracted from each data point. Fluorescence is measured as arbitrary units (A.U.). Data shown are the mean of 3 independent determinations. The box below the graph shows the  $r^2$  value for linear regression line obtained using Prism 4.

## 7.4 Blood quenches fluorescence of PicoGreen®

Following direct lysis of parasitized erythrocytes as described by Corbett and colleagues (Corbett *et al*, 2004), at best a very low level of PicoGreen® fluorescence was detected from wells containing *P. falciparum*-infected erythrocytes with haematocrit in the range of 0.5 – 5% and up to 10% parasitaemia. Since this observation was unexpected, further investigations were conducted to identify the factor responsible for the quenching of PicoGreen® fluorescence. Non-infected blood was therefore diluted to give a range of haematocrits from 0.5 to 5% and samples were spiked with salmon sperm DNA at a fixed concentration of 1000 ng/ml. One hundred and fifty microlitres each of the mixtures were dispensed into the wells of an opaque 96-well microtitre plate. A volume of 50 µL of the lysis/fluorescence mix was added and the fluorescence signal determined as usual (described in section 7.3). The fluorescence readings were plotted against percent haematocrit. Negative control wells consisted of 150 µl blood at 1.0% haematocrit but without salmon sperm DNA, whilst the positive control wells consisted of 150 µl of salmon sperm DNA (1000 ng/ml) without blood. The negative control wells gave a background reading of 11.4 arbitrary fluorescence units (Table 7.1). No fluorescence signal above background was obtained for any of the samples containing blood with haematocrit range 0.5-5%. The positive control gave a fluorescence reading of 400 AU.

Haematocrit	Fluorescence reading (AU)
0.5%	8.43
2%	8.59
3%	7.14
4%	7.02
5%	7.91
Negative control	11.4
Positive control	400

**Table 7.1** Fluorescence intensity reading for blood of haematocrit 1 - 5% spiked with 1000 ng/ml salmon sperm DNA.

The control consisted of 1.0% haematocrit blood in lysis/fluorescence-mix without salmon sperm DNA.

The result obtained from this investigation clearly showed that blood, or at least one of its constituents, quenches the fluorescence of PicoGreen<sup>®</sup>. It appears that that haemoglobin with its red pigment absorb most, if not all, of the fluorescence emitted by PicoGreen<sup>®</sup> (see absorbtion spectra in Figure 7.2). Attempts to solubilise and precipitate the haemoglobin with a cocktail of 5 parts of quaternary ammonium hydroxide, 2 parts 30% hydrogen peroxide and 2 parts glacial acetic acid, as reported by Biagini and colleagues (Biagini *et al*, 2004), did not reverse the observed quenching of PicoGreen<sup>®</sup> fluorescence. Furthermore, varying the emission and excitation wavelength did not improve the detection of the fluorescence signal.

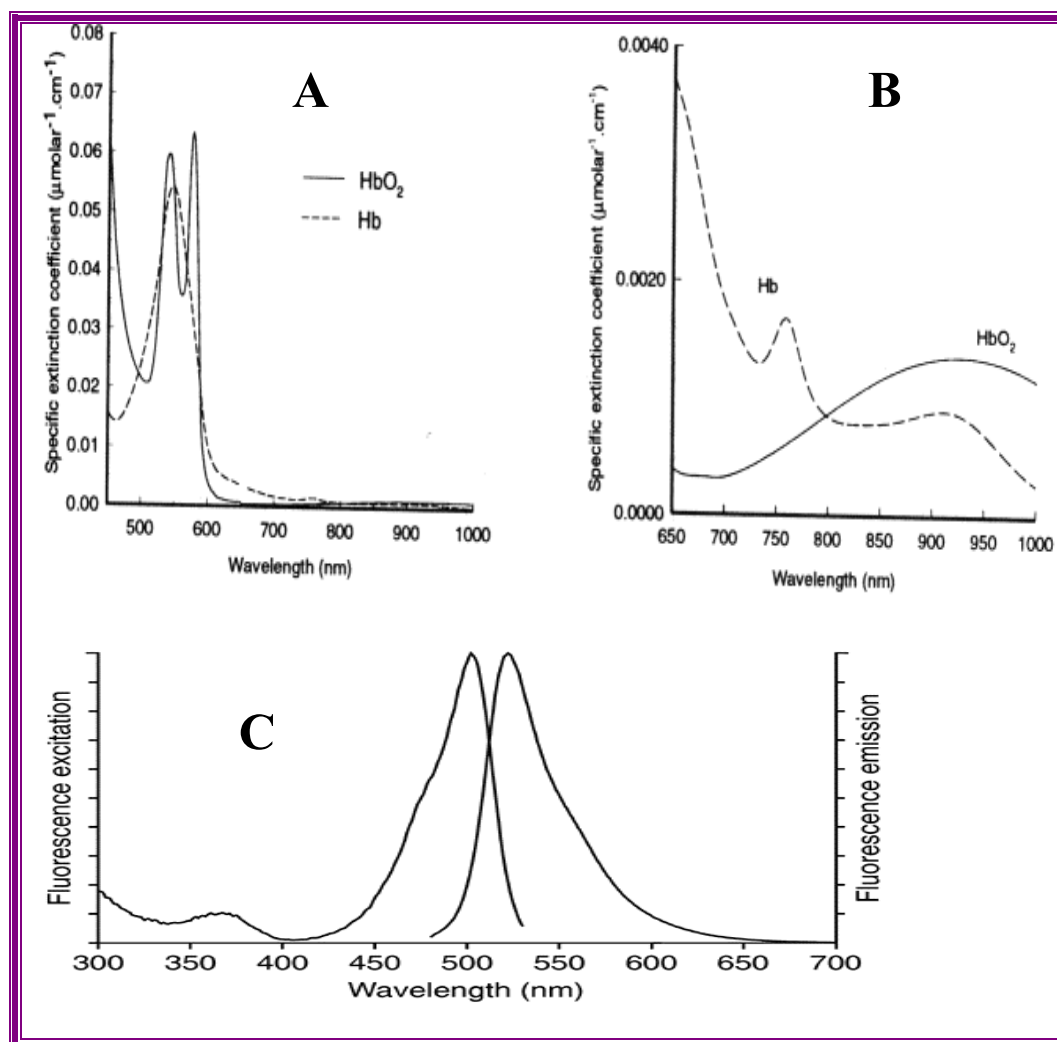


Figure 7.2: The absorption spectra of oxygenated haemoglobin and deoxy haemoglobin. The figures marked A or B shows the absorption spectra of oxygenated haemoglobin (HbO<sub>2</sub>) and deoxyhaemoglobin (Hb) in the wavelength range 450 - 1000 nm. (Source: [http://www.medphys.ucl.ac.uk/research/borg/research/NIR\\_topics/nirs.htm](http://www.medphys.ucl.ac.uk/research/borg/research/NIR_topics/nirs.htm)). The figure marked C shows the emission and excitation spectra of PicoGreen<sup>®</sup> (<http://probes.invitrogen.com/servlets/spectra?fileid=7581dna>).



## 7.5 Reversing the quenching effect of blood on PicoGreen® fluorescence by saponin treatment

In order to overcome the quenching of PicoGreen® fluorescence, the method described by Corbett and colleagues (Corbett *et al*, 2004) was modified. The modification involves additional steps to remove the haemoglobin suspected to be responsible for the quenching of the PicoGreen® fluorescence. A suspension of asexual parasites of *P. falciparum* clone 3D7 in a 2% haematocrit culture was serially diluted with uninfected erythrocytes (at 2% haematocrit) to yield parasitaemias of 0.5% to 15%. One hundred and fifty microlitres of each parasite concentration were dispensed into wells of two sets of microtitre plates. One set of the plates was processed to remove the haemoglobin as follows: (i) the microtitre plate containing the culture was centrifuged at  $500 \times g$  to pellet the cells; (ii) the supernatant was removed and the pellets were resuspended in saponin (0.15%, w/v) to lyse the erythrocytes and release the haemoglobin; (iii) the plate was centrifuged at  $500 \times g$  to sediment the parasites, and the supernatant was removed and discarded; (iv) traces of haemoglobin were removed through three washes with  $1 \times$  PBS; (v) The cell pellet was finally re-suspended in  $150 \mu\text{l}$   $1 \times$  PBS. The second set of plates remained untreated with saponin. Fifty microlitres of the lysis/fluorescence-mix was added to each well on the two sets of plates. The plates were incubated as previously in the dark at room temperature for 30 minutes. Measurement of fluorescence signals at 485 nm (Excitation) and 528 nm (Emission) was then performed as previously described. Fluorescence reading was plotted against parasitaemia for each of the two sets of plates.

After saponin treatment of parasite-infected erythrocytes, PicoGreen® fluorescence was restored, and a linear relationship was established between fluorescence of the dye and parasitaemia (Figure 7.2). The mean fluorescent signal obtained following saponin treatment was significantly different from that obtained in the untreated cultures (Student's t-test,  $P = 0.0009$ ).

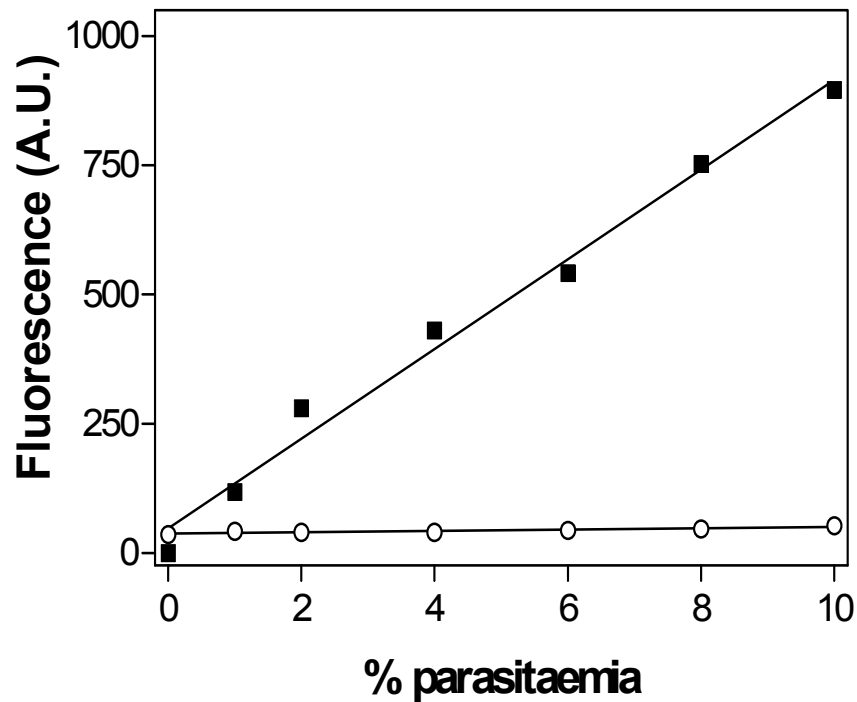


Figure 7.3: Effect of saponin treatment on PicoGreen® fluorescence.

PicoGreen® fluorescence is shown following saponin treatment of the parasite culture, followed by washing to remove haemoglobin (■), or with no saponin treatment (○), Parasitaemia was 1 - 10%. Background fluorescence was subtracted from each point. Lines were calculated by linear regression. The slope of the line for fluorescence in the absence of saponin treatment was significantly different from zero ( $P = 0.005$ ; F-test), but was only 1.5% of the slope for fluorescence after removal of haemoglobin ( $87 \pm 4$  versus  $1.3 \pm 0.3$  A.U.(% parasitaemia)<sup>-1</sup>).

## 7.6 Comparison of the improved PicoGreen® method with [<sup>3</sup>H]-hypoxanthine uptake method

Two culture-adapted standard laboratory lines of *P. falciparum*, 3D7 and K1, were tested for their sensitivity to chloroquine and pyrimethamine using the modified PicoGreen® method in parallel with the traditional [<sup>3</sup>H]-hypoxanthine accumulation test. The two selected parasite lines were known to differ in their sensitivity to antimalarial drugs *in vitro*: clone 3D7 is sensitive to chloroquine and pyrimethamine (Walliker *et al*, 1987) whilst K1 is resistant to both drugs (Thaithong, 1983).

Parasites were maintained in continuous culture using standard methods (Trager & Jensen, 1976; Haynes *et al*, 1976). Cultures used for the drug sensitivity assay contained predominantly ring-stages of the parasites. In some cases cultures were naturally synchronous, otherwise they were synchronized by brief incubation with 5% aqueous D-sorbitol using the standard method (Lambros & Vanderberg, 1979). All drug sensitivity assays were performed in 96-well microtitre plates using the method described by Rieckmann and others (Rieckmann *et al*, 1978). Briefly, stocks of drugs were prepared initially in DMSO and then diluted serially with incomplete RPMI 1640 culture medium to achieve the desired concentration range. The final drug concentrations were 3.8 nM - 500 nM for chloroquine (prepared from chloroquine sulphate, May and Baker, England), and 15.6 nM - 2000 nM for pyrimethamine. The pyrimethamine was a gift from Prof. David Walliker (University of Edinburgh) to Dr Lisa Ranford-Cartwright (University of Glasgow). Each well of a microtitre plate was pre-dosed with 50 µl of the appropriate drug solution. Parasite cultures were diluted with fresh uninfected erythrocytes and RPMI 1640 culture medium to achieve a starting parasitaemia of 0.5-1.0% and haematocrit of 2%. Two hundred microlitres of the diluted parasite culture were added to each well of the pre-dosed plates. Control wells consisted of 50 µl culture medium without drugs (but containing the same amount of DMSO as in drug wells) and 200 µl parasitized or uninfected erythrocytes. The plates were incubated at 37 °C for 42-48 hours in a modular incubator (FlowLabs), gassed with a mixture of 3% CO<sub>2</sub>, 1% O<sub>2</sub>, 96% N<sub>2</sub>.

For each test performed using the microfluorescence method, a second plate was set up for determination of IC<sub>50</sub> by the [<sup>3</sup>H]-hypoxanthine incorporation method. With regard to the isotopic method, cultures were initially plated as described and incubated at 37 °C for an

initial period of 24 hours. This was followed by the addition of 10  $\mu\text{l}$  of 1.87  $\mu\text{M}$  [ $^3\text{H}$ ]-hypoxanthine with a specific activity of 37 GBq/mmol (Amersham Biosciences) to each well, and a further incubation for 24 hours. The cells were then harvested from each well onto a fibreglass filter paper using a Filtermate Harvester (Packard Instruments). The filter paper was dried, sealed in a plastic bag and 3 ml scintillation fluid (OptiPhase HiSafe (Perkin Elmer)) added. Radioactivity incorporated into the parasites was counted with a Microbeta Wallac Trilux liquid scintillation and luminescence counter.

The  $\text{IC}_{50}$  value, representing 50% inhibition of uptake of [ $^3\text{H}$ ]-hypoxanthine, was determined from a non-linear regression analysis of log drug concentration against radiolabel incorporated into the parasites (Figure 7.4 and Figure 7.5). The  $\text{IC}_{50}$  value for chloroquine and pyrimethamine obtained using the PicoGreen<sup>®</sup> method was compared with the equivalent value determined using the traditional [ $^3\text{H}$ ]-hypoxanthine incorporation method. The overall results, which are shown in Table 7.2, indicate no statistically significant difference (Student's t-test;  $P > 0.05$ ) in the  $\text{IC}_{50}$  values using the two methods.

Parasite	Mean IC <sub>50</sub> values in nM (s.e.m.)			
	Drug	PicoGreen	[ <sup>3</sup> H]-hypoxanthine	P-value
3D7				
	Chloroquine	6.3 (0.39)	7.2 (1.05)	0.468
	Pyrimethamine	38.6 (7.6)	47.4 (9.6)	0.508
K1				
	Chloroquine	141 (29.4)	128 (7.4)	0.693
	Pyrimethamine	295 (115.2)	437 (133.4)	0.466

**Table 7.2 Mean  $\text{IC}_{50}$  values for chloroquine and pyrimethamine determined by the PicoGreen<sup>®</sup> or [ $^3\text{H}$ ]-hypoxanthine accumulation assay.**

Mean  $\text{IC}_{50}$  values for chloroquine and pyrimethamine were determined by the PicoGreen<sup>®</sup> or the [ $^3\text{H}$ ]-hypoxanthine accumulation assay for two laboratory lines of *P. falciparum*, 3D7 and K1. Data are the means of 3 independent determinations, and standard error of the mean (s.e.m.) in brackets. P-values were obtained from Student's t-test comparisons of  $\text{IC}_{50}$  values obtained for the two methods.

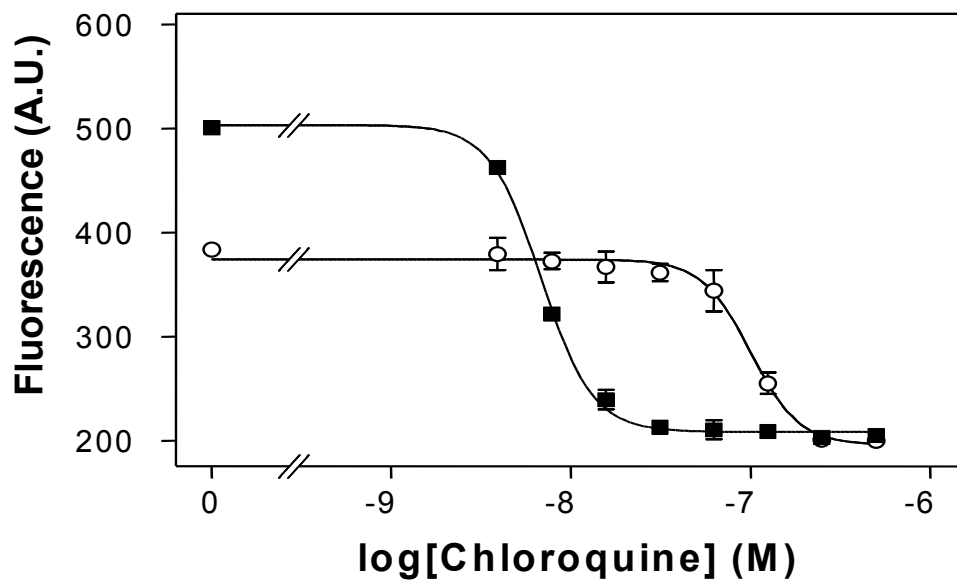


Figure 7.4: Representative graph showing chloroquine responses of *P. falciparum* lines obtained with the improved PicoGreen® method.

A typical sigmoidal graph showing the responses of *P. falciparum* lines 3D7 (■) and K1 (○) to different concentrations of chloroquine obtained with the improved PicoGreen® method. Each data point is the mean of two wells.

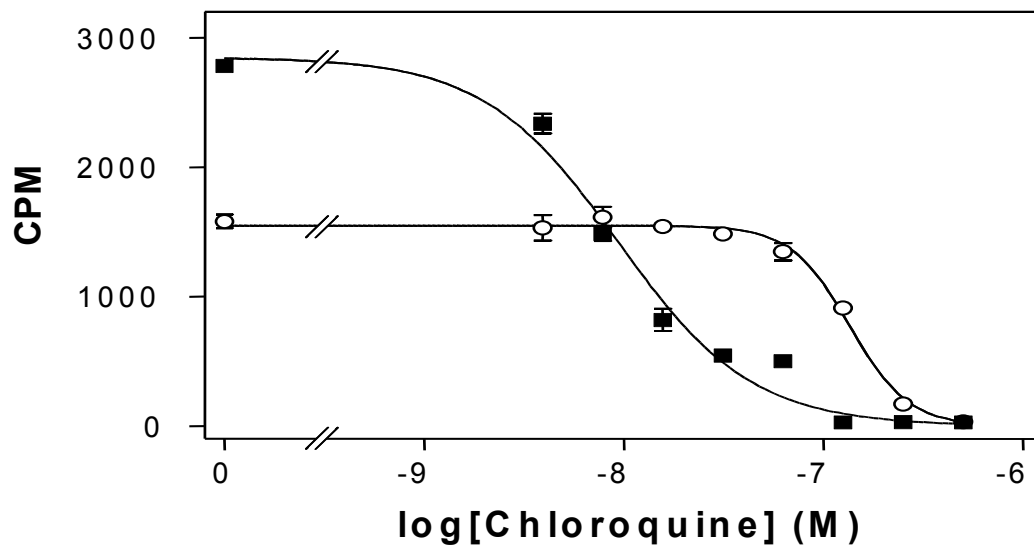
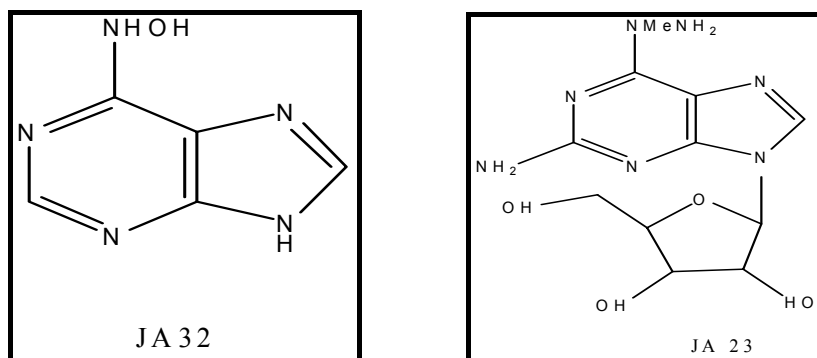


Figure 7.5: Representative graph showing chloroquine responses of *P. falciparum* lines obtained with the traditional [<sup>3</sup>H]-hypoxanthine incorporation method.

A typical sigmoidal graph showing the responses of *P. falciparum* lines 3D7 (■) and K1 (○) to different concentrations of chloroquine obtained with the traditional [<sup>3</sup>H]-hypoxanthine incorporation method. Each data point is the mean of two wells.

## 7.7 Test of purine analogues for antiplasmodial activities using the improved PicoGreen<sup>®</sup> method

The anti plasmodial activity of novel purine analogues synthesized at the Medical Research Council, Cambridge, and the University of Amsterdam, were investigated using the improved PicoGreen<sup>®</sup> method. The JA series of compounds (obtained from Dan Brown, the MRC Laboratory of Molecular Biology, Cambridge, UK and the NA-series of compounds (obtained from Gerrit-Jan Koomen, University of Amsterdam, The Netherlands) are analogues of purine nucleosides or nucleobases, with substitutions at various positions. Compound JA-23 is an N6-substituted analogue of 2,6-diaminopurine riboside and compound, JA-32, is N6-hydroxyadenine and is a substituted adenine analogue. Of all the purine compounds tested JA-32 is the closest to hypoxanthine by structure. Some of the compounds and their structures are shown in Figure 7.6.



**Figure 7.6: Structures of the purine analogues designated JA-32 and JA-23.**

These purines were received from Dan Brown, the MRC Laboratory of Molecular Biology, University of Cambridge.

A 40mM stock solution of each compound was prepared by dissolving the powder in 100% dimethylsulfoxide (DMSO, Sigma). Working solutions were prepared from the stock with incomplete RPMI 1640. From the working solutions, a concentration range of the compounds was prepared by serial dilution. Fifty microlitres of each concentration of the drug (JA- NA- compounds) were dispensed into each well, followed by the addition of 200 ml of *P. falciparum* culture to give a final parasitaemia of 0.5%, haematocrit of approximately 2% and DMSO concentrations  $\leq 0.01\%$ . The final concentration range of the compounds in the wells was 0.78-200  $\mu\text{M}$ . Control wells consisted of 50 ml culture medium without drugs (but contained the same amount of DMSO as in drug wells) and

200  $\mu$ l of parasitised or uninfected erythrocytes. A dilution series of chloroquine sulphate, at a final chloroquine concentration range of 3.9 – 500 nM, was included on each plate as a control. The plates were incubated at 37°C for 42 – 48 hours in a modular incubator, gassed with a mixture of 3% CO<sub>2</sub>, 1% O<sub>2</sub>, 96% N<sub>2</sub>. The plates were processed using the improved PicoGreen<sup>®</sup> method, and the IC<sub>50</sub> values determined appropriately. A representative curve obtained with these drugs is shown in Figure 7.7. A summary of the IC<sub>50</sub> values for JA- and NA-compounds is shown in Table 7.3. Generally, the JA-compounds were observed to have higher antiplasmodial activity than the NA-compounds.

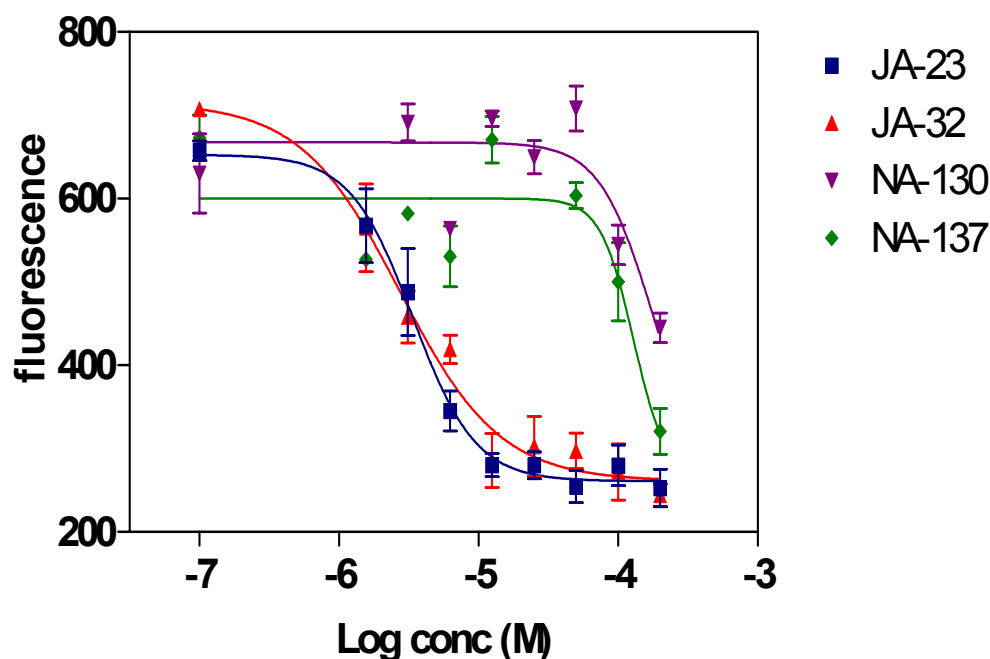


Figure 7.7: Representative graph showing the response of *P. falciparum* 3D7 clone to purine analogues.

The figure shows the responses of *P. falciparum* 3D7 clone to purine analogues JA-23 (■), JA-32 (▲), NA-130 (▼) and NA-137 (◆) obtained with the improved PicoGreen<sup>®</sup> method. Each data point is the mean of triplicate determinations and the error bars show the standard error of the mean.

---

Compound	Mean IC <sub>50</sub> ± S.E.M
JA-23	6.0 ± 2.4 µM
JA-32	2.0 ± 0.2 µM
NA-130	112.6 ± 33.9 µM
NA-137	112.9 ± 20 µM

---

Table 7.3: *In vitro* antiparasmodial activity of purine analogues against *P. falciparum* clone 3D7 using the improved PicoGreen® method.

IC<sub>50</sub> values presented are mean ± SEM of 3-4 determinations.



## 7.8 Discussion

It is important to have a suitable method for assessing the potential of purine analogues as antimalarial drugs. Since the popular isotopic method using [ $^3\text{H}$ ]-hypoxanthine is unsuitable for assessment of purine nucleobases, the microfluorimetric method using PicoGreen<sup>®</sup> became the method of choice in this study. The PicoGreen<sup>®</sup> method seems to offer advantages over some of the existing methods, especially as it is devoid of issues concerning detection, storage and waste disposal of radioactive compounds.

The outcome of a preliminary test using the PicoGreen<sup>®</sup> method showed a linear relationship between fluorescence of PicoGreen<sup>®</sup> and salmon sperm DNA concentration, with a clear signal from as little as 1 ng/ml DNA resuspended in PBS. However, the presence of uninfected erythrocytes, even at low haematocrit levels, abolished the fluorescence seen with salmon sperm DNA. Similarly, the fluorescence signal was barely detectable from cultures of *P. falciparum*-infected erythrocytes, even at high levels of parasitaemia. This phenomenon was attributable to the quenching of PicoGreen<sup>®</sup> fluorescence by haemoglobin, as the emission spectra for PicoGreen<sup>®</sup> and the absorption spectra for haemoglobin overlap in the relevant wavelengths (Figure 7.2).

Based on these observations, the method was modified to include removal of the haemoglobin using saponin lysis of the erythrocyte followed by washing with PBS to remove the released haemoglobin. Fluorescence of the dye was thus restored and a linear relationship between fluorescence and percent parasitaemia was established. This linearity was reliable between 0.5 – 15% parasitaemia and was not affected by the synchronicity of the culture. The method thus facilitates the evaluation of the antiplasmodial activities of potential new chemotherapeutic compounds.

Using the improved PicoGreen<sup>®</sup> method, the IC<sub>50</sub> values of chloroquine and pyrimethamine against *P. falciparum* laboratory lines 3D7 and K1 were determined and compared with those obtained using the isotopic method with [ $^3\text{H}$ ]-hypoxanthine. The IC<sub>50</sub> values obtained by the two methods were statistically identical and consistent with literature values. The PicoGreen<sup>®</sup> method is not technically demanding, though caution must be exercised during the removal of the supernatant after saponin lysis or during

washing with PBS, in order not to lose part of the parasite pellet. The procedure lends itself well to scaling up and gives clear, accurate and indisputable results.

The characterisation of the transporters of purines in *P. falciparum*, reported in chapter four of this thesis, paves the way for an intensive search of purine analogues as antimalarial drug candidates. Four transporters were found to be present in the parasite, and PfNT1 appears to be the most important. The presence of a high affinity hypoxanthine/nucleoside transporter in the parasite's plasma membrane can therefore be exploited for the efficient and selective targeting of purine antimetabolites. Interestingly, the outcome of a preliminary evaluation of hypoxanthine-like analogues received from the small libraries of a collaborator, Dan Brown, the MRC Laboratory of Molecular Biology, Cambridge, gave a promising results and confirmed the fact that PfNT1 can indeed be a good conduit for purine-based antimalarial drugs. Additionally, specific blockers of PfNT1, particularly those whose action may be non-competitive in nature, might make successful antimalarials, as PfNT1 is essential for growth under conditions of physiologically normal purine concentrations (El Bissati *et al*, 2006). It must however be emphasised that the presence of multiple transporters for purine salvage in *P. falciparum* poses a potential problem for the latter strategy, since there is the possibility of upregulation of the other transporters in compensation for the inhibition of purine uptake through PfNT1.

## 7.9 Conclusion

This study establishes the value of the microfluorimetric method using PicoGreen<sup>®</sup> dye for *in vitro* drug sensitivity testing of *P. falciparum*. IC<sub>50</sub> values obtained using the improved PicoGreen<sup>®</sup> method developed in this study were comparable with those of the traditional isotopic method for two different drugs (chloroquine or pyrimethamine) and two distinct parasite lines (3D7 or K1). Being simple and reliable, the modified PicoGreen<sup>®</sup> method should facilitate the screening of purine analogues for antiparasmodial activities. With the purine salvage mechanisms in *P. falciparum* parasites unveiled, it is now time to pursue a systematic purine-based antimalarial chemotherapy of malaria.

## **CHAPTER EIGHT**

### **8 General Discussion**

Purine nucleosides and nucleobases are essential to the malaria parasite as they form the basic constituents of nucleic acid and other important biomolecules. Since the parasite lacks the ability to synthesise these purines *de novo*, it has to rely solely on the host's purine for survival and proliferation (El Bissati *et al*, 2006). Although it is known that uptake of purine from the host milieu into the parasite is through specialized transporters, the exact mechanism involved in this salvage is not well understood. Information available on the kinetic properties of the parasite's purine transporters is shrouded in confusion and controversies. The availability of accurate and reliable information on the functional properties of purine transporters in *P. falciparum* should facilitate the development of a rational purine-based chemotherapy of malaria. The main aim of this project, therefore, was to provide detailed information on the kinetic characteristics of the transporters involved in purine salvage in *P. falciparum*, using biochemical and molecular methods.

Earlier studies on purine metabolism in malaria parasites were performed in the avian parasite, *P. lophurae* (Tracy & Sherman, 1972) and the rodent malaria, *P. berghei* (Hansen *et al*, 1980). In the year 2000, a gene encoding a purine transporter in *P. falciparum* was cloned and characterised after expression in *Xenopus laevis* oocytes. The investigations, carried out simultaneously by two independent groups of researchers, led to the identification of a low affinity adenosine transporter, denoted *PfNT1* or *PfENT1* (Parker *et al*, 2000; Carter *et al*, 2000). The *Xenopus* oocyte system has been widely used and accepted as a valuable tool for the expression of transporters and yielded highly valuable data on human transporters (Griffith & Jarvis, 1991; Wright *et al*, 2002; Beene *et al*, 2003). However, as is true with any heterologous expression system, the functional properties of the expressed proteins may be affected by the activities of indigenous proteins, codon preferences, post-translational modifications or membrane composition. It was thus reasoned that, since it has now become possible to study transport phenomena in the intact *P. falciparum* parasite, a study using freed (isolated) parasites would be complementary to the previous studies and secure accurate data of the kinetic characteristics of all the purine transporters expressed in the trophozoite stage.

## 8.1 Purine transport activity in *P. falciparum* parasites with intact erythrocyte membranes

In *P. falciparum* infected red blood cells, the growing parasite requires purines for the synthesis of important biomolecules. Although it has previously been suggested that movement of nutrients into parasitized red blood cell was through the New Permeation pathway (NPP) [(Gero *et al*, 1999)], data obtained from the current study clearly showed that uptake of purines into the infected erythrocyte cytosol was through the host nucleoside and nucleobase transporters, hFNT1 and hENT1. Hypoxanthine and adenine appear to cross the erythrocyte membrane mainly through the hFNT1 and nucleosides such as adenosine entered predominantly through the hENT1. The evidence for these assertions is based on observations (section 3.3) showing that adenosine uptake into the parasitised erythrocytes was not inhibited by furosemide, which is a known inhibitor of the NPP (Kirk, 2001). The observed free flow of purine into infected cells, even in the presence of high concentrations of furosemide, suggests that the NPP is not involved in nucleoside and nucleobase salvage in parasitised RBC. The NPP has also been reported to be non-saturable (Kirk, 2001), yet purine transport into the parasitised RBC as observed in the current study, was clearly saturable with 1mM permeant.

As reported in chapter three, the rate of adenosine uptake into *P. falciparum*-infected human RBC was approximately two fold higher than that of hypoxanthine. If hypoxanthine is, as reported, the preferred purine source for malaria parasites, it might be expected to have the highest rate of uptake. However, adenosine can easily be converted enzymatically to hypoxanthine, and the enzymes required, adenosine deaminase and purine nucleoside phosphorylase, are known to be present in the cytosol of the parasite (Gherardi & Sarciron, 2007). This perhaps explains the major focus on adenosine in previous studies of purine transporters in *P. falciparum*, when it is well known that presence of hypoxanthine enhances the growth of the parasite in culture.

The fate of the purine once it enters the cytosol of the erythrocyte was not investigated in the current study. However, given the reported presence of enzymes such as adenosine deaminase (Sherman, 1979; Gherardi & Sarciron, 2007) in the erythrocyte cytosol, it is likely that some of the nucleosides and nucleobases would be further metabolised accordingly. Since the erythrocyte is anucleate, purines may be necessary only for the synthesis of ATP and other biomolecules rather than for DNA or RNA. Therefore it is

expected that much of the purines salvaged from the external source would be available for use by the intracellular *P. falciparum* parasite to meet its physiological needs (see Table 1.1 for physiological average of salvageable purine in mammalian cells).

## **8.2 Purine transport activity in *P. falciparum* parasites with permeabilised erythrocyte membranes**

From the several published methods for the preparation of living *P. falciparum* parasites free of the host erythrocyte membrane, the method described by Ansorge and colleagues (1996) was chosen (Ansorge *et al*, 1996). The basis for the choice was its simplicity as well as the fact that it has been successfully used in other studies requiring permeabilised *P. falciparum* infected erythrocytes (Upston & Gero, 1995; Saliba *et al*, 1998). Even though the ghost of the erythrocytes in which the parasite originally resided is still present around the parasite in these preparations, it does not hinder the free movement of compounds into the parasite (Ansorge *et al*, 1996). The parasitophorous vacuole membrane remains intact around the parasite, but this is not a barrier to the translocation of compounds (Ansorge *et al*, 1996). *P. falciparum*- infected erythrocytes were permeabilised by this means in the current study. A series of investigations were carried out using the permeabilised cell (Chapter Four), which led to the characterisation of the proteins involved in purine salvage into *P. falciparum*. This allowed for the development of a model showing the proteins responsible for purine uptake from the external environment into the cytosol of the parasite (see Figure 8.1. for the model).

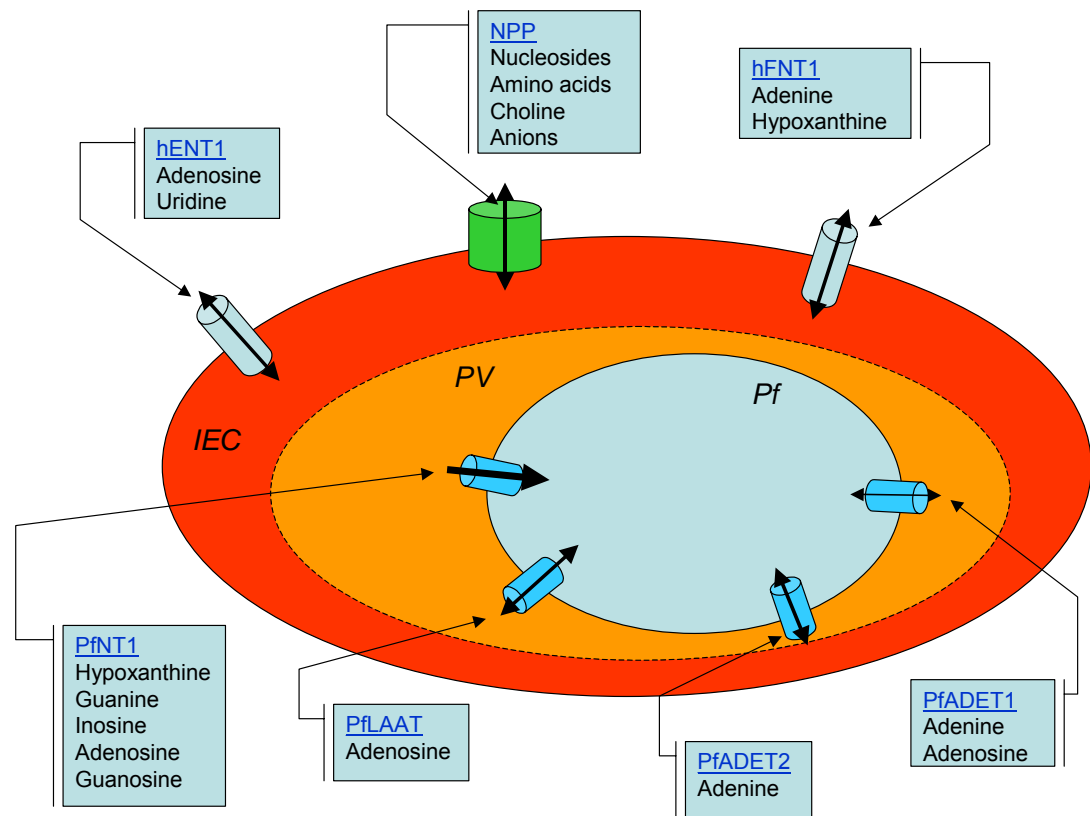


Figure 8.1: Model of purine uptake into intraerythrocytic *P. falciparum* trophozoites.

Double-headed arrows indicate presumed equilibrative transport, whereas the single headed arrow of PfNT1 indicates possible active transport. However, the assignment of active or equilibrative transport is speculative and was not investigated in the current study. hFNT1 and hENT1 are endogenous to the human erythrocyte whereas the origin of the NPP is unknown. The thickness of arrows for the *P. falciparum* transporters is meant to convey the relative flux of purines. NPP, New Permeation Pathways; PV, Parasitophorous vacuole; IEC, infected erythrocyte cytoplasm; Pf, *Plasmodium falciparum*.

Observations reported in chapter three of this thesis indicates that hypoxanthine is rapidly transported into *P. falciparum* trophozoites through a saturable, high affinity transporter, designated PfNT1. This protein was also found to transport adenosine, and is sensitive to inhibition by guanine, inosine and to a lesser extent guanosine, but not to adenine. A separate transporter with a lower affinity for adenosine (denoted PfLAAT) was also found to be present in the plasma membrane of the isolated parasite. Two other separate adenine transporters denoted PfADET1 and PfADET2, both being saturable, were found to be present. PfADET1 was observed to have a high affinity for adenine, while PfADET2 has low affinity for this permeant. Due to technical problems already discussed in chapter four of this thesis, the kinetic parameters of PfADET2 could not be accurately determined. The



adenine transporters were observed in this study to have the highest diffusion component compared with adenosine and the other permeants. This observation is consistent with published data for toxoplasma (de Koning *et al*, 2005). This is believed to be due to the comparatively lower number of electronegative atoms in adenine capable of hydrogen bond formation, relative to the other natural purines. The number of these electronegative atoms in a compound has an inverse relation with the rate of diffusion of that compound across the plasma membrane (Alberts *et al*, 1994). Since the number of such atoms is much higher in adenosine compared to adenine (due to the presence of the sugar moiety), the rate of diffusion is much higher with adenine than the adenosine diffusion rate.

There is considerable controversy about whether *Plasmodium* can utilise adenine at all, as several groups report the inability to identify genes encoding adenine phosphoribosyltransferase (APRT) and methylthioadenosine phosphorylase in any of the *Plasmodium* spp (Chaudhary *et al*, 2004; Ting *et al*, 2005) nor is there any evidence for the activity of adenine deaminase (Ting *et al*, 2005). Yet, the characterisation of APRT from *P. chabaudi* and *P. falciparum* has been reported (Walter & Konigk, 1974; Queen *et al*, 1989). In addition, *P. falciparum* is reportedly able to grow *in vitro* on adenine as the sole purine source (Geary *et al*, 1985) and *P. knowlesi* incorporated adenine into nucleic acids (Gutteridge & Trigg, 1970). Although these latter observations could be explained by conversion of the adenine to hypoxanthine in the host cell, Van Dyke reported that the free parasite can also incorporate adenine into nucleic acids, albeit at 1% of the efficiency by which hypoxanthine is incorporated (Van Dyke, 1975). However the reported uptake of adenine by *P. falciparum* trophozoites in the current study and its seemingly upregulation after deletion of the high affinity hypoxanthine transporter PfNT1, would be compatible with the view that adenine can be utilised in some way but is unlikely to play any major role in the overall synthesis of nucleotides. It is conceivable that the parasite has a different use for low levels of adenine, which it cannot generate itself from other purines (Ting *et al*, 2005), or that adenine at high concentrations could be deaminated by adenosine deaminase. In fact, the presence of PfADET 1 and PfADET2 in the parasite is difficult to explain currently, as the contribution of adenine to purine metabolism in the parasite is unclear. Probably these transporters play major role during conditions of low levels of hypoxanthine and adenosine, or that *P. falciparum* requires adenine for a function unrelated to nucleotide synthesis. Alternatively, PfADET 1 and PfADET2 could be 'primitive transporters' which have been retained after PfNT1 had emerged through years of evolution.

### 8.3 Purine transport in *P. falciparum* parasites lacking *PfNT1*.

Transgenic parasites lacking a full length *PfNT1* gene were generated (chapter five). The high affinity transport of adenosine and hypoxanthine observed in wild-type parasites was completely abolished in the transgenic parasite (3D7 $\Delta$ *PfNT1*), whereas there was no difference in the rate of uptake of adenosine through PfLAAT between the wild type and 3D7 $\Delta$ *PfNT1* parasites (chapter six). The initial rate of adenine uptake through PfADET1 was similar in both the gene-disrupted parasites and wild-type parasites. However there was a higher uptake of adenine during the period of maximum uptake into the transgenic parasites compared to wild-type (Figure 6.4, chapter six). We speculate that this observed difference in level of adenine uptake could compensate for the loss of the high affinity hypoxanthine/nucleoside transport in 3D7 $\Delta$ *PfNT1* parasites.

From a critical analysis of the data obtained in this study, it can be deduced that PfNT1 is likely to be the most important purine transporter for *P. falciparum*. This conclusion is based on: (1) its high affinity, allowing salvage at relatively low purine concentrations, (2) the preference for hypoxanthine, which was experimentally shown to be the most important source for the parasite, (3) its high capacity for both hypoxanthine and adenosine and (4) the observation that  $\Delta$ PfNT1 parasites are unable to survive without high concentrations of purines supplemented to the media. This saturable high affinity hypoxanthine/nucleoside transporter has some characteristics comparable to those reported by Carter's group and Parker's group (Parker *et al*, 2000; Carter *et al*, 2000), such as the ability to transport a broad range of purine nucleosides but not pyrimidines. The major difference between PfNT1 and the previously published transporters is the  $K_m$  value observed for adenosine. As reported in chapter six, PfNT1 has a much lower  $K_m$  value than that reported for any of the three previously published reports (see Table 8.1). However the  $K_m$  value of the previously reported adenosine transporter is similar to that reported for PfLAAT in this thesis.

Purine	Reported $K_m$ ( $\mu$ M)				
	Carter <i>et al.</i> , 2000	Parker <i>et al.</i> , 2000	Downie <i>et al.</i> , 2006	Quashie's PhD thesis	
	PfNT1	PfENT1		PfNT1	PfLAAT
Hypoxanthine		410*		0.34	
Adenosine	13.2*	320*	1450/1860*	2.0	197
Inosine				2.0	
Adenine		320*		>500	

Table 8.1: Comparison of  $K_m$  Values obtained from various studies.

\* NB= $K_m$  from uptake using the *Xenopus laevis* oocyte.

As can be seen on table 8.1 the hypoxanthine/adenosine transporters (PfNT1) reported in chapter four were of high affinity, contrasting with the relatively low affinity of the adenosine/hypoxanthine transporters denoted PfNT1/PfENT1 in previous work. One possible explanation for the apparent discrepancy is that the previous kinetic studies were performed in *Xenopus* oocyte expression systems, under conditions using relatively higher permeant concentration ( $>1\mu$ M). When exogenous purine concentrations are high, it would not be possible to identify high affinity transporters, as they would be rapidly saturated with the permeant. The studies presented in Chapter four used purine concentrations approximately four-fold lower, thus allowing the identification and characterisation of the high affinity transport activity.

During the current study, two further reports on purine transport using isolated *P. falciparum* parasites were published by the groups of Kirk (Downie *et al.*, 2006) and Mamoun (El Bissati *et al.*, 2006). Findings from these studies have not eased existing confusions on purine transporters in *P. falciparum*. In the first publication, El Bissati and co-workers disrupted the gene encoding the nucleoside transporter *PfNT1* in *P. falciparum* and studied the characteristics of the resultant phenotype (El Bissati *et al.*, 2006). They demonstrated that their  $\Delta$ *PfNT1* clones were auxotrophic for hypoxanthine, inosine, and

adenosine under physiological conditions and could only survive when the growth medium was supplemented with excess purine. Additionally the uptake of hypoxanthine into their  $\Delta PfNT1$  clones was significantly reduced, whereas adenosine and inosine transport were only partially affected. They reported that their finding supports the 'conjecture that nucleosides such as adenosine do not gain direct access to the parasite and that they require prior conversion into hypoxanthine using host enzymes, reactions that occur within the RBC cytoplasm followed by PfNT1-mediated transport into the parasite'. This assertion does contradict earlier reports (Parker *et al*, 2000; Carter *et al*, 2000) that adenosine is a major purine transported into the parasite. Such a situation makes the presence of significant levels of adenosine deaminase in the parasite's cytosol difficult to explain. However their report that their  $\Delta PfNT1$  clones needed excess purine to survive in culture is consistent with observations made in the current study (see chapter five). Findings by El Bissati and co are consistent with observations reported in this thesis that PfNT1 is responsible for the high affinity transport of hypoxanthine in *P. falciparum* and that this nucleobase is required to sustain growth of the parasites *in vitro*.

In the second publication, the group of Kirk (Downie *et al*, 2006) reported that salvage of nucleosides such as adenosine into freed parasites was through a low affinity transporter: the kinetic characteristics of which is similar to those of *PfNT1* expressed in *Xenopus* oocytes [ $K_m$  (adenosine) =  $1.86 \pm 0.28$  mM;  $K_m$  (thymidine) =  $1.33 \pm 0.17$  mM]. The group concluded that their data were consistent with PfNT1 serving as a major route for the uptake of nucleosides across the parasite plasma membrane.

It is however worth noting that in the most recent studies (Downie *et al*, 2006; El Bissati *et al*, 2006) high concentrations (micromolar range) of radiolabelled permeants were used in the uptake assays. As previously discussed, under such circumstances measurement of the transport activity of the high affinity transporter would not be possible, as the transporter would be saturated by the permeant. Any kinetic value measured would be that of the low affinity transporter. The use of 25  $\mu$ M of [ $^3$ H]-adenosine in the current study was intended to saturate the high affinity transporter and thus allow measurement of the low affinity adenosine transporter (PfLAAT). The  $K_m$  value of  $197 \pm 20$   $\mu$ M obtained for this transporter (PfLAAT) was lower than that reported (1.45mM) by the group of Kirk (Downie *et al*, 2006) for their transporter which we assert to be the same. Our assertion is supported by the observed rapidity at which adenosine uptake reached equilibrium, and the insensitivity of the transporter to the nucleoside transport inhibitor, dipyridamole. As to the

difference between the  $K_m$  value obtained by Downie and co and that in this study, physical conditions such as the difference in temperature (4°C or 6°C) at which the two uptake assays were performed, could perhaps, partly be an explanation.

In the current study, the ENT gene of the other three identified members of the purine transporters in *P.falciparum* were successfully disrupted and designated, 3D7 $\Delta$ PfNT2 (for Pf14\_0662), 3D7 $\Delta$ PfNT3 (for MAL8pl.32 ) and 3D7 $\Delta$ PfNT4 (for Pfa0160c). It is hoped that once clones are prepared from these and the kinetic property of the phenotype determined, a proper understanding of the entire purine transport in *P. falciparum* will be achieved.

Based on data obtained in the current study, it can be concluded that *P. falciparum* trophozoites expresses both high affinity purine nucleobase/nucleoside transport activities and a low affinity/ high capacity adenosine transport activities in addition to a saturable transport system for adenine. These findings are similar to the system of purine transport observed in the related apicomplexan parasite *T. gondii*. Available literature indicates the existence in *T. gondii* of a low affinity adenosine transporter denoted TgAT1 (Schwab *et al*, 1995; de Koning *et al*, 2003), as well as a high affinity adenosine transporter denoted TgAT2 that could also transport inosine (de Koning *et al*, 2003). However a major difference between purine salvage in the two apicomplexan species is that, unlike *P. falciparum*, *T. gondii* expresses a separate high affinity transporters for purine nucleosides (TgAT2) and the oxopurine nucleobases (TgNBT1). It is also worth noting that, just as observed for PfNT1 in the current study, TgNBT1 does not transport adenine (de Koning *et al*, 2003).

## 8.4 Purine-based antimalarial drugs

With detailed information on the kinetic properties of purine transporters made available through investigations carried out in this project, the stage has been set for an intense search for novel purine-based antimalarial drugs. *In vitro* assessment of purine analogues to ascertain their antiparasmodial potential would require the availability of a simple and reliable drug sensitivity testing method.

The traditional hypoxanthine uptake method (Desjardins *et al*, 1979) for assessing drug efficacy *in vitro* was found to be inappropriate for assessment of the suitability of purine analogues as potential antimalarial candidate. This is because the test compound could compete directly with the radiolabel for the transporter binding site or the enzymes for purine metabolism. The microscopic method (Rieckmann *et al*, 1978; WHO, 1990), which is the gold standard, is labour-intensive and time consuming and thus not suitable for even a semi-high throughput screening approach. A previously published microfluorimetric method (Corbett *et al*, 2004) involving the use of PicoGreen<sup>®</sup> dye to stain parasite's DNA was found to be the most appropriate for assessments of the purine analogues tested in preliminary experiments. However, the PicoGreen<sup>®</sup> method was initially found to be extremely insensitive due to quenching of the fluorescence signal, as discussed in chapter seven. The method was therefore modified appropriately to mend the defect and then used to assess the antimalarial potential of some purine analogues received from the libraries of collaborators. The modification involved removal by saponin lysis of the haemoglobin from red blood cells in the culture, which was thought to quench fluorescence of PicoGreen<sup>®</sup>. The improved method was found to provide reliable and reproducible results.

Using the newly improved PicoGreen<sup>®</sup> method, the antimalarial activity of a limited number of purine analogues, designated JA-compounds and NA-compounds, were investigated. JA-32 was found to be the compound with the most promising antiplasmodial activity. Interestingly, among the series of compounds from the library tested, JA-32 is the one with a chemical structure closest to hypoxanthine. This observation perhaps underlines the importance of hypoxanthine as the preferred purine source and the major permeant for PfNT1. With the presence of multiple purine transporters as observed in this study, a single purine-based antiplasmodial compound may not be enough to completely block the uptake of purine and thus prevent or slow the growth of the parasite. It is possible that when a major purine transporter is inhibited through competitive inhibition with a purine analogue, the parasite could obtain purines through the other transporters to compensate for the loss. This phenomenon was evident in the current study when adenine uptake was elevated in parasites lacking *PfNT1* (see Figure 6.4). Furthermore, the affinity of PfNT1 for hypoxanthine being already very high, a competitive inhibitor would need to either display an extremely and uniquely high affinity for the transporter, or be present locally in very high concentrations. Even then, the blockage of hypoxanthine uptake and utilization in the infected erythrocyte may well lead to a build up of free hypoxanthine generated by

adenosine deaminase and purine nucleoside phosphorylase, and again out-compete the inhibitor.

The work presented in this thesis has investigated purine uptake into trophozoite stages of *P. falciparum*. The results obtained do not exclude the possibility that some of the identified purine transporters of *P. falciparum* play important role in nucleoside transport at the other stages of the parasite life cycle.

## 9 Appendix



## 9.1 Composition of solutions

### 9.1.1 Cryopreservation solution

Glycerol	28%
Sorbitol	3%
NaCl	0.65%

Made with distilled water, filter sterilised and stored at 4°C.

### 9.1.2 Cytomix

KCl	120 mM
CaCl <sub>2</sub>	0.15 mM
EGTA	2 mM
MgCl <sub>2</sub>	5 mM
K <sub>2</sub> HPO <sub>4</sub> /KH <sub>2</sub> PO <sub>4</sub> at pH 7.6	10 mM
Hepes at pH 7.6	25 mM

### 9.1.3 Denaturation solution for Southern blot

NaCl	1.5 M
NaOH	0.5 M

Made with distilled water.

### 9.1.4 6 X DNA loading dye

Bromophenol blue	25 mg
Xylene cyanol FF	25 mg
Sucrose	4g

Made with double distilled water to 10 ml

.

### 9.1.5 LB agar

Lennox L agar	35 g
---------------	------

Made with distilled water in 1 litre and autoclaved. Liquified by melting the agar before making agar plates.

### 9.1.6 LB medium

Tryptone	10 g
Yeast extract	5 g
NaCl	10 g

Made with distilled water in 1 litre and pH adjusted at 7.0 with 5 M NaOH followed by autoclaving.

### 9.1.7 Neutralisation solution for Southern blot

NaCl	1.5 M
Tris-HCl at pH 7.2	0.5 M
EDTA	1 mM

Made with distilled water.

### 9.1.8 SOC

Tryptone	20 g
Yeast extract	5 g

NaCl	0.5 g
Dissolved in water	
250 mM KCl	10 ml
2 M MgCl <sub>2</sub>	5 ml

Made with distilled water in 1 litre and pH adjusted at 7.0 with 5 M NaOH followed by autoclaving. When cooled down  
1 M sterile glucose 20 ml added.

### 9.1.9 20 X SSC

NaCl	3 M
Sodium citrate (.2 H <sub>2</sub> O)	0.3 M

Made with distilled water and the pH was adjusted to 7.0 with NaOH. Diluted to 10 X / 6X/5 X before use.

### 9.1.10 50 X TAE

Tris base	2 M
Glacial acetic acid	57.1 ml
EDTA at pH 8.0	50 mM

Made with distilled water in 1 litre. Diluted to 1 X before use.

### 9.1.11 5 X TBE

Tris base	450 mM
Boric acid	27.5 g
EDTA at pH 8.0	10 mM

Made with distilled water in 1 litre. Diluted to 1 X before use.

### 9.1.12 1 X TE

1 M Tris.HCl	10 ml
0.5 M EDTA at pH 8.0	2 ml

Made with distilled water in 1 litre.

## 10 Reference List

## References

- Acimovic,Y. & Coe,I.R.** (2002) Molecular evolution of the equilibrative nucleoside transporter family: identification of novel family members in prokaryotes and eukaryotes. *Mol.Biol.Evol.*, **19**, 2199-2210.
- Alberts,B., Bray,D., Lewis,J., Raff,M., Roberts,K., & Watson,J.** (1994) *Molecular Biology of the Cell*, 3rd edn, Garland Publishing, New York.
- Aley,S.B., Barnwell,J.W., Daniel,W., & Howard,R.J.** (1984) Identification of parasite proteins in a membrane preparation enriched for the surface membrane of erythrocytes infected with *Plasmodium knowlesi*. *Mol.Biochem Parasitol*, **12**, 69-84.
- Allen,R.J. & Kirk,K.** (2004) The membrane potential of the intraerythrocytic malaria parasite *Plasmodium falciparum*. *J Biol.Chem.*, **279**, 11264-11272.
- Alonso,P.L., Sacarlal,J., Aponte,J.J., Leach,A., Macete,E., Milman,J., Mandomando,I., Spiessens,B., Guinovart,C., Espasa,M., Bassat,Q., Aide,P., Ofori-Anyinam,O., Navia,M.M., Corachan,S., Ceuppens,M., Dubois,M.C., Demoitie,M.A., Dubovsky,F., Menendez,C., Tornieporth,N., Ballou,W.R., Thompson,R., & Cohen,J.** (2004) Efficacy of the RTS,S/AS02A vaccine against *Plasmodium falciparum* infection and disease in young African children: randomised controlled trial. *Lancet*, **364**, 1411-1420.
- Anson,I., Benting,J., Bhakdi,S., & Lingelbach,K.** (1996) Protein sorting in *Plasmodium falciparum*-infected red blood cells permeabilized with the pore-forming protein streptolysin O. *Biochem.J.*, **315** ( Pt 1), 307-314.
- Asahi,H., Kanazawa,T., Kajihara,Y., Takahashi,K., & Takahashi,T.** (1996) Hypoxanthine: a low molecular weight factor essential for growth of erythrocytic *Plasmodium falciparum* in a serum-free medium. *Parasitology*, **113** ( Pt 1), 19-23.

- Baird, J.K.** (2004) Chloroquine resistance in *Plasmodium vivax*. *Antimicrob Agents Chemother*, **48**, 4075-4083.
- Baird, J.K., Basri, H., Purnomo, Bangs, M.J., Subianto, B., Patchen, L.C., & Hoffman, S.L.** (1991) Resistance to chloroquine by *Plasmodium vivax* in Irian Jaya, Indonesia. *Am.J.Trop.Med.Hyg.*, **44**, 547-552.
- Baird, J.K., Purnomo, & Jones, T.R.** (1992) Diagnosis of malaria in the field by fluorescence microscopy of QBC capillary tubes. *Trans.R.Soc.Trop.Med.Hyg.*, **86**, 3-5.
- Bakker-Grunwald, T.** (1992) Ion transport in parasitic protozoa. *J Exp.Biol.*, **172**, 311-322.
- Baldwin, S.A., Beal, P.R., Yao, S.Y., King, A.E., Cass, C.E., & Young, J.D.** (2004) The equilibrative nucleoside transporter family, SLC29. *Pflugers Arch.*, **447**, 735-743.
- Baldwin, S.A., Mackey, J.R., Cass, C.E., & Young, J.D.** (1999) Nucleoside transporters: molecular biology and implications for therapeutic development. *Mol.Med.Today*, **5**, 216-224.
- Baldwin, S.A., Yao, S.Y., Hyde, R.J., Ng, A.M., Foppolo, S., Barnes, K., Ritzel, M.W., Cass, C.E., & Young, J.D.** (2005) Functional characterization of novel human and mouse equilibrative nucleoside transporters (hENT3 and mENT3) located in intracellular membranes. *J Biol.Chem.*, **280**, 15880-15887.
- Becker, K. & Kirk, K.** (2004) Of malaria, metabolism and membrane transport. *Trends Parasitol*, **20**, 590-596.
- Beene, D.L., Dougherty, D.A., & Lester, H.A.** (2003) Unnatural amino acid mutagenesis in mapping ion channel function. *Curr.Opin.Neurobiol.*, **13**, 264-270.
- Benito, A., Roche, J., Molina, R., Amela, C., & Alvar, J.** (1994) Application and evaluation of QBC malaria diagnosis in a holoendemic area. *Appl.Parasitol.*, **35**, 266-272.

- Berman,P.A. & Human,L.** (1990) Regulation of 5-phosphoribosyl 1-pyrophosphate and of hypoxanthine uptake and release in human erythrocytes by oxypurine cycling. *J Biol.Chem.*, **265**, 6562-6568.
- Berman,P.A. & Human,L.** (1991) Hypoxanthine depletion induced by xanthine oxidase inhibits malaria parasite growth *in vitro*. *Adv.Exp.Med.Biol.*, **309A**, 165-168.
- Berman,P.A., Human,L., & Freese,J.A.** (1991) Xanthine oxidase inhibits growth of *Plasmodium falciparum* in human erythrocytes *in vitro*. *J.Clin.Invest*, **88**, 1848-1855.
- Beutler,E.** (1983) Red cell enzyme deficiencies as non-disease. *Biomed.Biochim.Acta*, **42**, S234-S241.
- Biagini,G.A., Pasini,E.M., Hughes,R., de Koning,H.P., Vial,H.J., O'Neill,P.M., Ward,S.A., & Bray,P.G.** (2004) Characterization of the choline carrier of *Plasmodium falciparum*: a route for the selective delivery of novel antimalarial drugs. *Blood*, **104**, 3372-3377.
- Black,R.H., Canfield,C.J., Clyde,D.F., Peters,W., & Werndorfer,W.H.** (1986) *Chemotherapy of malaria*, 2nd edn, WHO, Geneva.
- Bloand,P.B.** (2001) *Drug resistance in malaria*, p. 3. WHO/CDS/CSR/DRS, Geneva.
- Bojang,K.A., Milligan,P.J., Pinder,M., Vigneron,L., Alloueche,A., Kester,K.E., Ballou,W.R., Conway,D.J., Reece,W.H., Gothard,P., Yamuah,L., Delchambre,M., Voss,G., Greenwood,B.M., Hill,A., McAdam,K.P., Tornieporth,N., Cohen,J.D., & Doherty,T.** (2001) Efficacy of RTS,S/AS02 malaria vaccine against *Plasmodium falciparum* infection in semi-immune adult men in The Gambia: a randomised trial. *Lancet*, **358**, 1927-1934.
- Brown,D.M., Netting,A.G., Chun,B.K., Choi,Y., Chu,C.K., & Gero,A.M.** (1999) L-nucleoside analogues as potential antimalarials that selectively target *Plasmodium falciparum* adenosine deaminase. *Nucleosides Nucleotides*, **18**, 2521-2532.

- Bruce-Chwatt,L.** (1986) *Essential Malariology*, 2nd edn, William Heinemann Medical Books Ltd, London.
- Buyse,G., Voets,T., Tytgat,J., De Greef,C., Droogmans,G., Nilius,B., & Eggermont,J.** (1997) Expression of human pICln and ClC-6 in *Xenopus oocytes* induces an identical endogenous chloride conductance. *J Biol.Chem.*, **272**, 3615-3621.
- Cabantchik,Z.I.** (1989) Nucleoside transport across red cell membranes. *Methods Enzymol.*, **173**, 250-263.
- Cabantchik,Z.I.** (1990) Properties of permeation pathways induced in the human red cell membrane by malaria parasites. *Blood Cells*, **16**, 421-432.
- Capuozzo,E., Gigante,M.C., Salerno,C., & Crifo,C.** (1986) Hypoxanthine transport through human erythrocyte membranes. *Adv.Exp.Med.Biol.*, **195 Pt B**, 71-74.
- Carter,N.S., Ben Mamoun,C., Liu,W., Silva,E.O., Landfear,S.M., Goldberg,D.E., & Ullman,B.** (2000) Isolation and functional characterization of the *PfNT1* nucleoside transporter gene from *Plasmodium falciparum*. *J Biol.Chem.*, **275**, 10683-10691.
- Carucci,D.J., Gardner,M.J., Tettelin,H., Cummings,L.M., Smith,H.O., Adams,M.D., Venter,J.C., & Hoffman,S.L.** (1998) Sequencing the genome of *Plasmodium falciparum*. *Curr.Opin.Infect.Dis.*, **11**, 531-534.
- CDC.** Factors That Determine The Occurrence of Malaria. 2004. Atlanta, USA, Center for Disease Control.
- Ref Type: Report
- Chaudhary,K., Darling,J.A., Fohl,L.M., Sullivan,W.J., Jr., Donald,R.G., Pfefferkorn,E.R., Ullman,B., & Roos,D.S.** (2004) Purine salvage pathways in the apicomplexan parasite *Toxoplasma gondii*. *J Biol.Chem.*, **279**, 31221-31227.
- Chiang,C.W., Carter,N., Sullivan,W.J., Jr., Donald,R.G., Roos,D.S., Naguib,F.N., el Kouni,M.H., Ullman,B., & Wilson,C.M.** (1999) The adenosine transporter of *Toxoplasma gondii*. Identification by insertional mutagenesis, cloning, and recombinant expression. *J Biol.Chem.*, **274**, 35255-35261.

**Chongsuphajaisiddhi,T., Subchareon,A., Puangpartk,S., & Harinasuta,T.** (1979)

Treatment of falciparum malaria in Thai children. *Southeast Asian J.Trop.Med.Public Health*, **10**, 132-137.

**Chulay,J.D., Watkins,W.M., & Sixsmith,D.G.** (1984) Synergistic antimalarial activity of

pyrimethamine and sulfadoxine against *Plasmodium falciparum in vitro*.  
*Am.J.Trop.Med.Hyg.*, **33**, 325-330.

**Cohn,C.S. & Gottlieb,M.** (1997) The acquisition of purines by trypanosomatids.

*Parasitol.Today*, **13**, 231-235.

**Cook,G.C.** (1992) Malaria: an underdiagnosed and often neglected medical emergency.

*Aust.N.Z.J.Med.*, **22**, 69-82.

**Coomber,D.W., O'Sullivan,W.J., & Gero,A.M.** (1994) Adenosine analogues as

antimetabolites against *Plasmodium falciparum* malaria. *Int.J.Parasitol.*, **24**, 357-365.

**Corbett,Y., Herrera,L., Gonzalez,J., Cubilla,L., Capson,T.L., Coley,P.D.,**

**Kursar,T.A., Romero,L.I., & Ortega-Barria,E.** (2004) A novel DNA-based  
microfluorimetric method to evaluate antimalarial drug activity.

*Am.J.Trop.Med.Hyg.*, **70**, 119-124.

**Crawford,C.R., Patel,D.H., Naeve,C., & Belt,J.A.** (1998) Cloning of the human

equilibrative, nitrobenzylmercaptapurine riboside (NBMPR)-insensitive nucleoside  
transporter ei by functional expression in a transport-deficient cell line. *J*

*Biol.Chem.*, **273**, 5288-5293.

**Cumming,J.N., Ploypradith,P., & Posner,G.H.** (1997) Antimalarial activity of

artemisinin (qinghaosu) and related trioxanes: mechanism(s) of action.

*Adv.Pharmacol.*, **37**, 253-297.

**Daddona,P.E., Wiesmann,W.P., Lambros,C., Kelley,W.N., & Webster,H.K.** (1984)

Human malaria parasite adenosine deaminase. Characterization in host enzyme-  
deficient erythrocyte culture. *J Biol.Chem.*, **259**, 1472-1475.



- de Koning,H.P., Al Salabi,M.I., Cohen,A.M., Coombs,G.H., & Wastling,J.M.** (2003) Identification and characterisation of high affinity nucleoside and nucleobase transporters in *Toxoplasma gondii*. *Int.J.Parasitol.*, **33**, 821-831.
- de Koning,H.P., Bridges,D.J., & Burchmore,R.J.** (2005) Purine and pyrimidine transport in pathogenic protozoa: from biology to therapy. *FEMS Microbiol.Rev.*, **29**, 987-1020.
- de Koning,H.P. & Jarvis,S.M.** (1997) Purine nucleobase transport in bloodstream forms of *Trypanosoma brucei brucei*. *Biochem.Soc.Trans.*, **25**, 476S.
- Desai,S.A., Bezrukov,S.M., & Zimmerberg,J.** (2000) A voltage-dependent channel involved in nutrient uptake by red blood cells infected with the malaria parasite. *Nature*, **406**, 1001-1005.
- Desai,S.A., Krogstad,D.J., & McCleskey,E.W.** (1993) A nutrient-permeable channel on the intraerythrocytic malaria parasite. *Nature*, **362**, 643-646.
- Desjardins,R.E., Canfield,C.J., Haynes,J.D., & Chulay,J.D.** (1979) Quantitative assessment of antimalarial activity *in vitro* by a semiautomated microdilution technique. *Antimicrob Agents Chemother*, **16**, 710-718.
- Divo,A.A., Geary,T.G., Davis,N.L., & Jensen,J.B.** (1985) Nutritional requirements of *Plasmodium falciparum* in culture. I. Exogenously supplied dialyzable components necessary for continuous growth. *J.Protozool.*, **32**, 59-64.
- Divo,A.A. & Jensen,J.B.** (1982) Studies on serum requirements for the cultivation of *Plasmodium falciparum*. 2. Medium enrichment. *Bull.World Health Organ*, **60**, 571-575.
- Domin,B.A., Mahony,W.B., & Zimmerman,T.P.** (1988) Purine nucleobase transport in human erythrocytes. Reinvestigation with a novel "inhibitor-stop" assay. *J Biol.Chem.*, **263**, 9276-9284.

- Downie,M.J., Saliba,K.J., Howitt,S.M., Broer,S., & Kirk,K.** (2006) Transport of nucleosides across the *Plasmodium falciparum* parasite plasma membrane has characteristics of PfENT1. *Mol.Microbiol.*, **60**, 738-748.
- Dunham,P.B., Stewart,G.W., & Ellory,J.C.** (1980) Chloride-activated passive potassium transport in human erythrocytes. *Proc.Natl.Acad.Sci.U.S.A*, **77**, 1711-1715.
- Durantón,C., Huber,S., Tanneur,V., Lang,K., Brand,V., Sandu,C., & Lang,F.** (2003) Electrophysiological properties of the Plasmodium Falciparum-induced cation conductance of human erythrocytes. *Cell Physiol Biochem.*, **13**, 189-198.
- Egee,S., Lapaix,F., Decherf,G., Staines,H.M., Ellory,J.C., Doerig,C., & Thomas,S.L.** (2002) A stretch-activated anion channel is up-regulated by the malaria parasite *Plasmodium falciparum*. *J.Physiol*, **542**, 795-801.
- El Bissati,K., Zufferey,R., Witola,W.H., Carter,N.S., Ullman,B., & Ben Mamoun,C.** (2006) The plasma membrane permease PfNT1 is essential for purine salvage in the human malaria parasite *Plasmodium falciparum*. *Proc.Natl.Acad.Sci.U.S.A*, **103**, 9286-9291.
- Elford,B.C., Pinches,R.A., Newbold,C.I., & Ellory,J.C.** (1990) Heterogeneous and substrate-specific membrane transport pathways induced in malaria-infected erythrocytes. *Blood Cells*, **16**, 433-436.
- Fidock,D.A., Nomura,T., Cooper,R.A., Su,X., Talley,A.K., & Wellems,T.E.** (2000) Allelic modifications of the *cg2* and *cg1* genes do not alter the chloroquine response of drug-resistant *Plasmodium falciparum*. *Mol.Biochem Parasitol*, **110**, 1-10.
- Fidock,D.A. & Wellems,T.E.** (1997) Transformation with human dihydrofolate reductase renders malaria parasites insensitive to WR99210 but does not affect the intrinsic activity of proguanil. *Proc.Natl.Acad.Sci.U.S.A*, **94**, 10931-10936.
- Foster S & Phillips M** (1998) Economics and its contribution to the fight against malaria. *Annals of Trop Med Parasitol*, **92**, 391-398.

- Freese, J.A., Sharp, B.L., Ridl, F.C., & Markus, M.B.** (1988) In vitro cultivation of southern African strains of *Plasmodium falciparum* and gametocytogenesis. *S.Afr.Med.J.*, **73**, 720-722.
- Gallup, J.L. & Sachs, J.D.** (2001) The economic burden of malaria. *Am.J.Trop.Med.Hyg.*, **64**, 85-96.
- Garcia-Romeu, F., Cossins, A.R., & Motais, R.** (1991) Cell volume regulation by trout erythrocytes: characteristics of the transport systems activated by hypotonic swelling. *J.Physiol*, **440**, 547-567.
- Gardiner, D.L., McCarthy, J.S., & Trenholme, K.R.** (2005) Malaria in the post-genomics era: light at the end of the tunnel or just another train? *Postgrad.Med J*, **81**, 505-509.
- Gardner, M.J., Hall, N., Fung, E., White, O., Berriman, M., Hyman, R.W., Carlton, J.M., Pain, A., Nelson, K.E., Bowman, S., Paulsen, I.T., James, K., Eisen, J.A., Rutherford, K., Salzberg, S.L., Craig, A., Kyes, S., Chan, M.S., Nene, V., Shallom, S.J., Suh, B., Peterson, J., Angiuoli, S., Pertea, M., Allen, J., Selengut, J., Haft, D., Mather, M.W., Vaidya, A.B., Martin, D.M., Fairlamb, A.H., Fraunholz, M.J., Roos, D.S., Ralph, S.A., McFadden, G.I., Cummings, L.M., Subramanian, G.M., Mungall, C., Venter, J.C., Carucci, D.J., Hoffman, S.L., Newbold, C., Davis, R.W., Fraser, C.M., & Barrell, B.** (2002) Genome sequence of the human malaria parasite *Plasmodium falciparum*. *Nature*, **419**, 498-511.
- Geary, T.G., Divo, A.A., Bonanni, L.C., & Jensen, J.B.** (1985) Nutritional requirements of *Plasmodium falciparum* in culture. III. Further observations on essential nutrients and antimetabolites. *J.Protozool.*, **32**, 608-613.
- Gengenbacher, M., Fitzpatrick, T.B., Raschle, T., Flicker, K., Sinning, I., Muller, S., Macheroux, P., Tews, I., & Kappes, B.** (2006) Vitamin B6 biosynthesis by the malaria parasite *Plasmodium falciparum*: biochemical and structural insights. *J Biol.Chem.*, **281**, 3633-3641.
- Gero, A.M., Bugledich, E.M., Paterson, A.R., & Jamieson, G.P.** (1988) Stage-specific alteration of nucleoside membrane permeability and nitrobenzylthioinosine

insensitivity in *Plasmodium falciparum* infected erythrocytes.  
*Mol.Biochem.Parasitol.*, **27**, 159-170.

**Gero,A.M., Dunn,C.G., Brown,D.M., Pulenthiran,K., Gorovits,E.L., Bakos,T., & Weis,A.L.** (2003) New malaria chemotherapy developed by utilization of a unique parasite transport system. *Curr.Pharm.Des*, **9**, 867-877.

**Gero,A.M. & Hall,S.T.** (1997) *Plasmodium falciparum*: transport of enantiomers of nucleosides into Sendai-treated trophozoites. *Exp.Parasitol.*, **86**, 228-231.

**Gero,A.M. & O'Sullivan,W.J.** (1990) Purines and pyrimidines in malarial parasites. *Blood Cells*, **16**, 467-484.

**Gero,A.M., Perrone,G., Brown,D.M., Hall,S.T., & Chu,C.K.** (1999) L-purine nucleosides as selective antimalarials. *Nucleosides Nucleotides*, **18**, 885-889.

**Gherardi,A. & Sarciron,M.E.** (2007) Molecules targeting the purine salvage pathway in Apicomplexan parasites. *Trends Parasitol.*, **23**, 384-389.

**Giacomello,A. & Salerno,C.** (1979) Role of human hypoxanthine guanine phosphoribosyltransferase in nucleotide interconversion. *Adv.Exp.Med.Biol.*, **122B**, 93-101.

**Ginsburg,H.** (1994) Transport pathways in the malaria-infected erythrocyte. Their characterization and their use as potential targets for chemotherapy. *Biochem.Pharmacol.*, **48**, 1847-1856.

**Ginsburg,H. & Krugliak,M.** (1983) Uptake of L-tryptophan by erythrocytes infected with malaria parasites (*Plasmodium falciparum*). *Biochim.Biophys.Acta*, **729**, 97-103.

**Ginsburg,H. & Stein,W.D.** (1987) New permeability pathways induced by the malarial parasite in the membrane of its host erythrocyte: potential routes for targeting of drugs into infected cells. *Biosci.Rep.*, **7**, 455-463.

**Goman,M., Langsley,G., Hyde,J.E., Yankovsky,N.K., Zolg,J.W., & Scaife,J.G.** (1982) The establishment of genomic DNA libraries for the human malaria parasite

*Plasmodium falciparum* and identification of individual clones by hybridisation. *Mol.Biochem.Parasitol.*, **5**, 391-400.

**Gray,J.H., Owen,R.P., & Giacomini,K.M.** (2004) The concentrative nucleoside transporter family, SLC28. *Pflugers Arch.*, **447**, 728-734.

**Griffith,D.A. & Jarvis,S.M.** (1991) Expression of sodium-dependent nucleoside transporters in *Xenopus* oocytes. *Adv.Exp.Med Biol.*, **309A**, 431-434.

**Griffiths,M., Yao,S.Y., Abidi,F., Phillips,S.E., Cass,C.E., Young,J.D., & Baldwin,S.A.** (1997) Molecular cloning and characterization of a nitrobenzylthioinosine-insensitive (ei) equilibrative nucleoside transporter from human placenta. *Biochem.J.*, **328 ( Pt 3)**, 739-743.

**Gubler,D.J.** (1998) Resurgent vector-borne diseases as a global health problem. *Emerg.Infect.Dis.*, **4**, 442-450.

**Gutteridge,W.E. & Trigg,P.I.** (1970) Incorporation of radioactive precursors into DNA and RNA of *Plasmodium knowlesi* in vitro. *J.Protozool.*, **17**, 89-96.

**Hansen,B.D., Sleeman,H.K., & Pappas,P.W.** (1980) Purine base and nucleoside uptake in *Plasmodium berghei* and host erythrocytes. *J.Parasitol.*, **66**, 205-212.

**Harmse,L., van Zyl,R., Gray,N., Schultz,P., Leclerc,S., Meijer,L., Doerig,C., & Havlik,I.** (2001) Structure-activity relationships and inhibitory effects of various purine derivatives on the *in vitro* growth of *Plasmodium falciparum*. *Biochem.Pharmacol.*, **62**, 341-348.

**Haynes,J.D., Diggs,C.L., Hines,F.A., & Desjardins,R.E.** (1976) Culture of human malaria parasites *Plasmodium falciparum*. *Nature*, **263**, 767-769.

**Hiebsch,R.R., Raub,T.J., & Wattenberg,B.W.** (1991) Primaquine blocks transport by inhibiting the formation of functional transport vesicles. Studies in a cell-free assay of protein transport through the Golgi apparatus. *J Biol.Chem.*, **266**, 20323-20328.

- Howard,R.J., Uni,S., Aikawa,M., Aley,S.B., Leech,J.H., Lew,A.M., Wellems,T.E., Rener,J., & Taylor,D.W.** (1986) Secretion of a malarial histidine-rich protein (Pf HRP II) from *Plasmodium falciparum*-infected erythrocytes. *J.Cell Biol.*, **103**, 1269-1277.
- Huber,S.M., Uhlemann,A.C., Gamper,N.L., Duranton,C., Kremsner,P.G., & Lang,F.** (2002) *Plasmodium falciparum* activates endogenous Cl(-) channels of human erythrocytes by membrane oxidation. *EMBO J.*, **21**, 22-30.
- Hyde,J.E.** (2002) Mechanisms of resistance of *Plasmodium falciparum* to antimalarial drugs. *Microbes.Infect.*, **4**, 165-174.
- Hyde,R.J., Cass,C.E., Young,J.D., & Baldwin,S.A.** (2001) The ENT family of eukaryote nucleoside and nucleobase transporters: recent advances in the investigation of structure/function relationships and the identification of novel isoforms. *Mol.Membr.Biol.*, **18**, 53-63.
- Jensen,J.B.** (1988) *Malaria: Principles and Practice of Malariology*, pp. 307-320. Churchill Livingstone Ltd, London.
- Jensen,J.B., Trager,W., & Beaudoin,R.L.** (1979) *Techniques for in vitro cultivation of erythrocytic and exo-erythrocytic stages of malaria parasites.*In 'Practical tissue culture applications', pp. 255-266. Academic Press, New York.
- Joet,T., Eckstein-Ludwig,U., Morin,C., & Krishna,S.** (2003) Validation of the hexose transporter of *Plasmodium falciparum* as a novel drug target. *Proc.Natl.Acad.Sci.U.S.A.*, **100**, 7476-7479.
- Jongwutiwes,S., Putaporntip,C., Iwasaki,T., Sata,T., & Kanbara,H.** (2004) Naturally acquired *Plasmodium knowlesi* malaria in human, Thailand. *Emerg.Infect.Dis.*, **10**, 2211-2213.
- Kawamoto,F.** (1991) Rapid diagnosis of malaria by fluorescence microscopy with light microscope and interference filter. *Lancet*, **337**, 200-202.

- Kirk,K.** (2001) Membrane transport in the malaria-infected erythrocyte. *Physiol Rev.*, **81**, 495-537.
- Kirk,K. & Horner,H.A.** (1995) In search of a selective inhibitor of the induced transport of small solutes in *Plasmodium falciparum*-infected erythrocytes: effects of arylaminobenzoates. *Biochem.J.*, **311 ( Pt 3)**, 761-768.
- Kirk,K., Horner,H.A., Elford,B.C., Ellory,J.C., & Newbold,C.I.** (1994) Transport of diverse substrates into malaria-infected erythrocytes via a pathway showing functional characteristics of a chloride channel. *J Biol.Chem.*, **269**, 3339-3347.
- Kirk,K., Staines,H.M., Martin,R.E., & Saliba,K.J.** (1999) Transport properties of the host cell membrane. *Novartis.Found.Symp.*, **226**, 55-66.
- Komarova,S.V., Mosharov,E.V., Vitvitsky,V.M., & Ataulakhanov,F.I.** (1999) Adenine nucleotide synthesis in human erythrocytes depends on the mode of supplementation of cell suspension with adenosine. *Blood Cells Mol.Dis.*, **25**, 170-179.
- Kong,W., Engel,K., & Wang,J.** (2004) Mammalian nucleoside transporters. *Curr.Drug Metab*, **5**, 63-84.
- Kraupp,M., Marz,R., Prager,G., Kommer,W., Razavi,M., Baghestanian,M., & Chiba,P.** (1991) Adenine and hypoxanthine transport in human erythrocytes: distinct substrate effects on carrier mobility. *Biochim.Biophys.Acta*, **1070**, 157-162.
- Krishna,S., Eckstein-Ludwig,U., Joet,T., Uhlemann,A.C., Morin,C., Webb,R., Woodrow,C., Kun,J.F., & Kremsner,P.G.** (2002) Transport processes in *Plasmodium falciparum*-infected erythrocytes: potential as new drug targets. *Int.J.Parasitol.*, **32**, 1567-1573.
- Krug,E.C., Marr,J.J., & Berens,R.L.** (1989) Purine metabolism in *Toxoplasma gondii*. *J Biol.Chem.*, **264**, 10601-10607.

- Krugliak,M., Zhang,J., & Ginsburg,H.** (2002) Intraerythrocytic *Plasmodium falciparum* utilizes only a fraction of the amino acids derived from the digestion of host cell cytosol for the biosynthesis of its proteins. *Mol.Biochem.Parasitol.*, **119**, 249-256.
- Lambros,C. & Vanderberg,J.P.** (1979) Synchronization of *Plasmodium falciparum* erythrocytic stages in culture. *J.Parasitol.*, **65**, 418-420.
- Landfear,S.M., Ullman,B., Carter,N.S., & Sanchez,M.A.** (2004) Nucleoside and nucleobase transporters in parasitic protozoa. *Eukaryot.Cell*, **3**, 245-254.
- Lassen,U.V.** (1967) Hypoxanthine transport in human erythrocytes. *Biochim.Biophys.Acta*, **135**, 146-154.
- Li,W., Mo,W., Shen,D., Sun,L., Wang,J., Lu,S., Gitschier,J.M., & Zhou,B.** (2005) Yeast model uncovers dual roles of mitochondria in action of artemisinin. *PLoS.Genet.*, **1**, e36.
- Liu,J., Istvan,E.S., Gluzman,I.Y., Gross,J., & Goldberg,D.E.** (2006) *Plasmodium falciparum* ensures its amino acid supply with multiple acquisition pathways and redundant proteolytic enzyme systems. *Proc.Natl.Acad.Sci.U.S.A*, **103**, 8840-8845.
- Makler,M.T., Ries,J.M., Williams,J.A., Bancroft,J.E., Piper,R.C., Gibbins,B.L., & Hinrichs,D.J.** (1993) Parasite lactate dehydrogenase as an assay for *Plasmodium falciparum* drug sensitivity. *Am.J.Trop.Med.Hyg.*, **48**, 739-741.
- Makler,M.T., Ries,L.K., Ries,J., Horton,R.J., & Hinrichs,D.J.** (1991) Detection of *Plasmodium falciparum* infection with the fluorescent dye, benzothiocarboxypurine. *Am.J.Trop.Med.Hyg.*, **44**, 11-16.
- Malaney,P., Spielman,A., & Sach,J.** (2004) The malaria gap. *Am.J.Trop.Med.Hyg.*, **71**, 141-146.
- Marr,J.J., Nilsen,T.W., & Komuniecki,R.** (2003) *Molecular Medical Parasitology*, Academic Press, New York.



- Martin,R.E., Henry,R.I., Abbey,J.L., Clements,J.D., & Kirk,K.** (2005) The 'permeome' of the malaria parasite: an overview of the membrane transport proteins of *Plasmodium falciparum*. *Genome Biol.*, **6**, R26.
- Matesanz,F., Duran-Chica,I., & Alcina,A.** (1999) The cloning and expression of Pfacs1, a *Plasmodium falciparum* fatty acyl coenzyme A synthetase-1 targeted to the host erythrocyte cytoplasm. *J.Mol.Biol.*, **291**, 59-70.
- Matias,C., Nott,S.E., Bagnara,A.S., O'Sullivan,W.J., & Gero,A.M.** (1990) Purine salvage and metabolism in *Babesia bovis*. *Parasitol Res.*, **76**, 207-213.
- McCoubrie,J.E., Miller,S.K., Sargeant,T., Good,R.T., Hodder,A.N., Speed,T.P., Koning-Ward,T.F., & Crabb,B.S.** (2007) Evidence for a common role for the serine-type *Plasmodium falciparum* serine repeat antigen proteases: implications for vaccine and drug design. *Infect.Immun.*, **75**, 5565-5574.
- McCutchan,T.F., Dame,J.B., Miller,L.H., & Barnwell,J.** (1984) Evolutionary relatedness of *Plasmodium* species as determined by the structure of DNA. *Science*, **225**, 808-811.
- Menard,R. & Janse,C.** (1997) Gene targeting in malaria parasites. *Methods*, **13**, 148-157.
- Mitamura,T. & Palacpac,N.M.** (2003) Lipid metabolism in *Plasmodium falciparum*-infected erythrocytes: possible new targets for malaria chemotherapy. *Microbes.Infect.*, **5**, 545-552.
- Mohrenweiser,H.W., Fielek,S., & Wurzinger,K.H.** (1981) Characteristics of enzymes of erythrocytes from newborn infants and adults: activity, thermostability, and electrophoretic profile as a function of cell age. *Am.J.Hematol.*, **11**, 125-136.
- Molina-Arcas,M., Moreno-Bueno,G., Cano-Soldado,P., Hernandez-Vargas,H., Casado,F.J., Palacios,J., & Pastor-Anglada,M.** (2006) Human equilibrative nucleoside transporter-1 (hENT1) is required for the transcriptomic response of the nucleoside-derived drug 5'-DFUR in breast cancer MCF7 cells. *Biochem.Pharmacol.*, **72**, 1646-1656.

- Moore,D.V. & Lanier,J.E.** (1961) Observations on Two *Plasmodium falciparum* Infections with an Abnormal Response to Chloroquine. *Am.J.Trop.Med.Hyg.*, **10**, 5-9.
- Mubagwa,K. & Flameng,W.** (2001) Adenosine, adenosine receptors and myocardial protection: an updated overview. *Cardiovasc.Res.*, **52**, 25-39.
- Musto,H., Caccio,S., Rodriguez-Maseda,H., & Bernardi,G.** (1997) Compositional constraints in the extremely GC-poor genome of *Plasmodium falciparum*. *Mem.Inst.Oswaldo Cruz*, **92**, 835-841.
- Nakazawa,S., Kanbara,H., & Aikawa,M.** (1995) *Plasmodium falciparum*: recrudescence of parasites in culture. *Exp.Parasitol.*, **81**, 556-563.
- Ngo,H.M., Ngo,E.O., Bzik,D.J., & Joiner,K.A.** (2000) *Toxoplasma gondii*: are host cell adenosine nucleotides a direct source for purine salvage? *Exp.Parasitol.*, **95**, 148-153.
- Paglia,D.E., Valentine,W.N., Nakatani,M., & Brockway,R.A.** (1986) Mechanisms of adenosine 5'-monophosphate catabolism in human erythrocytes. *Blood*, **67**, 988-992.
- Parker,M.D., Hyde,R.J., Yao,S.Y., McRobert,L., Cass,C.E., Young,J.D., McConkey,G.A., & Baldwin,S.A.** (2000) Identification of a nucleoside/nucleobase transporter from *Plasmodium falciparum*, a novel target for anti-malarial chemotherapy. *Biochem.J.*, **349**, 67-75.
- Pastor-Anglada,M., Cano-Soldado,P., Molina-Arcas,M., Lostao,M.P., Larrayoz,I., Martinez-Picado,J., & Casado,F.J.** (2005) Cell entry and export of nucleoside analogues. *Virus Res.*, **107**, 151-164.
- Patz,J.A. & Olson,S.H.** (2006) Malaria risk and temperature: influences from global climate change and local land use practices. *Proc.Natl.Acad.Sci.U.S.A*, **103**, 5635-5636.

- Payne,D.** (1987) Spread of chloroquine resistance in *Plasmodium falciparum*. *Parasitol.Today*, **3**, 241-246.
- Payne,D.** (1988) Did medicated salt hasten the spread of chloroquine resistance in *Plasmodium falciparum*? *Parasitol Today*, **4**, 112-115.
- Perrett,D.** (1976) Simplified low-pressure high-resolution nucleotide analyser. *J.Chromatogr.*, **124**, 187-196.
- Plagemann,P.G.** (1986) Transport and metabolism of adenosine in human erythrocytes: effect of transport inhibitors and regulation by phosphate. *J.Cell Physiol*, **128**, 491-500.
- Plagemann,P.G. & Woffendin,C.** (1988) Species differences in sensitivity of nucleoside transport in erythrocytes and cultured cells to inhibition by nitrobenzylthioinosine, dipyridamole, dilazep and lidoflazine. *Biochim.Biophys.Acta*, **969**, 1-8.
- Plagemann,P.G., Wohlhueter,R.M., & Woffendin,C.** (1988) Nucleoside and nucleobase transport in animal cells. *Biochim.Biophys.Acta*, **947**, 405-443.
- Podgorska,M., Kocbuch,K., & Pawelczyk,T.** (2005) Recent advances in studies on biochemical and structural properties of equilibrative and concentrative nucleoside transporters. *Acta Biochim.Pol.*, **52**, 749-758.
- Pollack,Y., Katzen,A.L., Spira,D.T., & Golenser,J.** (1982) The genome of *Plasmodium falciparum*. I: DNA base composition. *Nucleic Acids Res.*, **10**, 539-546.
- Price,R.N., Nosten,F., Luxemburger,C., Ter Kuile,F.O., Paiphun,L., Chongsuphajaisiddhi,T., & White,N.J.** (1996) Effects of artemisinin derivatives on malaria transmissibility. *Lancet*, **347**, 1654-1658.
- Queen,S.A., Jagt,D.L., & Reyes,P.** (1990) In vitro susceptibilities of *Plasmodium falciparum* to compounds which inhibit nucleotide metabolism. *Antimicrob Agents Chemother*, **34**, 1393-1398.

- Queen,S.A., Vander Jagt,D.L., & Reyes,P.** (1989) Characterization of adenine phosphoribosyltransferase from the human malaria parasite, *Plasmodium falciparum*. *Biochim.Biophys.Acta*, **996**, 160-165.
- Rager,N., Mamoun,C.B., Carter,N.S., Goldberg,D.E., & Ullman,B.** (2001) Localization of the *Plasmodium falciparum* PfNT1 nucleoside transporter to the parasite plasma membrane. *J Biol.Chem.*, **276**, 41095-41099.
- Rapoport,I., Rapoport,S.M., & Gerber,G.** (1987) Degradation of AMP in erythrocytes of man. Evidence for a cytosolic phosphatase activity. *Biomed.Biochim.Acta*, **46**, 317-329.
- Reyes,P., Rathod,P.K., Sanchez,D.J., Mrema,J.E., Rieckmann,K.H., & Heidrich,H.G.** (1982) Enzymes of purine and pyrimidine metabolism from the human malaria parasite, *Plasmodium falciparum*. *Mol.Biochem.Parasitol.*, **5**, 275-290.
- Rieckmann,K.H.** (1983) Falciparum malaria: the urgent need for safe and effective drugs. *Annu.Rev.Med.*, **34**, 321-335.
- Rieckmann,K.H., Campbell,G.H., Sax,L.J., & Mrema,J.E.** (1978) Drug sensitivity of *Plasmodium falciparum*. An in-vitro microtechnique. *Lancet*, **1**, 22-23.
- Rieckmann,K.H., Davis,D.R., & Hutton,D.C.** (1989) *Plasmodium vivax* resistance to chloroquine? *Lancet*, **2**, 1183-1184.
- Rodenko,B., van der Burg,A.M., Wanner,M.J., Kaiser,M., Brun,R., Gould,M., de Koning,H.P., & Koomen,G.J.** (2007) 2,N6-disubstituted adenosine analogs with antitrypanosomal and antimalarial activities. *Antimicrob Agents Chemother*, **51**, 3796-3802.
- Rosales,O.R., Eades,B., & Assali,A.R.** (2004) Cardiovascular drugs: adenosine role in coronary syndromes and percutaneous coronary interventions. *Catheter.Cardiovasc.Interv.*, **62**, 358-363.
- Rosario,V.** (1981) Cloning of naturally occurring mixed infections of malaria parasites. *Science*, **212**, 1037-1038.

- Rudzinska,M.A., Trager,W., & Bray,R.S.** (1965) Pinocytotic uptake and the digestion of hemoglobin in malaria parasites. *J.Protozool.*, **12**, 563-576.
- Russell,s.** (2004) The economic burden of illness for households in developing countries: A review of studies focusing on malaria, tuberculosis, and Human Immunodeficiency Virus/Acquired Immunodeficiency Syndrome. *Am.J.Trop.Med.Hyg.*, **71**, 147-155.
- Saliba,K.J., Horner,H.A., & Kirk,K.** (1998) Transport and metabolism of the essential vitamin pantothenic acid in human erythrocytes infected with the malaria parasite *Plasmodium falciparum*. *J Biol.Chem.*, **273**, 10190-10195.
- Saliba,K.J. & Kirk,K.** (2001) H(+)-coupled pantothenate transport in the intracellular malaria parasite. *J Biol.Chem*, M010942200.
- Sambrook,J., Fritsch,E.F., & Maniatis,T.** (1989) *Molecular cloning: A laboratory manual*, 2nd edn, New York.
- Scheibel,L.W. & Sherman,I.W.** (1988) *Malaria: principles and practice of malariology*, pp. 234-242. Churchill Livingstone Ltd, London.
- Schrader,W.P., Harder,C.M., & Schrader,D.K.** (1983) Adenosine deaminase complexing proteins of the rabbit. *Comp Biochem.Physiol B*, **75**, 119-126.
- Schwab,J.C., Afifi,A.M., Pizzorno,G., Handschumacher,R.E., & Joiner,K.A.** (1995) *Toxoplasma gondii* tachyzoites possess an unusual plasma membrane adenosine transporter. *Mol.Biochem.Parasitol.*, **70**, 59-69.
- Schwab,J.C., Beckers,C.J., & Joiner,K.A.** (1994) The parasitophorous vacuole membrane surrounding intracellular *Toxoplasma gondii* functions as a molecular sieve. *Proc.Natl.Acad.Sci.U.S.A*, **91**, 509-513.
- Schwartzman,J.D. & Pfefferkorn,E.R.** (1982) *Toxoplasma gondii*: purine synthesis and salvage in mutant host cells and parasites. *Exp.Parasitol.*, **53**, 77-86.

- Shepard,D.S., Ettling,M.B., Brinkmann,U., & Sauerborn,R.** (1991) The economic cost of malaria in Africa. *Trop.Med.Parasitol.*, **42**, 199-203.
- Sherman,I.W.** (1979) Biochemistry of *Plasmodium* (malarial parasites). *Microbiol.Rev.*, **43**, 453-495.
- Shi,M.M. & Young,J.D.** (1986) [3H]dipyridamole binding to nucleoside transporters from guinea-pig and rat lung. *Biochem J*, **240**, 879-883.
- Siddiqui,W.A., Kan,S.C., Kramer,K., & Richmond-Crum,S.M.** (1979) *In vitro* production and partial purification of *Plasmodium falciparum* antigen. *Bull World Health Organ*, **57 Suppl 1**, 75-82.
- Sidhu,A.B., Valderramos,S.G., & Fidock,D.A.** (2005) pfmdr1 mutations contribute to quinine resistance and enhance mefloquine and artemisinin sensitivity in *Plasmodium falciparum*. *Mol.Microbiol.*, **57**, 913-926.
- Singh,B., Kim,S.L., Matusop,A., Radhakrishnan,A., Shamsul,S.S., Cox-Singh,J., Thomas,A., & Conway,D.J.** (2004) A large focus of naturally acquired *Plasmodium knowlesi* infections in human beings. *Lancet*, **363**, 1017-1024.
- Smeijsters,L.J., Franssen,J., Naesens,L., de Vries,E., .Holý,A., Balzarini,J., de Clercq,E., & Overdulve,P.** (1999) Inhibition of the *in vitro* growth of *Plasmodium falciparum* by acyclic nucleoside phosphonates. *Int J Antimicrob Agents*, **12**, 53-61.
- Staines,H.M., Ellory,J.C., & Kirk,K.** (2001) Perturbation of the pump-leak balance for Na(+) and K(+) in malaria-infected erythrocytes. *Am.J.Physiol Cell Physiol*, **280**, C1576-C1587.
- Staines,H.M., Powell,T., Thomas,S.L., & Ellory,J.C.** (2004) *Plasmodium falciparum*-induced channels. *Int.J.Parasitol.*, **34**, 665-673.
- Sundaram,M., Yao,S.Y., Ingram,J.C., Berry,Z.A., Abidi,F., Cass,C.E., Baldwin,S.A., & Young,J.D.** (2001) Topology of a human equilibrative, nitrobenzylthioinosine (NBMPR)-sensitive nucleoside transporter (hENT1) implicated in the cellular uptake of adenosine and anti-cancer drugs. *J Biol.Chem.*, **276**, 45270-45275.

- Tanabe,K.** (1990a) Glucose transport in malaria infected erythrocytes. *Parasitol.Today*, **6**, 225-229.
- Tanabe,K.** (1990b) Ion metabolism in malaria-infected erythrocytes. *Blood Cells*, **16**, 437-449.
- Thaithong,S.** (1983) Clones of different sensitivities in drug-resistant isolates of *Plasmodium falciparum*. *Bull.World Health Organ*, **61**, 709-712.
- Thaithong,S. & Beale,G.H.** (1981) Resistance of ten Thai isolates of *Plasmodium falciparum* to chloroquine and pyrimethamine by *in vitro* tests. *Trans.R.Soc.Trop.Med.Hyg.*, **75**, 271-273.
- Ting,L.M., Shi,W., Lewandowicz,A., Singh,V., Mwakingwe,A., Birck,M.R., Ringia,E.A., Bench,G., Madrid,D.C., Tyler,P.C., Evans,G.B., Furneaux,R.H., Schramm,V.L., & Kim,K.** (2005) Targeting a novel *Plasmodium falciparum* purine recycling pathway with specific immucillins. *J Biol.Chem.*, **280**, 9547-9554.
- Too,K., Brown,D.M., Loakes,D., Bongard,E., & Vivas,L.** (2007) *In vitro* anti-malarial activity of n(6)-modified purine analogs. *Nucleosides Nucleotides Nucleic Acids*, **26**, 579-583.
- Tracy,S.M. & Sherman,I.W.** (1972) Purine uptake and utilization by the avian malaria parasite *Plasmodium lophurae*. *J.Protozool.*, **19**, 541-549.
- Trager,W. & Jensen,J.B.** (1976) Human malaria parasites in continuous culture. *Science*, **193**, 673-675.
- Traut,T.W.** (1994) Physiological concentrations of purines and pyrimidines. *Mol.Cell Biochem*, **140**, 1-22.
- Upston,J.M. & Gero,A.M.** (1995) Parasite-induced permeation of nucleosides in *Plasmodium falciparum* malaria. *Biochim.Biophys.Acta*, **1236**, 249-258.

- Uyemura,S.A., Luo,S., Moreno,S.N., & Docampo,R.** (2000) Oxidative phosphorylation, Ca(2+) transport, and fatty acid-induced uncoupling in malaria parasites mitochondria. *J Biol.Chem.*, **275**, 9709-9715.
- Van Dyke,K.** (1975) Comparison of tritiated hypoxanthine, adenine and adenosine for purine-salvage incorporation into nucleic acids of the malarial parasite, *Plasmodium berghei*. *Tropenmed.Parasitol.*, **26**, 232-238.
- Verloo,P., Kocken,C.H., Van der,W.A., Tilly,B.C., Hogema,B.M., Sinaasappel,M., Thomas,A.W., & De Jonge,H.R.** (2004) *Plasmodium falciparum*-activated chloride channels are defective in erythrocytes from cystic fibrosis patients. *J Biol.Chem.*, **279**, 10316-10322.
- Vu,T.T., Tran,V.B., Phan,N.T., Le,T.T., Luong,V.H., O'Brien,E., & Morris,G.E.** (1995) Screening donor blood for malaria by polymerase chain reaction. *Trans.R.Soc.Trop.Med.Hyg.*, **89**, 44-47.
- Wagner,C.A., Friedrich,B., Setiawan,I., Lang,F., & Broer,S.** (2000) The use of *Xenopus laevis* oocytes for the functional characterization of heterologously expressed membrane proteins. *Cell Physiol Biochem.*, **10**, 1-12.
- Wallace,L.J., Candlish,D., & de Koning,H.P.** (2002) Different substrate recognition motifs of human and trypanosome nucleobase transporters. Selective uptake of purine antimetabolites. *J Biol.Chem.*, **277**, 26149-26156.
- Walliker,D., Quakyi,I.A., Wellems,T.E., McCutchan,T.F., Szarfman,A., London,W.T., Corcoran,L.M., Burkot,T.R., & Carter,R.** (1987) Genetic analysis of the human malaria parasite *Plasmodium falciparum*. *Science*, **236**, 1661-1666.
- Walter,R.D. & Konigk,E.** (1974) Hypoxanthine-guanine phosphoribosyltransferase and adenine phosphoribosyltransferase from *Plasmodium chabaudi*, purification and properties. *Tropenmed.Parasitol.*, **25**, 227-235.
- Ward,G.E., Miller,L.H., & Dvorak,J.A.** (1993) The origin of parasitophorous vacuole membrane lipids in malaria-infected erythrocytes. *J Cell Sci.*, **106 ( Pt 1)**, 237-248.



**Ward,S.A.** (1988) Mechanisms of chloroquine resistance in malarial chemotherapy.

*Trends Pharmacol.Sci.*, 9, 241-246.

**Webster,H.K. & Whaun,J.M.** (1981) Purine metabolism during continuous erythrocyte culture of human malaria parasites (*P. falciparum*). *Prog.Clin.Biol.Res.*, **55**, 557-573.

**White,N.J.** (2004) Antimalarial drug resistance. *J.Clin.Invest*, **113**, 1084-1092.

**WHO** (1990) Severe and complicated malaria. *Trans.R.Soc.Trop.Med.Hyg.*, **84**, 1-65.

WHO. World Malaria Report. 2005.

Ref Type: Report

**Wilairatana,P., Chanthavanich,P., Singhasivanon,P., Treeprasertsuk,S., Krudsood,S., Chalermrut,K., Phisalaphong,C., Kraisintu,K., & Looareesuwan,S.** (1998) A comparison of three different dihydroartemisinin formulations for the treatment of acute uncomplicated falciparum malaria in Thailand. *Int.J.Parasitol.*, **28**, 1213-1218.

**Wright,E.M., Turk,E., & Martin,M.G.** (2002) Molecular basis for glucose-galactose malabsorption. *Cell Biochem.Biophys.*, **36**, 115-121.

**Yakuob,A.A., Gustafsson,L.L., Ericsson,O., & Hellgren,U.** (1995) *Handbook of Drugs for Tropical Parasitic Infections*, pp. 155-159. Taylor and Francis Publication, UK.

**Yao,S.Y., Ng,A.M., Vickers,M.F., Sundaram,M., Cass,C.E., Baldwin,S.A., & Young,J.D.** (2002) Functional and molecular characterization of nucleobase transport by recombinant human and rat equilibrative nucleoside transporters 1 and 2. Chimeric constructs reveal a role for the ENT2 helix 5-6 region in nucleobase translocation. *J Biol.Chem.*, **277**, 24938-24948.

**Yeung,S.M. & Green,R.D.** (1983) Agonist and antagonist affinities for inhibitory adenosine receptors are reciprocally affected by 5'-guanylylimidodiphosphate or N-ethylmaleimide. *J Biol.Chem.*, **258**, 2334-2339.

- Zoig, J.W., McLeod, A.J., & Dickson I.H. (1982) *Plasmodium falciparum*: modifications of the *in vitro* culture improving parasitic yields. *J. Parasitol*, **68**, 1072-1080.